THE UNIVERSITY OF MICHIGAN

INDUSTRY PROGRAM OF THE COLLEGE OF ENGINEERING

EXPERIMENTAL AND ANALYTICAL STUDY OF VISCOUS COMPRESSIBLE FLOW IN A UNIFLOW VORTEX TUBE

Joachim Joseph Ellery Lay

This dissertation was submitted in partial fulfillment of the requirements for the degree of Doctor of Philosophy in the University of Michigan, 1957.

December, 1956

IP-193

Doctoral Committee:

Professor F. N. Calhoon, Chairman
Professor D. L. Katz
Professor H. E. Keeler
Professor A. Marin
Associate Professor G. J. Van Wylen
Professor E. T. Vincent

PREFACE

The purpose of this work is to provide a better understanding of the separation of a gas stream into regions of high and low stagnation temperatures in a vortex field. Its motivation is the Ranque-Hilsch tube, which produces from a single source of compressed air, a hot stream and a cold stream of widely different temperatures.

The Ranque-Hilsch effect is a fairly recent discovery, having been first reported in 1931. Its history follows the familiar pattern of initial enthusiasm, then apathy, and later, renewed interest. As a phenomenon, relatively little is known concerning it, except for its spectacular effect of producing hot and cold air simultaneously. Despite various hypotheses advanced, there is to date, no general agreement as to its theory of operation. Consequently, there is need for a systematic study of the phenomenon from the ground up. The current work represents such a study. It is hoped that it will be of help in the understanding of the Ranque-Hilsch tube and of vorticity in general.

The author wishes to express his thanks to the Doctoral Committee for its interest, encouragement, and suggestions. He is particularly grateful to Professor F. N. Calhoon, Chairman, who, despite the pressure of many duties, was always available for consultation and advice.

The author also wishes to express his appreciation to the people who have been of help in the accomplishment of the project. To Mr. W. Salva, of the Mechanical Engineering Machine Shop, for constructing the model from the detailed plans. To Drs. R. Leite, M. Uberoi, and Mr. K. Raman, of the Aeronautical Engineering Department, for initiation to the technique of hot wire anemometry. To Messrs. C. Ronsdahl and A. Menner, of the Mechanical Engineering Laboratory, for their help in erecting the

test installation. To Mr. J. Davenport, of the Photography Department, for taking pictures of the model and test installation. To Miss M. Runkel and Mr. R. Harrell, of the Engineering Library, for their courteous service. And to the College of Engineering Industry Program, for the typing and printing of the thesis.

TABLE OF CONTENTS

PART IV. DISCUSSION AND CONCLUSION

LIST OF TABLES

LIST OF FIGURES

LIST OF FIGURES (Cont'd)

LIST OF FIGURES (Cont'd)

LIST OF FIGURES (Cont'd)

LIST OF FIGURES (Cont'd)

LIST OF SYMBOLS

A = Constant in the entropic equation of state. Also, ratio of local to stagnation sound velocity. Also, constant in the hot wire velocity relation. As a subscript, denotes axial component of velocity.

B = Constant in the entropic equation of state. Also, coefficient in the hot wire velocity relation.

C = Constant in hot wire calibration relation. Also, constant of integration.

D = Constant in hot wire calibration relation.

G = Modulus of elasticity in torsion.

H = Hot wire heat loss in the Boussinesq-King relation.

J = Jacobian $x_u y_v - x_v y_u$. Also, function as defined by Equation (8-34).

K = Constant in irrotational flow.

L = Axial length; length of hot wire.

M = Mach number. Also, total mass. Also moment of shearing forces.

P_r = Prandtl number.

N_u = Nusselt's number.

Q = Strength of source or sink. Also, heat transfer rate.

R = Radial distance. Also, hot wire resistance. Also, radius of curvature. Also, gas constant.

R_e = Reynolds number.

S = Entropy. Also, displacement vector in stress-strain relations.

T = Absolute temperature. As a subscript, denotes stagnation or total conditions. Also, torque.

V = Velocity, of components u, v, w. Also, volume.

W = Velocity parameter in sink flow as per Equation (11-5).

X, Y, Z = Body forces in Navier-Stokes equations.

a = Hot wire overheating ratio. Also, acceleration. As a subscript, denotes axial component of velocity.

c = Speed of sound.

c_p, c_v = Specific heats at constant pressure and volume.

g = Acceleration of gravity. Also, gravity force in Navier-Stokes and change of circulation equations.

h = Coefficient of convective heat transfer in the cross-convection equation $N_u = .3\ (R_e)^{.57}$. Also, enthalpy.

i = Summation index. Also, unit vector along x axis.

j = Jacobian $u_x v_y - u_y v_x$. Also, function as defined by Equation (8-35). Also, unit vector along y axis.

k = Thermal conductivity. Also, unit vector along z axis.

ℓ = Distance normal to flow direction.

m = Mass. Also, sink strength.

n = Normal component in curvilinear coordinates.

o = As a subscript, denotes stagnation conditions; also reference condition; also outer radius as against inner radius.

p = Pressure.

q = Velocity in the hodograph plane. Also, velocity in physical space, of components u, v, w. Used to denote velocity in preference to V whenever the latter may be confused with its component v. Also, strength of source or sink.

r = Radial distance.

s = Specific entropy. As a subscript, denotes static conditions.

t = Time. Also, temperature Fahrenheit. As a subscript, denotes stagnation or total conditions.

LIST OF SYMBOLS (Cont'd)

u, v, w = Components of velocity in physical space.

x, y, z = Coordinate axes. Also, as double subscripts, denote partial differentiation.

α = Temperature coefficient of resistivity. Also, inverse Reynold's number. Also, flow angle. When paired with β, summation suffix in tensor notation.

β = Angle in Biot-Savart vorticity theorem. When paired with α, summation suffix in tensor notation.

γ = Ratio of specific heats at constant pressure and constant volume. Also, angular displacement in stress-strain relations.

Γ = Circulation.

ϵ = Emissivity. Also, turbulent exchange rate in turbulent shear equation.

$\epsilon_x, \epsilon_y, \epsilon_z$ = Elongation along coordinate axes.

ξ, η, ζ = Components of displacement vector in stress-strain relations.

η = Efficiency.

θ = Velocity angle in hodograph plane. Also, cylindrical coordinate angle.

λ = Coefficient relating laminar and turbulent shear stresses.

μ = Coefficient of viscosity.

ρ = Density.

σ = Stefan-Boltzmann constant. Also, strength of source or sink. Also, normal stress.

τ = Shear stress.

φ = Potential function.

ψ = Streamline function.

ω = Rotation.

$*$ = Denotes sonic conditions.

ABSTRACT

The present investigation is an experimental and analytical study of viscous compressible flow in a uniflow vortex tube. There is need for such a study from the ground up, for to date, no general agreement on the theory of the vortex tube has yet been reached.

The problem is first approached from the experimental standpoint. A large, multi-purpose vortex tube is designed and built of lucite. Design features enable traverse measurements of pressure, temperature, and velocity to be taken at six different stations throughout the length of the tube. The pressure and temperature probes are of the hypodermic type with minimum flow disturbance. The velocity probe is a miniature hot wire anemometer which is revolvable for measurement of direction as well as magnitude. Data is taken for five runs of different inlet pressures.

The analytical approach consists of a mathematical treatment of vorticity in general. It begins with potential vortex flow in the plane. This is characterized by the existence of sonic or limit circles. An axial velocity is then added to yield the solution in space. The effect of viscosity is considered, and the potential or free vortex is shown to change into a forced vortex. The general solution is arrived at by superposing a viscous compressible sink with the vortex flow. Performance or energy separation is expressed as a function of the ratio between vortex strength and sink strength.

Part I

INTRODUCTION, DEFINITION OF PROBLEM, AND REVIEW OF PREVIOUS WORK

CHAPTER 1

DEFINITION OF PROBLEM AND REVIEW OF PREVIOUS WORK

1.1 Introduction

The initial motivation for this work is the perplexing phenomenon of separation of a gas stream simultaneously into hot and cold streams known as the Ranque-Hilsch effect. The beautiful and altogether extensive characteristics of vorticity, however, have also been a factor in the attempt to give the work an engineering and mathematical unity.

The vortex, or Ranque-Hilsch, tube is a remarkably uncomplicated device which simultaneously produces hot and cold streams from a single source of compressed gas. The device has no moving parts, but merely consists of a straight length of tubing with a tangential entry for the supply air, and à smaller tube for tapping off the cold stream that is produced (Fig. 1-1); the hot stream leaving through the larger tube. By throttling the far end of the larger tube, various proportions of hot and cold gas may be obtained with various degrees of temperature difference.

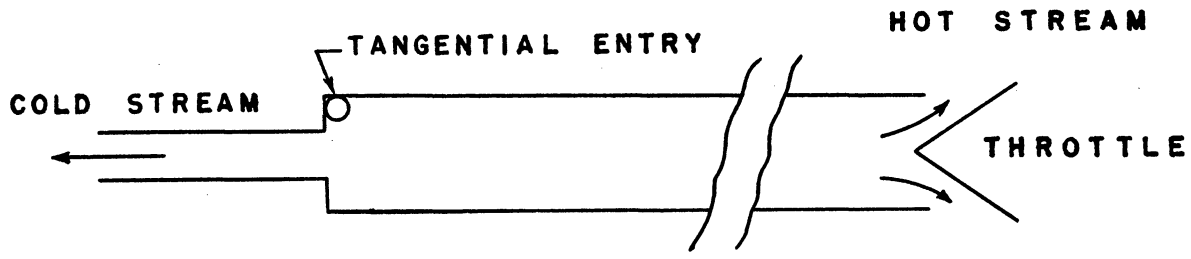

Figure 1-1. Simple Counterflow Vortex Tube

As a phenomenon, relatively little is known concerning its details or performance laws except that the effect occurs when a gas expands in a centrifugal field such as exists in cyclone separators, or when it flows through valves such as nozzles. Despite various hypotheses advanced, there is to date no general agreement or treatment as to its theory of operation (39). It thus represents a most interesting item to be studied.

1.2 The Problem

One of the most spectacular facts concerning the vortex tube is the wide spread in the temperature of the hot and cold stream temperatures that can be obtained under certain conditions. Experimenting with a simplified form of Hilsch's original device, Blaber (11) obtained hot stream and cold stream temperatures of 88°C and -20°C respectively from a source of compressed air at 4 atm. and room temperature (15°C). Hilsch (50) has claimed hot stream temperatures as high as 154°F and cold stream temperatures as low as 10°F in experiments involving tubes of approximately .3" diameter and 18" long. The device thus separates air into two streams: one, as if it were heated by compression near the wall, and the other, as if it were cooled by expansion near the axis. Hilsch termed the device a wirbelrohr, or vortex tube.

A hypothesis on the Ranque-Hilsch tube must explain not only the cooling of the one stream from expansion of the supply stream, but also the mechanism by which the energy abstracted from the other stream is added to the portion of gas that becomes the hot stream. An energy balance indicates that such an exchange exists (56), but does not show how it is done. Since 1946, writers of widely varying backgrounds have undertaken to explain the phenomenon, but with little

success. There is at present an almost complete lack of agreement as to the mechanism of flow (59). The following quotation from Fulton (40) sums up the present status of affairs: "At least ten theories have been proposed....some of them turn out to say nothing at all...in some others, equations have been tortured to show two different temperatures, while in still others the mass of manipulations has grown so great as to be incomprehensible."

The author is in agreement with Webster, Scheper, and Fulton (130,100,40,) that there is need to fall back to the beginning and start in the right fashion with a traverse of pressures, temperatures, and velocities inside the vortex tube. This is not only the most down-to-earth starting point for an understanding of the phenomenon, but it is also good scientific procedure in that relatively fewer assumptions need then be made for the analysis that is to follow. Heretofore, the usual tubes tested have been too small to contemplate making traverses. The original Hilsch apparatus consisted of a 6 mm hot tube, a 1 mm entry tube, with a 1.5 mm orifice opening to tap off the cold air. Under such conditions, it was well nigh impossible to take data inside the device.

It is the object of the present investigation to provide for a direct attack of the problem by constructing a set of lucite tubes big enough to enable traverses to be taken. Temperature and pressure traverses are obtained by means of hypodermic probes unobtrusively inserted, while velocity traverses are obtained by means of very small sized hot-wire probes so constructed as not to disturb the flow. From the data thus taken, correlation with theory is attempted and the laws of vortex flow evolved in terms of pertinent parameters.

Another object of the investigation is to study the uniflow type of vortex tube. There are essentially two types of vortex tubes: uniflow and counterflow. While the counterflow type shown in Fig. (1-1 has been the more often studied by writers, the uniflow type, shown in Fig. (1-2) has not been extensively investigated heretofore (73,131, 39). To establish a proper balance between the two types of vortex tubes, the present investigation concentrates on the uniflow type, inasmuch as the author believes that a more basic study of the vortex

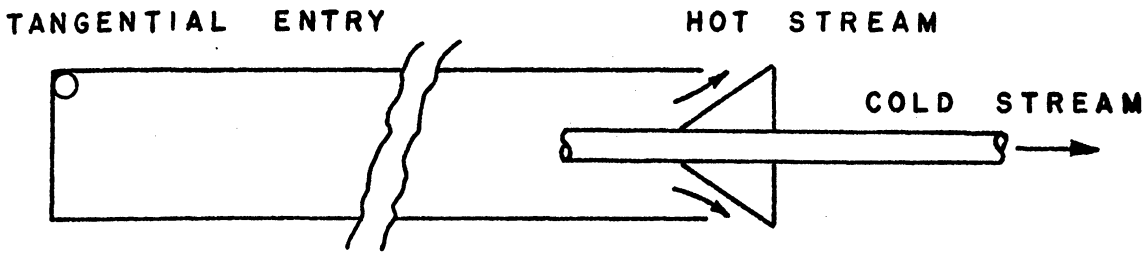

Figure 1-2. Simple Uniflow Vortex Tube

phenomenon should start with the uniflow type, since it is the one that occurs more often in nature as compared with the counterflow type which is based on an arbitrary subdivision of the directions of flow, and thus is more artificial.

1.3 Historical Background

The vortex tube is a relatively recent discovery, having been first reported by George Ranque in 1931. Its history follows the pattern of many inventions of the past two centuries, namely that of initial interest, then skepticism and apathy, and later, renewed interest. Ranque was a metallurgist at a steel works in Moutluçon,

Central France, and he may have noticed the vortex cooling affect in connection with cyclone separators. He constructed a device to duplicate the effect and applied for a French patent in December, 1931. The invention was called "an apparatus for obtaining from a fluid under pressure two currents of fluids at different temperatures" and the patent was assigned to the company of "La Giration Des Fluids." A similar patent was applied for in the United States in December, 1932, and was granted in March, 1934 (91).

In the patents, Ranque gave various arrangements of the counterflow and parallel flow types of vortex tube, along with an explanation of the phenomenon which is not commonly accepted theory at present. Ranque realized later that his explanation was incorrect, and presented a revised version in form of a paper (90) read to the Societé Française de Physique. Considerable skepticism was expressed in the Societé Française de Physique, and in a discussion (14) E. Brun, a member of the Society and an aerodynamicist, dismissed Ranque's discovery on the grounds that he had confused static temperature with total temperature. Ranque did not reply to the criticism and did not demonstrate his device to convince the skeptics. It may have been that he desired to maintain secrecy in order to further his invention, for the company to which he assigned his patent was none other than the one he himself had formed. Subsequent developments, however, probably brought the disappointing realization that the vortex tube was inefficient as a refrigerator, for nothing more was heard concerning the device in Europe or in the United States until 1946, when Rudolph Hilsch (76,50) of the Physikalischen Institute, Erlangen, Germany, published a paper concerning his work with the device.

Hilsch became interested in the vortex tube after reading Ranque's paper, and he proceeded to build some counterflow-type tubes which he tested (50). Hilsch's purpose was to design a tube of maximum efficiency for cooling underground mines and shafts. He did not realize his goal, but did succeed in using the vortex tube as a substitute for the ammonia precooler in his laboratory's air liquifying machine (Fig. 1-3).

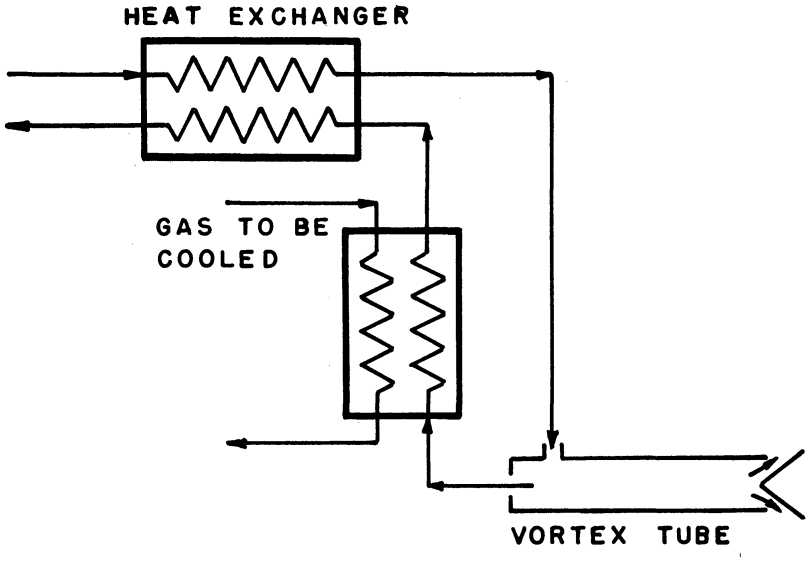

Figure 1-3. Vortex Tube in Gas Liquefaction Process

In June, 1945, at the end of the war in Europe, C. W. Hansell, an investigator for the United States and British Technical Industrial Intelligence Committee, visited Erlangen University and rediscovered the vortex tube (47,48). About the same time, R. M. Milton, of Johns Hopkins also visited Erlangen and brought back a model and a thesis by Hilsch. The thesis was translated by I. Estermann, of Carnegie Institute of Technology, and the translation was circulated through Wright Field. Hilsch's original paper was published in Germany in April 1946 (50,108), and gave performance data and some optimum dimensions for two vortex tubes. Hilsch's translated paper was printed unabridged in "The Review of Scientific Instruments" of February, 1947.

Widespread American interest has been given the vortex tube ever since Milton published a short descriptive article in "Refrigerating Engineering," May, 1946. The extreme simplicity of the device suggested that it might replace many of the more complicated refrigeration designs. However, subsequent investigations showed that the power required to operate the vortex tube was many times that required by a conventional refrigerator, and that, in spite of its simplicity, it would not be practical as a regular refrigerator. Nevertheless, the vortex tube has presented a new and intriguing phenomenon in fluid dynamics, and interest in the device continues.

1.4 Review of Past Work

Relatively little information is known on the working process of the vortex tube, despite the vast amount of literature both technical and non-technical that has been written on the subject. Many theories have been advanced to explain the operation of the tube, but none has been accepted with any widespread agreement. In passing, it should be mentioned that some writers have, facetiously or otherwise, resorted to the "Maxwell Demon" explanation for the device to the extent that the vortex tube is sometimes classified as a Maxwell Demon Device. Maxwell, of course, once suggested that in the realm of molecular motion, it would conceivably be possible to tap energy from a gas by utilizing the non-uniformity of the velocity or kinetic energy of its molecules. According to this scheme, a chamber filled with gas would be envisioned to be divided into two portions by a partition. Fast and slow molecules would then impinge on this partition. Now, the random distribution of molecules can be changed by permitting the fast molecules to accumulate on one side of the partition and the slow molecules to accumulate on the other. For changing

the random distribution into one of higher degree of order, Maxwell facetiously pictured a small gate with a doorkeeper (the demon) opening the gate and allowing the fast molecules to pass in one direction, and the slow ones in the opposite direction. Thus, a temperature gradient is established without addition or subtraction of energy to the system. Maxwell's demon, of course, is of no help in explaining the vortex tube, since the latter is neither a molecular sorting device, nor a device that violates the Second Law of Thermodynamics. An attempt to explain the vortex effect on the basis of the Joule-Thomson effect was disproved by Milton when he showed that the effect could be observed in the same direction when pure nitrogen and hydrogen were used, whereas the Joule-Thomson effect would show an inversion on hydrogen.

Following Hilsch's paper, the next contribution to the subject were in six theses (74,44,92,46,21,32), mainly experimental, which were completed at the Massachusetts Institute of Technology. Mayer, Hunter, and Greene (74,44) gave performance data on the effects of inlet air pressure, cold orifice diameter, and nozzle diameter. Reed (92) gave results on internal flow, and Corliss and Solnick (21) overall data, along with sediment flow pictures and static pressure distribution over the cold outlet plate. Fattah and Sweeney (32) used convergent-divergent nozzle for the flow entry, and their investigation included pressure and temperature measurements on the inside surface of the vortex tube.

Johnson (56), of the University of Toronto, also initiated experimental investigation of the vortex tube, and his results were published in September, 1947. He confirmed Hilsch's work in its

general aspects and gave brief results when CO_2 and H_2 were used as the working fluid in place of air. Samples of air were also taken from the two ends of the vortex tube and analyzed. The results gave no indication of any separation of the air into its components in passing through the device.

Until the end of 1947, explanation of the vortex process had only been suggested in general terms; there was no universal agreement or confirmation. The first important theoretical work was published in November, 1947, by Kassner and Knoernschild (58), of Wright Patterson Air Force Base. The analysis assumes that a free vortex is initially formed inside the tube due to the tangential position of the nozzle with respect to the tube. This vortex complies with the law of constant angular momentum ($m \frac{d}{dt} rv = 0$, $rv = const.$), i.e., the velocity times the radius of any particle is a constant. A radial velocity gradient thus exists in the fluid ($vr = const.$, $rdv + vdr = 0$, $\frac{dv}{dr} = -\frac{v}{r}$), with the inner layers at high tangential velocity and the outer layers at low tangential velocity. This is a characteristic of irrotational flow. A radial pressure gradient is likewise established ($\frac{dp}{dr} = p \frac{v^2}{r}$), which causes the air to expand on its spiral inward path. With sufficient pressure gradient acting, the velocity of the air in the center of the tube would increase to supersonic speed. Viscous shear stress, however, take over in this region with a resulting tendency to equalize velocity distribution. The irrotational character of the flow changes to rotational flow (constant angular velocity or forced vortex), with the normal velocity gradient tending to disappear. The higher velocity layers of the center accelerate the lower velocity layers at the periphery, causing a transfer of kinetic energy outward from the tube axis. This kinetic energy transfer raises the temperature

of the outer gas layers and lowers the temperature of the inner layers. Now, however, a temperature difference exists in the gas, and a heat transfer results, whereby the heat flows from the hot outer layer to the cold inner layers. The pressure of the gas near the axis increases, and a pressure gradient towards the cold orifice (at atmospheric pressure) appears. The innermost layers separate under the influence of this axial pressure gradient and the remaining gas under conditions of rotational flow, progress axially along to the end of the tube. The resulting difference in temperature of the two streams of gas is due to the fact that the overall kinetic energy flux outward is greater than the heat flux inward. By making these various assumptions, Kassner and Knoernschild calculated the velocity and temperature in the resultant vortex, and an estimate of the tube's performance was made and compared with Hilsch's results.

Such explanation did not appear entirely satisfactory to some writers (5,13), who contended that the ideal free vortex of the mathematician (VR = const.) does not exist in a real gas that has the three transport properties of diffusion, viscosity and thermal conduction. It called for radial velocity gradients that are very large and cannot exist in a gas with viscosity. It also called for radial static temperature gradients that resulted in high rates of radial heat transfer, and it furnished no rational solution near the center when an actual gas is considered.

Still in 1948, this time in Norway, attention was drawn on the vortex tube by Haar and Wergeland (45) who published a brief theoretical analysis based on the assumption that the process was simply adiabatic cooling in passing through the pressure gradient

caused by the centrifugal field ($\frac{dp}{dr} = \rho\omega^2 r$, $p\rho^{-\gamma} = \text{constant}$). Haar and Wergeland's presentation is an oversimplification: the radial temperature variation does not coincide with that of an adiabatic line (due to viscous forces near the axis), for with air entering the nozzle at 70°F a temperature of -74°F would have to be attained in an expansion to atmospheric pressure (13), and no such gradient has been experimentally reported. Burkhardt (15), of Germany, also presented a simplified theoretical investigation of performance without analysis of the internal flow by calculating the hot and cold stream temperatures as functions of the fraction of cold air flow rate, and a coefficient α (the separating factor).

Fulton (38,39) began his theoretical investigation by endeavoring to solve the equations for a three dimensional compressible vortex subjected to viscous or turbulent shear with an approximate expression for the temperature drop across the vortex. However, he concluded that Kassner's and Knoernschild's analysis (which did not consider compressibility) involved fewer uncertainties and that it appeared to agree satisfactorily with experiments. Fulton also pointed out that if the hot air from the vortex tube is deliberately wasted, then the power required to drive a vortex refrigerator would be of the order of 100 times that of a conventional refrigerator.

The first report to be concerned solely with the application of the vortex tube came from Knoernschild and Morgensen (61). It discussed the cooling of high-speed aircraft or missiles, and compared the performance of the vortex tube with that of the expansion turbine. For small requirements of cooling, the vortex tube operating on ram intake or jet-engine pressure bleed would be a very good means because it has superior efficiency with respect to an expansion

turbine of very low specific speed.

On the experimental side, Corr (23) carried out some tests at the General Electric Research Division by using a multi-nozzle inlet chamber. Pressure measurements taken at the hot tube outlet and cold outlet diaphragm were then chosen as parameters of performance. Corr also made brief tests on a supersonic inlet nozzle, but the results indicated a decrease of the temperature drop. Other aspects of his investigation included the use of a glass tube to observe flow and a spectrograph analysis of hot and cold air samples to test for separation of component gases. None was observed. Humidity measurements also revealed negligible increase of water vapor in the hot air.

Barnes (6), in another of M.I.T.'s theses on the subject, assumed that the flow in the tube was that of a two-dimensional symmetric and compressible vortex with small radial flow with cases of both laminer and turbulent shear being considered. Mathematical difficulties prevented the completion of the laminar flow analysis, whereas additional assumption had to be made for the turbulent flow case. Nickerson (79) attempted completion of Barnes' work by making several assumptions and by using a somewhat different approach to the equations of two-dimensional compressible turbulent flow. An approximate solution was obtained for the temperature distribution which agreed fairly well with the experimental results of Fattah and Sweeney (32). Nickerson, however, expressed the opinion that in view of the assumptions made, the agreement may be somewhat of a coincidence.

Scheper (100,101), of Union College, investigated the internal flow of the vortex tube by means of short silk threads. He also proposed a theory by which heat transfer occured radially from the core outward by virtue of static temperature gradients in that direction.

The heat sink is provided by the outer gas layers which are at lower static temperature due to the nozzle expansion. This heat transfer raises the stagnation temperature of the outer gas which produces the hot flow, while at the same time the stagnation temperature of the core is lowered, thus producing a cold flow through the orifice. Scheper's theory is original in that it is based on forced convection due to static temperature gradients whereas previous investigators used the principle of energy transfer due to shear stress. Other academic contributions during this period (1949) were those of Sochor (113), of Syracuse University, and of Levitt (65), of Rensselaer Polytechnic Institute.

1.5 From 1950 to Present

Webster (130) carried out an investigation of vortex tubes at the Engineering Research Laboratory of E. I. du Pont de Nemours and Co. Inc., and presented a paper to the 45th Annual Meeting of the American Society of Refrigerating Engineers which was published in Refrigerating Engineering in February, 1950. He reviewed most of Hilsch's work and he also gave an explanation which was very lively and critically commented upon (5,13,43).

Lustich (69), of Syracuse University, reviewed previous work on the vortex tube and gave a theory based on thermodynamic considerations. He also pointed out that the efficiency of the vortex tube could be considerably increased if the availability of the energy of the higher pressure hot gas could be realized instead of being rejected through the throttling valve.

In the same year, MacGee, of Boston University, reviewed work on the vortex tube and reported on his experimental investigations concerning the pitch of the vortex along the hot tube. He also, with

Curley (72,25), completed a comprehensive list of works and papers on the subject.

Dornbrand (28) meanwhile, wrote a report of the work done at the Republic Aviation Corporation under U. S. Government contract. The report included experimental data on the effects of such parameters as inlet temperature and the pressure ratio across the vortex inlet and the cold outlet. Internal investigations included pressure, velocity and temperature traverses and visual flow pattern on the internal walls. A theory was developed for the case of a two-dimensional laminar compressible vortex formed between two rotating cylinders. Attempts were also made to improve the tube's performance by adding an internal guide vane.

In England, one of the first attempts to use the vortex device was given in a report by De Havilland Aircraft (27). The report listed the applicability of the vortex tube for the cooling of a Vampire cockpit with air, under pressure, to be supplied from the jet engine to the vortex tube. A tube was developed, but it was not considered adequate in view of all the cooling requirements.

Although immediately after the publication of Hilsch's paper most of the vortex work was carried out in the United States, by 1951, however, the European contribution began to appear. In January 1951, Elser and Hoch (31) described experiments in which various gases and gas mixtures were used as the working fluid. Samples of gases leaving the hot and cold outlets were analyzed, and it was found that separation differences of about one percent could occur between the hot and cold mixtures. Elser and Hoch also tried to ascertain if a centrifugal field was necessary for the Ranque effect. They reported

a similar but smaller effect to be observed in the temperature distribution across four parallel air jets when placed in echelon.

In March 1951, Williamson and Tompkins (135) stated in a Technical note that an inlet chamber with multi-inlet nozzles and with a diameter larger than that of the hot tube would give improved performance. Their experimental results, however, were difficult to compare with those of other investigators because the usual hot valve had been replaced by a fixed orifice which had the same diameter as that of the cold outlet.

Sprenger (114), in July 1951, gave an account of several qualitative studies which were carried out at the E.T.H., Zurich. Hilsch and other investigators had commented on the loud noise which was produced in the vortex tube. To investigate this effect, Sprenger attached a tube, containing lycopodium powder, to the hot tube and detected an ultrasonic standing wave. Sprenger's tests included the verification of Hilsch's results, and the measurement of the temperature distribution along a simple vortex tube which had no hot flow and was without a cold diaphragm. Other features were the use of temperature indicating points, comparison of internal flow pattern when the working fluid was air or water, and the effect of rotating the hot tube while the inlet nozzle remained at rest. Sprenger observed that previous explanations of the vortex device did not appear to be completely satisfactory, and in a later paper suggested that the cooling and heating phenomenon was due to an ultrasonic effect which was not solely restricted to circular flow. The heating and cooling effects experienced in a modified Hartmann type generator were cited as an example.

From around 1952-53, interest on the Hilsch tube has centered on its practical applications, especially as regards to high-speed aircraft. Vonnegut (127,128), of General Electric Co., developed a vortex tube which measured free air temperatures for aircraft speeds up to 250 mph. More elaborate developments by Ruskin, Scheter, Merrill, and Dinger (96,97), increased the speed to 500 mph.

In February 1952, Packer (80,81), of Cornell Aeronautical Laboratory, issued a progress report on work being carried out for the Navy Department (Project Vortex), the object of which was to develop a free air thermometer for use on aircraft over the range of Mach numbers 0.3 to 0.95. The report dwelt on an experimental design to investigate vortex tube flow and performance characteristics. A list of references was also included.

Further application of the vortex tube was discussed at a "Proceedings of the Conference on Cooling of Airborne Electronic Equipment," held at the Ohio State University (3). A vortex tube for cooling and pressurizing an airborne, 400 amps, 70 volt generator was described. The vortex device consisted of a bank of 20 tubes located between an air to air heat exchanger and the generator. Pressurized air was bled from the engine and precooled by ram air passing through the heat exchanger. This precooled air was then passed through the bank of vortex tubes to the generator. Preliminary experiments revealed that increased efficiency was obtained by cooling the outsides of the hot tubes, and this effect was therefore incorporated in the air to air heat exchanger.

The application of the vortex tube, this time, to cooling ventilated suits in aircraft, was discussed by Westley in 1953 (134) in a technical note. It was reported that under certain conditions, the

vortex device represented a very simple method for cooling ventilated suits. The vortex tube, however, was not as efficient as the more conventional and more complicated expansion turbine, inasmuch as the latter had a usually larger temperature drop.

Back to the theoretical side, a significant contribution to the literature on the vortex tube was that of Van Deemter (124) of the Royal Dutch Shell Laboratory, Amsterdam. His paper combined the concepts of Hilsch (20) and Prins (88) on the subject. Van Deemter adopted an approach similar to that of Fulton (39), in which the temperature distribution was determined by the ratio of the work flux to heat flux, but he pointed out that the heat flux in turbulent circular flow was not solely proportional to the temperature gradient, but included a term which was proportional to the radial acceleration. More recently, pressure and temperature measurements have been made inside the vortex tube with the aid of miniaturized versions of NACA probes, and this, in conjunction with the trend of using larger vortex tubes, seems to represent the thinking of the day. As of the writing of this work, two research papers along these lines have been delivered (30,129) and will be available in journal form in the near future. In common with these efforts, the present work aims to synthesize and extend the knowledge of vorticity in general.

PART II

EXPERIMENTAL STUDY

CHAPTER 2

TEST PROGRAM

2.1 Basic Design

The main consideration in the test program is the design of a vortex tube of sufficient size and flexibility as to allow velocity, temperature and pressure traverses to be taken without causing major disturbances in the flow field. There are inherent limitations to the experimental study of vortex flow, and until recently they have kept the systematic investigation of the vortex tube from progressing very far. Both Ranque's and Hilsch's original models were of very small diameters (4 mm to 18 mm tubes with 2 mm to 7 mm orifices) wherein fairly impressive effects were obtainable with relatively low or moderate supply pressures. Such small size models, however, are not suitable to any basic study of the vortex phenomenon, since they do not lend themselves to any velocity, pressure, or temperature traverses. To perform these operations, considerably larger size models have to be designed, and this in turn requires very high pressures and very high flow rates of supply air. In addition to all this, great care must be given to the fact that whatever probes are to be inserted in the tube, the flow pattern must not be disturbed.

With these considerations in mind, it was decided to design a 2 inch diameter vortex tube (Figs. 2-1, -2, -3, -4, -5, -6, -7) made of lucite. This is considerably larger than the majority of previously reported designs, and just about taxes the limit of most available sources of compressed air. The choice of lucite, of course, is to permit flow visualization studies in addition to the systematic probe traverses.

2.2 Apparatus

The installation evolved is flexible for many kinds of traverses at different stations along the length of the vortex tube; nevertheless, it has been kept simple and devoid of unnecessary apparatus. Compressed air at room temperature is fed tangentially into a nozzle block (Figs. 2-1, -2, -3) from which it spirals downward along a tube (Figs. 2-1, -4) of any desired length. Stagnation temperature, stagnation pressure, static pressure, and velocity traverses are taken at various stations down the length of the vortex tube (Fig. 2-7). The exit end of the tube is fitted with a cone-shaped valve (Figs. 2-1, -5, -6) which is movable in and out.

The flow circuit is the following. Referring to Figs. (2-8)and (2-9), compressed air from the University Power House is supplied by means of Valve #1 to a New Jersey constant head, variable area flow meter of the multiple orifice, cylinder and piston type. It then passes through a DeVilbiss (type HB) Regulator and drier, from whence it is fed by a simple flexible hose to the nozzle block of the vortex tube. Pressure Gage #1 and Thermocouple #1 are installed between the Jersey flow meter and the DeVilbiss drier, and a mercury U-tube is installed at the outlet of the drier so as to record the pressure of the air at entrance to the vortex tube. Later on, when it came to running the installation at those relatively high pressures and high rates of flow which exceeded the capacity of the DeVilbiss drier, a by-pass circuit (Valve #3) was used, and Pressure Gage #3 was used to record the entry pressure to the vortex tube, since continued use of a U-tube would have necessitated a mercury tube of ceiling height. It was felt that the use of a low-pressure range diaphragm gage more then gained in convenience what it might have lost in accuracy had a U-tube been maintained.

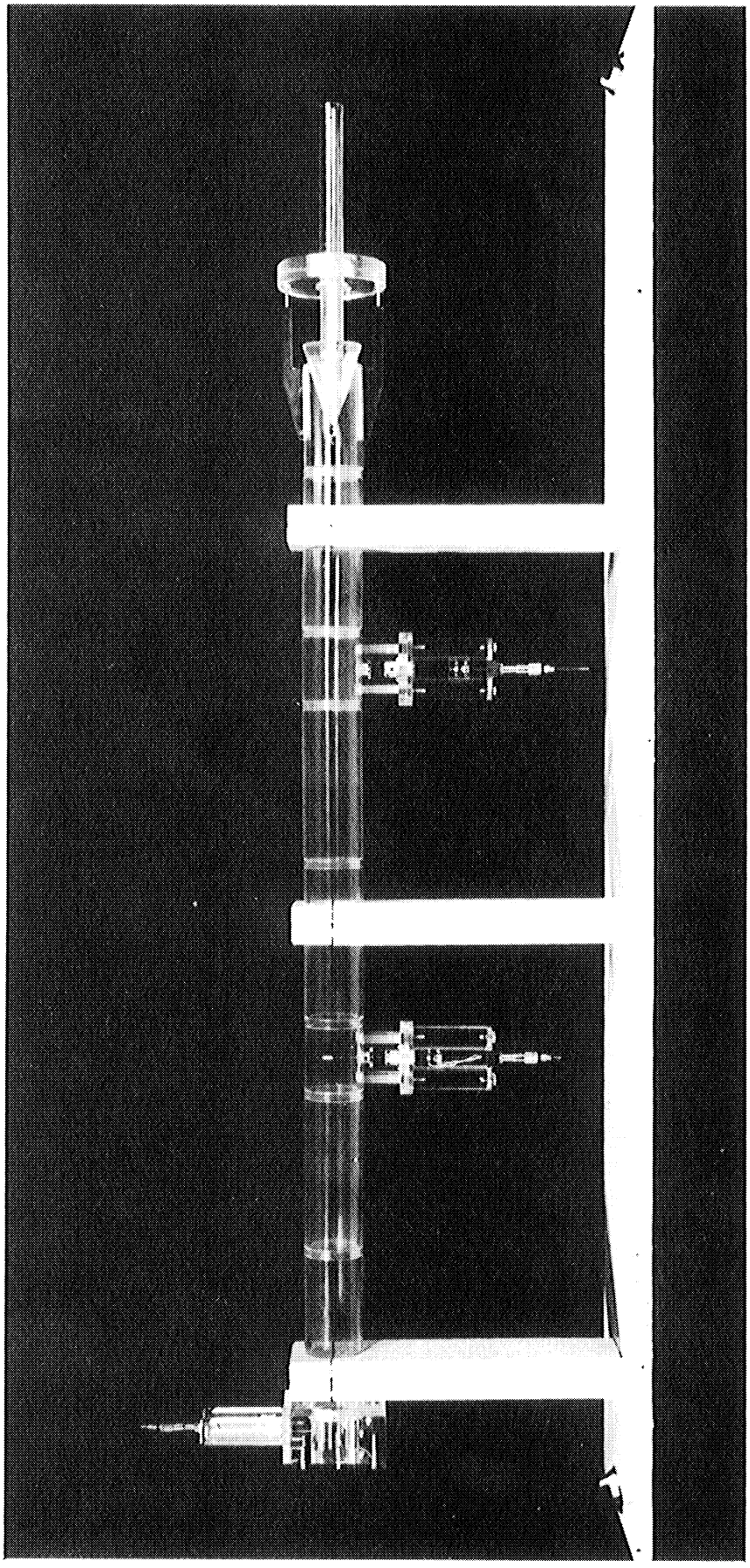

Figure 2-1. Vortex Tube Design

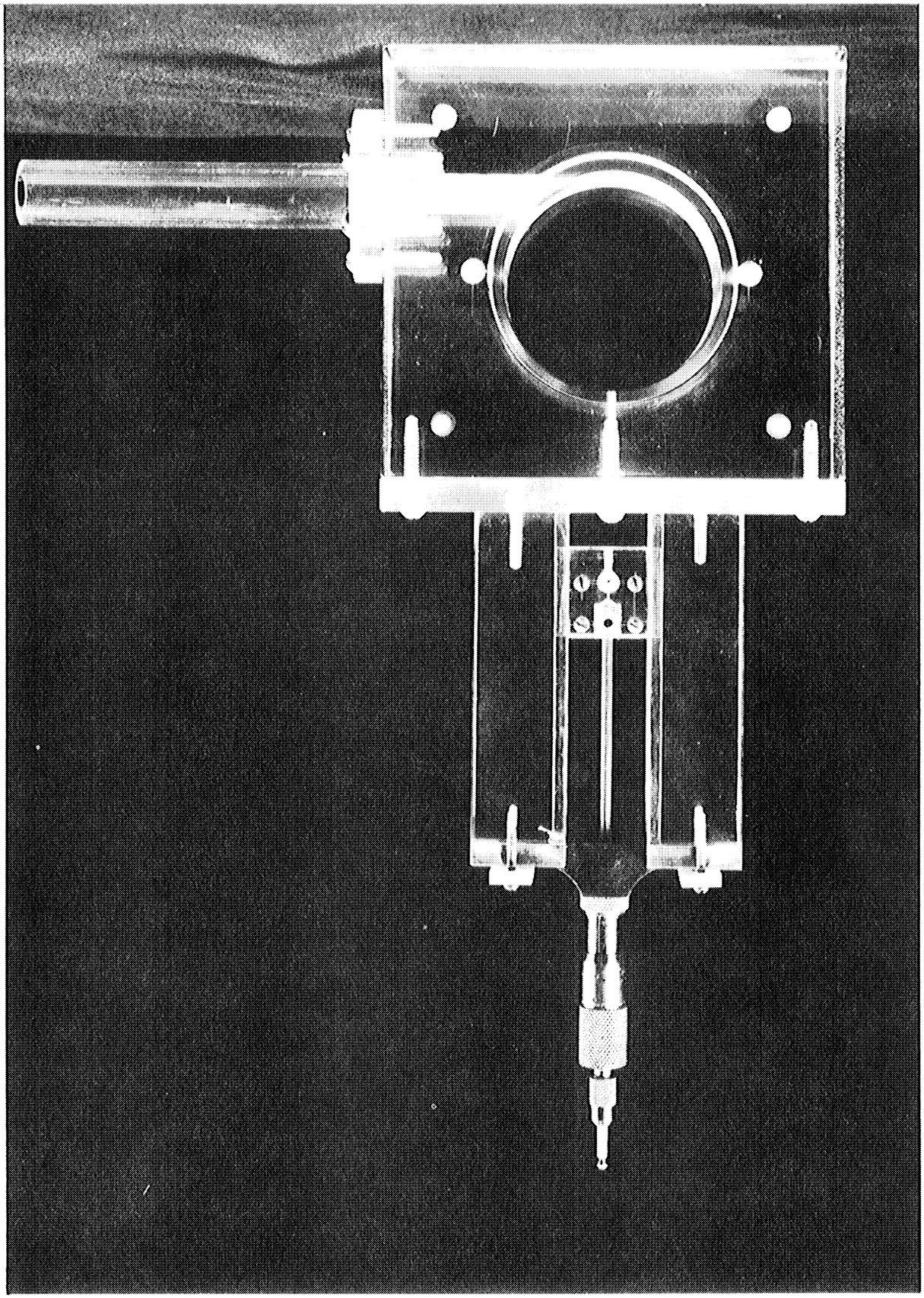

Figure 2-2. Center Block and Probe

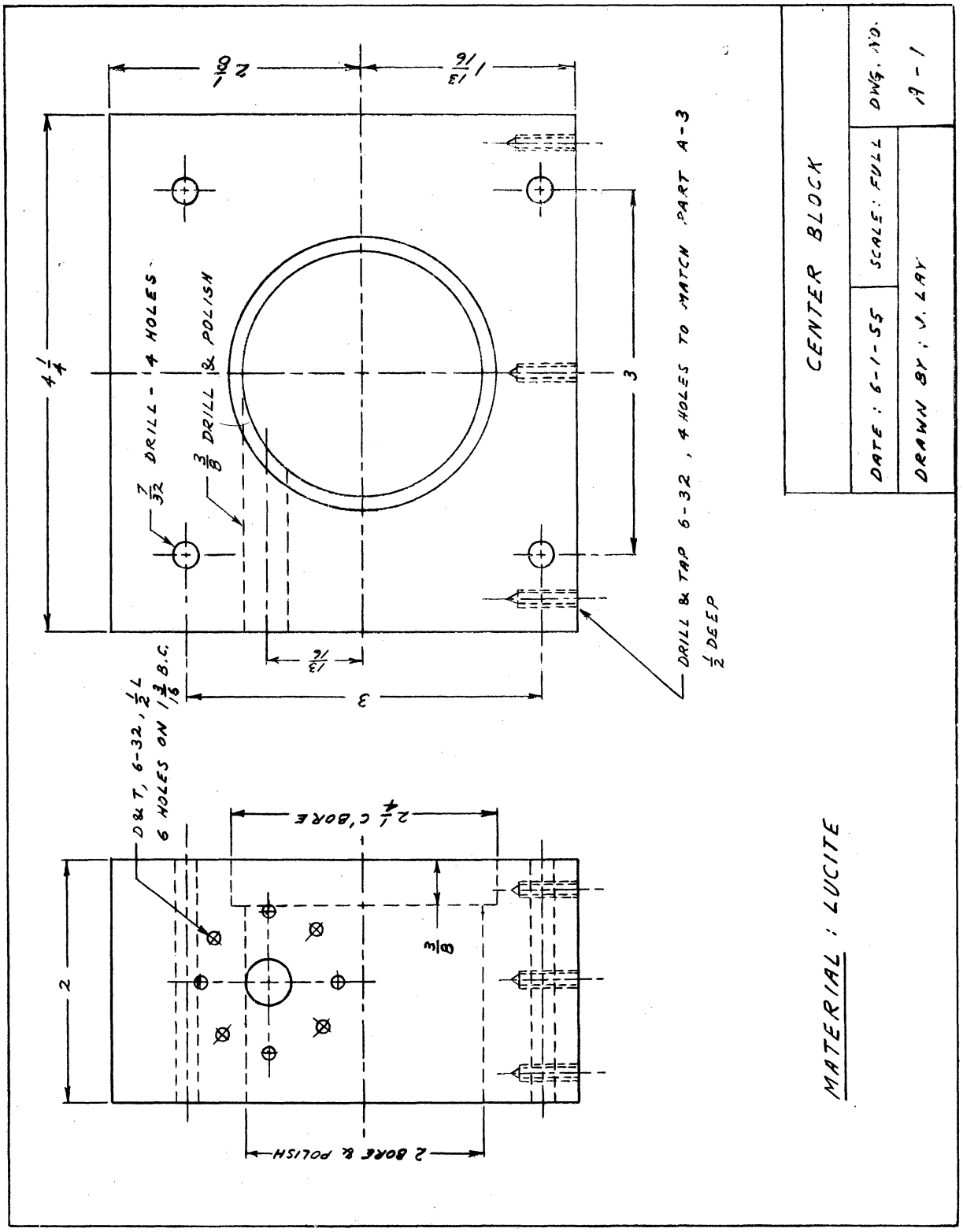

Figure 2-3. Detail of Center Block

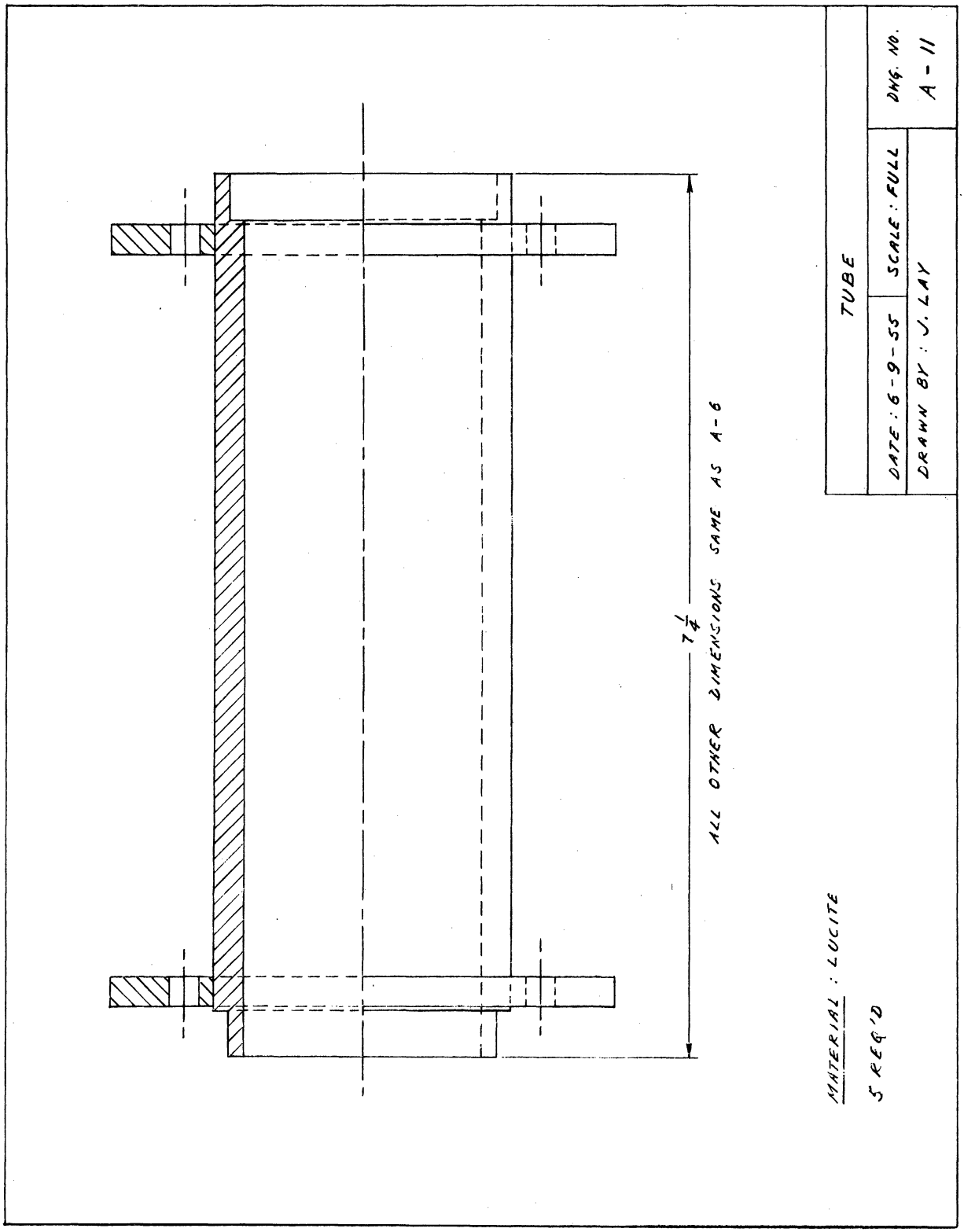

Figure 2-4. Tube Section

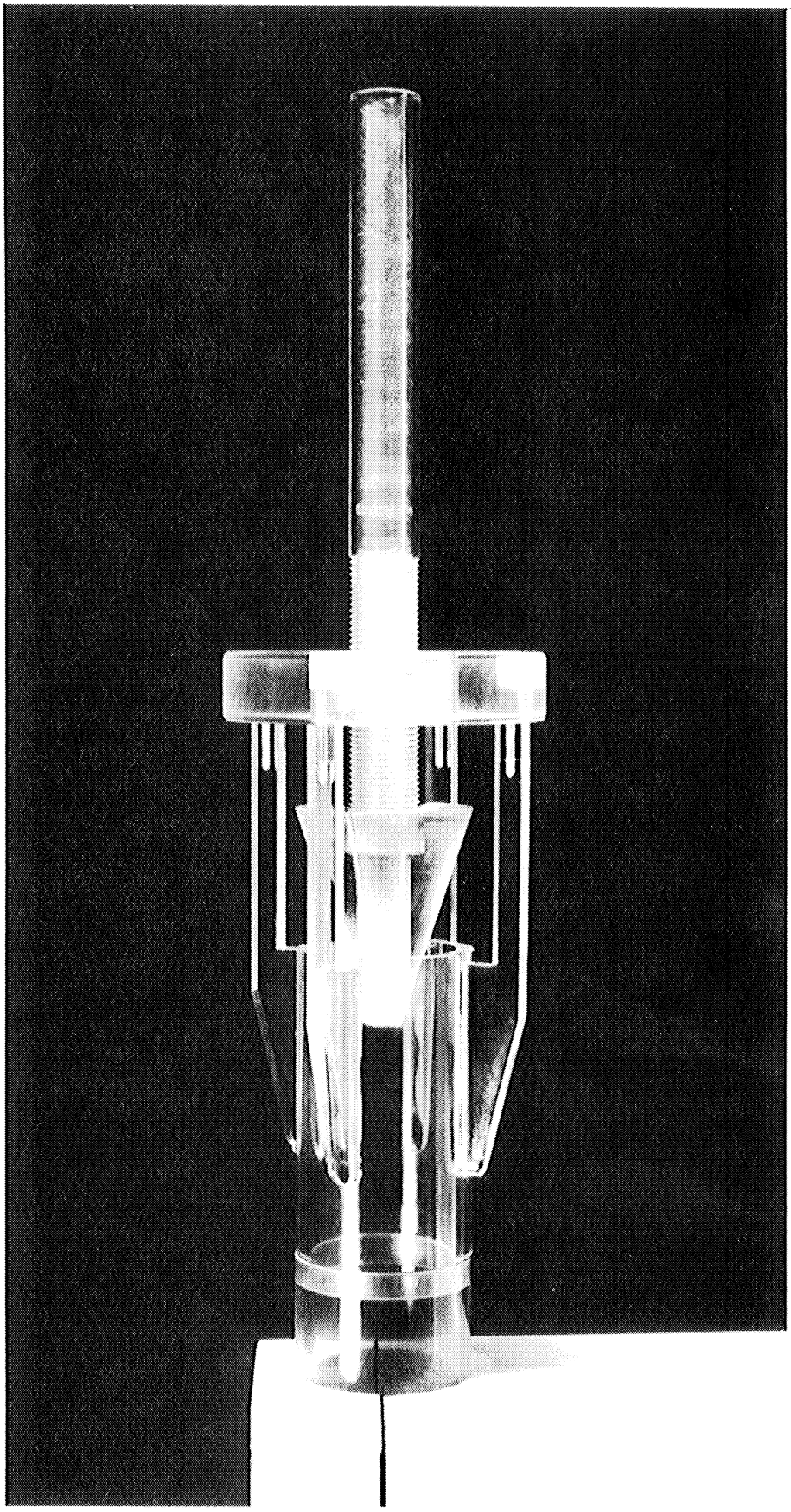

Figure 2-5. Tail Assembly

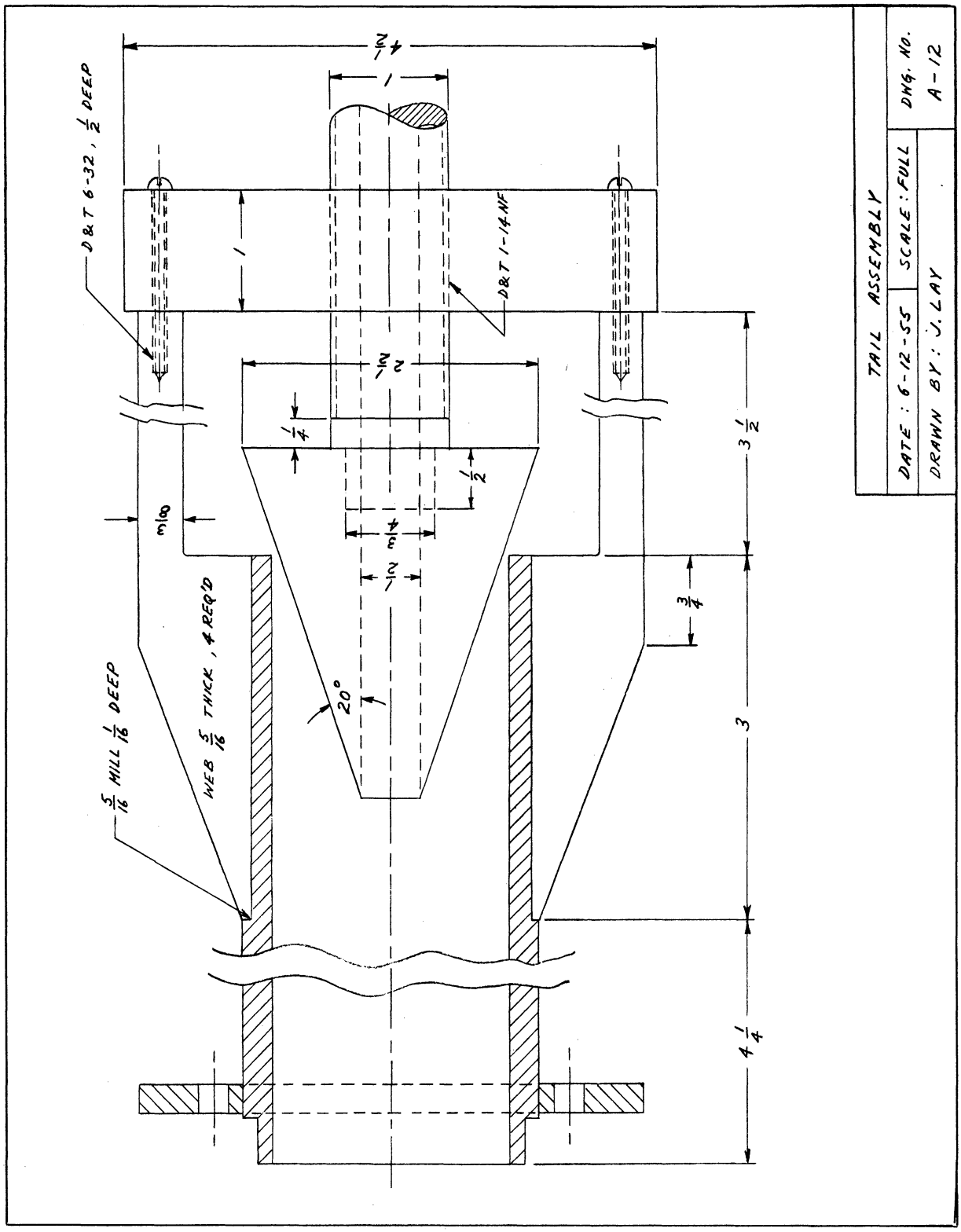

Figure 2-6. Detail of Tail Assembly

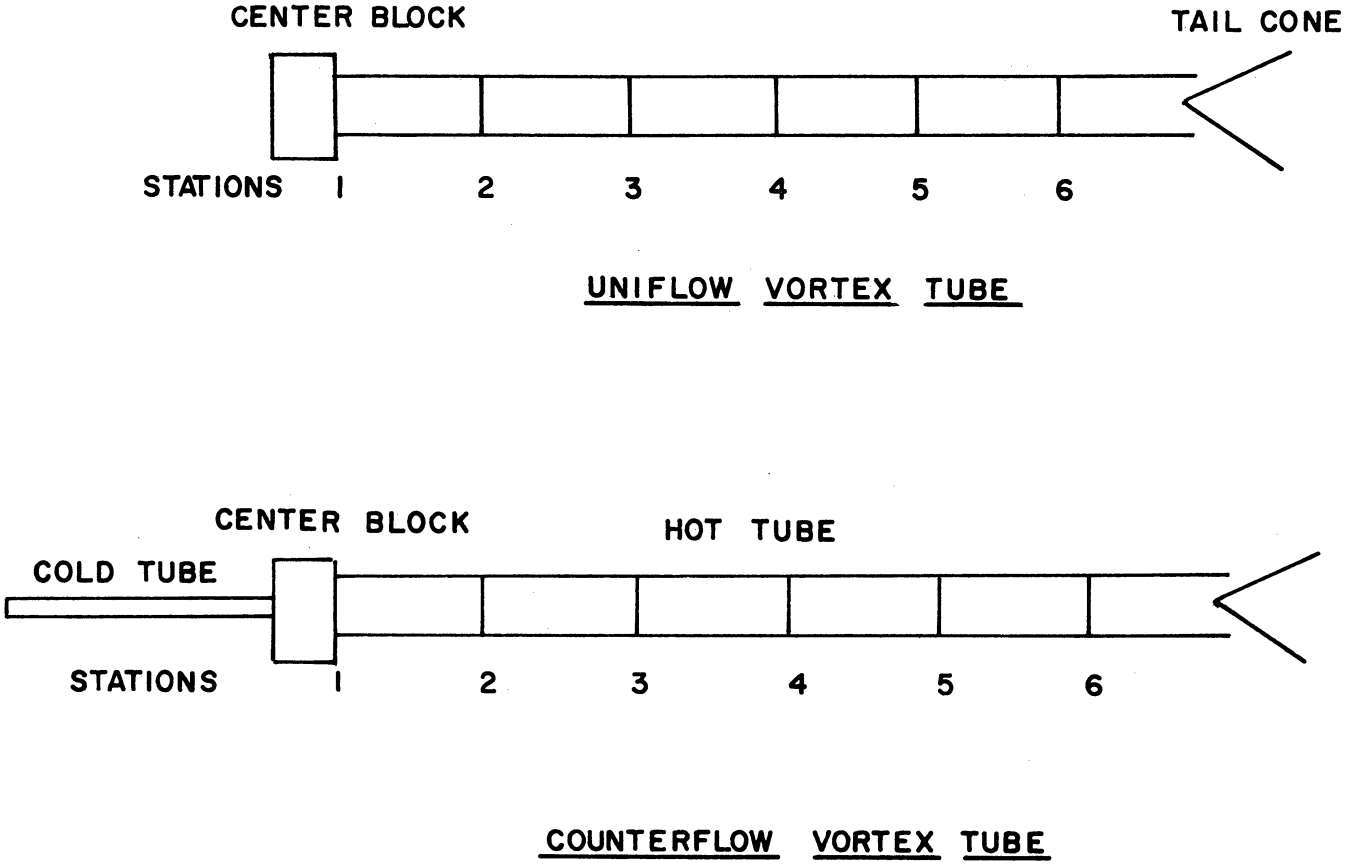

Figure 2-7. Location of Traverse Stations

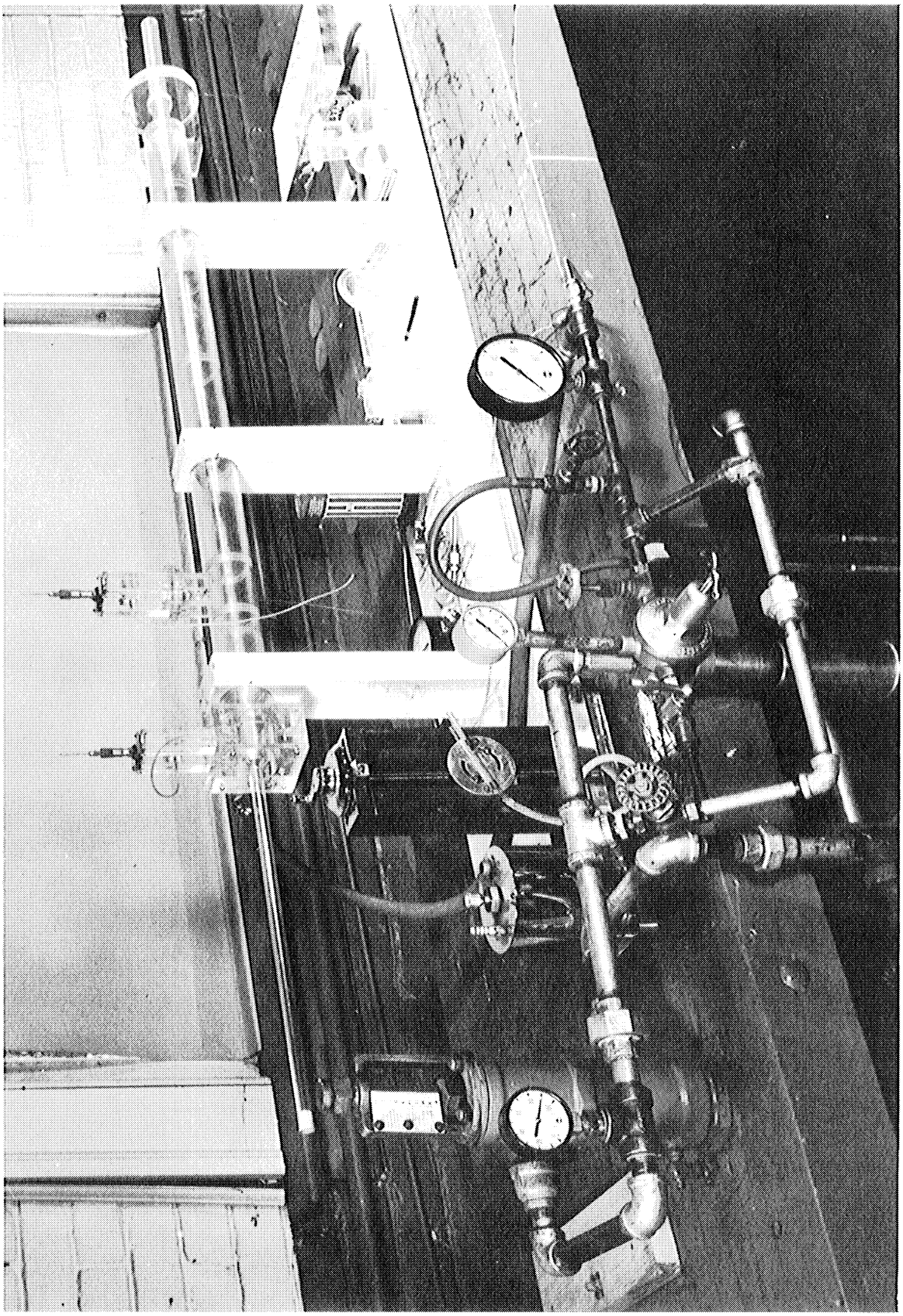

Figure 2-8. Test Installation

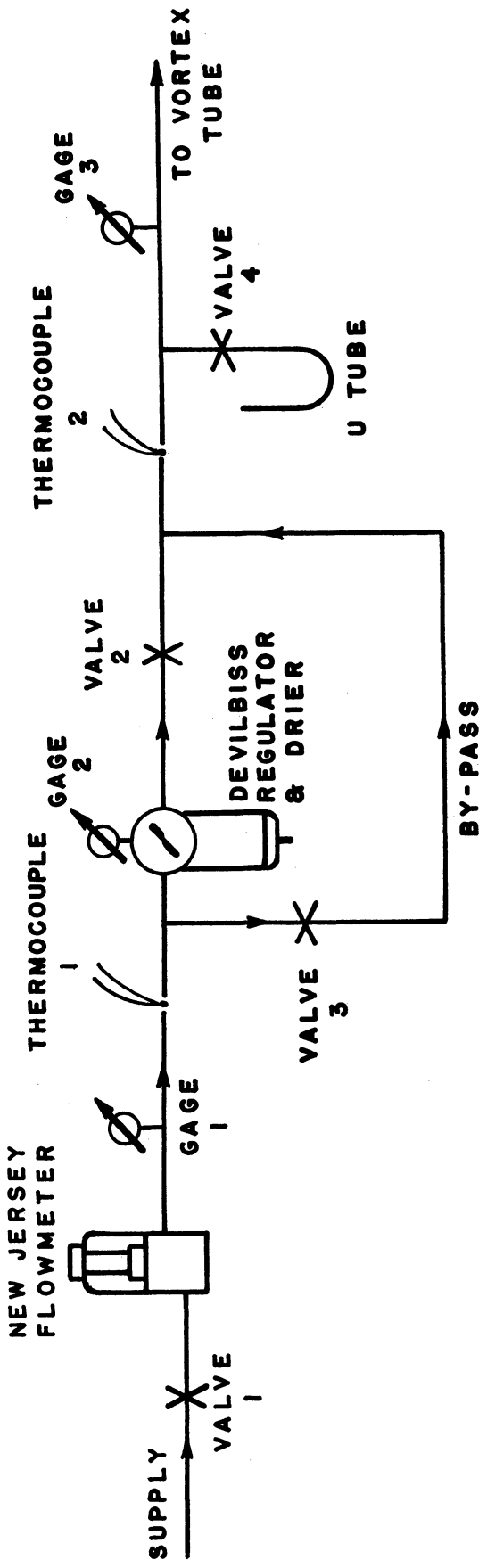

Figure 2-9. Flow Circuit

No further instrumentation than the above is needed for the study of the uniflow type of vortex tube. For the counter-flow type of vortex tube, a specially constructed miniature Pitot tube (Fig. 2-17) is used to traverse the cold tube, and thus measure its outflow; the outflow of the hot tube being obtained by difference between the supply flow and the cold tube flow, since it is ineffectual to directly measure the flow through a conical area.

2.3 Instrumentation

For the experiments described in this report, special velocity, pressure, and temperature probes were designed. The key feature is a "probe assembly" (Figs. 2-10, -11) which can be inserted at any station along the length of the vortex tube, and constructed in such a way that a hypodermic needle probe may be raised, lowered, or even completely revolved within the flow field. Referring to Fig. (2-11), a hypodermic needle probe is raised or lowered by means of a Brown and Sharpe 605 Depth gage and a slider and bearing assembly (Figs. 2-12, -13) which is mounted on a stand (Fig. 2-14). This stand is itself lightly clamped by means of adjusting screws to another stand (Fig. 2-15), with the latter being glued in place to the probe tube (Fig. 2-4). Thus, the hypodermic needle is free to move to any radial position within the vortex tube, and it may also be revolved so as to be sensible to direction as well as to magnitude of velocities. (Fig. 2-10, -11) show a probe assembly designed for insertion along stations 1, 2, 3, etc., Fig. (2-7), whereas Fig. (2-2) shows a probe assembly for insertion at the nozzle block itself.

The velocity, pressure, and temperature probes are shown in Figs. (2-15, -16). Velocity measurements are made by means of a hot wire anemometer, the theory, electric circuit, and control panel of which is described in the Appendix section of this report. The hot

wire anemometer itself is a special miniature version of the more bulky types made by the University Aerodynamic Laboratory or by commercial houses. Referring to (Fig. 2-15), it consists of inserting two insulated copper leads through a small (#18 gage) stainless steel hypodermic tubing, and soldering two sewing needles to these leads. The needles are held apart and in rigid position by binding them with fine thread and then carefully coating the whole with shallow layers of electrical insulation which are allowed ample time to dry and harden. Next, the hardened base is reduced to proper size by means of a grinding wheel, and finally it is given several coverings of aircraft "dope" alternated with sanding operations to smooth the surface. Across the sewing needles is soldered a very fine Wollaston or Tungsten wire ranging in size from .00015 in. diameter to .00035 in. diameter. Depending on occasions, different wires and different sizes are used. Also, for extreme sensitivity to velocity changes, the center portion of the wire is etched to a still finer diameter by means of a nitric acid solution and an electric circuit.

The pressure probes (Fig. 2-16) consist of a static pressure probe, which is simply a stainless steel hypodermic tubing (#18 gage) well polished and left open at the end, and of a stagnation pressure probe. The static probe is always inserted in such a way that it is perpendicular to the direction of flow. The stagnation pressure probe is more elaborate, but essentially, it consists of a stainless steel hypodermic tube of similar size as the one for static pressure measurement, except that the open end is soldered closed, square cut, and polished. Near the tip of this hypodermic needle, there is drilled a

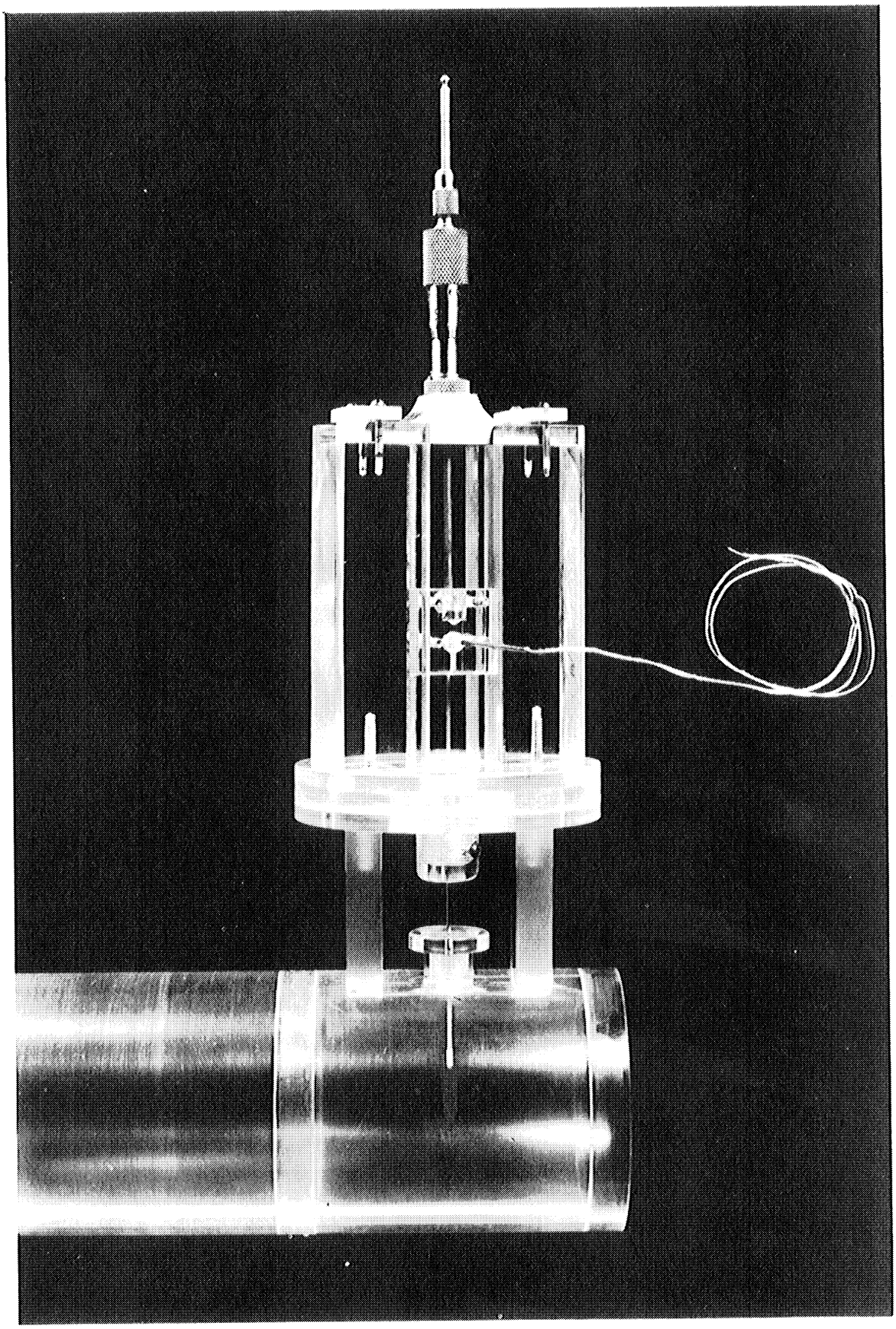

Figure 2-10. Probe Assembly

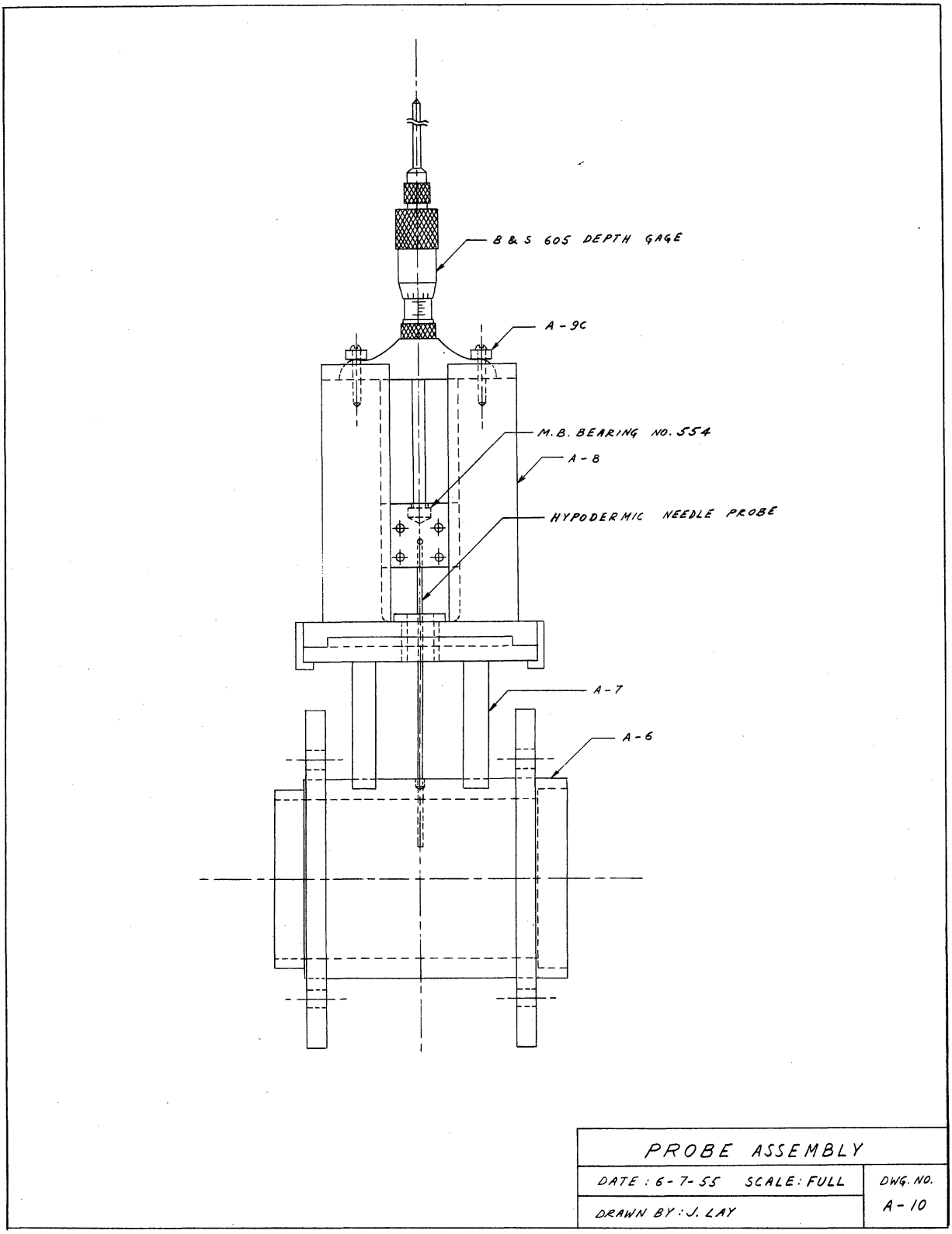

Figure 2-11. Detail of Probe Assembly

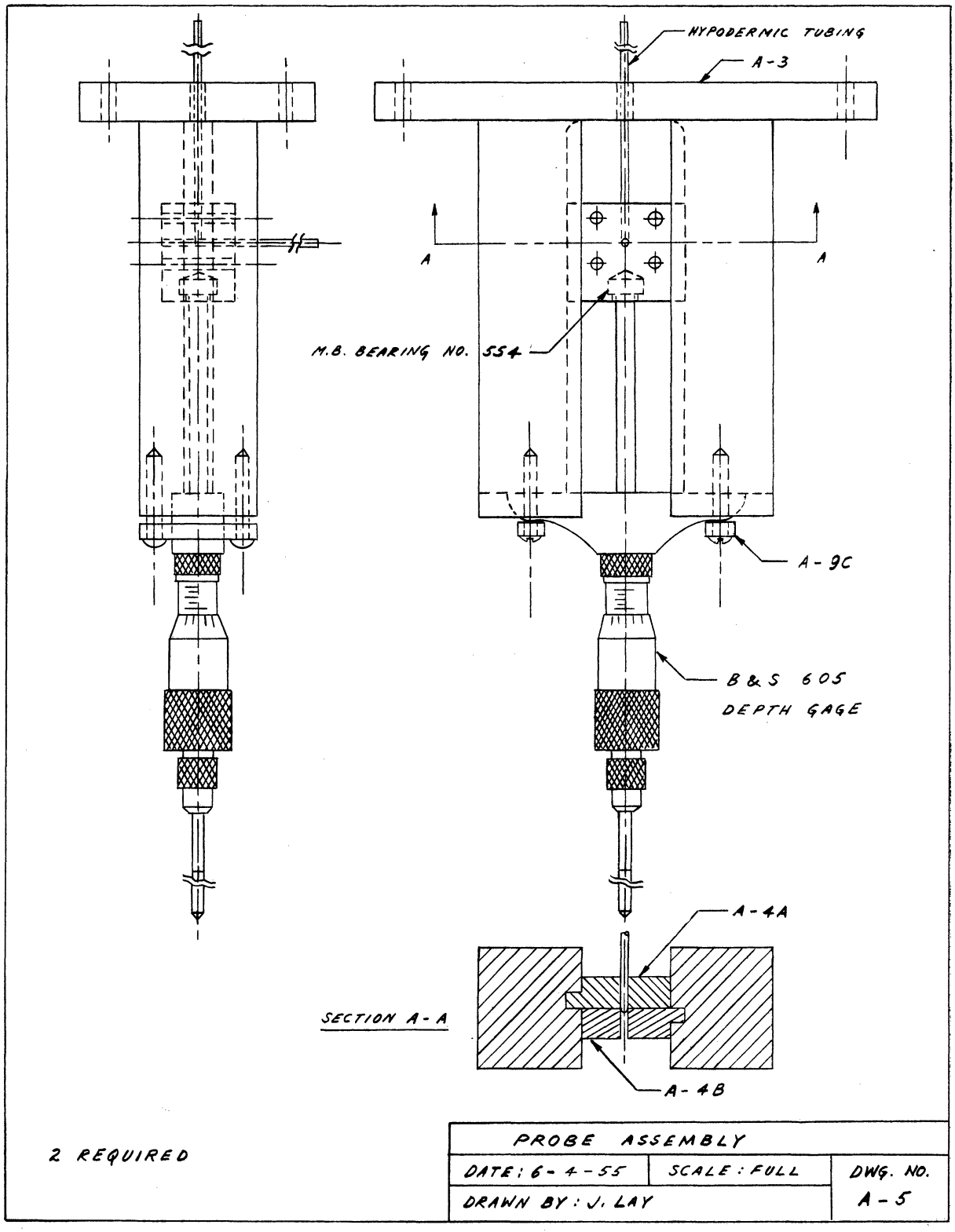

Figure 2-12. Slider and Depth Gage Assembly

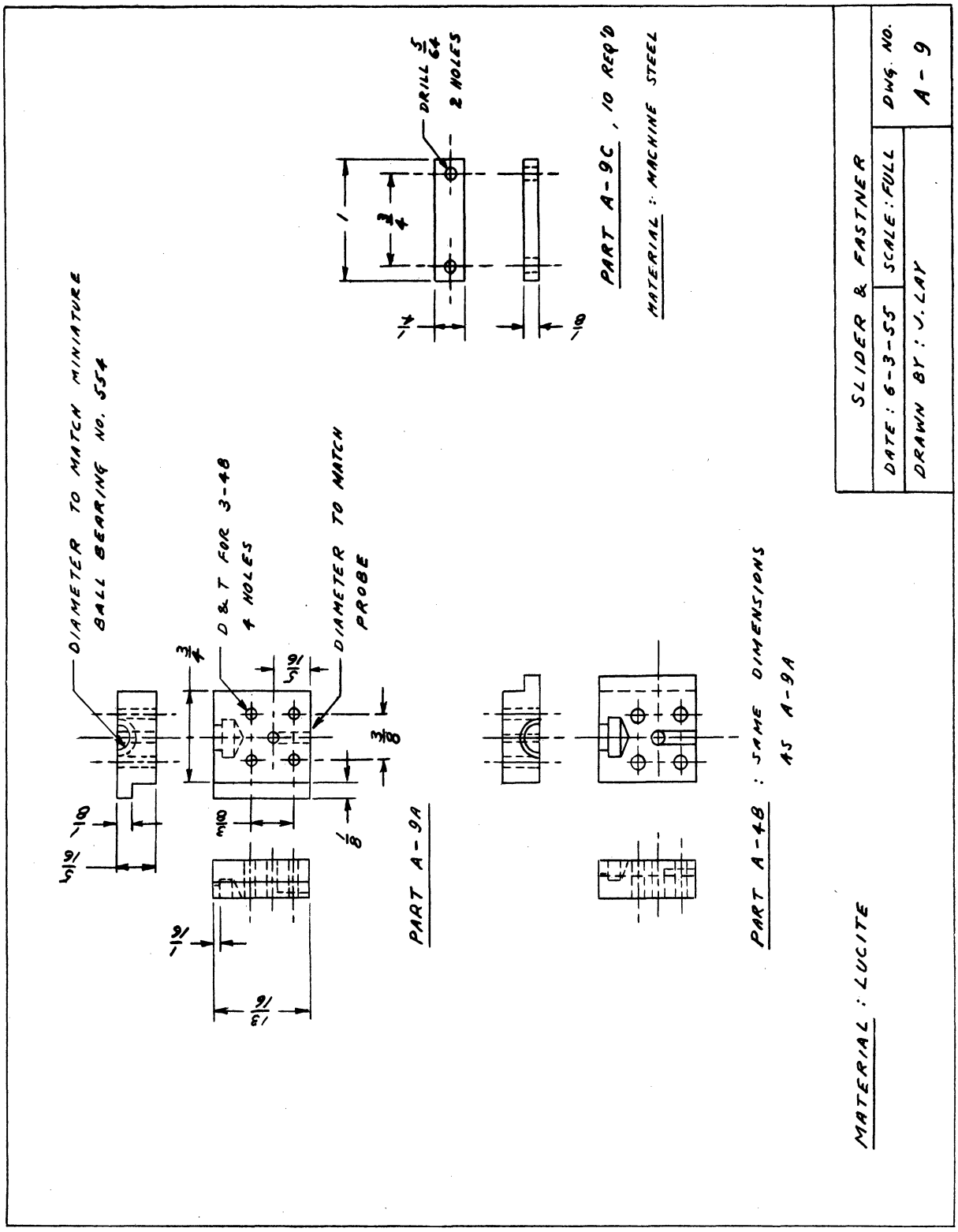

Figure 2-13. Detail of Slider

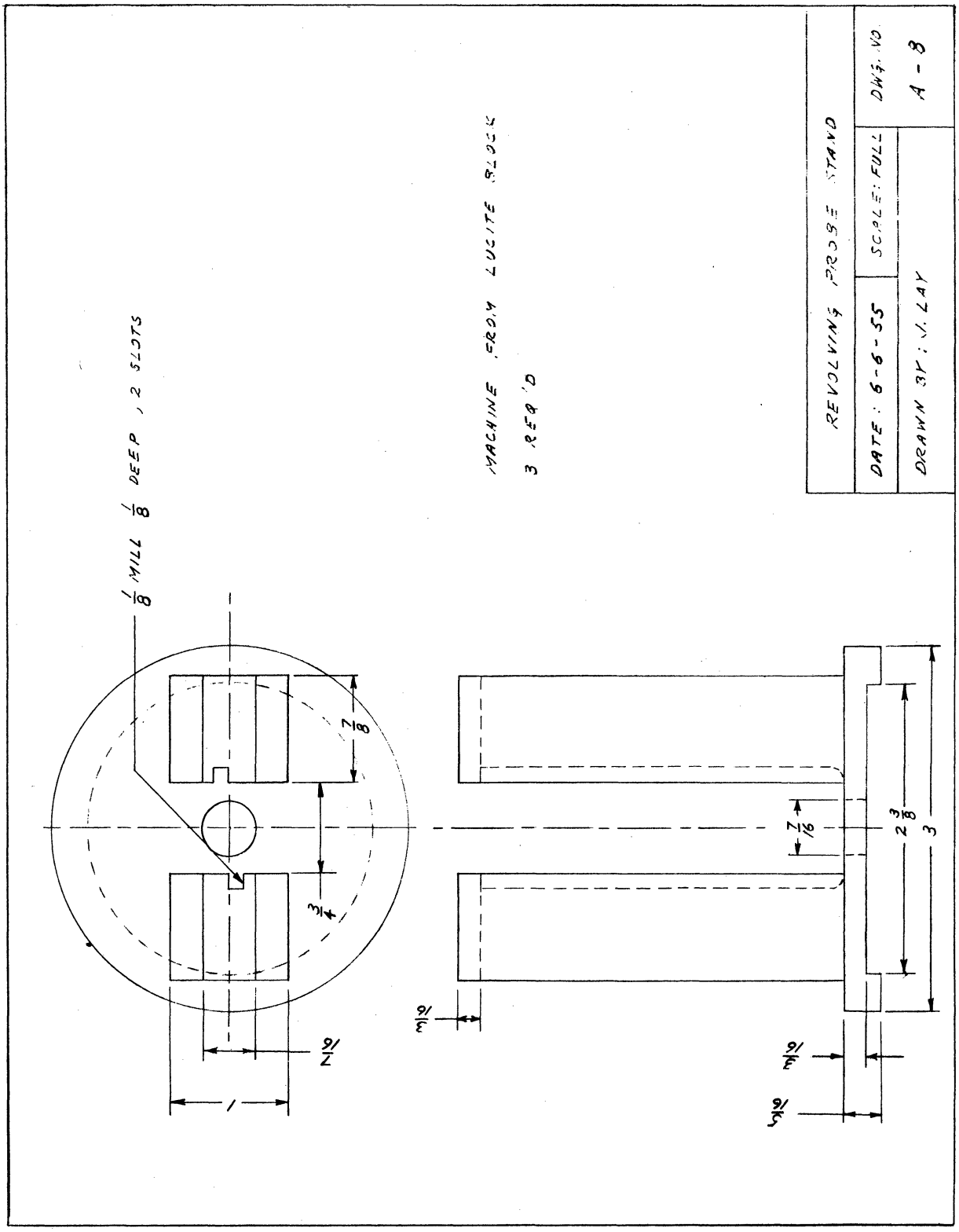

Figure 2-14a. Probe Upper Stand

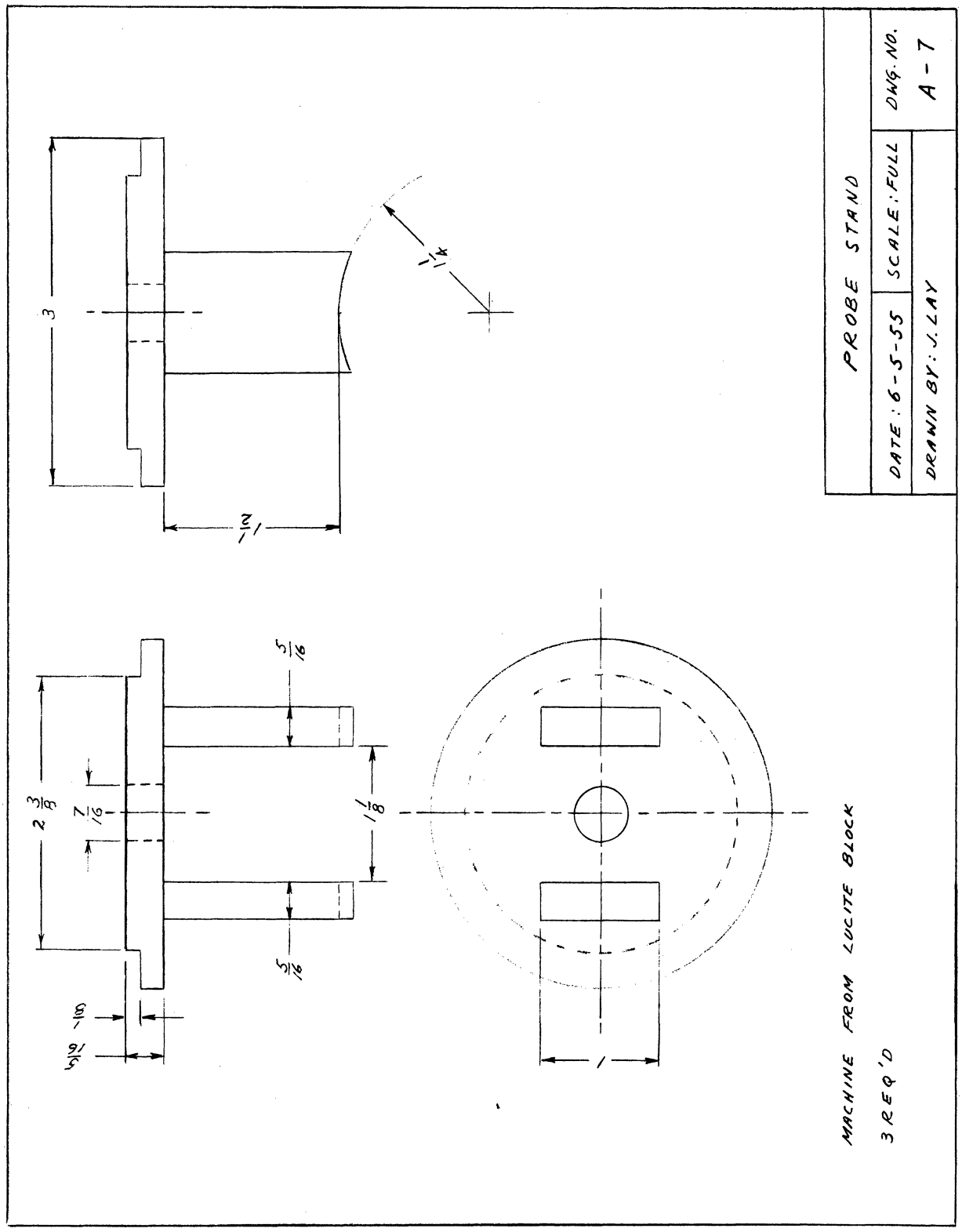

Figure 2-14b. Probe Lower Stand

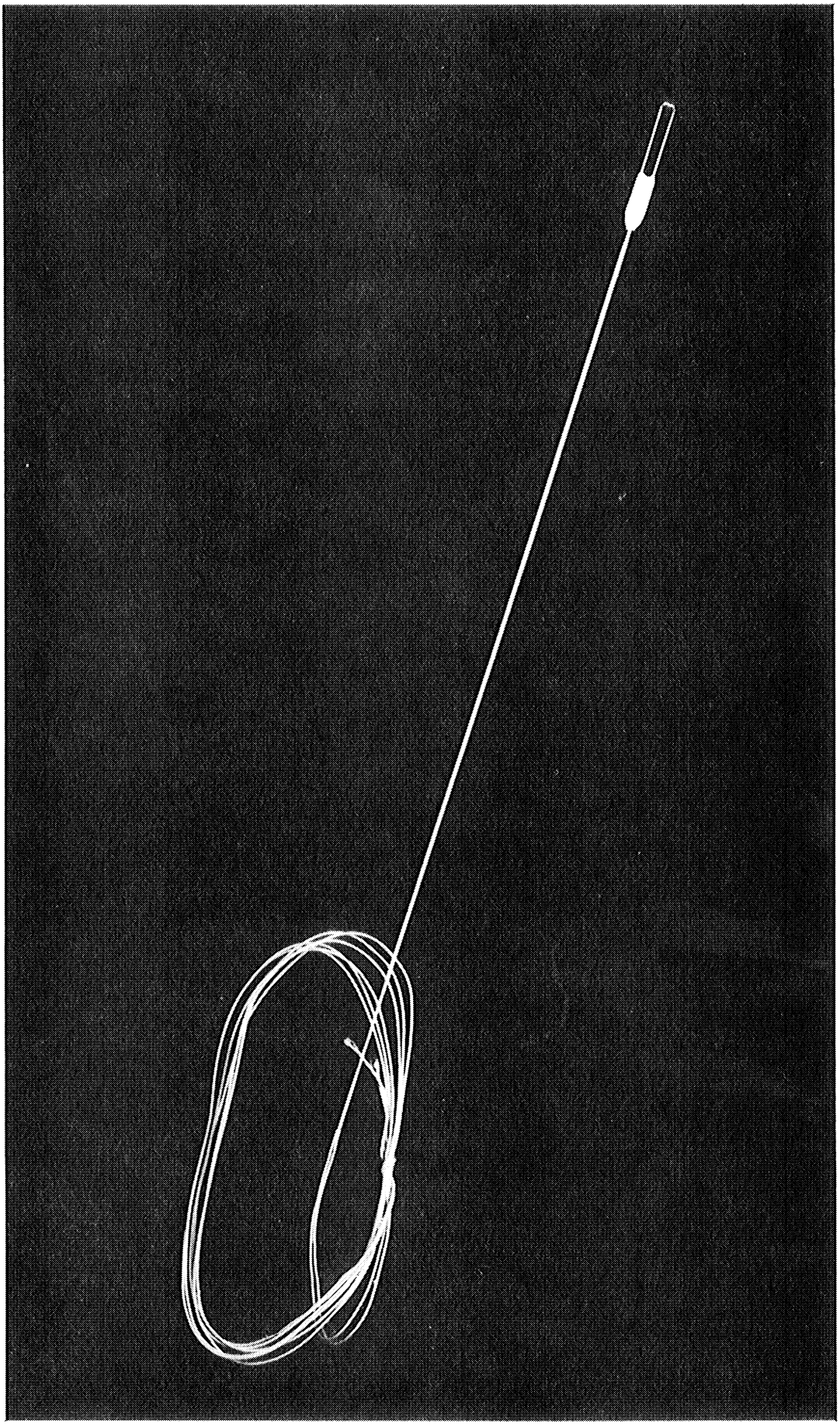

Figure 2-15. Hot-Wire Velocity Probe

small hole perpendicularly to the axis of the tube. This opening, being always in the direct line of flow (since the axis of the tube is perpendicular to the line of flow), serves as an impact tube for the measurement of total pressure. By difference, the velocity head is obtained from the total and static pressure readings and thus serves as a check on the velocity readings as obtained by means of the hot-wire anemometer probe. Where space permitted it, such as at the "cold" exit of the counterflow vortex tube, a miniature Pitot tube (Fig. 2-17) is also used to measure velocity. The smallness of its size may be seen when compared to a cigarette and a packet of matches photographed next to it.

As for the stagnation temperature probe, it consists of a stainless steel hypodermic tubing of similar size (#18 gage) as those used for velocity and pressure probes, this time with two dissimilar but insulated leads (iron and constantan, or copper and constantan) inserted through it. The ends of the leads are bared and fused together by acetylene torch or carbon arc, then pulled back close to the end of the tube to make the assembly compact. Since all probes had to be kept as minute as possible so as not to disturb the flow field, no further elaboration (such as shielding for radiation, etc.) was included in the manufacture of the probes. All the probes used were calibrated and typical calibration curves are included in the Appendix.

2.4 Test Configurations

The primary objective of the experimental program was to obtain basic knowledge of the velocity, pressure and temperature distributions in the vortex field of flow. The emphasis of study was

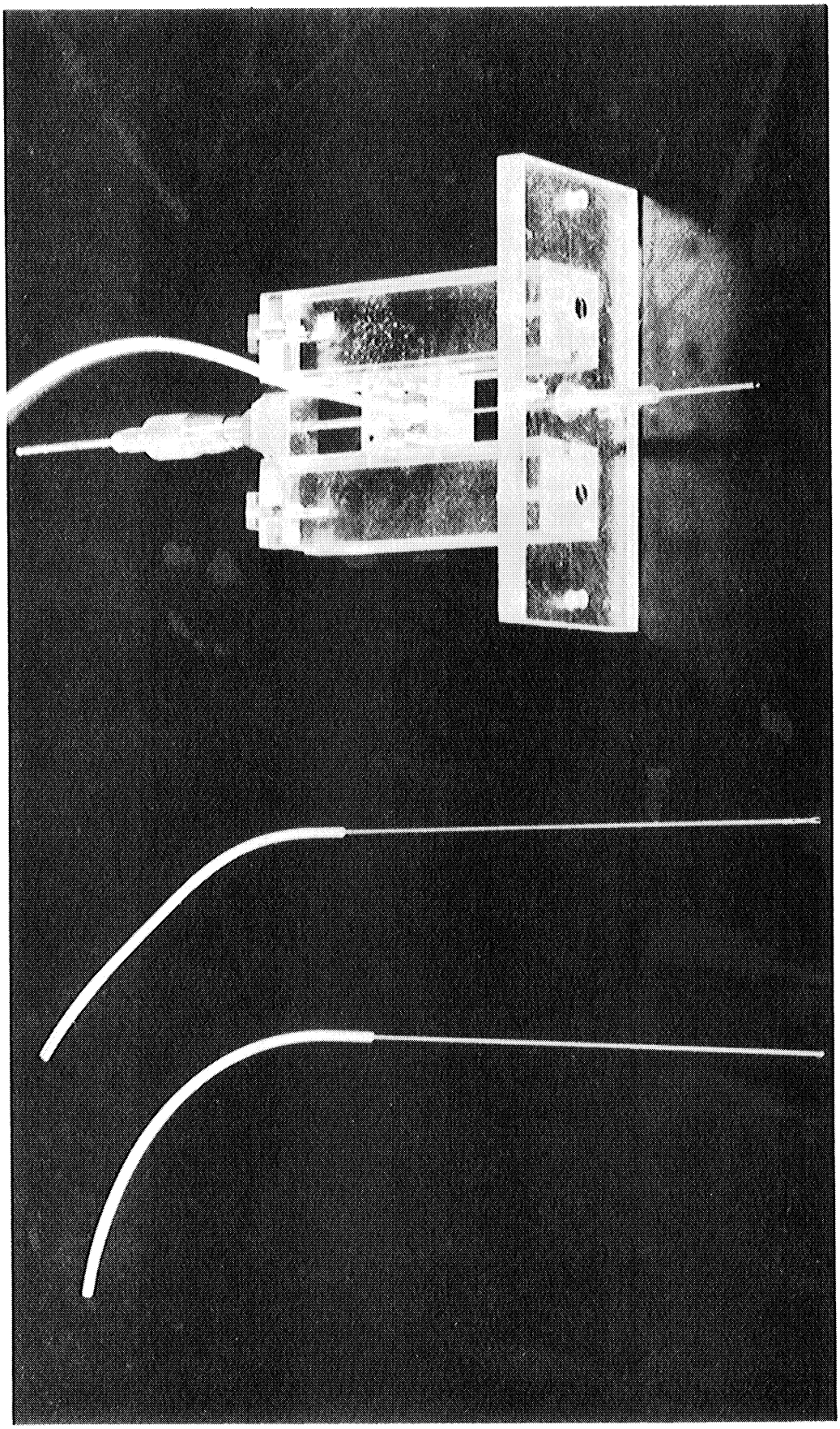

Figure 2-16. Pressure and Temperature Probes

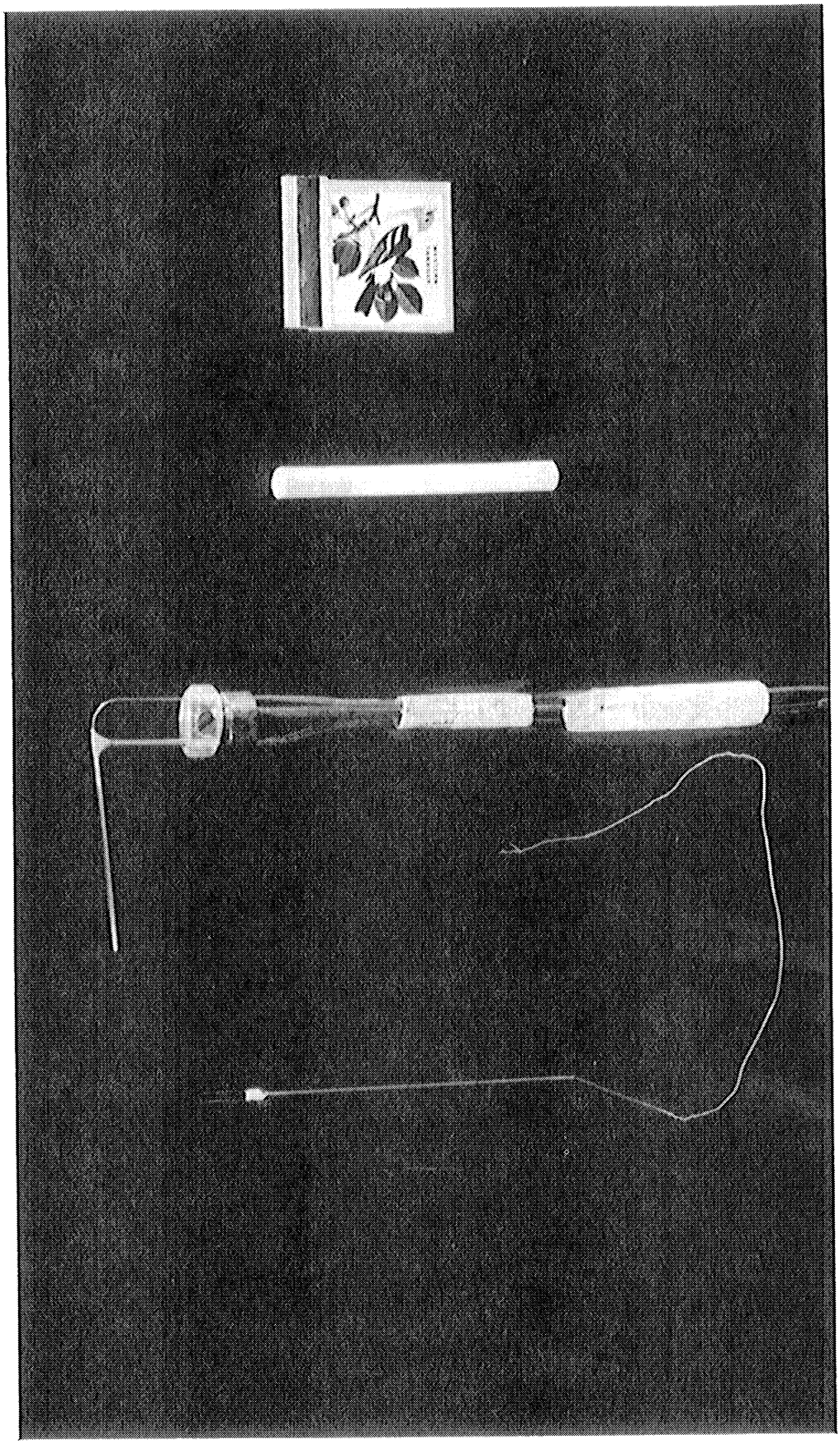

Figure 2-17. Size of Hot-Wire and Pitot Tube Probe as Compared to Cigarette and Matches

directed to a vortex which is generated at the nozzle cross section, and which proceeds in one direction down the tube to be discharged through the exit at the far end of the tube. This is the so-called "uniflow" flow type of vortex tube which heretofore has not been extensively reported upon in the literature. A secondary, though interesting part of the study, was devoted to the "counterflow" vortex tube, which is commonly known as the Ranque-Hilsch tube.

To adequately cover most of the geometry of flow, the test cases were subdivided into various flow configurations based on the selected length of tube. These were denoted as "Uniflow Configuration A", "Uniflow Configuration B," . . . . and "Counterflow Configuration A," "Counterflow Configuration B ", etc. These configurations are shown in Figs.(2-18, -19). Within each geometrical configuration, quantitative measurements were obtained for inlet pressures of 10, 15, 20, etc. psig, maintained by the pressure regulator valve. These quantitative measurements included flow rates, velocity, pressure, and temperature traverses taken at the various stations (1), (2), (3), etc. All of the runs were made at a given opening of the cone shaped discharge valve in the case of the "uniflow" vortex tube, and at the "optimum" opening in the case of the "counterflow" vortex tube; the optimum opening being that which corresponds to the largest temperature difference between hot and cold streams.

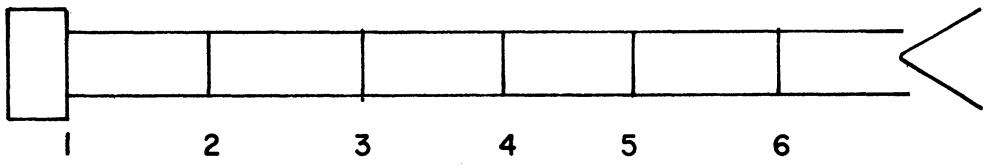

CONFIGURATION A

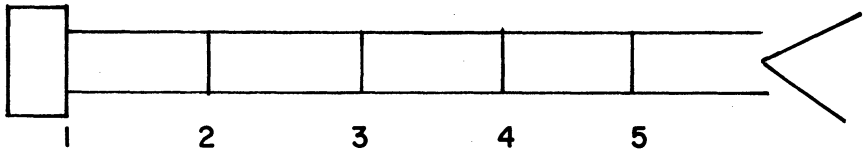

CONFIGURATION B

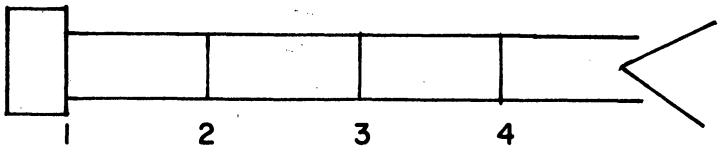

CONFIGURATION C

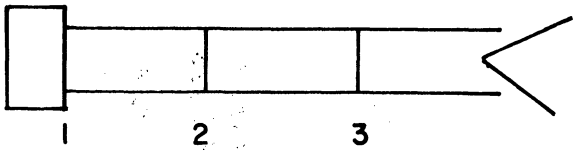

CONFIGURATION D

Figure 2-18. Uniflow Vortex Tube Configuration

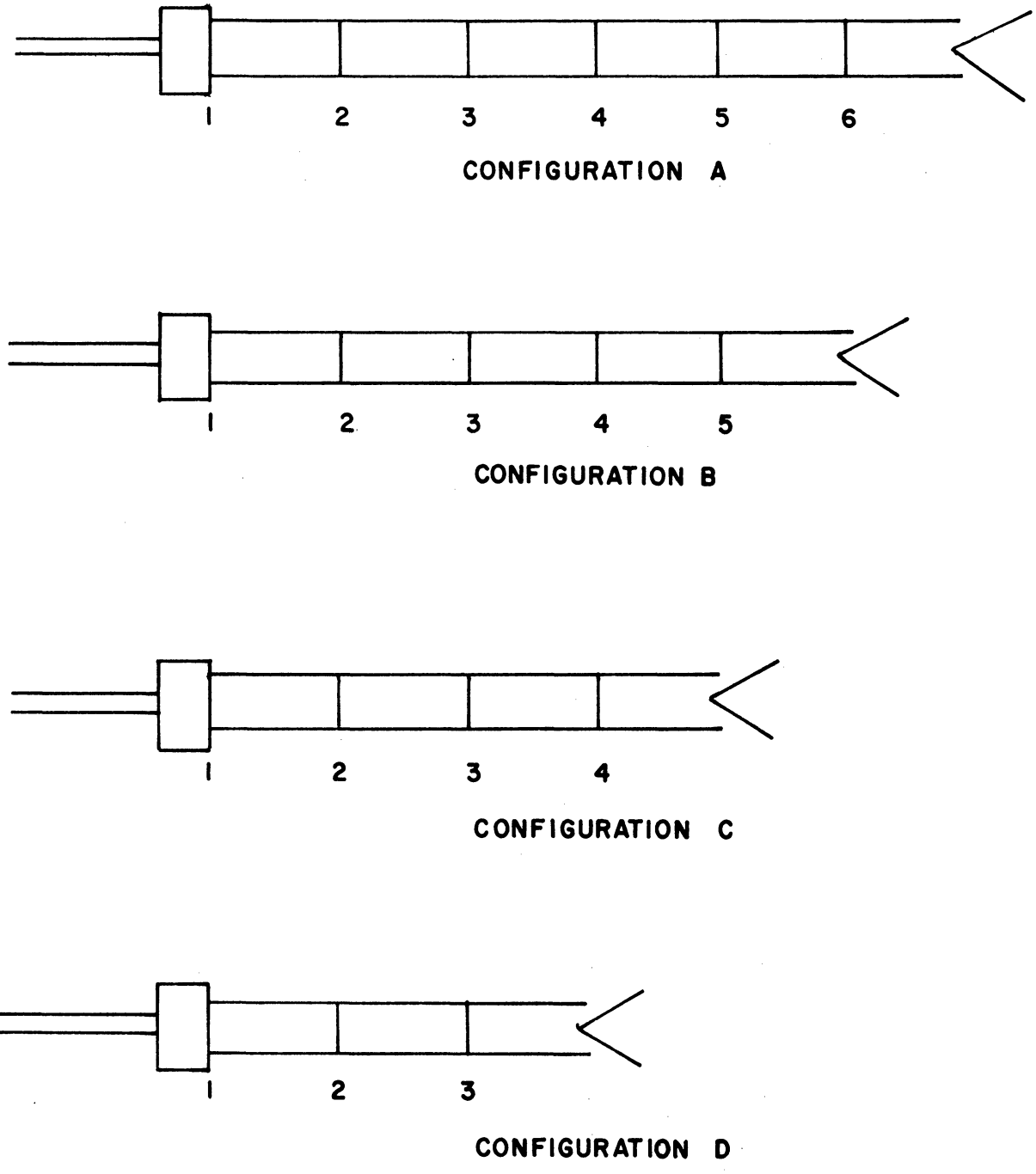

Figure 2-19. Counterflow Vortex Tube Configuration

CHAPTER 3

TEST RESULTS

This chapter is primarily concerned with the presentation of test data. Comments and explanations are included wherever necessary, but analysis and discussion are deferred to chapters 8, 10, 11, and 12.

3.1 Velocity, Pressure, Temperature Traverse

Quantitative measurements of velocity, pressure, and temperature were obtained by placing, respectively, a velocity-hypodermic-probe, a pressure-hypodermic-probe, and a temperature-hypodermic-probe at various distances from the axis of the vortex tube. Specifically, beginning with a probe placed near the wall, readings were taken for every tenth of an inch that the probe was moved toward the axis of the vortex tube. The radial movement was controlled by means of the micrometer depth gage and slider assembly described in Chapter 2. The traverse of velocities, pressures, and temperatures was performed at each station along the length of the vortex tube, with the inlet pressure maintained at a constant value throughout a given run.

The results are plotted in the form of velocity, stagnation or total temperature, static temperature, stagnation or total pressure, and static pressure curves in Figures (3-1) through (3-6, and (3-8) through (3-13). The measured quantities are stagnation temperatures, hot-wire velocities, and stagnation pressures. The computed quantities are static pressures and static temperatures.

Each run consisted of the following operational procedures. i) The valves of the flow circuit Figure (2-9) were cracked open and the inlet valve to the vortex tube adjusted for the desired pressure of the run. ii) The exit cone was turned all the way in, then backed out

fairly slow until the greatest Ranque-Hilsch effect is obtained, and left in that position for the remainder of the run. iii) After allowing time for steady-state conditions to be reached, the process of traversing the tube was undertaken. Beginning with the probe assembly Figure (2-10) placed in position at station 1, the hypodermic probes for velocity, pressure, and temperature were introduced, one at a time, into the vortex tube and positioned at every tenth of an inch along the radius. The reason for introducing only one probe at a time was to keep the disturbance of the flow field to a minimum. For each radial position of a probe, two readings were taken, one corresponding to the probe on its way from the tube wall to the center of the tube, and the other corresponding to the probe on its way back from the tube center to the tube wall. The two readings were averaged, and this is the value that was recorded as being the probe reading at a given radial position. Since the vortex tube had a radius of one inch, twenty readings were thus taken per item, and ten averages were recorded for that item in the table of results. With the existance of the three items of velocity, pressure, and temperature, this meant sixty readings per traverse per station. With six stations along the length of the vortex tube, a given run involved no less than three hundred and sixty readings or a hundred and eighty averages to be entered in the tabulation of results. With the additional factors that time had to be allowed for readings to stabilize, and ambient conditions to be fairly uniform throughout, it can be seen that it is not easy to make a good run. At that, five decent runs, corresponding to inlet pressures of 10, 15, 20, 25, 30, and 35 psig were obtained. The results of the first two runs have been plotted in the form of curves in the aforementioned Figures (3-1) to

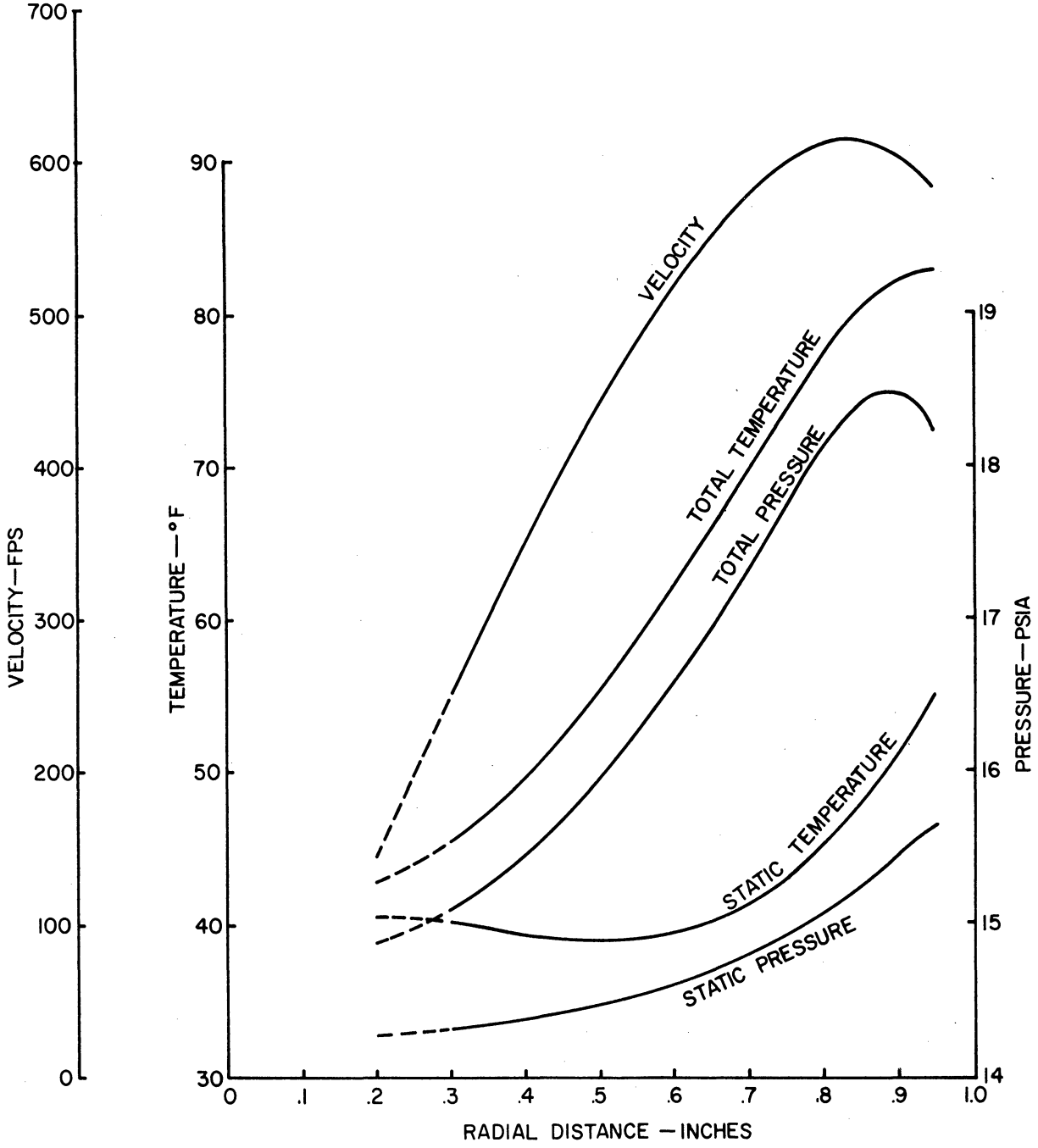

Figure 3-1. Velocity, Pressure, Temperature Traverse. Station 1, Configuration A, P_{inlet} = 10 psig.

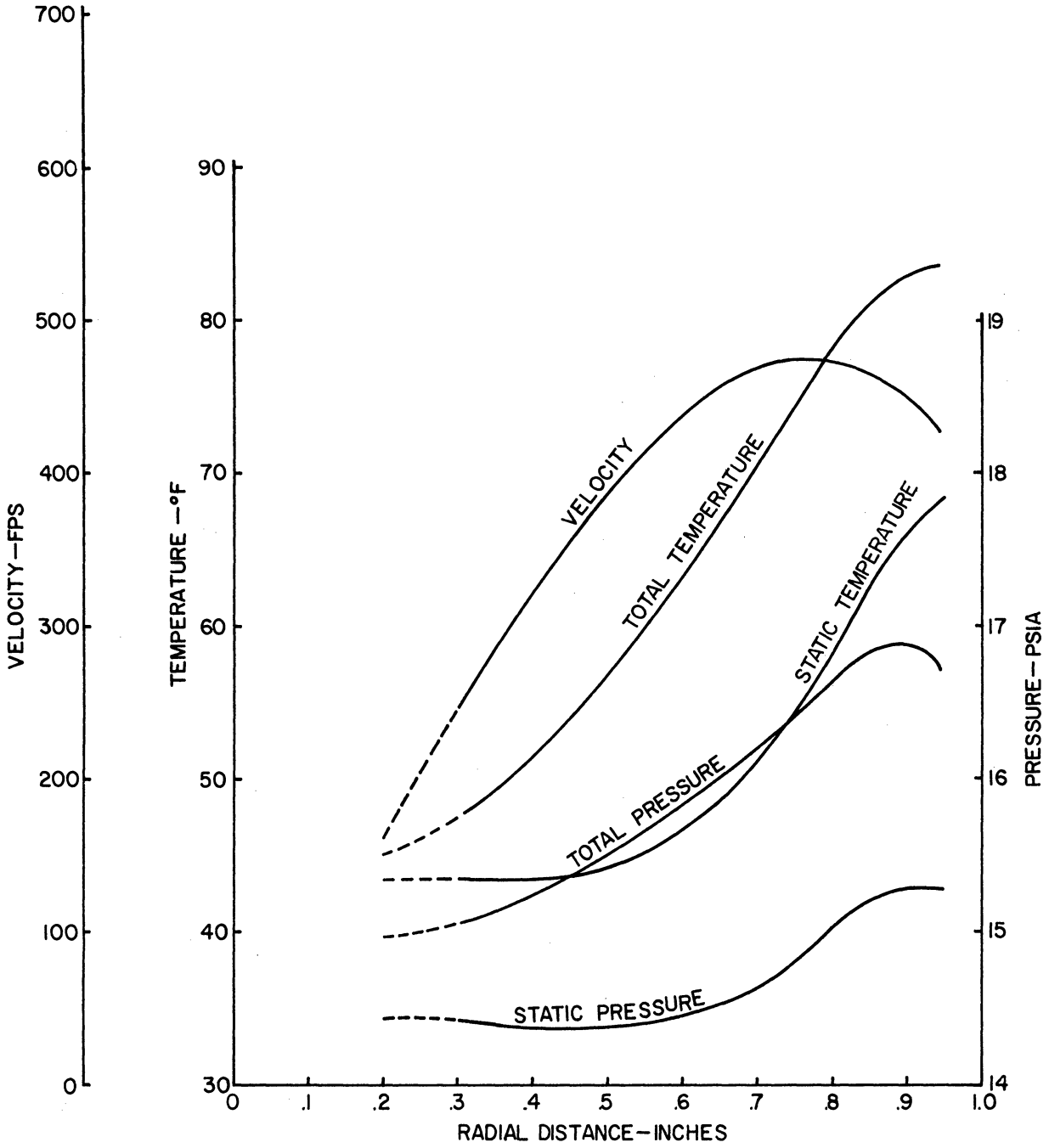

Figure 3-2. Velocity, Pressure, Temperature Traverse. Station 2, Configuration A, P_{inlet} = 10 psig.

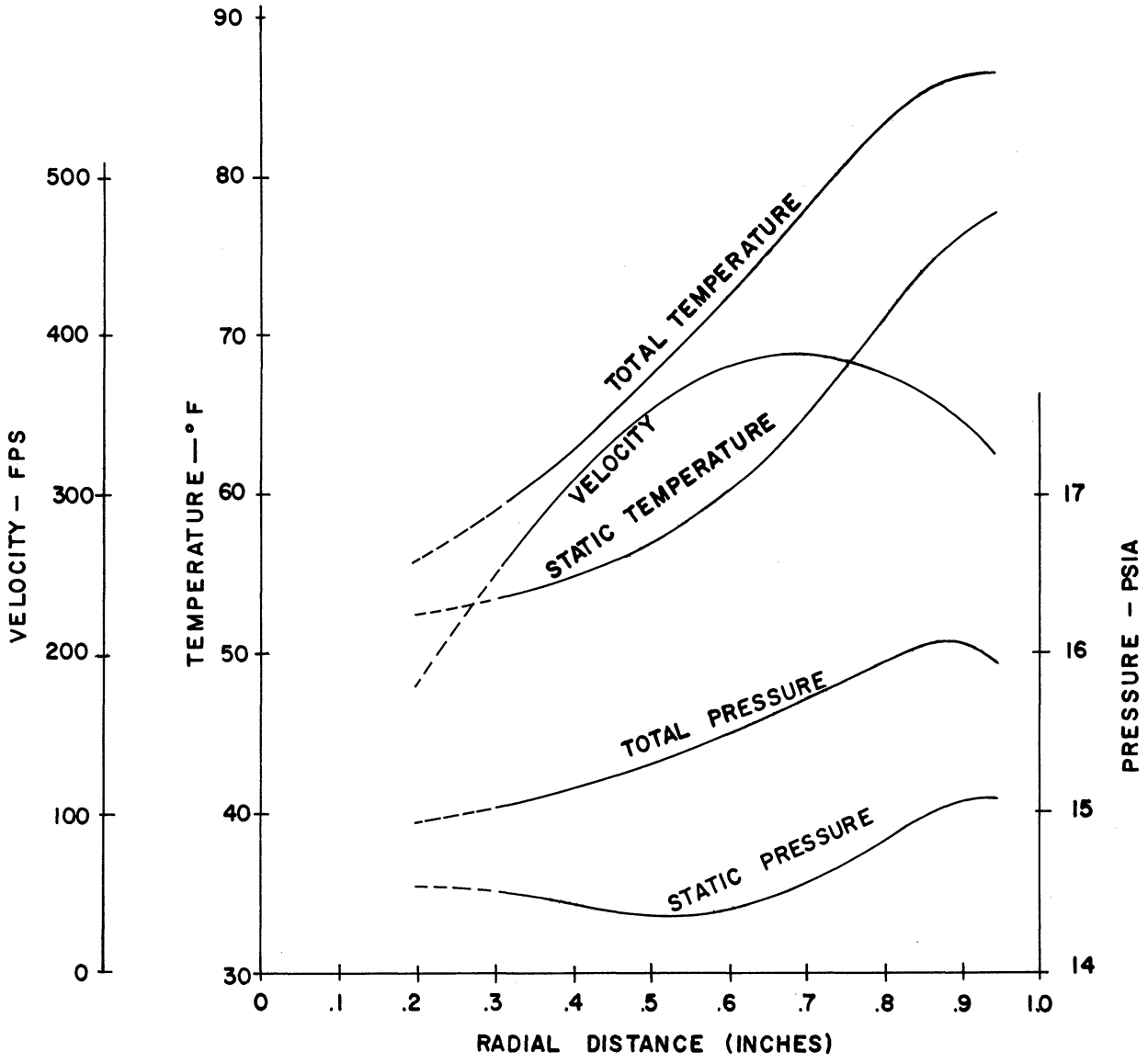

Figure 3-3. Velocity, Pressure, Temperature Traverse. Station 3, Configuration A, P_{inlet} = 10 psig.

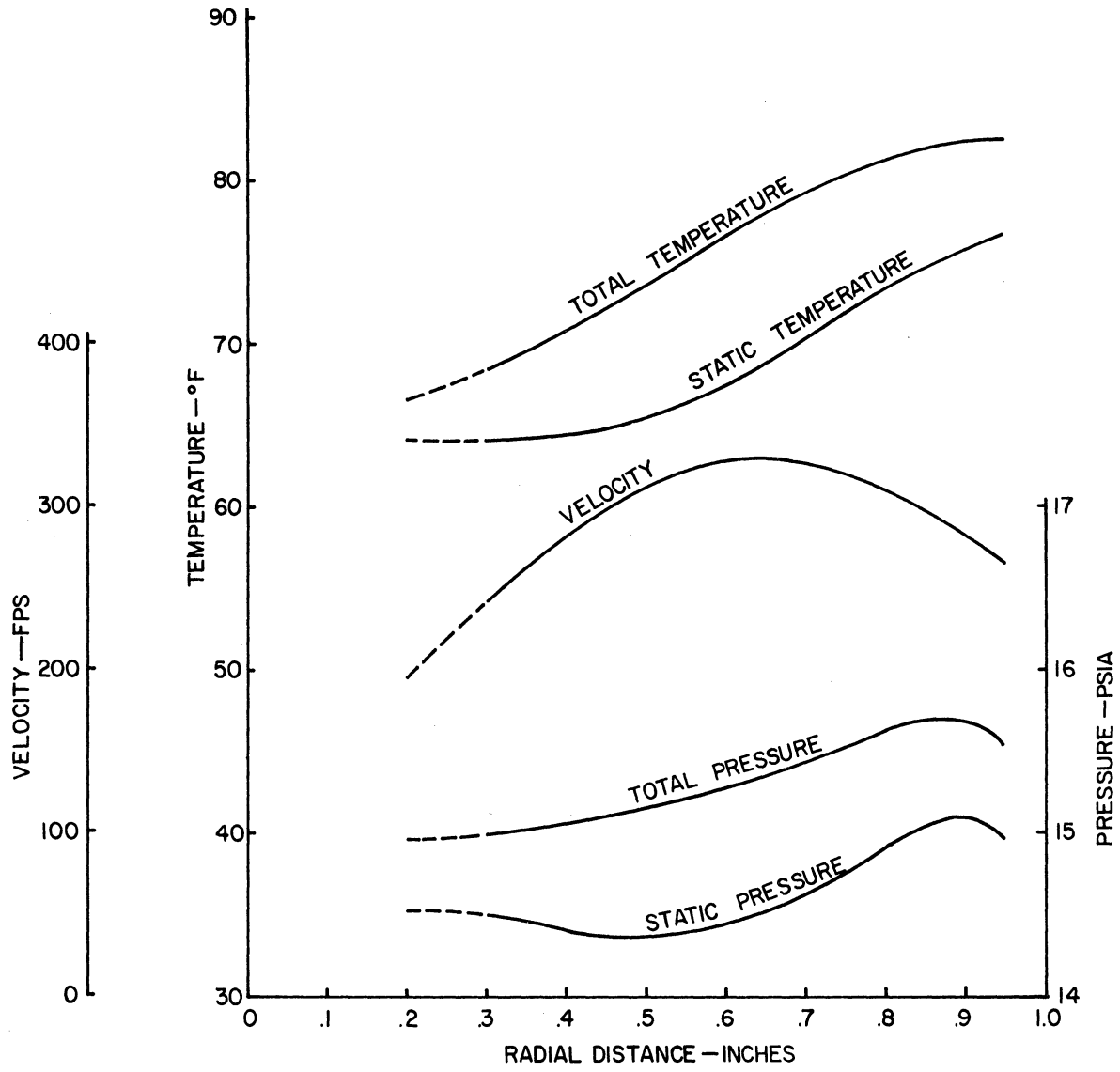

Figure 3-4. Velocity, Pressure, Temperature Traverse. Station 4, Configuration A, P_{inlet} = 10 psig.

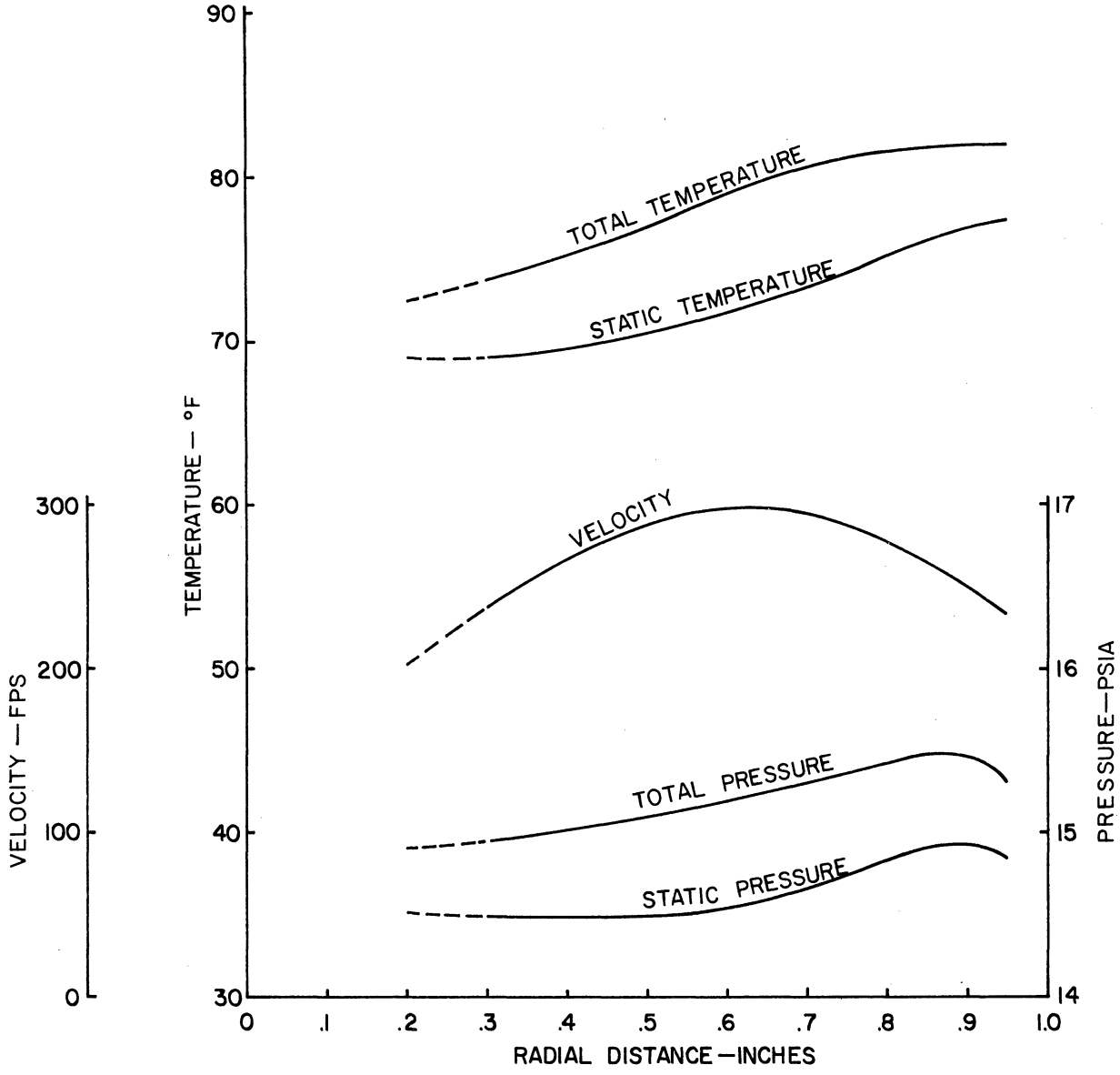

Figure 3-5. Velocity, Pressure, Temperature Traverse. Station 5, Configuration A, P_{inlet} = 10 psig.

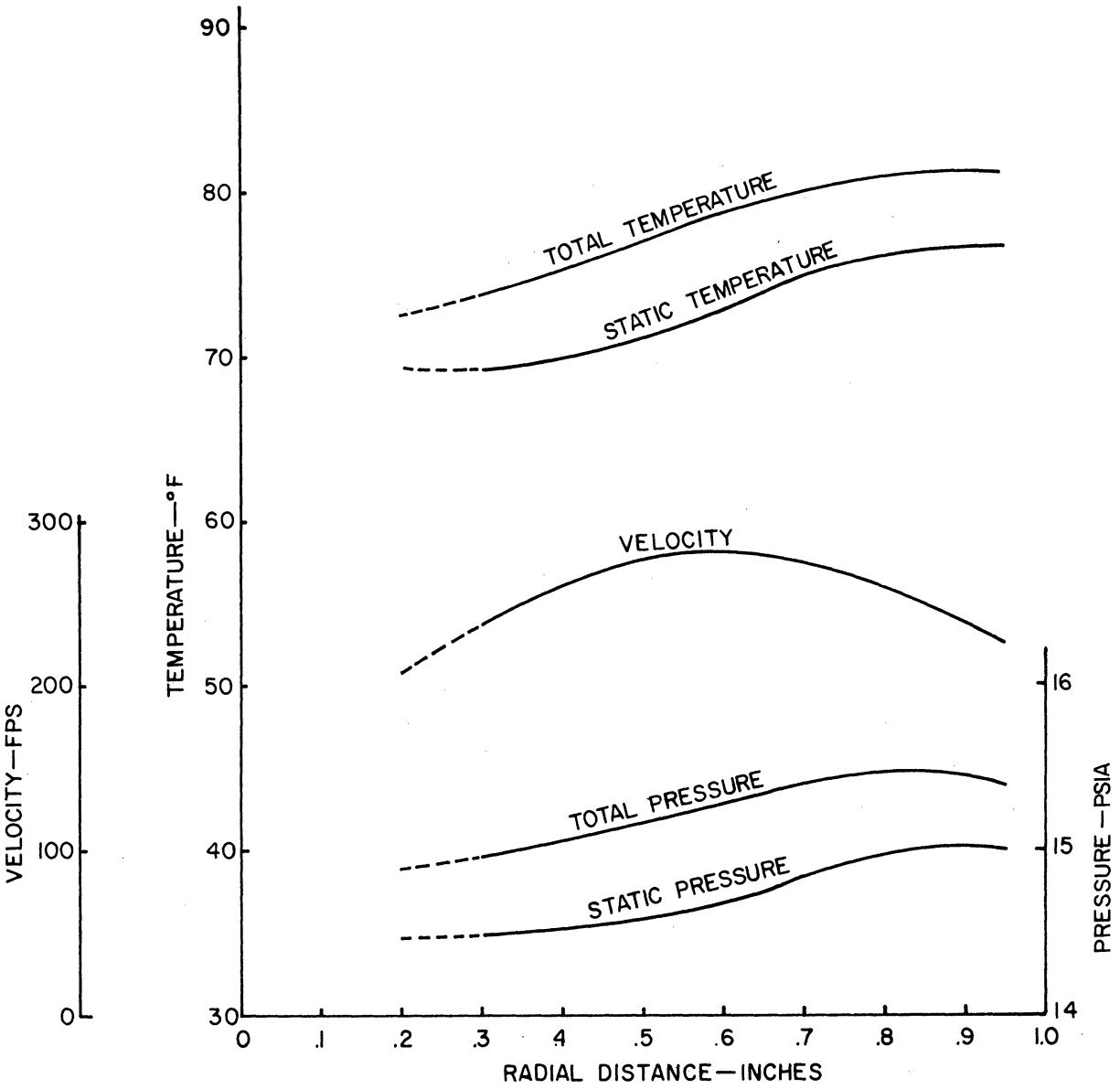

Figure 3-6. Velocity, Pressure, Temperature Traverse. Station 6, Configuration A, P_{inlet} = 10 psig.

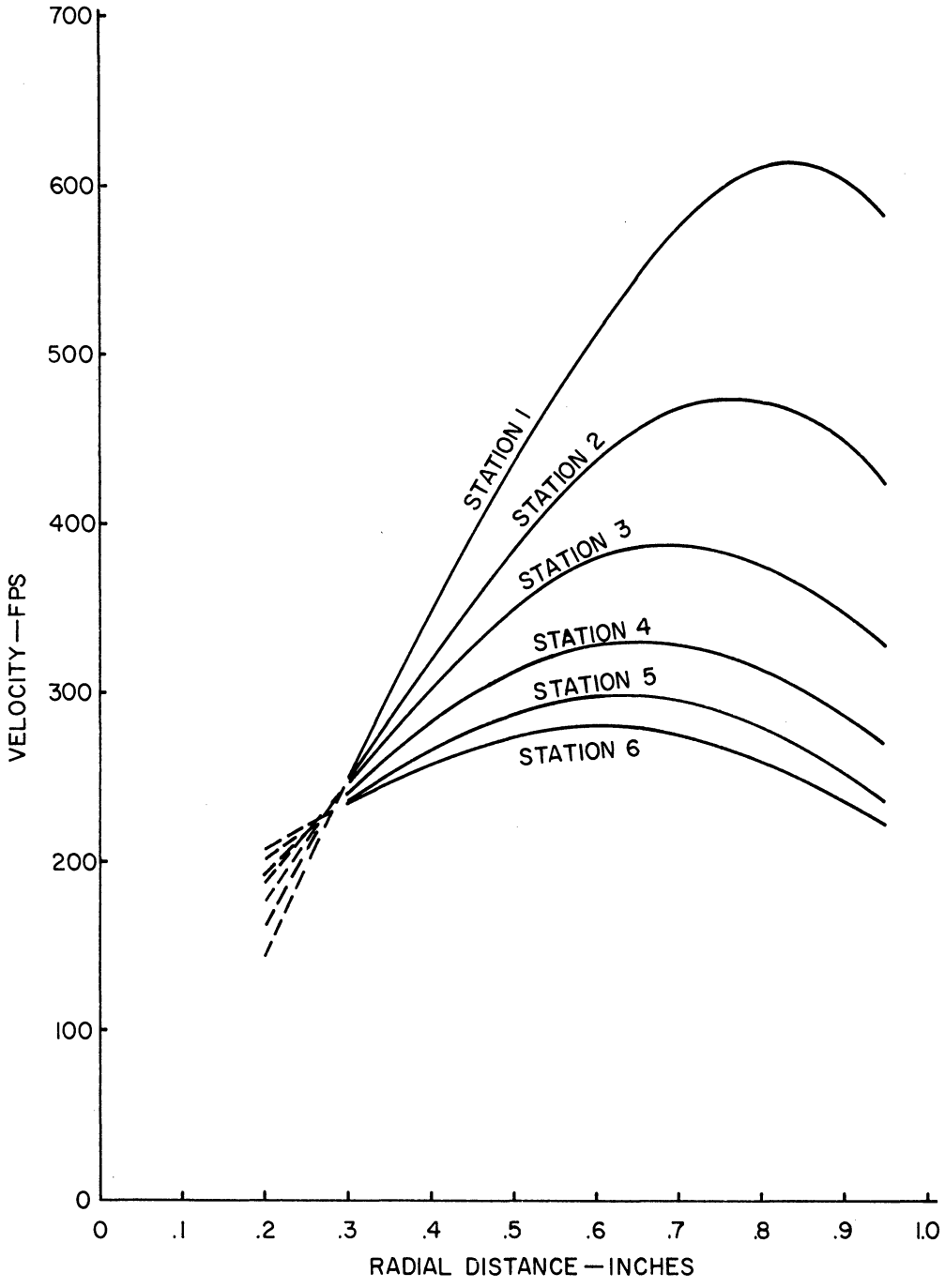

Figure 3-7. Velocity-Profile Change, Configuration A, P_{inlet} = 10 psig.

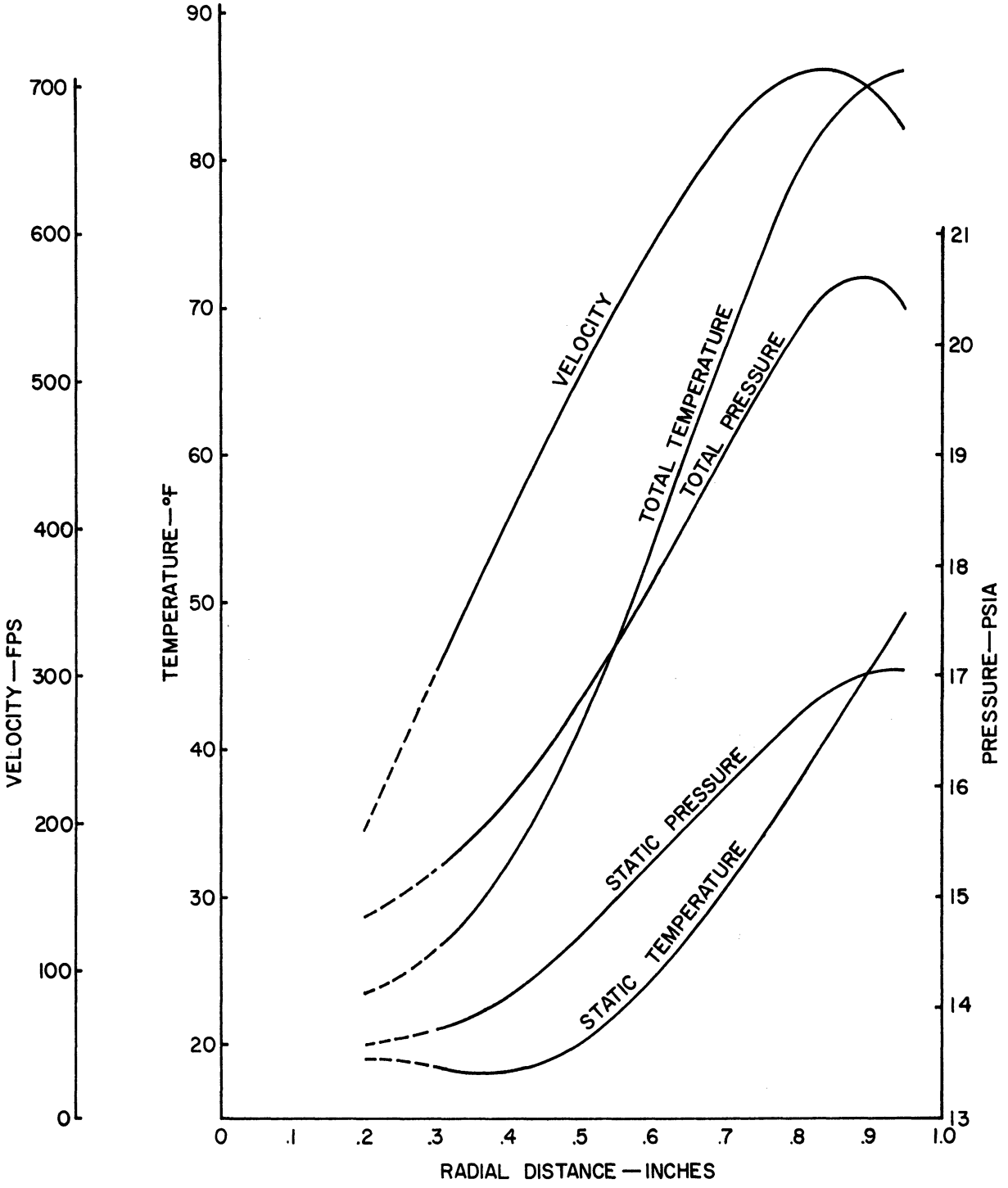

Figure 3-8. Velocity, Pressure, Temperature Traverse. Station 1, Configuration A, P_{inlet} = 15 psig.

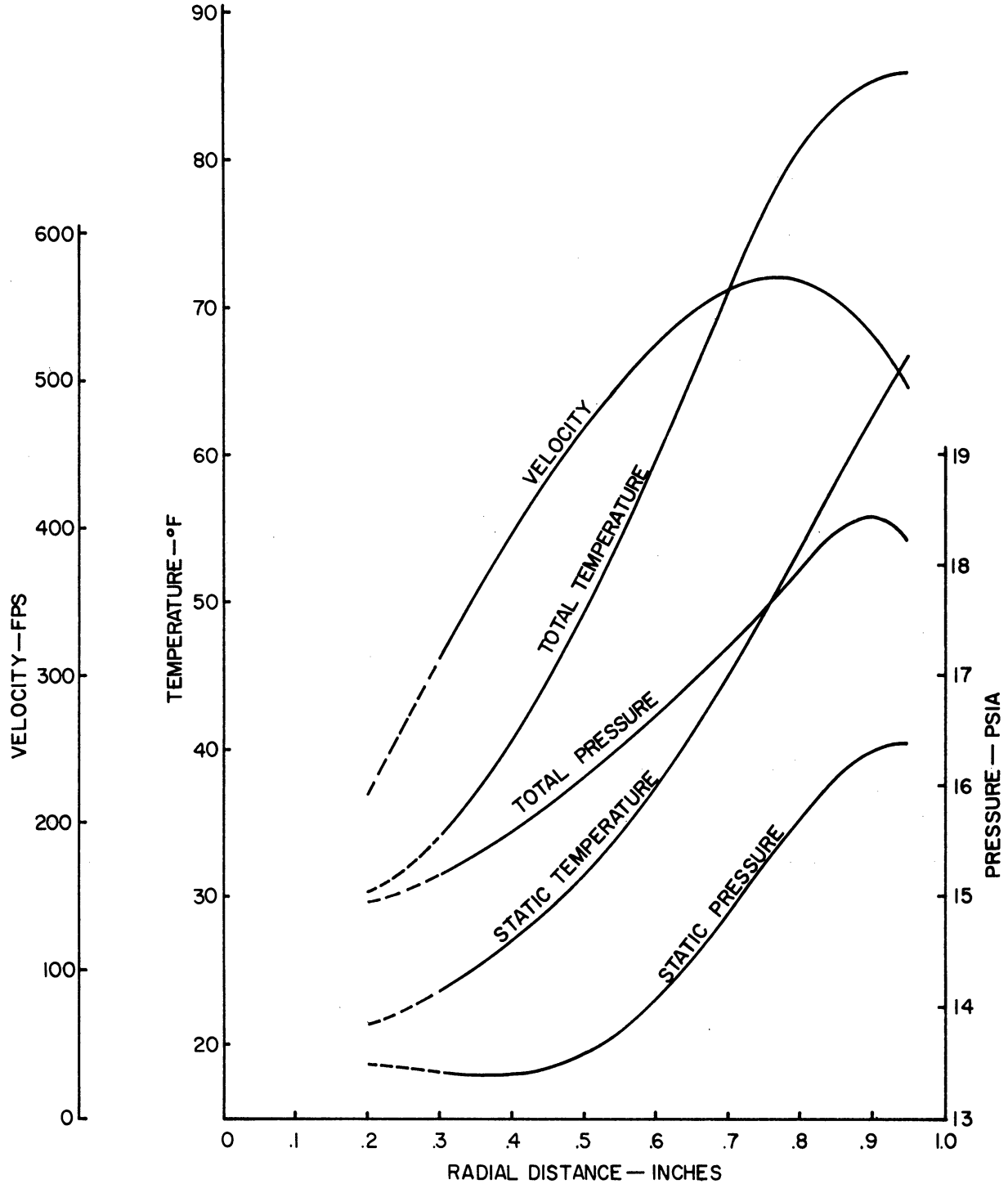

Figure 3-9. Velocity, Pressure, Temperature Traverse. Station 2, Configuration A, P_{inlet} = 15 psig.

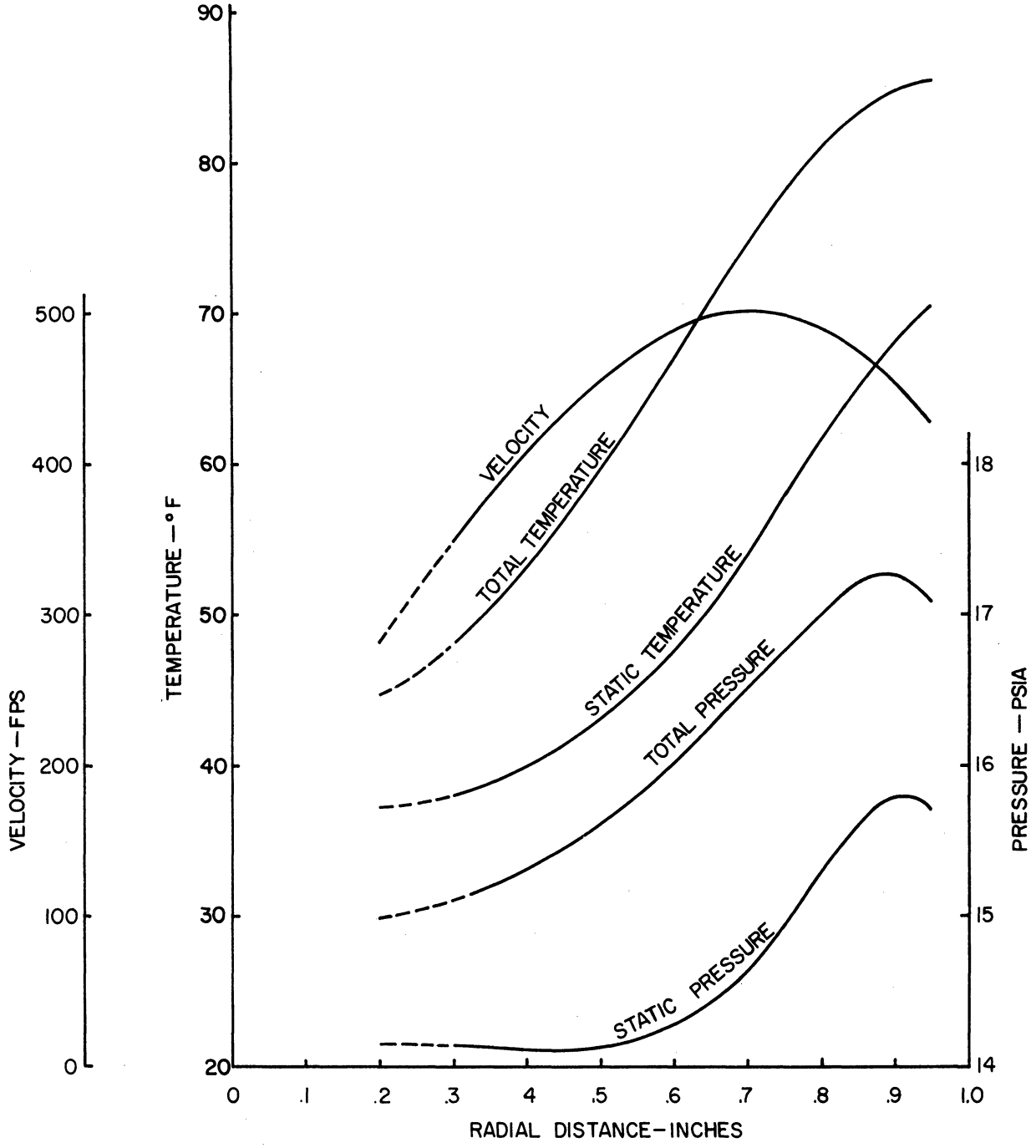

Figure 3-10. Velocity, Pressure, Temperature Traverse. Station 3, Configuration A, P_{inlet} = 15 psig.

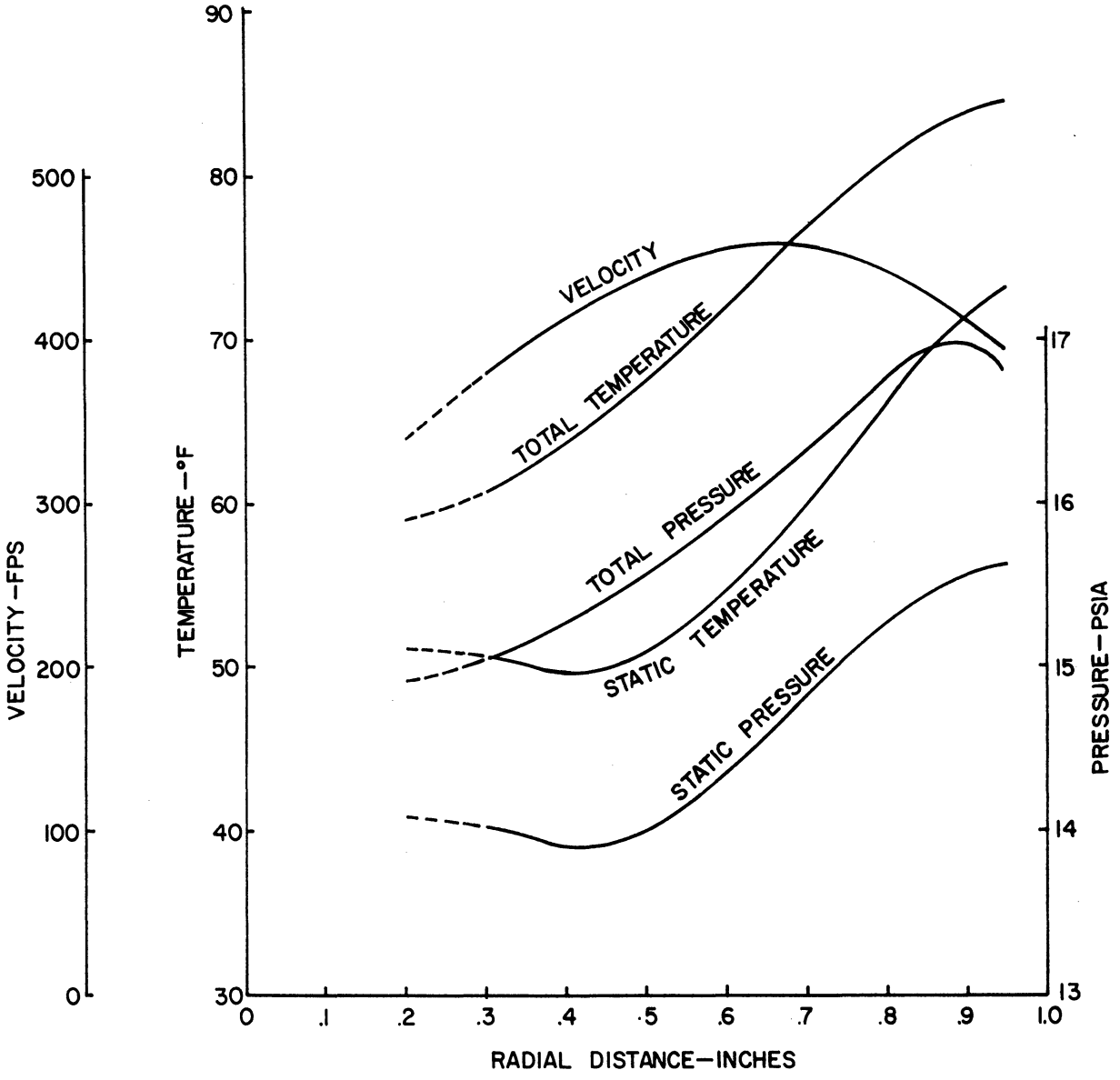

Figure 3-11. Velocity, Pressure, Temperature Traverse. Station 4, Configuration A, P_{inlet} = 15 psig.

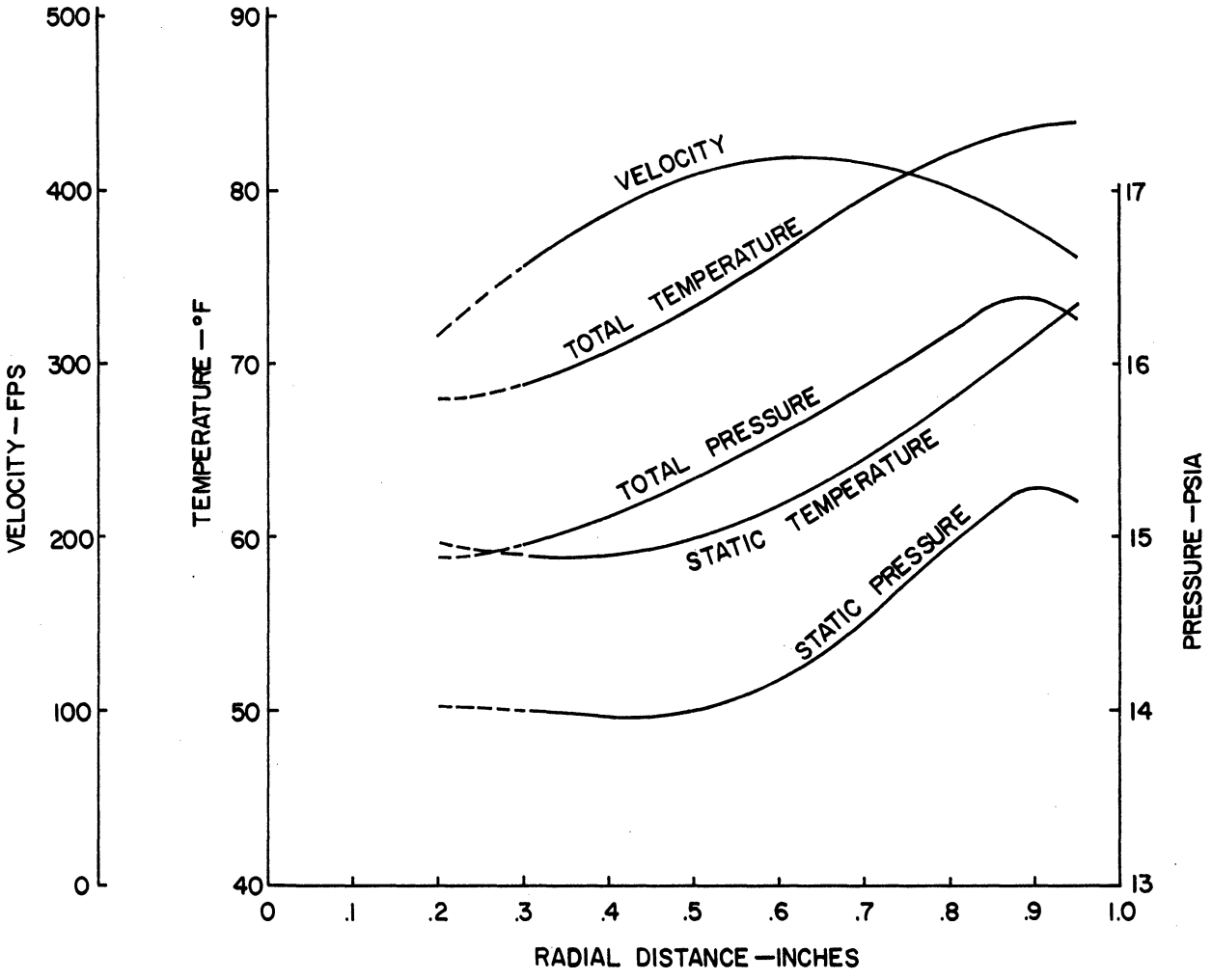

Figure 3-12. Velocity, Pressure, Temperature Traverse. Station 5, Configuration A, P_{inlet} = 15 psig.

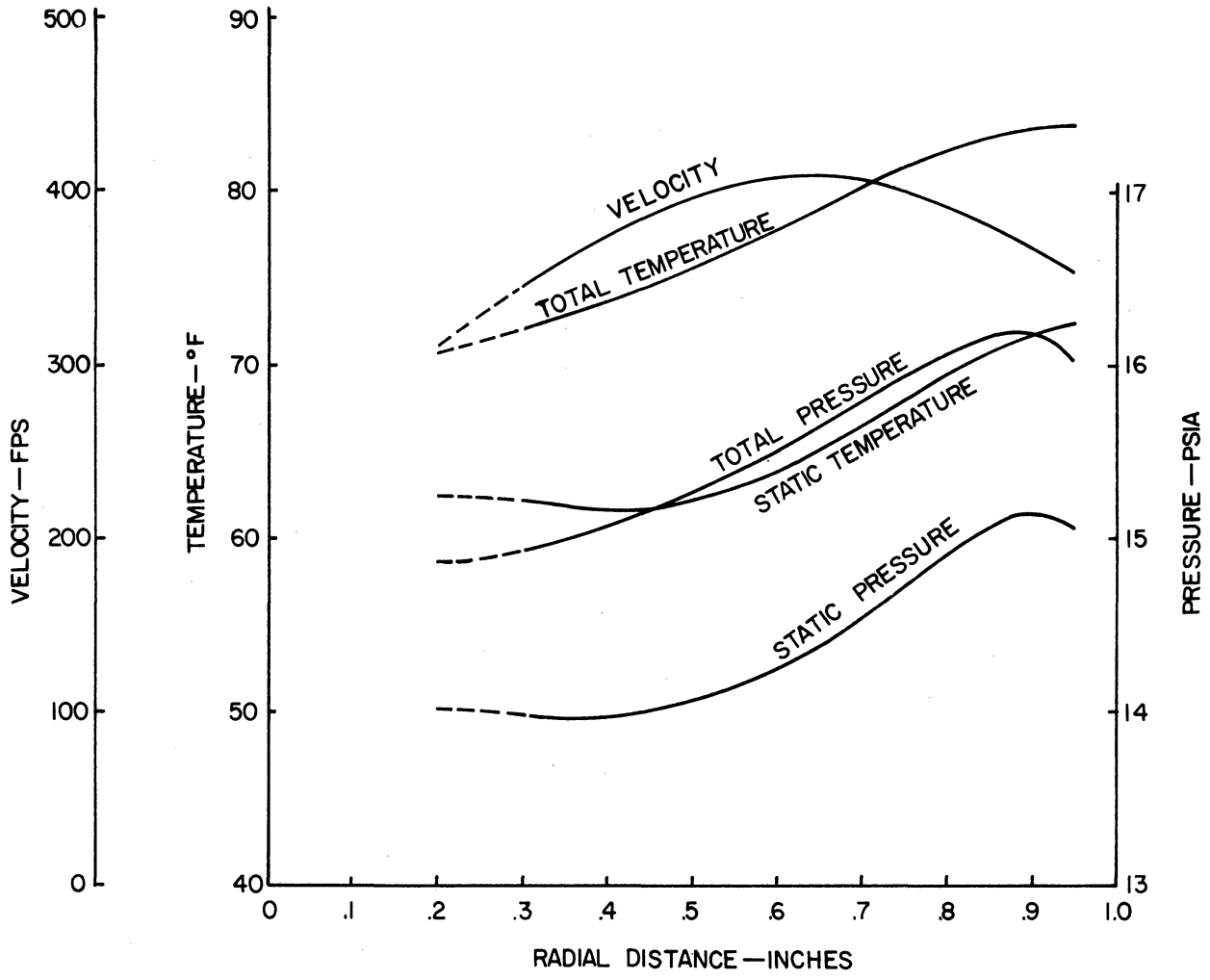

Figure 3-13. Velocity, Pressure, Temperature Traverse. Station 6, Configuration A, P_{inlet} = 15 psig.

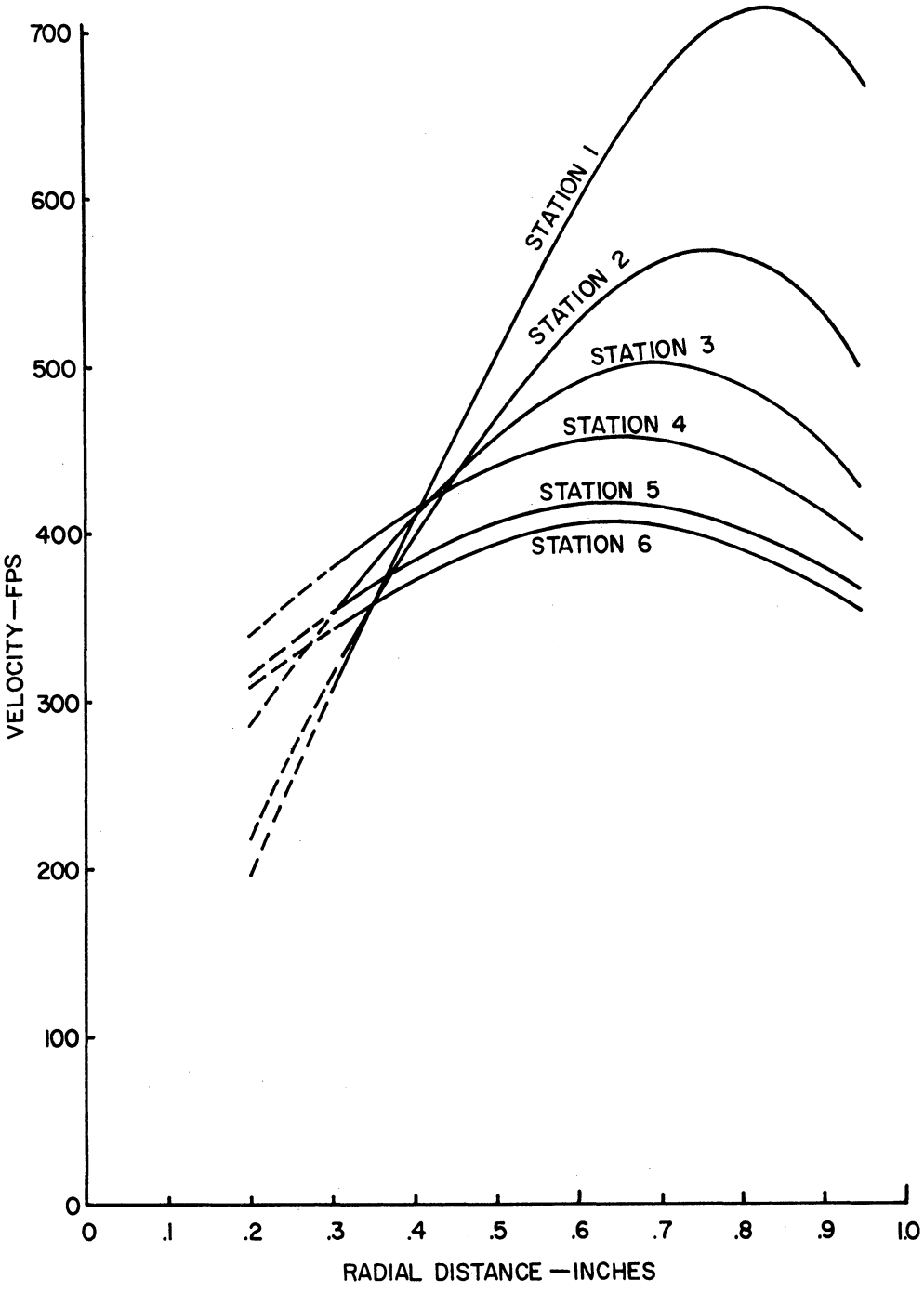

Figure 3-14. Velocity-Profile Change, Configuration A, P_{inlet} = 15 psig.

TABLE 3-1. Traverse Data; P_{inlet} = 20 psig

Station 1

r(inches)	V(fps)	T_T(°F)	p_T(psia)	V_A(fps)
.2	300	8	15.1	45
.3	405	17	14.9	15
.4	505	27	15.3	-8
.5	606	41	18.8	-14
.6	695	55	20.3	10
.7	760	70	21.7	125
.8	795	80	22.4	250
.9	770	84	22.5	293

Station 2

r(inches)	V(fps)	T_T(°F)	p_T(psia)	V_A(fps)
.2	350	21	15	25
.3	430	29	15.4	-8
.4	510	40	16	-14
.5	580	51	16.9	-10
.6	635	63	17.8	42
.7	660	75	18.8	150
.8	650	82	19.7	254
.9	615	85.5	20	272

Station 3

r(inches)	V(fps)	T_T(°F)	p_T(psia)	V_A(fps)
.2	375	38.5	15	12
.3	440	43	15.2	-7
.4	495	50.5	15.8	-11
.5	545	58.5	16.4	-2
.6	575	68.5	17	52
.7	590	77	17.7	151
.8	575	82	18.3	213
.9	530	84	18.7	246

Station 4

r(inches)	V(fps)	T_T(°F)	p_T(psia)	V_A(fps)
.2	410	56	15	3
.3	455	58	15.2	-8
.4	490	61.5	15.7	-9
.5	525	66	16.1	2
.6	540	71.5	16.5	63
.7	540	77.5	17	150
.8	520	82	17.3	208
.9	475	85	17.7	252

Station 5

r(inches)	V(fps)	T_T(°F)	p_T(psia)	V_A(fps)
.2	405	64.5	14.9	6
.3	445	67	15.1	-2
.4	475	69	15.3	-12
.5	500	72	15.7	-2
.6	510	77	16.1	50
.7	505	80.5	16.5	149
.8	485	83	16.9	206
.9	450	85.5	17.1	212

Station 6

r(inches)	V(fps)	T_T(°F)	p_T(psia)	V_A(fps)
.2	395	69	14.8	2
.3	430	70	15	-2
.4	455	71.5	15.2	-3
.5	475	73	15.6	2
.6	490	76	15.9	175
.7	480	79	16.3	159
.8	465	82	16.7	200
.9	435	84	16.8	201

TABLE 3-2. Traverse Data; P_{inlet} = 25 psig

Station 1

r(inches)	V(fps)	T_T(°F)	p_T(psia)	V_A(fps)
.2	355	-1.5	15.7	65
.3	413	4	16.8	6
.4	500	16	84	-20
.5	525	30	20.5	-30
.6	745	45	22.6	45
.7	824	62	24.5	150
.8	858	78.5	26.1	270
.9	849	86	26.3	340

Station 2

r(inches)	V(fps)	T_T(°F)	p_T(psia)	V_A(fps)
.2	385	15	15.5	35
.3	480	22	16.5	-10
.4	575	30	17.7	-30
.5	655	39.5	18.9	-10
.6	715	51	20.4	60
.7	824	65	21.8	165
.8	859	78	23.3	260
.9	845	85	23.2	325

Station 3

r(inches)	V(fps)	T_T(°F)	p_T(psia)	V_A(fps)
.2	430	43	15.3	20
.3	530	48	16	-14
.4	604	52	16.9	-25
.5	655	58.5	17.9	0
.6	715	64.5	18.9	70
.7	741	71	20.2	160
.8	740	79	21.4	260
.9	715	85	21.5	315

Station 4

r(inches)	V(fps)	T_T(°F)	p_T(psia)	V_A(fps)
.2	450	56	15.2	15
.3	516	59	15.7	-20
.4	575	62	16.4	-20
.5	608	66	17.1	25
.6	626	71	17.9	100
.7	627	55.5	19	195
.8	608	80.5	20	270
.9	575	84.5	20.1	300

Station 5

r(inches)	V(fps)	T_T(°F)	p_T(psia)	V_A(fps)
.2	465	63	14.9	10
.3	510	64.5	15.4	-20
.4	549	68	16	-17
.5	575	71	16.6	30
.6	590	74.5	17.4	104
.7	586	78.5	18.1	180
.8	560	81.5	18.5	255
.9	540	84	19	286

Station 6

r(inches)	V(fps)	T_T(°F)	p_T(psia)	V_A(fps)
.2	450	65.5	14.8	5
.3	480	66	15.2	-18
.4	525	70	15.7	-16
.5	550	72	16.3	27
.6	560	75	16.9	92
.7	555	79	17.5	175
.8	540	81	18.3	245
.9	511	83.5	18.2	272

TABLE 3-3. Traverse Data; P_{inlet} = 30 psig

Station 1

r(inches)	V(fps)	T_T(°F)	p_T(psia)	V_A(fps)
.2	385	-9	16.8	85
.3	435	-3.5	18.4	25
.4	536	7	20.4	-15
.5	675	21	22.6	-32
.6	800	40	25.2	25
.7	877	60	27.8	145
.8	900	78.5	30	275
.9	872	88	30.9	365

Station 2

r(inches)	V(fps)	T_T(°F)	p_T(psia)	V_A(fps)
.2	410	3	16.5	65
.3	512	10	17.8	10
.4	640	19.5	17.2	-30
.5	750	31	20.8	-15
.6	775	45	22.4	55
.7	790	63	24.2	170
.8	775	79	26.2	285
.9	740	87	27.3	352

Station 3

r(inches)	V(fps)	T_T(°F)	p_T(psia)	V_A(fps)
.2	450	33	16.4	45
.3	550	37.5	17.5	-4
.4	635	45	18.7	-25
.5	678	53.5	19.9	-10
.6	706	61.5	21.3	65
.7	705	71	22.7	165
.8	681	80.5	24.1	270
.9	638	87	24.6	340

Station 4

r(inches)	V(fps)	T_T(°F)	p_T(psia)	V_A(fps)
.2	480	52	16.3	35
.3	560	55	17.2	-5
.4	610	60	18.1	-24
.5	650	65	17.1	-8
.6	665	71	20.1	62
7	655	77	21.4	165
.8	630	83.5	22.5	280
.9	592	86.5	23.1	334

Station 5

r(inches)	V(fps)	T_T(^oF)	p_T(psia)	V_A(fps)
.2	480	60	16.2	25
.3	530	62	16.9	-11
.4	585	66	17.6	-23
.5	615	70	18.4	4
.6	627	74.5	19.3	84
.7	620	80	20.2	175
.8	598	84	21	270
.9	560	86	21.5	330

Station 6

r(inches)	V(fps)	T_T(^oF)	p_T(psia)	V_A(fps)
.2	450	65	16.1	15
.3	535	68	16.6	-18
.4	565	70	17.3	-23
.5	594	73.5	17.9	14
.6	598	76	18.6	80
.7	586	80.5	19.3	160
.8	564	84.5	20	250
.9	530	86	20.3	305

(3-13), and the remainder left in tabular form in Tables (3-1,2,3) for the sake of economy of labor. No runs were made above 35 psig because of the large consumption of air and of the noise involved. It should be noted that the readings near the center of the tube and near the wall of the tube were very erratic, and for that reason, neither traverse curves nor traverse data are drawn or given for radial distances less than 0.3 inches or more than 0.9 inches. The explanation for this condition is found in chapters 8 and 12.

3.2 Axial Distribution

The variation of velocity, pressure, and temperature with axial distance is shown by cross plotting the data as in Figures (3-7), (3-14), (3-15), and (3-16). The former figures are a juxtaposition of the velocity traverses, and shows not only how the whirl velocity decreases as flow progresses down the vortex tube, but that there is actually a sort of leveling off, indicating that flow becomes more and more axial as it moves down the tube. This means that the strength of the vortex filament (Chapter 4), unlike the situation for a perfect fluid, is no longer constant, but decreases as flow progresses along the tube. The latter figures show the variation of maximum values of total temperature, total pressure, and velocity in the axial direction. It is seen that the maximum Ranque-Hilsch effect occurs near the inlet of the vortex tube rather than farther down the tube.

The axial length of the tube did not appreciably affect the character of the flow. Several runs were made at various configurations other than A. Except for axial gradients that are somewhat larger for the shorter configurations, i.e., pressures and velocities dropping over a smaller axial distance, the results have the same general appearance as those for configuration A, and for the sake of economy, they are

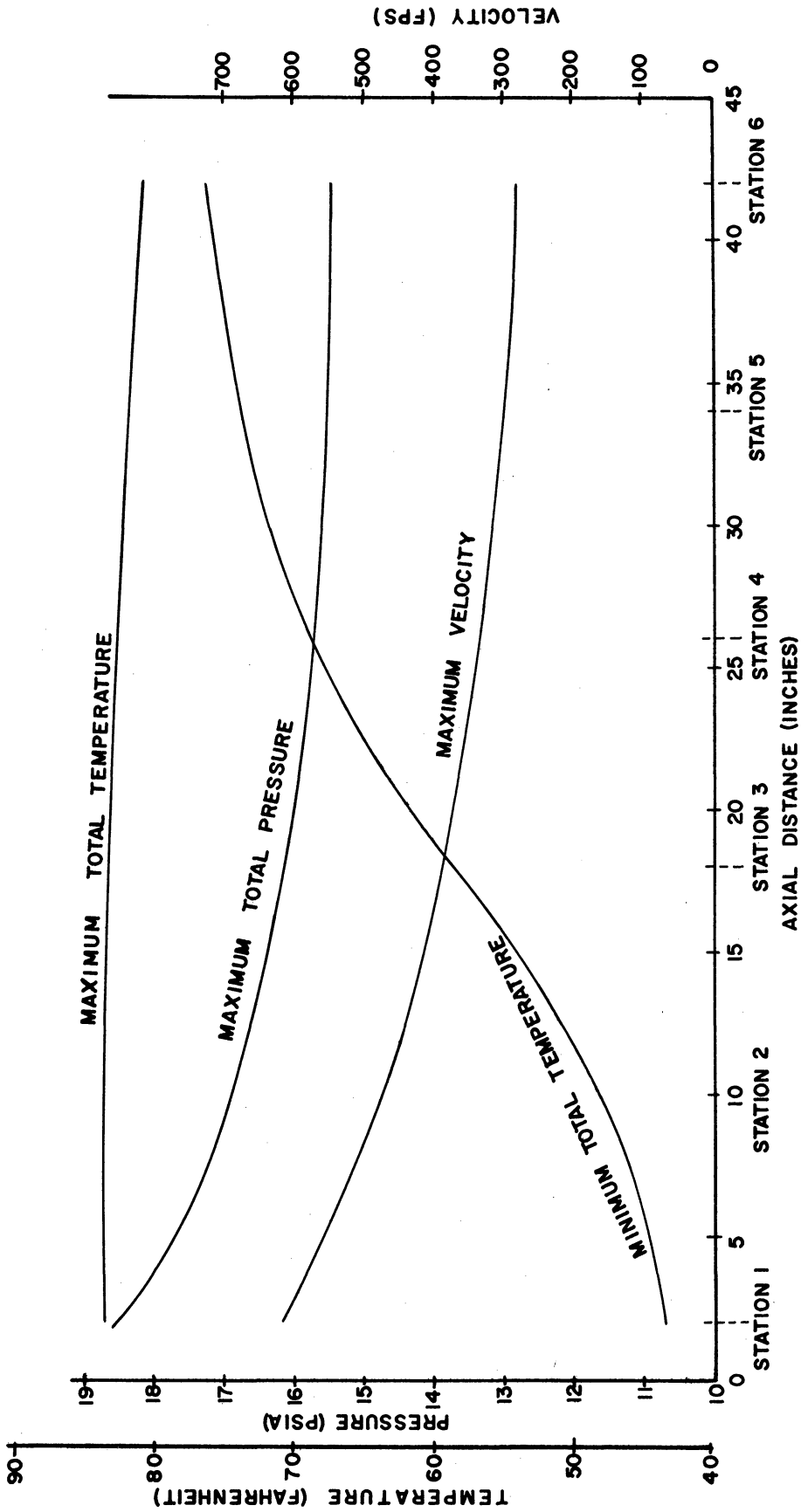

Figure 3-15. Axial Variation of Pressure, Temperature, and Velocity. Configuration A, P_{inlet} = 10 psig.

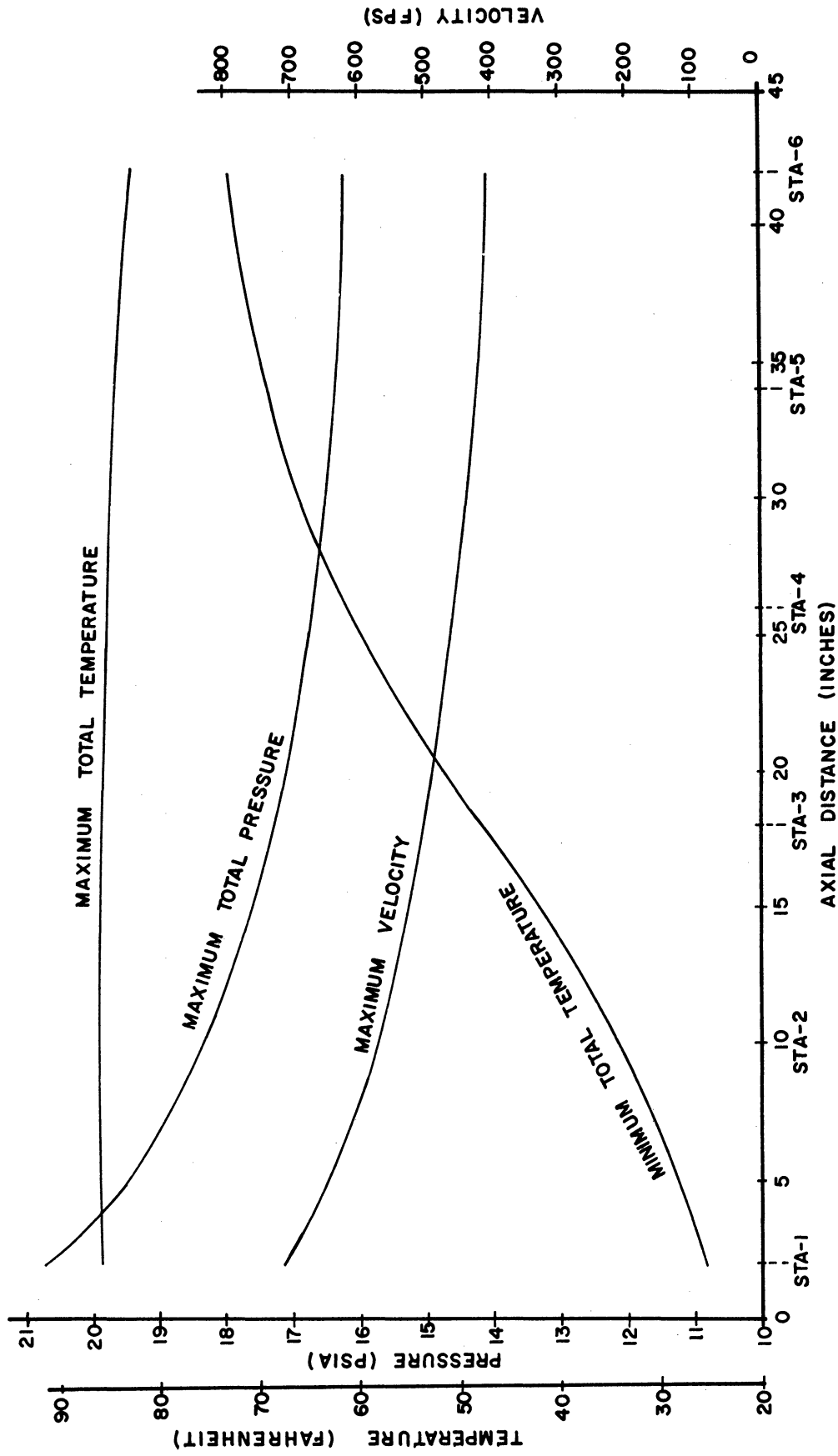

Figure 3-16. Axial Variation of Pressure, Temperature, and Velocity. Configuration A, P_{inlet} = 15 psig.

Table 3-4. Axial Distribution of Pressure, Temperature and Velocity; P_{inlet} = 20 psig.

Station	Axial Distance	Max.T_T (^oF)	Min.T_T (^oF)	Max. P_T (Psia)	Max. V (fps)
1	2	86	9	22.9	780
2	10	86	22	20	660
3	18	85.5	40	18.6	590
4	26	85	56	17.6	545
5	34	84.5	66	17.1	510
6	42	83.5	69	16.8	490

Table 3-5. Axial Distribution of Pressure, Temperature and Velocity; P_{inlet} = 25 psig.

Station	Axial Distance	Max.T_T (^oF)	Min.T_T (^oF)	Max. P_T (Psia)	Max. V (fps)
1	2	87	-4	26.9	860
2	10	87	15	23.5	760
3	18	86.5	42	21.8	690
4	26	86.5	56	20.3	630
5	34	85.5	63	19.3	590
6	42	84	65.5	18.4	560

Table 3-6. Axial Distribution of Pressure, Temperature and Velocity; P_{inlet} = 30 psig.

Station	Axial Distance	Max. T_T (^oF)	Min. T_T (^oF)	Max. P_T (Psia)	Max. V (fps)
1	2	88	-11.5	30.5	890
2	10	88	2	27.5	780
3	18	87.5	33	25	710
4	26	87.5	51.5	23	765
5	34	86.5	60	21.6	730
6	42	85	65	20.4	605

not included here.

3.3 Axial Velocity

The velocities concerned up to this point represent the magnitude of the velocity vector. The velocity probe, however, can detect direction. It can be rotated 360 degrees on its stand(Figures 2-10) and 2-14), so that in its postion of maximum reading, that direction perpendicular to the hot wire indicates the direction of the velocity. With this information, it is possible to resolve velocities into axial and tangential components. Figure (3-17) shows the flow angle and the axial velocity traverses at a typical station, namely, 2. Traverses at other stations show curves of similar shape, and hence are not drawn. For convenience, the stagger or tangential angel ($90-\alpha$) is plotted, rather than the flow angle itself. Incidently, it was found that the flow angle is rather independent of changes in inlet pressure over the range of values tested. Figure (3-18) shows that the axial velocities are uniformly small when compared to tangential velocities or to total velocities of Figures (3-7) and (3-15). As for distribution, the predominant axial velocities are concentrated in a small annular region near the wall of the vortex tube. The axial velocity falls off sharply toward the center of the tube, and actually indicates a reverse flow near the center. This explains partly how the hot stream travels in one direction, and the cold stream in the other in the case of previous investigations of the vortex tube (50, 108).

A reasoning concerning the wall friction throws considerable light on the tangential velocity distribution. Inspection of the data reveals that the tangential or total velocity peaks do not coincide with the axial velocity peaks, but are located more toward the center of the

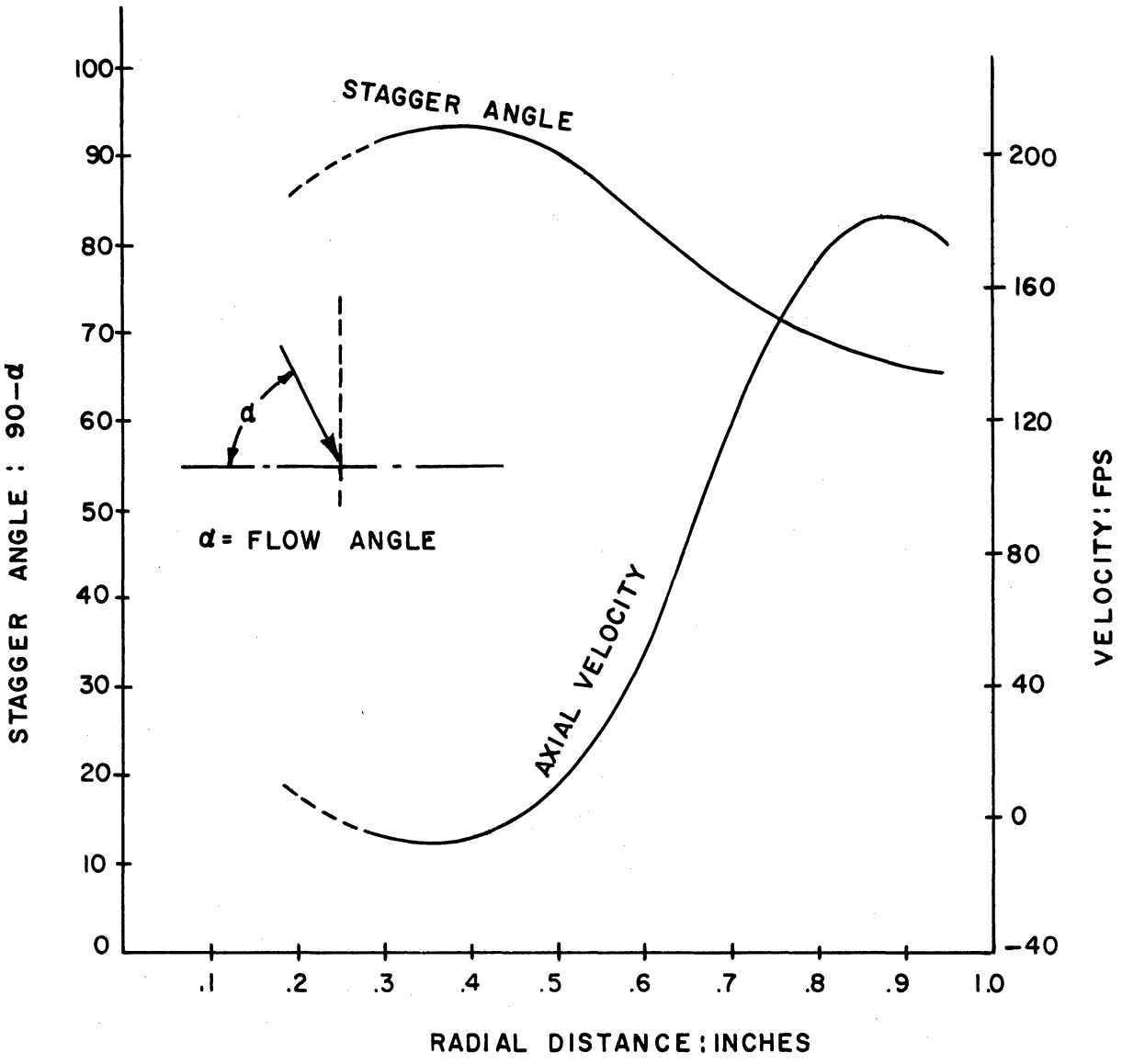

Figure 3-17. Flow Angle and Axial Velocity. Station 2, Configuration A, P_{inlet} = 10 psig.

tube. This can be explained on the basis that wall friction causes a decrease in both the axial and tangential velocities near the wall as the flow moves along. From continuity considerations, this results in an increase in axial and tangential velocities in regions farther away from the wall. It indicates that some air must move in toward the center as flow progresses down the tube. In so doing, the air tends to conserve its angular momentum, thereby resulting in an increase in angular velocity in those regions farther away from the wall. The tangential velocity, however, drops off at the center of the tube, for as shown in Chapter 8, there is theoretically no flow "in the plane", but only axial flow.

It is interesting to compare the axial velocity distribution with that obtained by superposition of a vortex flow and a longitudinal flow. From the relations to be developed in Chapter 5, Euler's equation becomes

$$\frac{dp}{\rho} + \frac{V_T\, dV_T}{g} + \frac{V_a\, dV_a}{g} = 0 \qquad (3\text{-}1)$$

where p denotes pressure, and V_T, V_a denote tangential and axial velocities respectively. The differentiation is with respect to radial distance r. The pressure gradient relation becomes

$$\frac{dp}{dr} = \frac{\rho V_T^2}{gr} \qquad (3\text{-}2)$$

while the "free" vortex condition is

$$r\, V_T = \text{constant} \qquad (3\text{-}3)$$

From Equation (3-2), $dp/\rho = V_T^2\, dr/gr$, and from Equation (3-3), $dr/r = -\, d\, V_T/V_T$. Substituting these into Equation (3-1) yields

$$V_a\, dV_a = 0 \qquad (3\text{-}4)$$

Rejecting the trivial solution $V_a = 0$ (no flow), Equation (3-4) yields V_a = constant for the combination of "free" vortex flow with longitudinal flow.

The velocity distribution in the vortex tube, however, is more characteristic of the "forced" vortex type than of the free vortex type. Therefore, combining a "forced" vortex flow with a longitudinal flow, the Euler equation, the pressure gradient equation are the same as Equations (3-1) and (3-2), but the vortex condition is now

$$\frac{V_T}{r} = \text{constant} = \omega \qquad (3\text{-}5)$$

Equations (3-5) and (3-2) give $dp/\rho = \omega^2 r\, dr/g$, while Equation (3-5) becomes $d V_T = \omega\, dr$. Substitution of these into Euler's equation, however, no longer result in a constant V_a, but a $V_a = f(r)$ which is more complex, having nevertheless the general character of the distribution curve shown in Figure (3-18).

3.4 Interrelationship of Internal Data

The experimental study of the vortex tube "from the inside", as is the case in the present investigation, affords some interesting cross checking of data. It was previously pointed out that the plot of axial velocities showed some negative values in the neighborhood of the axis, indicating the existence of a backward flow. This may be verified by considering the pressure relation for circulatory flow:

$$\frac{dps}{dr} = \frac{\rho}{r} V_T^2 \qquad (3\text{-}6)$$

Figures (3-8) through (3-14) show an increase in tangential velocities near the center of the tube. Since Equation (3-6) must be satisfied, it follows that there must be an increase in the pressure differential between the center line and the region immediately away from it as flow progresses down the tube. Now, static pressure measurements along the center line itself showed fairly constant values along the length of the vortex tube. Therefore, the static pressure in the neighborhood of the center line must increase from station 1 to

station 6. Such a pressure gradient explains the tendency for backward flow near the center of the tube, especially in the case of the counterflow vortex tube (50, 108).

Nor is the foregoing the only case of data cross checking. The axial velocity distribution may be used in conjunction with the local values of the density to determine by integration, the mass rate of flow down the tube. This mass rate can then be compared with the mass rate obtained from the flowmeter. Similarly, an energy balance may be performed by taking the product of the meter flow rate, the specific heat, and the inlet temperature, and comparing with the integrated energy flow at various cross sections along the tube length. This was done on several occasions, and the results agreed well enough for peace of mind. This is one of the many advantages occurring from the "internal" approach to the study of the vortex tube.

3.5 Flow Visualization

Construction of a vortex tube of lucite afforded good opportunity for the study of flow patterns by means of visual methods. Accordingly, a smoke chamber was first constructed and connected to the inlet hose. The injected smoke showed up well at low speeds, but at moderate or high speeds, it became invisible. Also, there was considerable difficulty in getting the smoke into the vortex tube center block. The pressure in the smoke chamber being low compared to the air supply pressure and to the vortex tube pressure, the smoke had a tendency of flowing out of the tube rather than into the tube.

After smoke, balsa sawdust was tried, but it did not show up well at high speeds, and it was messy to work with, since it covered everything in the vicinity with a coat of dust. Next, fine confetti

was tried, with a laundry bag covering the vortex tube exit cone to prevent the confetti from blanketting the adjacent laboratory space. It worked for short bursts of speeds, but then the confetti, in rubbing against the lucite, developed static electricity, and it simply clung to the walls of the tube to no avail.

The final and most successful method of flow visualization was the injection of clear or colored water into the vortex tube. The injections were made by means of a horse syringe, and clear water was first used, because it kept the installation clean. Later on, for the sake of taking photographs, colored liquid was used. This entailed washing and cleaning the entire installation after an injection, however, it was not too high a price to pay for the obtention of good photographes. Figure (3-18) shows the flow pattern immediately after entry into the vortex tube. The circle in the field of flow is the limit circle, and represents the inner boundary of the vortex flow. Its existence is a characteristic of compressible flow, and its theory is developed in Chapter 8. Figure (3-19) shows the same condition, but for the case of the counterflow vortex tube. These are interesting pictures, for the existence of limit circles (circles beyond which the flow does not penetrate) has not been discussed in previous investigations.

Figure (3-20) shows another example of limit line in plane flow. It was, however, obtained by injecting a trace of clear water, and it represents one of the few cases where a "clear" trace photographed well. Figure (3-21) shows a spiral streamline in three-dimensional flow. It was obtained by means of clear liquid, but using a short configuration, namely configuration D. A similar streamline in space, but using a longer configuration is shown in Chapter 9, where it was included to correlate the theoretical study with some of the experimental results.

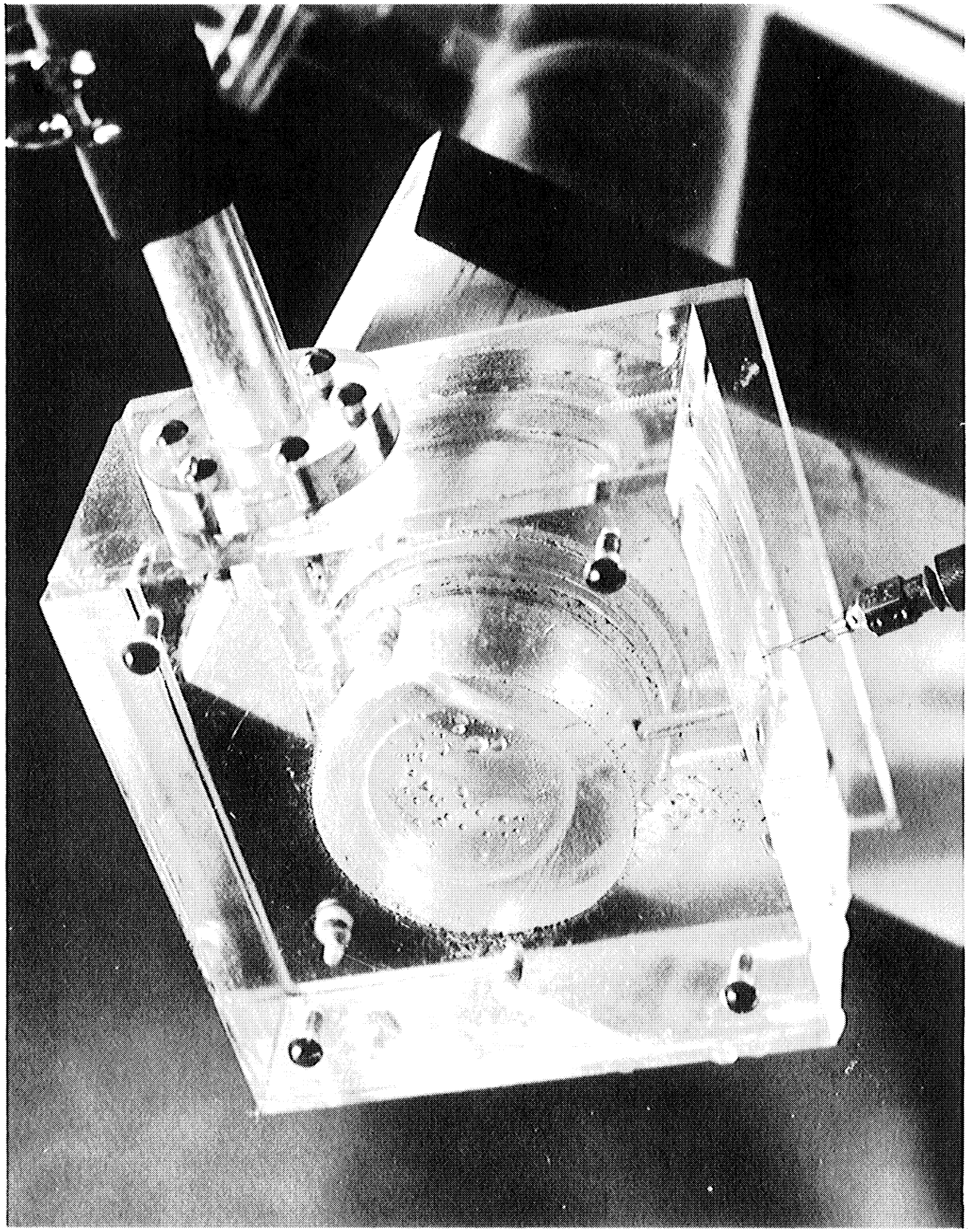

Figure 3-18. Limit Circle in Uniflow Vortex Tube

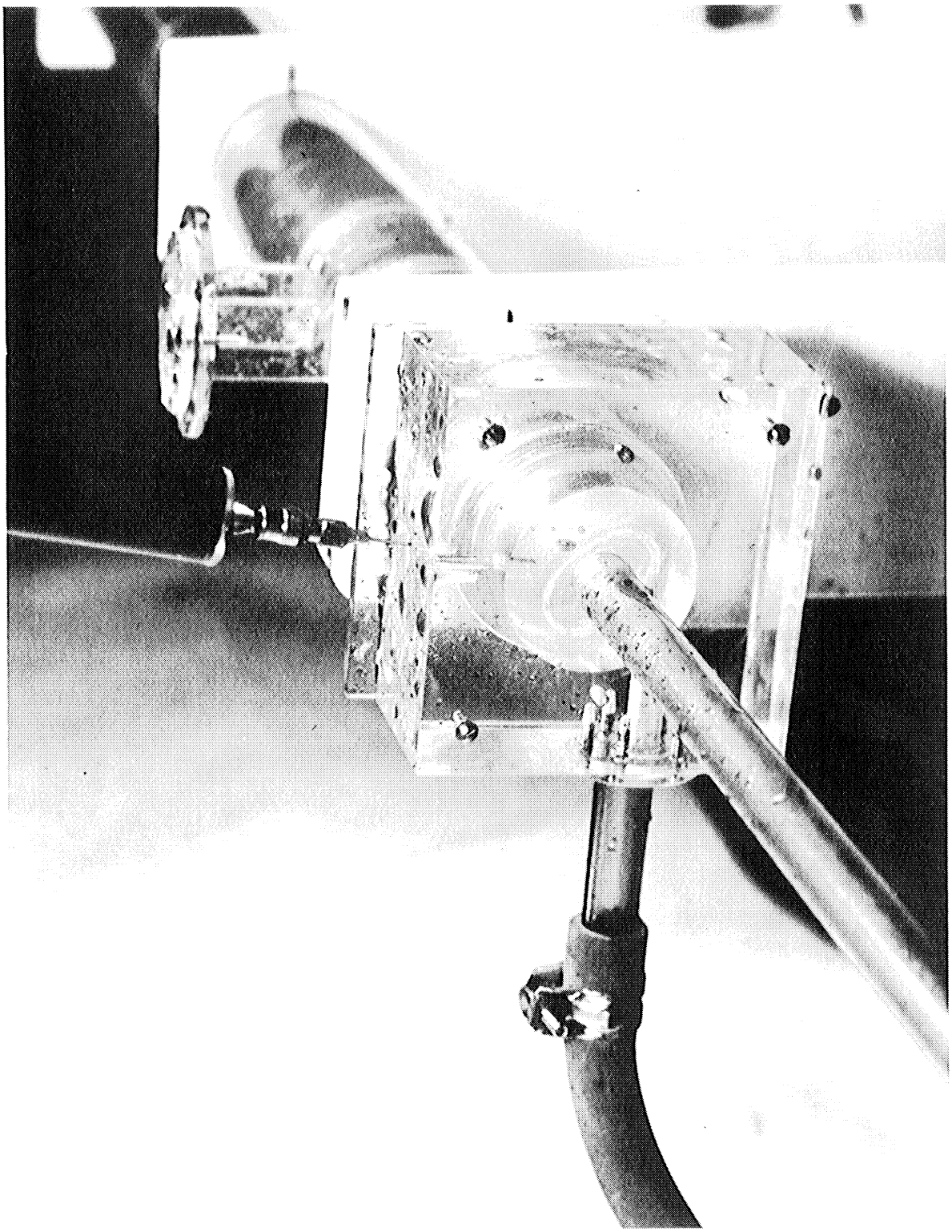

Figure 3-19. Limit Circle in Counterflow Vortex Tube

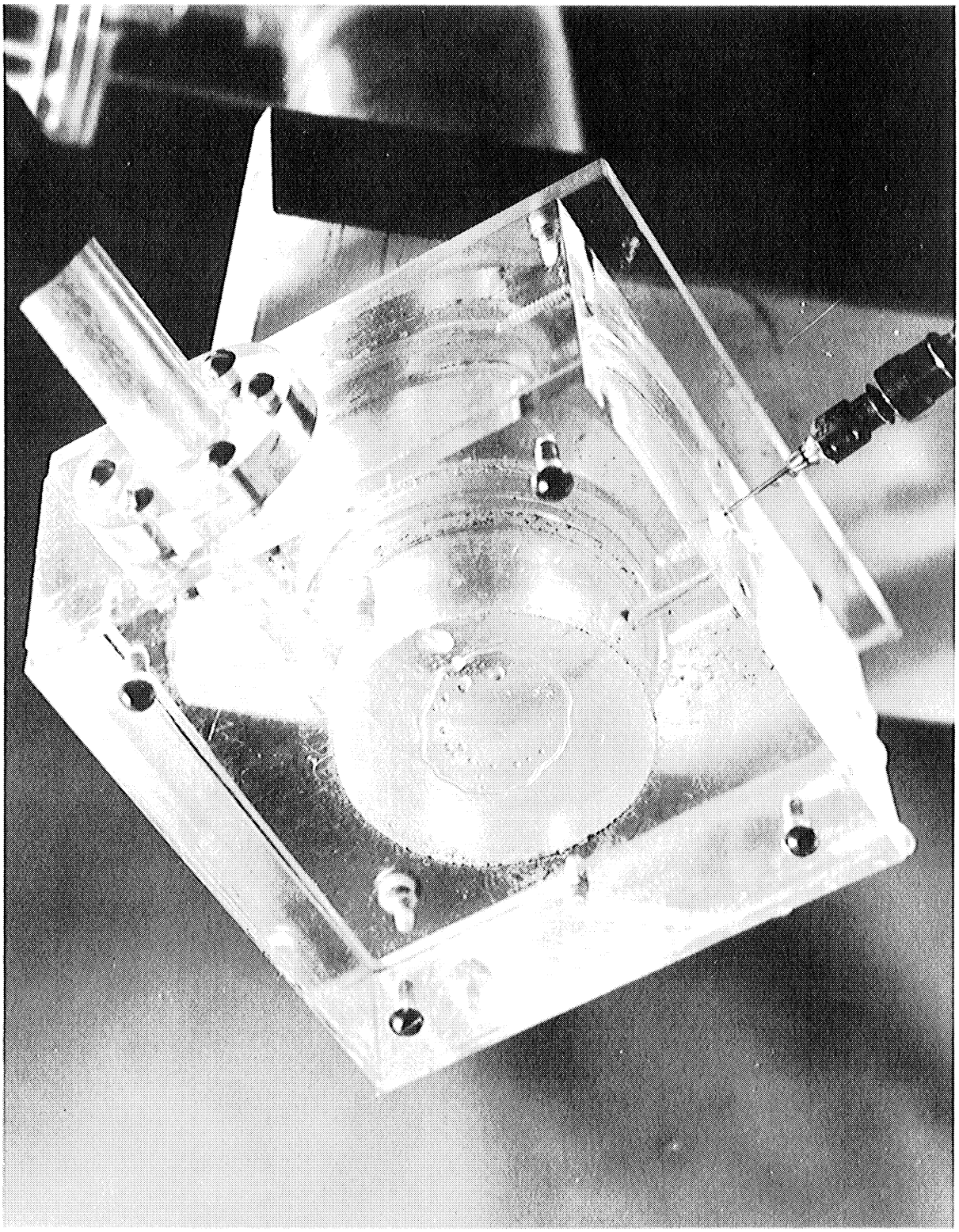

Figure 3-20. Limit Circle (Clear Water Injection)

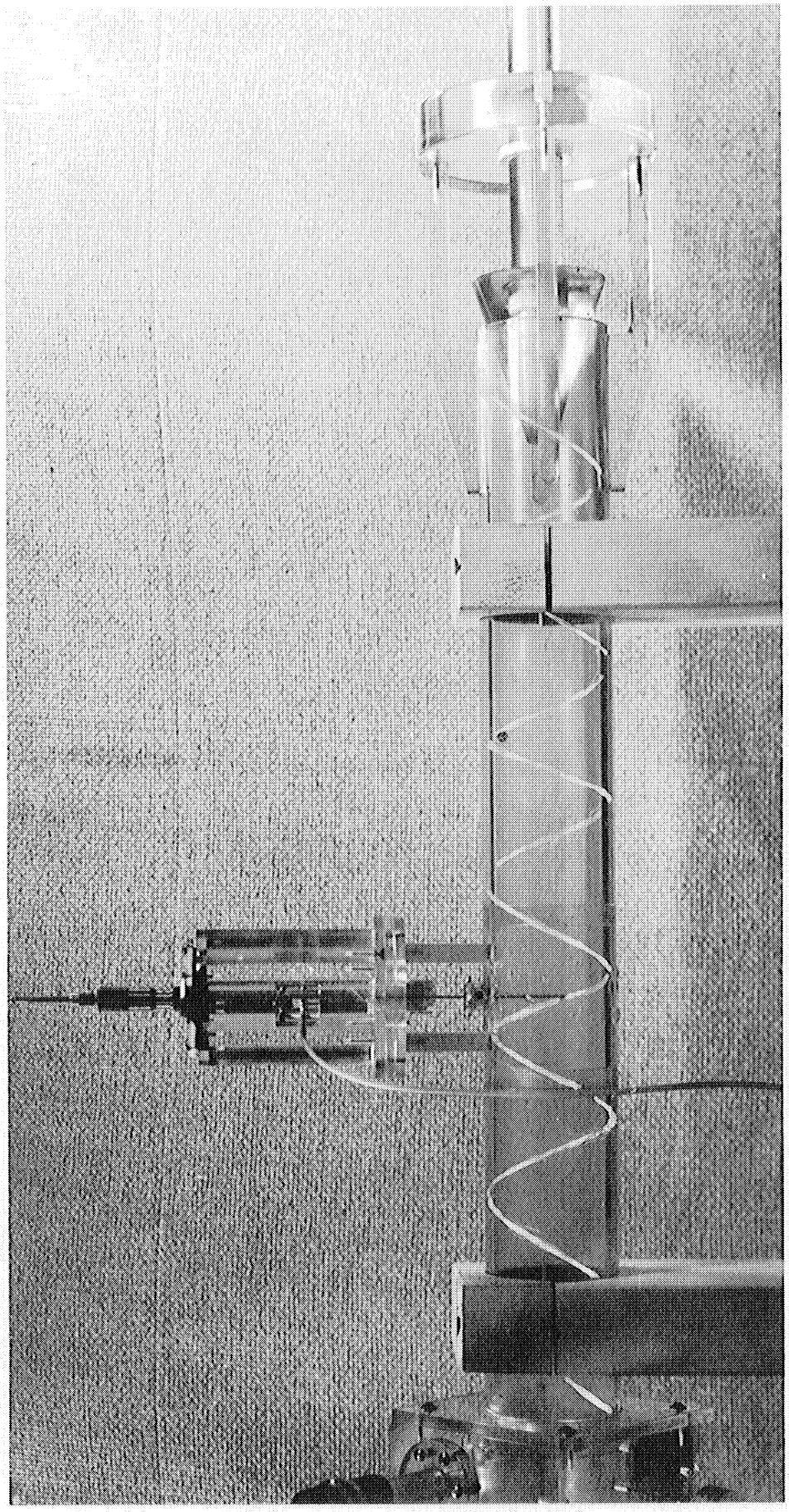

Figure 3-21. Experimental Streamline (Configuration D)

PART III

THEORETICAL STUDY

CHAPTER 4

VORTEX FLOW IN THE PLANE

4.1 Potential Vortex

Consider the flow of air upon its entrance into the vortex tube. Its motion is circulatory, and is as shown in Figure (4-1). The analytical treatment of the problem will proceed along the following line of thought. The instrinsic equations of compressible fluid flow, if tackled head-on in their most general form, i.e., three-dimensional, with viscosity and heat transfer included, involve mathematical difficulties beyond the power of present-day methods of analysis. It is, therefore, only natural that simpler solutions be sought from simpler, if more restricted models of flow, and by superposing these individual solutions, to arrive at the general solution.

Using Prandtl's concept of the boundary layer, it is possible to ignore friction and heat transfer for the region of potential flow outside the boundary layer. Shearing stresses and heat transfer are small compared to dynamic effects, except in a thin film near the solid boundaries, and the flow can be considered as frictionless adiabatic within a space the outline of which is displaced by an amount equal to the thickness of the boundary layer. Shock waves do not occur in regions where the flow is entirely subsonic. In transonic and supersonic flow, they are present, but even so, the flow patterns upstream and downstream of the shock can be treated as shock-free.

In the present work, the fluid is treated as a continuum, which is equivalent to working with macroscopic properties of the fluid, rather than with the instantaneous states of its innumerable

molecules. This assumption is valid, since the mean free path of the molecules (3.5×10^{-6} in. for air) is nowhere of comparable size with the smallest significant dimension of the problem. Because of most problems in compressible flow, the concept of irrotational, frictionless, adiabatic, shock-free motion of a perfect gas permits great mathematical simplifications with scarcely any sacrifice in accuracy, the present study begins with the flow in the vortex tube being expressed as irrotational or potential. Viscosity effects are taken into account in Chapter 10.

4.2 Irrotational Flow

This is one instance when the flow is amenable to exact solution, for the differential equations of flow reduce to systems of quasi-linear partial differential equations of the first order for functions of two independent variables. Advantage is taken of this fact, and the flow, upon entry of the compressed air into the vortex tube is then expressed as follows.

Consider, in that region excluding the boundary layer, a perfect fluid moving in a circular path with no external torque applied:

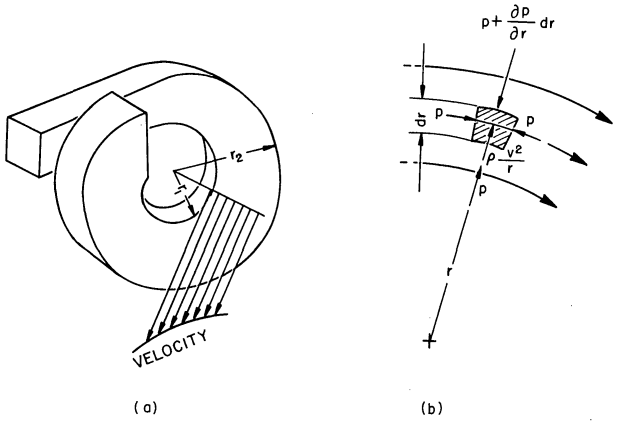

Figure 4-1. Flow in Circular Path

$$T = m \frac{d}{dt} (rV) = 0$$

Integrating:

$$rV = \text{constant} = K$$

or

$$V = \frac{K}{r} \tag{4-1}$$

The significance of this equation will now be developed.

Equation (4-1) is characteristic property of a free vortex; the velocity distribution being of the type (hyperbolic) shown in Figure (4-2).

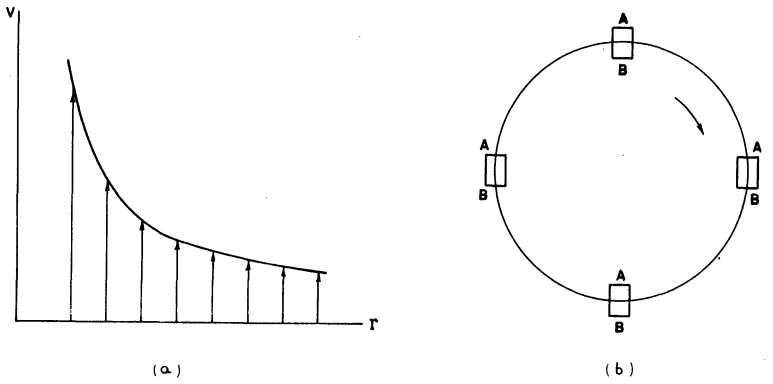

Figure 4-2. Velocity Distribution and Irrotational Motion of Free Vortex

The flow in a free vortex is also irrotational, i.e., an infinitesimal fluid particle does not rotate about its own axis. As shown in Figure (4-2), it has but translational motion, even though it travels a circular path.

The pressure distribution in a free vortex is determined by considering the force balance in Figure (4-1). The centrifugal force on the fluid element is balanced by the resultant force due to pressures over the surfaces. Neglecting infinitesimals of higher order than the first, the force balance in the radial direction is

$$dpdA = (dm)\frac{V^2}{r} = (\rho\ dr\ dA)\frac{V^2}{r}$$

or

$$dp = \frac{V^2}{r}\rho\ dr \tag{4-2}$$

Substituting K/r for V into Equation (4-2) results in

$$dp = \rho\ K^2\ \frac{dr}{r^3}$$

or

$$\frac{dp}{\rho} = K^2\ \frac{dr}{r^3} \tag{4-3}$$

Integrating:

$$\int_1^2 \frac{dp}{\rho} = K^2 \int_1^2 \frac{dr}{r^3}$$

$$\int_0^2 \frac{dp}{\rho} - \int_0^1 \frac{dp}{\rho} = \frac{K^2}{2} \quad \left(\frac{1}{r_1^2} - \frac{1}{r_2^2}\right) = \frac{V_1^2}{2} - \frac{V_2^2}{r}$$

$$\int_0^1 \frac{dp}{\rho} + \frac{V_1^2}{2} = \int_0^2 \frac{dp}{\rho} + \frac{V_2^2}{2} \tag{4-4}$$

For a perfect gas, $\rho = \frac{p}{RT}$, and Equation (4-3) becomes

$$dp = \frac{p}{RT}\ K^2\ \frac{dr}{r^3}$$

or

$$\frac{dp}{p} = \frac{K^2}{RT}\ \frac{dr}{r^3}$$

which integrates into

$$\ln \frac{p_2}{p_1} = \frac{K^2}{2RT} \quad \left(\frac{1}{r_1^2} - \frac{1}{r_2^2}\right) \tag{4-5}$$

Equation (4-4) shows that the total energy in any stream tube is the same as that in any other stream tube. No energy is added to the vortex by torque, and no energy is dissipated by friction.

Having established the existance of a "free vortex" inside the tube, the characteristic properties of such a flow field will now be developed. To this end, and also for the sake of continuity, a certain amount of mathematical derivation is included.

4.3 Circulation of Free Vortex

The potential, or free vortex, is a case of irrotational flow; it describes the motion in whirlpools and tornados, and in its simplest form, is a two-dimensional motion in which the streamlines are concentric circles, with the tangential velocity along any streamline being inversely proportional to the radius of the streamline. The circulation of an area enclosing and not enclosing the origin will now be evaluated for this type of flow.

By definition, the circulation is the line integral of the velocity field around any closed curve. It is the sum of the products of elements $\vec{dl}$ of a curve drawn in the plane of the flow and the corresponding component of velocity tangent to the curve.

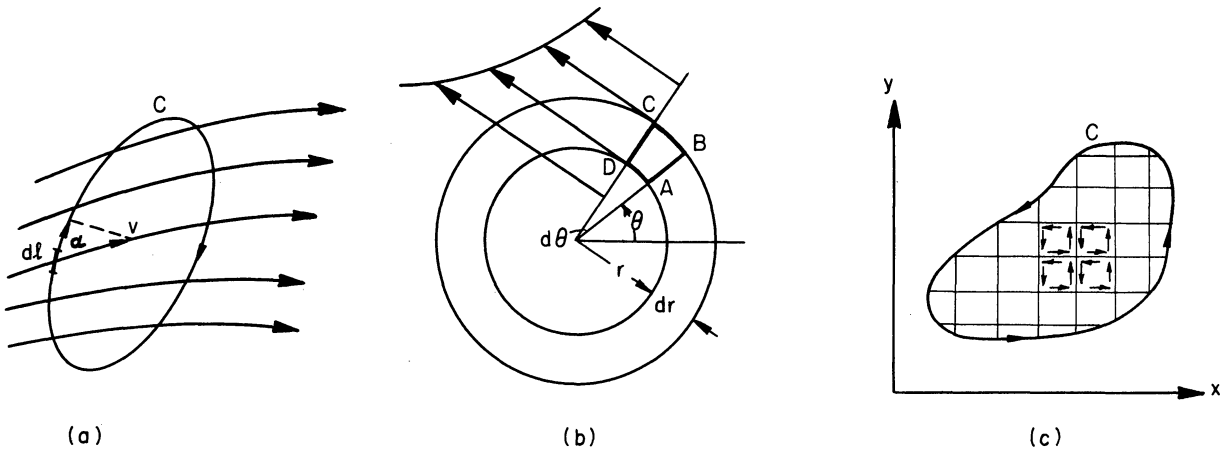

Figure 4-3. Circulation for Free Vortex

Referring to the closed curve c of Figure (4-3), the circulation is

$$\Gamma = \oint_c V \cos \alpha \, dl = \int_c \vec{V} \quad \vec{dl} \tag{4-6}$$

where $\vec{V}$ denotes the velocity vector and $\vec{dl}$ the displacement vector. If u and v denote respectively the velocity components in the x and y directions, then the Cartesian form of Equation (4-6) is

$$\Gamma = \oint (u \, dx + v \, dy) \tag{4-7}$$

Equation (4-6) is now applied to the free vortex. First, consider the circulation around a closed curve enclosing the origin, such as a streamline of radius r in Figure (4-3b). Noting that cos α = cos 0 = 1,

$$\Gamma = \int_0^{2\pi} V \, r d\theta = \int_0^{2\pi} K d\theta = 2\pi K \tag{4-8}$$

Next, consider the circulation around a closed curve not enclosing the origin, such as element ABCD in Figure (4-3b). Noting that the line integral is zero along the sides AB and CD, (cos α = cos $\pi/2$ = 0), the circulation is

$$\Gamma_{ABCD} = (V + dV)(r + dr)\, d\theta - V \, r d\theta$$
$$= (V \, dr + r dV)\, d\theta = \left[d(Vr) \right] d\theta$$

But from the definition of the free vortex, Vr = const. = K, or d(Vr) = 0, and

$$\Gamma_{ABCD} = \left[d(Vr) \right] d\theta = 0 \tag{4-9}$$

The circulation for an element of area not enclosing the origin is thus zero. The circulation for a finite area Figure (4-3c) not enclosing the origin is also zero, since the line integral around the bounding curve of the finite area is the algebraic sum of all the line integrals around the elementary elements comprising the finite area:

$$\Gamma = \oint (u dx + v dy) = \iint_A \left(\frac{\partial v}{\partial x} - \frac{\partial u}{\partial y} \right) dx \, dy = 0 \tag{4-10}$$

Equation (4-10) represents Green's Theorem for the transformation from line integral to surface integral in two-dimensional space, and its truth is evident from the fact that each interior line of each element is traversed twice but in opposite directions, and hence only the exterior line of the elements contribute to the circulation.

It may be noted that the generalization of Equation (4-10) to three dimensional is

$$\Gamma = \oint (u\,dx + V\,dy + w\,dz) = \oint \vec{V} \cdot \vec{dl}$$

$$= \iint \left[\left(\frac{\partial V}{\partial x} - \frac{\partial u}{\partial y}\right) dx\,dy + \left(\frac{\partial w}{\partial y} - \frac{\partial V}{\partial z}\right) dy\,dz + \left(\frac{\partial u}{\partial z} - \frac{\partial w}{\partial x}\right) dz\,dx \right]$$

$$= \iint \vec{\nabla} \times \vec{V} \cdot \vec{dA} \qquad (4\text{-}11)$$

By Equation (4-8), the circulation for any closed curve enclosing the vortex center is $2\pi K$. The rotational properties of the vortex are thus concentrated at its center, a "singular point", where the velocity is infinite and the radius is zero, while the product of the two is the constant K. The circulation Γ about a vortex is a constant, and is a measure of its strength. A vortex may thus be designated by the shorthand rotation Γ  to indicate its strength and direction of rotation, and the velocity at any radius may be expressed in terms of it by

$$V = \frac{\Gamma}{2\pi r} \qquad (4\text{-}12)$$

Figure (4-4) shows the circulation for any closed curve in a field of flow where several vortices are present. It is readily seen how the shorthand notation can be used to advantage.

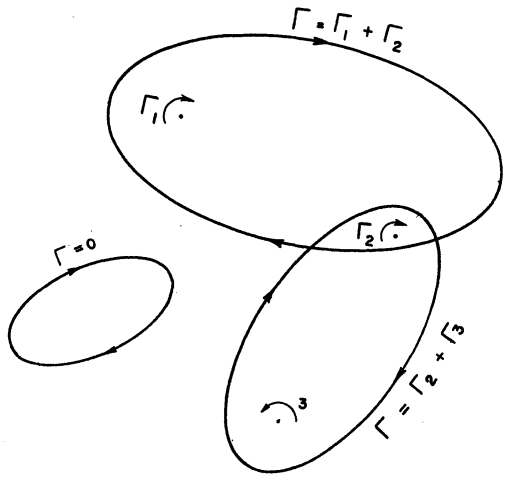

Figure 4-4. Circulation for a Multiple-Vorticity Field

Physically speaking, each particle of fluid in a free vortex undergoes a shearing deformation, but the rotation of each particle is zero. The free vortex is irrotational, except for a singularity at the origin, and is therefore called potential vortex. This is illustrated in Figure (4-2b). An element of fluid will travel in a circle, but if a straight line AB were to be painted on the element, it would be observed that this line has a rectilinear motion, i.e., the line always remains parallel to its original direction and consequently has zero angular velocity.

4.4 Circulation per Unit Area

It is convenient at this point to employ the concept of circulation to define an important kinematical property of the velocity field, namely the curl. Consider the circulation $d\Gamma$ around a small element in the x,y- plane as shown in Figure (4-5).

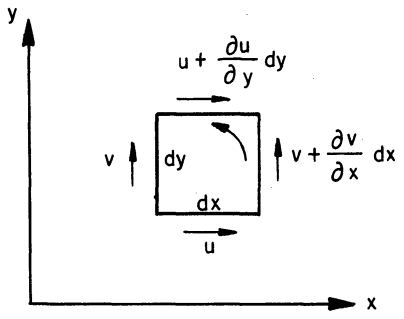

Figure 4-5. Circulation for Element of Area

Using Equation (4-7), and proceeding counter-clockwise, the circulation amounts to:

$$d\Gamma = udx + (v + \frac{\partial v}{\partial x} dx)\, dy - (u + \frac{\partial u}{\partial y} dy)\, dx - vdy$$

$$= (\frac{\partial v}{\partial x} - \frac{\partial u}{\partial y})\, dx\, dy = (\frac{\partial v}{\partial x} - \frac{\partial u}{\partial y})\, dA$$

The circulation per unit area in the xy plane is thus

$$\frac{d\Gamma}{dA} = (\frac{\partial v}{\partial x} - \frac{\partial u}{\partial y}) \qquad (4\text{-}13)$$

Similar expressions may be found for the circulation per unit area in the (yz), and (zx) planes by rotation of indices. This serves to define the curl of a velocity field: it is a vector whose component in any direction $\vec{n}$ is defined as:

$$\text{curl}_n \vec{V} = \lim_{\Delta A \to 0} \frac{\oint \vec{V} \cdot \vec{dl}}{\Delta A} \qquad (4\text{-}14)$$

where ΔA is the area enclosed by the path about which the line integral is taken, and $\vec{n}$ is the direction of the normal to the surface. The sense is given by the right hand rule. It is seen that in vectorial rotation:

$$\text{curl } \vec{V} = (\frac{\partial}{\partial y} w - \frac{\partial}{\partial z} v)\, \vec{i} + (\frac{\partial}{\partial z} u - \frac{\partial}{\partial x} w)\, \vec{j} + (\frac{\partial}{\partial x} v - \frac{\partial}{\partial y} u)\, \vec{k}$$

$$= \vec{\nabla} \times \vec{V} \qquad (4\text{-}15)$$

where

$$\vec{\nabla} = \vec{i} \frac{\partial}{\partial x} + \vec{j} \frac{\partial}{\partial y} + \vec{k} \frac{\partial}{\partial z}$$

is the usual vector differential operator "del" or "nabla".

4.5 Fluid Rotation at a Point

The fluid rotation at a point is the mean angular velocity of two infinitesimal and mutually perpendicular fluid lines instantaneously passing through the point.

To find an analytical expression for the fluid rotation at a point, consider the infinitesimal and mutually perpendicular fluid lines OA and OB in Figure (4-6).

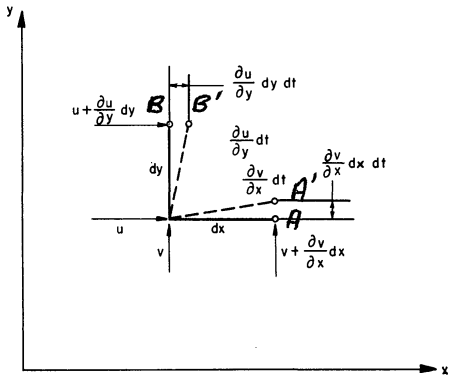

Figure 4-6. Fluid Rotation at a Point

During an infinitesimal time interval dt, OA rotates to position OA', and the vertical displacement is

$$A\,A' = \frac{\partial v}{\partial x}\,dx\,dt$$

The angle AOA', positive when measured counter-clockwise, is

$$\measuredangle AOA' = \frac{\partial v}{\partial x}\,dt$$

and its time rate of change or angular velocity is thus $\frac{\partial v}{\partial x}$.

Similarly, it may be shown that the angular velocity of the fluid line OB is $-\frac{\partial u}{\partial y}$. The average rotation of the fluid element is therefore:

$$\omega_z = \frac{1}{2}\left(\frac{\partial v}{\partial x} - \frac{\partial u}{\partial y}\right) \qquad (4\text{-}16)$$

Referring to Equation (4-13), it is seen that the circulation for unit area is twice the average rotation of the fluid particle:

$$\frac{\partial \Gamma}{\partial A} = \text{curl } \vec{V} = \left(\frac{\partial v}{\partial x} - \frac{\partial u}{\partial y}\right) = 2\omega_z \tag{4-17a}$$

$$\text{vorticity} = \omega_z = \frac{1}{2} \text{ curl } \vec{V}$$

For a free vortex, it was found from Equation (4-10) that the circulation for an area excluding the origin was zero. Therefore, from Equation (4-17a), $\left(\frac{\partial v}{\partial x} - \frac{\partial u}{\partial y}\right)$ must be zero, or $\frac{\partial v}{\partial x} = \frac{\partial u}{\partial y}$, which is the condition for irrotational flow.

For a rotation in space, the x and y components of the rotation vector ω may be found from Equation (4-17a) by rotation of indices, i.e,

$$2\omega_z = \frac{\partial w}{\partial y} - \frac{\partial v}{\partial z} \tag{4-17b}$$

and

$$2\omega_y = \frac{\partial u}{\partial z} - \frac{\partial w}{\partial x} \tag{4-17c}$$

In vectorial notation, the general expression for the "vorticity" or angular velocity vector is thus

$$2\vec{\omega} = \vec{i}\left(\frac{\partial w}{\partial y} - \frac{\partial v}{\partial Z}\right) + \vec{j}\left(\frac{\partial u}{\partial Z} - \frac{\partial w}{\partial x}\right) + \vec{k}\left(\frac{\partial v}{\partial x} - \frac{\partial u}{\partial y}\right) = \nabla \times \vec{V} \tag{4-18}$$

4.6 Shear Deformation Rate and Angular Velocity

Before leaving Figure (4-6), it is of interest to note that the rate of shear deformation in a fluid is defined as the rate of change of the angle between two mutually perpendicular fluid lines. Thus, for the angle between lines OA and OB, the change in angle during a time interval dt is

$$\frac{\partial v}{\partial x} dt + \frac{\partial u}{\partial y} dt$$

and its rate of change is $(\frac{v}{x} + \frac{u}{y})$. Consequently,

$$\text{Rate of shear deformation} = (\frac{\partial v}{\partial x} + \frac{\partial u}{\partial y}) \qquad (4\text{-}19)$$

There is a parallel between these expressions and the corresponding expressions for the deformation of elastic solids. In the case of a fluid particle, velocity is the quantity dealt with, whereas for a deformable solid, it is the displacement. The average rotation of a fluid particle corresponds to the average rotation of a solid particle, and the rate of shear deformation of a fluid particle corresponds to the shear strain of an elastic solid body.

A physical picture of Equations (4-17a) and (4-19) is provided by considering the following two cases;

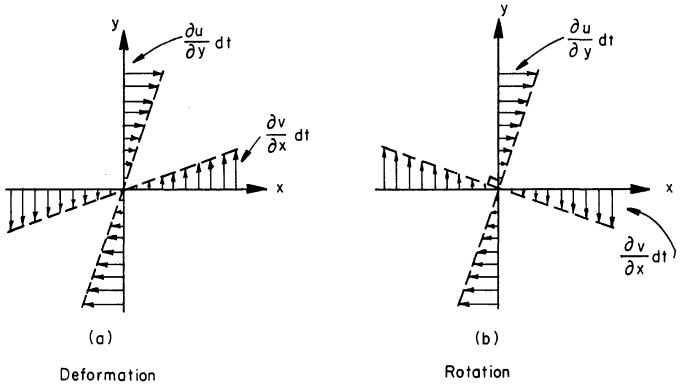

Figure 4-7. Shear Deformation and Rotation

In Figure (4-7a), let $\frac{\partial v}{\partial x}$ and $\frac{\partial u}{\partial y}$ have equal positive values. From Equations (4-17a) and (4-19), the angular velocity vanishes, and the fluid element is undergoing pure shear deformation.

In Figure (4-7b), let $\frac{\partial v}{\partial x}$ and $\frac{\partial u}{\partial y}$ have equal magnitudes, but opposite signs. For this case, Equation (4-19) gives zero strain, and Equation (4-17a) gives a finite value for the rotation. The fluid element undergoes pure rotation. Use of the foregoing will be made in Chapter 10 when viscosity effects are taken into account in the flow field.

4.7 Rotation in Natural Coordinates

It is advantageous, whenever possible, to express the angular velocity or vorticity in terms of the natural coordinates of a system. Referring to Figure (4-8a), let the streamlines and the radius lines (normal) comprise a system of curvilinear coordinates.

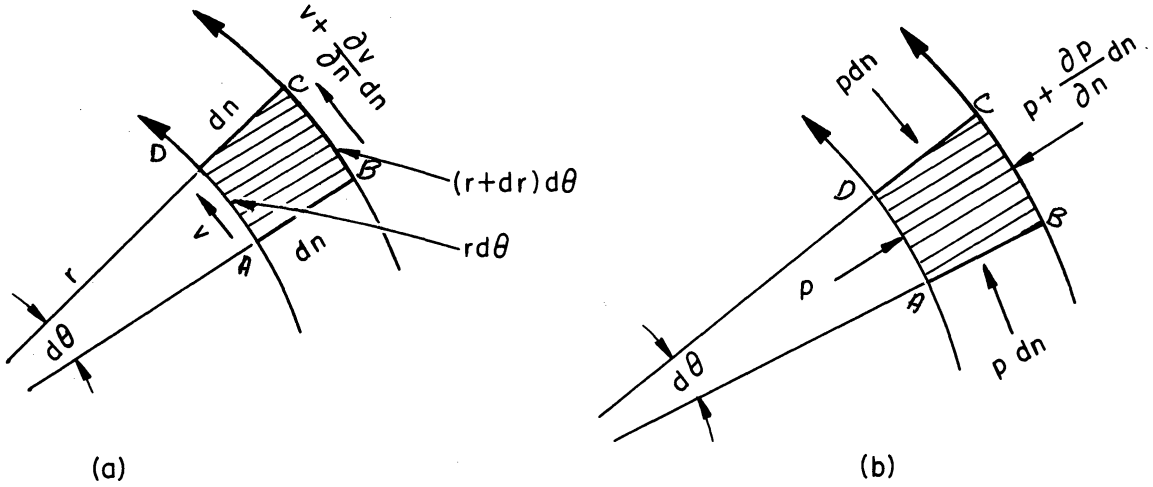

Figure 4-8. Circulation and Rotation in Natural Coordinates

The circulation of element ABCD is

$$d\Gamma = \left(V + \frac{\partial V}{\partial n}\, dn\right)(r + dn)\, d\theta - V\, r\, d\theta$$

$$= \left(r\,\frac{\partial V}{\partial n} + V\right) dn\, d\theta$$

and the rotation is

$$2\omega = \frac{d}{dA} = \frac{\left(r\,\frac{\partial V}{\partial n} + V\right) dn\, d\theta}{r\, dn\, d\theta} = \frac{\partial V}{\partial n} + \frac{V}{r} \qquad (4\text{-}20)$$

The condition of irrotationality in curvilinear coordinates then becomes

$$\frac{\partial V}{\partial n} + \frac{V}{r} = 0$$

or

$$\frac{\partial V}{\partial n} = -\frac{V}{r} \qquad (4\text{-}21)$$

This relation is the restriction that potential flow places upon the flow field in order to achieve mathematical solution.

4.8 Dynamic Equation Normal to Streamlines

This is the statement of Newton's second law of motion in the direction $\vec{n}$ normal to the streamlines. Referring to Figure (4-8b), the mass of the element is $\rho\, r d\theta\, dn$, and its acceleration toward the center of curvature of the streamline is the expression for the centrifugal acceleration V^2/r. In the absence of friction and body forces, the only forces acting are those owing to pressure. The net force along the normal drawn through the center of the element is thus:

$$\left(p + \frac{\partial p}{\partial n}\, dn\right)(r + dn)\, d\theta - p\, r\, d\theta - 2\, p\, dn\, \frac{d\theta}{2}$$

or, after simplification:

$$\frac{\partial p}{\partial n}\, r\, d\theta\, dn$$

This force must, by Newton's law, be equal to the product of mass and acceleration $\rho r d\theta\, dn\, \frac{V^2}{r}$. Thus

$$\frac{\partial p}{\partial n}\, r d\theta\, dn = \rho\, r d\theta\, dn\, \frac{V^2}{r}$$

or

$$\frac{\partial p}{\partial n} = \rho\, \frac{V^2}{r} \qquad (4\text{-}22)$$

In the case of the free vortex, the condition of irrotationality as given by Equation (4-21) is $\frac{V}{r} = -\frac{\partial V}{\partial n}$, and this can be used in Equation (4-22) to integrate it:

$$\frac{p}{n} = -\rho\, V\, \frac{\partial V}{\partial n} = -\rho\, \frac{\partial}{\partial n}\, \frac{V^2}{2}$$

$$\frac{\partial p}{\rho \partial n} + \frac{\partial}{\partial n}\left(\frac{V^2}{2}\right) = 0$$

and since this relation is true regardless of the normal that was chosen,

$$\int \frac{dp}{\rho} + \frac{V^2}{2} = \text{constant} \qquad (4\text{-}23)$$

which agrees with the previous result provided by Equation (4-3) that the total energy in any stream tube is equal to that in any other stream tube.

4.9 Crocco's Theorem

This theorem provides the connection between the rotation and the thermodynamic properties of the flow. Consider the stagnation or total enthalpy h_o. It is related to the velocity and the static enthalpy by

$$h_o = h + \frac{V^2}{2} \qquad (4\text{-}24)$$

or, differentiating in the n-direction.

$$\frac{\partial h_o}{\partial n} = \frac{\partial h}{\partial n} + V \frac{\partial V}{\partial n} \qquad (4\text{-}25)$$

The first law of thermodynamics and the definition of enthalpy yield

$$Tds = du + pdv$$

$$dh = du + pdv + vdp$$

Hence

$$Tds = dh - vdp$$

$$= dh - \frac{1}{\rho} dp \qquad (4\text{-}26)$$

and this may be differentiated to give

$$T \frac{\partial s}{\partial n} = \frac{\partial h}{\partial n} - \frac{1}{\rho} \frac{\partial p}{\partial n}$$

or

$$\frac{1}{\rho} \frac{\partial p}{\partial n} = - T \frac{\partial s}{\partial n} + \frac{\partial h}{\partial n}$$

and, replacing h in terms of h_o as per Equation (4-25):

$$\frac{1}{\rho}\frac{\partial p}{\partial n} = -T\frac{\partial s}{\partial n} + \frac{\partial}{\partial n}h_o - V\frac{\partial V}{\partial n}$$

or

$$\frac{1}{\rho V}\frac{\partial p}{\partial n} = -\frac{T}{V}\frac{\partial s}{\partial n} + \frac{1}{V}\frac{\partial}{\partial n}h_o - \frac{\partial V}{\partial n} \qquad (4\text{-}27)$$

The rotation, as given by Equation (4-20) is

$$2\omega = \frac{\partial V}{\partial n} + \frac{V}{r}$$

which, with the aid of Equation (4-22), can be written as

$$2\omega = \frac{\partial V}{\partial n} + \frac{1}{\rho V}\frac{\partial p}{\partial n} \qquad (4\text{-}28)$$

Finally, replacing the second term of the right hand side of this expression by its equivalent as given in Equation (4-27) yields

$$2\omega = \frac{\partial V}{\partial n} - \frac{T}{V}\frac{\partial s}{\partial n} + \frac{1}{V}\frac{\partial}{\partial n}h_o - \frac{\partial V}{\partial n} \qquad (4\text{-}29)$$

$$= \frac{1}{V}\left(\frac{\partial h_o}{\partial n} - T\frac{\partial s}{\partial n}\right) \qquad (4\text{-}30)$$

which is the special form for Crocco's Theorm in two dimensional flow. Equation (4-30) enables the calculation of the thermodynamic properties of the flow field within the vortex tube.

4.10 Velocity Induced by Vortex Filament

The two-dimensional velocity field previously described is a vortex flow in the xy-plane, with the point vortex at the origin of coordinates. This means that the flow pattern is identical in all planes parallel to the xy-plane from $-\infty$ to $+\infty$. The point vortex is duplicated in every parallel plane, the configuration of the points forming a straight line perpendicular to the xy-plane and extending from $-\infty$ to $+\infty$. In space, such a line is called a vortex filament,

and it may be visualized as the line around which successive fluid elements travel.

It is of interest to detemine the velocity induced in a region surrounding the vortex filament by an element dz of the filament. Figure (4-9) shows a vortex filament of infinite length normal to the xy-plane.

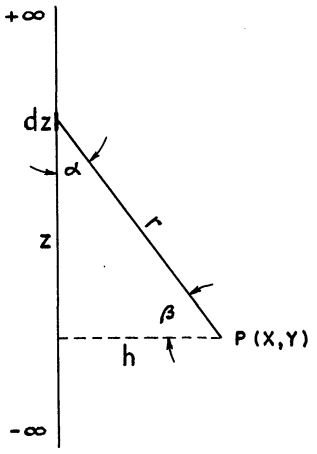

Figure 4-9. Velocity Induced by Vortex Filament

The velocity induced at point P by an element dz of the filament is determined from the Biot-Savart law, which states that an element dz of a vortex filament of strength Γ induces at a point P the velocity

$$dV = \frac{\Gamma}{4\pi} \frac{\sin \alpha}{r^2} dz \qquad (4\text{-}31)$$

where r is the distance from the element to P, and α is the angle between the radius vector from the element to P and the filament. The induced velocity lies in a plane through P perpendicular to the element of filament. It is seen that Equation (4-31) is analogous to the law concerning the strength of a magnetic field induced in a region surrounding a wire that is carrying a current.

The velocity at P indiced by the entire filament is obtained by integrating Equation (4-31)

$$V = \int_{-\infty}^{+\infty} \frac{\Gamma}{4\pi} \frac{\sin \alpha}{r^2} \, dz \tag{4-32}$$

To solve Equation (4-32), express everything in terms of h and β:

$$z = h \tan \beta; \quad dz = h \sec^2 \beta \, d\beta:$$

$$r = h \sec \beta$$

$$\sin \alpha = \cos \beta$$

Thus:

$$V = \int_{-\frac{\pi}{2}}^{+\frac{\pi}{2}} \frac{\Gamma}{4\pi} \frac{\cos \beta}{h^2 \sec^2 \beta} h \sec^2 \beta \, d\beta$$

$$= \int_{-\frac{\pi}{2}}^{+\frac{\pi}{2}} \frac{\Gamma}{4\pi} \frac{\cos \beta}{h} \, d\beta = \frac{\Gamma}{4\pi h} \left[\sin \beta\right]_{-\frac{\pi}{2}}^{+\frac{\pi}{2}}$$

$$= \frac{\Gamma}{2\pi h} \tag{4-33}$$

This is precisely the velocity induced at P due to a point vortex at the origin as given by Equation (4-12); this is a necessary agreement for consistency between the two and three-dimensional cases.

4.11 Vorticity Theorems

It is of interest to include in the present study of vorticity fields several important theorems which govern their behavior. These theorems are:

Helmholtz's First Theorem: In a perfect fluid, the strength of a vortex filament is constant along its length.

The proof of this statement is shown by the following device. Enclose a segment of the vortex filament with a sheath from which a slit has been removed, as shown in Figure (4-10).

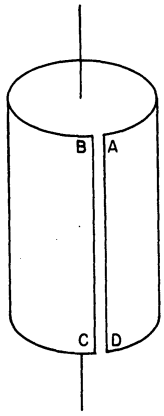

Figure 4-10. Demonstration of Helmholtz's Theorem

The cylindrical surface enclosed by the perimeter ABCD contains no vortex points, hence the curl of the velocity at every point on the surface is zero, and it follows by Stokes' Theorem that the line integral of the velocity along the perimeter is also zero. In traversing the perimeter, the constributions to the total circulation of the line integrals from B to C and from D to A are of equal magnitude and opposite sign, assuming the slit to be narrow. This means that for the total circulation to be zero, the remaining line integrals from A to B and C to D must also be of equal magnitude and opposite sign. The consequence of this is that the vorticity enclosed by the top and bottom perimeters of the cylinder is the same, which means that the vortex filament stays constant in strength.

Helmholtz's Second Theorem: In a perfect fluid, a vortex filament can neither begin nor end; it must extend to the boundaries of the fluid, or form a closed path, or extend to infinity.

To prove this, simply revert to the demonstration of Figure (4-10): assume the split sheath so placed that the filament ends

midway between the top and bottom edges. The line integrals around the sheath from A to B and from C to D are then no longer of equal magnitude and opposite sign, and the condition of zero circulation around the perimeter can no longer be maintained. Since this violates the state of irrotationality of the cylindrical flow surface, the ending of the vortex filament within the sheath cannot hold.

Helmholtz's Third Theorem (Kelvin's Theorem): In a perfect fluid, in the absence of rotational external forces, a fluid that is initially irrotational remains irrotational.

A simple proof of this is obtained from Crocco's Theorem, Equation (4-30). If the fluid is originally in parallel motion with uniform properties, and if the fluid along each streamline undergoes adiabatic, reversible changes, it follows from Equation (4-30) that the flow is everywhere irrotational since both terms of the right hand side of the equation are zero. But the stipulation of reversible flow is precisely equivalent to the statement that there is no frictional forces in the fluid.

Finally, a corollary may be added to these vorticity theorems. From Stokes; theorem, it can be stated that: In a perfect fluid, in the absence of rotational forces, if the circulation around a closed path enclosing a definite group of fluid particles is initially zero, it will remain zero.

These theorems apply to perfect fluids, or fluids with small viscosity. The effect of frictional forces on the "free-vortex" field will be considered in Chapter 10.

CHAPTER 5

INTRINSIC EQUATIONS OF COMPRESSIBLE FLOW

5.1 Differential Equations of Fluid Motion

Before attempting the mathematical solution for the flow field inside the vortex tube, it is necessary to express in differential form the physical principles which the flow must satisfy in order to possibly exist. The equations of fluid dynamics can be expressed in two different forms, Lagrange's form, and Euler's form. The Lagrangian method describes the motion in terms of the paths of the individual particles of gas, i.e., the coordinates x, y, z of the particles as functions of the time t and three parameters a, b, c, which characterize the individual particle. The Eulerian method directs attention to definite points (x,y,z), and to what happens in the course of time t. The motion is then described by giving as functions of x, y, z, and t the velocity components u, v, and $\dot{w}$ of the particle that happens to be at the point (x,y,z) at the time t. It is Euler's representation which is adopted in the present work.

The basic relations which govern the motion of a fluid medium, except at discontinuities, are i) the equation of continuity, ii) the equation of motion, iii) the reversible-adiabatic change of state relation, and iv) the equation of state of the medium.

These equations, together with the condition of irrotationality, form the basis upon which a mathematical solution is built, and because of their importance, they will be developed in some detail.

5.2 Equation of Continuity

To express the principle of conservation of mass, consider the infinitesimal cube of fluid shown in Figure (5-1).

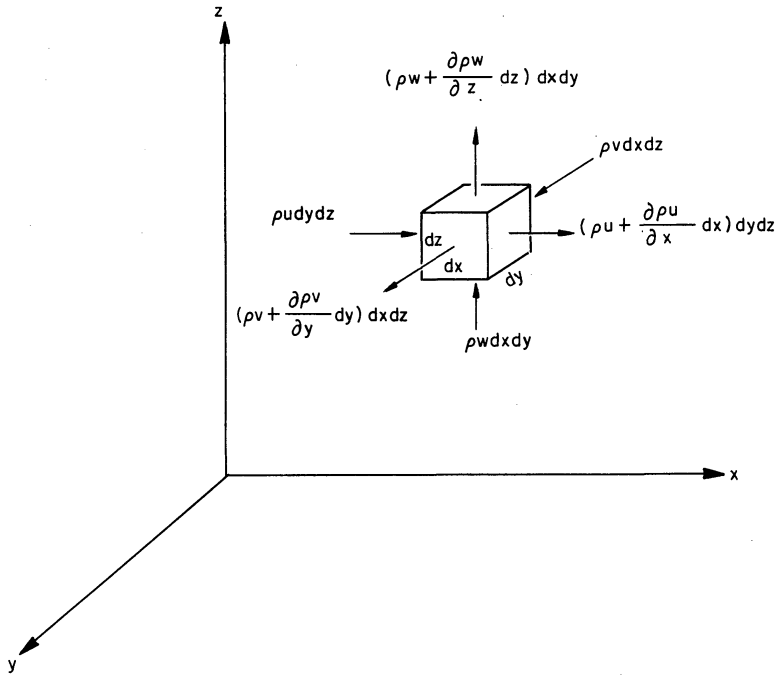

Figure 5-1. Interpretation of Divergence

Let dx, dy, dz be the dimensions of the cube. The fluid mass entering the cube in the x direction is then $(\rho\, u\, dy\, dz)$, and the fluid mass leaving the cube in the same direction is $(\rho u + \frac{\partial \rho u}{\partial x} dx)(dy\, dz)$. The mass flux in the x direction is thus

$$\rho\, u\, dy\, dz - (\rho\, u + \frac{\partial \rho u}{\partial x} dx)\, dy\, dz = - \frac{\partial \rho u}{\partial x} dx\, dy\, dz$$

Similarly, the mass flux in the y direction is $- \frac{\partial \rho v}{\partial y} dx\, dy\, dz$, and the mass flux in the z direction is $- \frac{\partial \rho w}{\partial z} dx\, dy\, dz$. The mass flux through the entire cube is thus

$$- \left[\frac{\partial (\rho u)}{\partial x} + \frac{\partial (\rho v)}{\partial y} + \frac{\partial (\rho w)}{\partial z} \right] dx\, dy\, dz \qquad (5\text{-}1)$$

which, per unit volume, becomes

$$-\left[\frac{\partial(\rho u)}{\partial x} + \frac{\partial(\rho v)}{\partial y} + \frac{\partial(\rho w)}{\partial z}\right] = -\,\mathrm{div}(\rho\vec{q}) \qquad (5\text{-}2)$$

where $\vec{q}$ is the flow velocity.

The mass flux must, of course, equal to the change of density $\frac{\partial \rho}{\partial t}$ at the point in question. Thus:

$$-\,\mathrm{div}\,(\rho\vec{q}) = \frac{\partial \rho}{\partial t}$$

or

$$\mathrm{div}\,(\rho\vec{q}) + \frac{\partial \rho}{\partial t} = 0 \qquad (5\text{-}3)$$

Equation (5-3) is the continuity equation, and in Cartesian form, is written as

$$\frac{\partial(\rho u)}{\partial x} + \frac{\partial(\rho v)}{\partial y} + \frac{\partial(\rho w)}{\partial z} + \frac{\partial \rho}{\partial t} = 0 \qquad (5\text{-}4)$$

For steady-flow, the field properties are not functions of time, and Equation (5-4) reduces to

$$\frac{\partial(\rho u)}{\partial x} + \frac{\partial(\rho v)}{\partial y} + \frac{\partial(\rho w)}{\partial z} = 0 \qquad (5\text{-}5)$$

Finally, if the flow is both steady and incompressible, then

$$\frac{\partial u}{\partial x} + \frac{\partial v}{\partial y} + \frac{\partial w}{\partial z} = 0 \qquad (5\text{-}6)$$

5.3 Equation of Motion

In this section, the application of Newton's second law of motion to a fluid flowing without friction is considered. This assumption is valid since at present, the boundary layer is excluded from the region of flow.

Newton's second law states that the time rate of change of momentum of a mass particle is equal to the sum of the external forces acting on the particle in both magnitude and direction. In Figure (5-2),

let dx, dy, dz be an incremental volume of fluid.

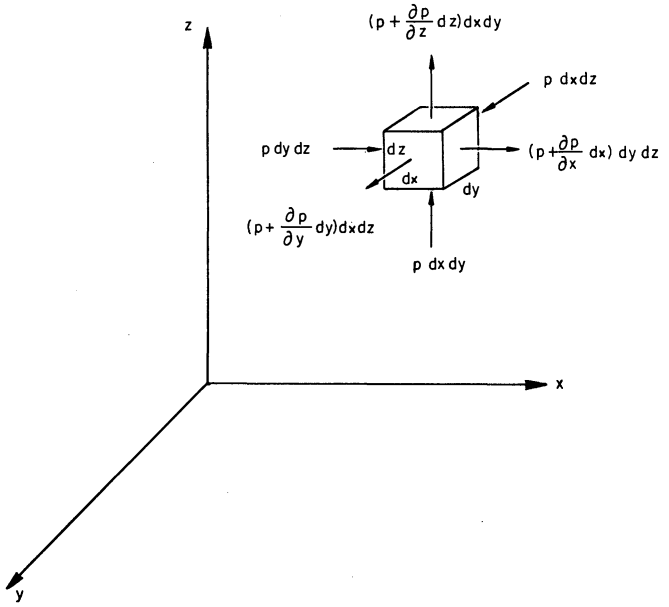

Figure 5-2. Pressure Forces on Fluid Element

The mass of the fluid element being (ρ dx dy dz), Newton's second law, namely that the time rate of change of momentum equals the sum of external forces becomes

$$\Sigma \vec{F} = \frac{D}{Dt} \quad (\rho \; dx \; dy \; dz) \; \vec{q} \tag{5-7}$$

The symbol $\frac{D}{Dt}$ represents the substantive or total derivative with respect to time, and denotes that the differentiation is to be carried out while following the fluid particle. This is because in general, the velocity $\vec{q}$ (x, y, z, t) is a function of time as well as of the coordinates of the field. Because a fixed mass (ρ dx dy dz) is being dealt with, Equation (5-7) is more conveniently written as

$$\Sigma \vec{F} = (\rho \; dx \; dy \; dz) \; \frac{D}{Dt} \; \vec{q}$$

which, in Cartesian coordinates becomes

$$\Sigma F_x = (\rho \; dx \; dy \; dz) \; \frac{Du}{Dt} \tag{5-8a}$$

$$\Sigma F_y = (\rho \; dx \; dy \; dz) \; \frac{Dv}{Dt} \tag{5-8b}$$

$$\Sigma F_z = (\rho \; dx \; dy \; dz) \; \frac{Dw}{Dt} \tag{5-8c}$$

where

$$\frac{Du}{Dt} = \frac{u_{x + dx,\ y + dy,\ z + dz,\ t + dt} - u_{x,y,z,t}}{dt}$$

$$= \frac{\partial u}{\partial x} dx + \frac{\partial u}{\partial y} dy + \frac{\partial u}{\partial z} dz + \frac{\partial u}{\partial t} dt$$

$$= u \frac{\partial u}{\partial x} + v \frac{\partial u}{\partial y} + w \frac{\partial u}{\partial z} + \frac{\partial u}{\partial t} \qquad (5\text{-}9a)$$

The first three terms of the right hand side of Equation (5-9a) form the convective acceleration, whereas the last term is the local acceleration. Likewise,

$$\frac{Dv}{Dt} = u \frac{\partial v}{\partial x} + v \frac{\partial v}{\partial y} + w \frac{\partial v}{\partial z} + \frac{\partial v}{\partial t} \qquad (5\text{-}9b)$$

$$\frac{Dw}{Dt} = u \frac{\partial w}{\partial x} + v \frac{\partial w}{\partial y} + w \frac{\partial w}{\partial z} + \frac{\partial w}{\partial t} \qquad (5\text{-}9c)$$

As for the forces, the resultant pressure force in the direction of each of the x,y,z axes is

$$p\ dy\ dz - \left(p + \frac{\partial p}{\partial x} dx\right) dy\ dz = - \frac{\partial p}{\partial x} dx\ dy\ dz \qquad (5\text{-}10a)$$

$$p\ dx\ dz - \left(p + \frac{\partial p}{\partial y} dy\right) dx\ dz = - \frac{\partial p}{\partial y} dx\ dy\ dz \qquad (5\text{-}10b)$$

$$p\ dx\ dy - \left(p + \frac{\partial p}{\partial z} dz\right) dx\ dy = - \frac{\partial p}{\partial z} dx\ dy\ dz \qquad (5\text{-}10c)$$

Equations (5-10a,b,c) show that the resultant pressure force on the fluid is seen to be the negative of the pressure gradient multiplied by the incremental volume. Thus:

$$\text{pressure force} = - (\text{grad } p)\ dx\ dy\ dz \qquad (5\text{-}11)$$

In the absence of body forces, such as gravity, electromagnetic, etc.,

Equation (5-11) or its equivalent, Equation (5-10) represents all the external forces acting on the fluid particle. Inserting the expressions for ΣF_x, ΣF_y, and ΣF_z from equations (5-10a,b,c) and the expressions for $\frac{Du}{Dt}$, $\frac{Dv}{Dt}$, and $\frac{Dw}{Dt}$ from equations (5-9a,b,c), and simplifying, the following is obtained:

$$u\frac{\partial u}{\partial x} + v\frac{\partial u}{\partial y} + w\frac{\partial u}{\partial z} + \frac{\partial u}{\partial t} + \frac{1}{\rho}\frac{\partial p}{\partial x} = 0 \qquad (5\text{-}12a)$$

$$u\frac{\partial v}{\partial x} + v\frac{\partial v}{\partial y} + w\frac{\partial v}{\partial z} + \frac{\partial v}{\partial t} + \frac{1}{\rho}\frac{\partial p}{\partial y} = 0 \qquad (5\text{-}12b)$$

$$u\frac{\partial w}{\partial x} + v\frac{\partial w}{\partial y} + w\frac{\partial w}{\partial z} + \frac{\partial w}{\partial t} + \frac{1}{\rho}\frac{\partial p}{\partial z} = 0 \qquad (5\text{-}12c)$$

Equations (5-12a, b, c) are the Euler's equation of motion, and in vectorial notation, may be written simply as

$$\frac{D\vec{q}}{Dt} + \frac{1}{\rho}\,\text{grad}\, p = 0 \qquad (5\text{-}13)$$

where the derivative $\frac{D}{Dt}$ represents the substantive or total derivative.

There are two sets of circumstances for which the system of Equations (5-12) can be integrated: first, along a streamline; and second, throughout the entire flow field, provided that the flow be irrotational.

To integrate along a streamline, consider the fact that at each instant, the velocity vector being tangent to the streamline, the equation for the latter is then given by

$$\frac{dy}{dx} = \frac{v}{u}\ ;\ \frac{dz}{dy} = \frac{w}{v}\ ;\ \frac{dx}{dz} = \frac{u}{w} \qquad (5\text{-}14)$$

Multiplying Equations (5-12) by dx, dy, and dz respectively, assuming

steady-state conditions, and making use of Equations (5-14), there is obtained:

$$-\frac{1}{\rho}\frac{\partial p}{\partial x}dx = u\frac{\partial u}{\partial x}dx + v\frac{\partial u}{\partial y}dx + w\frac{\partial u}{\partial z}dx = u\frac{\partial u}{\partial x}dx + u\frac{\partial u}{\partial y}dy + u\frac{\partial u}{\partial z}dz$$

$$-\frac{1}{\rho}\frac{\partial p}{\partial y}dy = u\frac{\partial v}{\partial x}dy + v\frac{\partial v}{\partial y}dy + w\frac{\partial v}{\partial z}dy = v\frac{\partial v}{\partial x}dx + v\frac{\partial v}{\partial y}dy + v\frac{\partial v}{\partial z}dz$$

$$\frac{1}{\rho}\frac{\partial p}{\partial z}dz = u\frac{\partial w}{\partial x}dz + v\frac{\partial w}{\partial y}dz + w\frac{\partial w}{\partial z}dz = w\frac{\partial w}{\partial x}dx + w\frac{\partial w}{\partial y}dy + w\frac{\partial w}{\partial z}dz$$

Adding the three equations results in

$$-\frac{1}{\rho}\left(\frac{\partial p}{\partial x}dx + \frac{\partial p}{\partial y}dy + \frac{\partial p}{\partial z}dz\right) = u\frac{\partial u}{\partial x}dx + u\frac{\partial u}{\partial y}dy + u\frac{\partial u}{\partial z}dz$$

$$+ v\frac{\partial v}{\partial x}dx + v\frac{\partial v}{\partial y}dy + v\frac{\partial v}{\partial z}dz$$

$$+ w\frac{\partial w}{\partial x}dx + w\frac{\partial w}{\partial y}dy + w\frac{\partial w}{\partial z}dz$$

which can be written as

$$-\frac{1}{\rho}dp = udu + vdv + wdw = d\left(\frac{u^2 + v^2 + w^2}{2}\right)$$

or

$$\frac{dp}{\rho} + d\left(\frac{q^2}{2}\right) = 0 \qquad (5\text{-}15)$$

where $q = (u^2 + v^2 + w^2)^{1/2}$ is the magnitude of the flow velocity.

Equation (5-15) is integrated to

$$\int \frac{dp}{\rho} + \frac{q^2}{2} = \text{constant (along a streamline)} = \frac{q_{max}^2}{2} \qquad (5\text{-}16)$$

The integration constant in Equation (5-16) is the Bernoulli constant, and it has the same value from any point to another point of a given streamline. For different streamlines, it will assume different values, unless, of course, all streamlines are from a region of uniform velocity, in which case the same constant would prevail throughout the flow field.

For the general case, Bernoulli's constant, $\frac{1}{2} q_{max}^2$ may, of course, have different values along different streamlines. The same is true of the entropy s, which is also constant along each streamline. The rates of change of the Bernoulli constant and the entropy across the streamlines are coupled with the vorticity of the flow. For, Equation (5-13) may be rewritten with the use of the enthalpy equation

$$dh = d\,(u + pv) = Tds + vdp = Tds + \frac{dp}{\rho} \qquad (5\text{-}17)$$

into the form of

$$d(\vec{q}) + \text{grad } h = T \text{ grad } s \qquad (5\text{-}18)$$

Expanding and rearranging terms, there is obtained

$$\frac{\partial \vec{q}}{\partial t} + \frac{1}{2} \text{ grad } q^2 - \vec{q} \times \text{curl } \vec{q} + \text{grad } h = T \text{ grad } s \qquad (5\text{-}19)$$

Now, the adiabatic change of state relation in its vector form

$$\frac{\partial s}{\partial t} + \vec{q} \cdot \text{grad } s = 0;\ \vec{q} \cdot \text{grad } s = 0 \text{ (steady-state)} \qquad (5\text{-}20)$$

yields, with the use of Equation (5-18)

$$\vec{q} \cdot d(\vec{q}) + \vec{q} \cdot \text{grad } h = \frac{d}{dt}\left(\frac{1}{2} q^2 + h\right) = \vec{q} \cdot T \text{ grad } s = 0$$

from which

$$\frac{1}{2} q^2 + h = \text{constant} = \frac{1}{2} q_{max}^2 \qquad (5\text{-}21)$$

Equation (5-21) is known as the Bernoulli law, and is a particular form of the energy relation. With it, Equation (5-19) may be written as

$$\text{grad } \frac{1}{2} q_{max}^2 - T \text{ grad } s = \vec{q} \times \text{curl } \vec{q} \qquad (5\text{-}22)$$

An immediate conclusion to be drawn from this equation is that in the case of steady flow which is irrotational (curl $\vec{q} = 0$), and isentropic (grad $s = 0$), the Bernoulli constant $\frac{1}{2} q_{max}^2$ is the same on every streamline in the region. This is the strong form of Bernoulli's law. A similar conclusion is arrived at by integrating Euler's equation throughout the flow field, provided that irrotational flow (curl $\vec{q} = 0$) be assumed. For, again multiplying Equations (5-12) by dx, dy, and dz respectively, assuming steady-state conditions, and making use of the irrotationality conditions

$$\frac{\partial v}{\partial x} - \frac{\partial u}{\partial y} = 0; \quad \frac{\partial w}{\partial y} - \frac{\partial v}{\partial z} = 0; \quad \frac{\partial u}{\partial z} - \frac{\partial w}{\partial x} = 0$$

instead of restricting to a streamline, results in

$$-\frac{1}{\rho}\frac{\partial p}{\partial x} dx = u\frac{\partial u}{\partial x} dx + v\frac{\partial u}{\partial y} dx + w\frac{\partial u}{\partial z} dx = u\frac{\partial u}{\partial x} dx + v\frac{\partial v}{\partial x} dx + w\frac{\partial w}{\partial x} dx$$

$$-\frac{1}{\rho}\frac{\partial p}{\partial y} dy = u\frac{\partial v}{\partial x} dy + v\frac{\partial v}{\partial y} dy + w\frac{\partial v}{\partial z} dy = u\frac{\partial u}{\partial y} dy + v\frac{\partial v}{\partial y} dy + w\frac{\partial w}{\partial y} dy$$

$$-\frac{1}{\rho}\frac{\partial p}{\partial z} dz = u\frac{\partial w}{\partial x} dz + v\frac{\partial w}{\partial y} dz + w\frac{\partial w}{\partial z} dz = u\frac{\partial u}{\partial z} dz + v\frac{\partial v}{\partial z} dz + w\frac{\partial w}{\partial z} dz$$

Adding the three equations yields

$$-\frac{1}{\rho}\left[\frac{\partial p}{\partial x} dx + \frac{\partial p}{\partial y} dy + \frac{\partial p}{\partial z} dz\right] = udu + vdv + wdw$$

$$= d\left(\frac{u^2}{2}\right) + d\left(\frac{v^2}{2}\right) + d\left(\frac{w^2}{2}\right) \qquad (5\text{-}23)$$

which integrates into

$$\int \frac{dp}{\rho} + \frac{q^2}{2} = \text{constant through the flow field}$$

$$= \frac{q_{max}^2}{2} \qquad (5\text{-}24)$$

where $q = (u^2 + v^2 + w^2)^{1/2}$. For irrotational flow, the Bernoulli constant is the same for all streamlines, and Equation (5-24) may be used for relating the flow properties between any two points in the field of flow. The assumption of irrotationality is thus an important simplification.

5.4 Reversible Adiabatic Change of State

Unless discontinuities exist in the flow field, it is possible to assume that the specific entropy has the same value throughout the medium for irrotational flow, and that it retains this value throughout the medium for all time. Thus:

$$\frac{\partial s}{\partial t} + u \frac{\partial s}{\partial x} + v \frac{\partial s}{\partial y} + w \frac{\partial s}{\partial z} = 0 \qquad (5\text{-}25)$$

This simplifies the mathematical situation by thinking of s as a constant, and thus eliminating one equation and one unknown.

More important yet, is the fact that such an assumption enables the solution of the flow without requiring an energy relation in addition to Euler's equation. This is because an integral of Euler's equation involves only those energies which are associated with inertia forces and pressure forces. If thermal energy is added to a flow either by direct application of heat from an outside source or by dissipation of the fluid's kinetic energy through viscous effects, a more general energy relation, one which includes thermal effects, is needed. Equation (5-21), when written in the form

$$1/2\ q^2 + u + \frac{p}{\rho} = \text{constant} \qquad (5\text{-}25)$$

does represent the energy equation, however, in the case of reversible adiabatic flow. For, by using the equation of state and replacing u by $c_v T$, it may be written as

$$1/2\ q^2 + (c_v + R)T = \text{constant}$$

or, since $(c_v + R) = c_p T$,

$$1/2\ q^2 + c_p = \text{constant} = c_p T_o \qquad (5\text{-}26)$$

Although shear stresses have been neglected in obtaining Equation (5-26), the usefulness of the latter may be vastly increased by the following consideration. The dissipation of kinetic energy $1/2\ q^2$ of the fluid in overcoming friction is accompanied by the generation of an equivalent amount of heat. If the process is adiabatic, this heat remains in the fluid element and produces a temperature rise which is reflected in the temperature dependent term $c_p T$. Thus, the sum $1/2\ q^2 + c_p T$ remains constant even though shearing stresses may be present.

5.5. Equation of State

Except where the motion is discontinuous, the fluid medium may be idealized, and viscosity, heat conduction, and deviation from thermodynamic equilibrium may be neglected. At each instant and each point of the fluid, there is a definite thermodynamic state defined by: p - the pressure, t - the temperature, v - the specific volume, ρ - the density, s - the entropy, u - the internal energy, and h - the enthalpy.

From thermodynamics, it is known that for any given medium, only two of these parameters are independent, i.e., only two properties are required to specify the state of the system. In fact, they may all be considered as functions of v and s. The functions giving p in terms of v or ρ, and s, occur frequently in fluid flow; they are noted by

$$p = f(v, s) = g(\rho, s) \tag{5-27}$$

and are often labeled as the caloric equation of state of the medium. When viscosity and heat conduction are neglected, Equations (5-27) become functions of only v and ρ respectively, since the entropy remains fixed, and the equations

$$p = f(v) = g(\rho) \tag{5-28}$$

then become the reversible adiabatic equation.

It is a fundamental property of all actual media that, entropy remaining constant, the pressure increases with increasing density, i.e.:

$$\frac{\partial}{\partial \rho} g(\rho,s) > 0; \quad \frac{\partial}{\partial v} f(v,s) < 0 \tag{5-29}$$

except in the limiting case $\rho = 0$, for which $\frac{\partial}{\partial \rho} g(\rho,s) = 0$. Equation (5-29) defines a positive quantity c, with the dimension of speed, by setting

$$c^2 = \frac{\partial}{\partial \rho} g(\rho,s) = \frac{\partial p}{\partial \rho} \tag{5-30}$$

$$\rho^2 c^2 = - \frac{\partial}{\partial v} f(v,s) = - \frac{\partial p}{\partial v} \tag{5-31}$$

The quantity c is the speed of sound, and the quantity ρc is often labeled the acoustic impedence.

As for the definition of a perfect gas, it is in two parts. First, in practically all applications, the medium may, with sufficient accuracy, be assumed to obey the laws of Boyle and Gay-Lussac as expressed by the equation of state

$$pv = \frac{p}{\rho} = RT \tag{5-32}$$

In an ideal gas the internal energy is a function of the temperature alone. If, in particular, the internal energy is simply proportional to the temperature, the gas is called polytropic, and the internal energy is expressed as $u = c_v T$ where c_v is a constant.

The second part of the definition of a perfect gas involves gases which obey Equation (5-32), but have specific heats varying with temperature. These gases are labeled "semi-perfect" gases.

The assumption of a polytropic gas is adopted in the present work. It leads, together with Equation (5-32), to the entropic equation of state

$$p = g(\rho,s) = A\rho^{\gamma} \tag{5-33}$$

in which the coefficient A depends on the entropy s, and the adiabatic exponent γ is a constant (= 1.4 for air), and

$$A = (\gamma - 1) \exp c_v^{-1} (s - s_o) \tag{5-34}$$

It is of interest to note that in gases, the pressure depends noticeably on the specific entropy, whereas in liquids, the influence of entropy change is negligible, so that p may be considered as a function of density alone, i.e., $p = g(\rho) = f(v)$, and as a consequence, the internal energy relation

$$du = Tds - pdv \tag{5-35}$$

becomes an equation of the variables separable type. The internal energy may be then written as

$$u = u(v) + u(s) \tag{5-36}$$

Conversely, separable energy, as expressed by Equation (5-36), implies the entropic equation of state $p = f(v) = g(\rho)$. Similarly, the condition that T depends only on s is equivalent to that of separable energy. The most noteworthy example of medium with separable energy is water. Its caloric equation of state is

$$p = A \left(\frac{\rho}{\rho_o}\right)^{\gamma} - B \tag{5-37}$$

where ρ_o is the density at 0° Centigrade, A, B, γ are independent of entropy, and have the values of A = 3001 atm, B = 3000 atm, and $\gamma = 7$.

Assuming a perfect gas, the following relations will be of future usefulness.

$$dh = c_p dT;\ c_p = \left(\frac{\partial h}{\partial T}\right)_p = \frac{\partial}{\partial T}(u + pv) = \frac{du}{dT} + \frac{d}{dT} RT = c_v + R \tag{5-38}$$

$$\gamma = \frac{c_p}{c_v};\ c_p = \frac{\gamma}{\gamma - 1} R;\ c_v = \frac{R}{\gamma - 1} \tag{5-39}$$

$$ds = \frac{du}{T} + \frac{pdv}{T} = c_v \frac{dT}{T} + R \frac{dv}{v} = c_v \frac{dT}{T} - R \frac{d\rho}{\rho} = d \ln \frac{T^{c_v}}{\rho^R} \tag{5-40}$$

$$s - s_o = c_v \ln \frac{T}{T_o} + R \ln \frac{v}{v_o} = c_v \ln \left(\frac{T}{T_o}\right)\left(\frac{v}{v_o}\right)^{\gamma - 1} = \ln \frac{T^{c_v}}{\rho^R} \tag{5-41}$$

Alternately, either T or v may be eliminated with the aid of $pv = RT$ to obtain

$$s - s_o = c_v \ln \frac{p}{p_o} + c_p \ln \frac{v}{v_o} = c_v \ln \left(\frac{p}{p_o}\right)\left(\frac{v}{v_o}\right)^{\gamma} \tag{5-42}$$

or

$$s - s_o = c_p \ln \frac{T}{T_o} - R \ln \frac{p}{p_o} = c_v \ln \left(\frac{T}{T_o}\right)^{\gamma} \left(\frac{p}{p_o}\right)^{-(\gamma - 1)} = c_v \ln \frac{p}{\rho^{\gamma}} \tag{5-43}$$

Equations (5-40) to (5-43) enable entropy changes to be calculated in terms of end properties. If the entropy remains constant, then T and v; p and v; and T and p are connected with each other during the process by the relations

$$Tv^{\gamma-1} = \text{constant} \tag{5-44}$$

$$pv^{\gamma} = \frac{p}{\rho^{\gamma}} = \text{constant} \tag{5-45}$$

$$\frac{1}{p} T^{\frac{\gamma}{\gamma-1}} = \text{constant} \tag{5-46}$$

The foregoing relations represent the contribution of thermodynamics to the treatment of irrotational, frictionless flow. With the possibly additional second law statement of $\Delta s \geq 0$, it is the only contribution required.

CHAPTER 6

ISENTROPIC FLOW PARAMETERS

6.1 Choice of Parameters

The equation of continuity, the three coordinate-equations of Euler's equation, the reversible adiabatic change of state relation, and the equation of state developed in the preceeding chapter form six equations in the six unknowns u, v, w, p, ρ, and s. The number of equations is equal to the number of unknowns, and this completely describes the flow, without recourse to any further physical principles. Thus, irrotational, frictionless flow represents a conservative system which can be dealt with almost solely by Newton's law of motion and the principle of conservation of mass. The only contribution required of thermodynamics is to provide the relation between pressure and density for the reversible adiabatic process so that Euler's equation may be integrated into useful form. For, in the preceding chapter, the equation of motion was integrated to

$$\int \frac{dp}{\rho} + \frac{q^2}{2} = \text{constant throughout flow field.}$$

It can be rewritten with the aid of the isentropic relation

$$\frac{p}{\rho^\gamma} = \frac{p_o}{\rho_o{}^\gamma} \tag{6-1}$$

to

$$\left(\frac{\gamma}{\gamma-1}\frac{p_o}{\rho_o{}^\gamma}\right)\rho^{\gamma-1} + \frac{q^2}{2} = \text{constant} \tag{6-2}$$

The constant in Equation (6-2) may be evaluated by using the known values of q, ρ and p at any station. In particular, for the stagnation

station 0, $q_o = 0$, and the constant in Equation (6-2) becomes $\frac{\gamma}{\gamma-1}\frac{p_o}{\rho_o}$. Thus Equation (6-2) is finally written as

$$\frac{q^2}{2} + \left[\frac{\gamma}{\gamma-1}\frac{p_o}{\rho_o^{\gamma}}\right]\rho^{\gamma-1} = \frac{\gamma}{\gamma-1}\frac{p_o}{\rho_o} \qquad (6\text{-}3a)$$

or

$$\frac{q^2}{2} + \left[\frac{\gamma}{\gamma-1}\frac{p_o^{1/\gamma}}{\rho_o}\right]p^{1-1/\gamma} = \frac{\gamma}{\gamma-1}\frac{p_o}{\rho_o} \qquad (6\text{-}3b)$$

Equation (6-3) is Bernoulli's equation for a compressible isentropic flow; p_o is the stagnation or total pressure, and corresponds to the $(p + \rho\frac{q^2}{2})$ of incompressible flow. Equation (6-3) is sometimes called the weak form of Bernoulli's equation because it is based on the condition of isentropy, Equation (6-1).

Bernoulli's equation and the energy equation are equivalent when isentropic flow is assumed. This is readily seen from the fact that the energy equation was previously integrated to

$$c_pT + \frac{q^2}{2} = c_pT_o \qquad (5\text{-}26)$$

Employing the relations $T = p/\rho R$ and $c_p = \frac{\gamma}{\gamma-1}R$, Equation (5-26) becomes:

$$\frac{\gamma}{\gamma-1}RT + \frac{q^2}{2} = \frac{\gamma}{\gamma-1}\frac{p}{\rho} + \frac{q^2}{2} = \frac{\gamma}{\gamma-1}\left(\frac{p_o}{\rho_o}\right)\rho^{\gamma-1} + \frac{q^2}{2} = \text{constant}$$

or

$$\frac{q^2}{2} + \frac{\gamma}{\gamma-1}\frac{p_o}{\rho_o^{\gamma}}\rho^{\gamma-1} = \text{constant} = \frac{\gamma}{\gamma-1}\frac{p_o}{\rho_o}$$

which is identical to Equation (6-3). Thus, Bernoulli's equation is in fact an energy relation when heat transfer and viscous dissipation are not taken into account.

To determine a network of p, ρ, q, and T for the flow field, it is convenient to form the parameters $\frac{p}{p_o}$, $\frac{\rho}{\rho_o}$, $\frac{q}{q_o}$, and $\frac{T}{T_o}$, and to evaluate them in terms of an independent variable. The independent variable selected here will be the Mach number. However, before evaluating the flow parameters, it is useful to introduce the concept of a reference speed.

6.2 Reference Speeds

Equation (5-26) is used to define the flow velocity

$$q = \sqrt{2\, c_p\, (T_o - T)} = \sqrt{\frac{2\gamma}{\gamma-1} R\, (T_o - T)} \qquad (6\text{-}4)$$

From this it is seen that for a fixed stagnation temperature T_o, all states with the same temperature have the same velocity. Referring to Figure (6-1), lines of constant velocity are horizontal, and the vertical distance between T_o and T is proportional to the square of the velocity

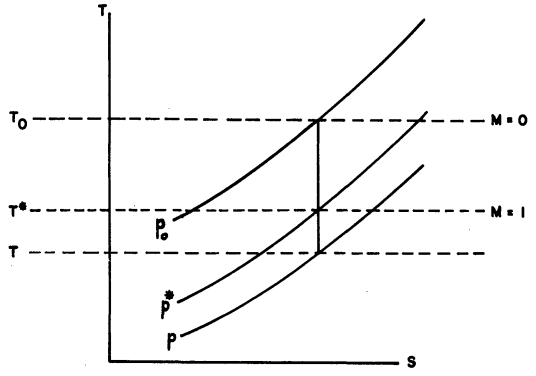

Figure 6-1. Isentropic Flow Process

From Equation (6-4), it is evident that the maximum velocity corresponding to a given stagnation temperature is when T = 0 (corresponding to expansion into a vacuum). Thus

$$q_{max} = \sqrt{\frac{2\gamma}{\gamma-1} RT_o} \qquad (6\text{-}5)$$

may be used as a reference velocity.

Another reference velocity is the speed of sound at the stagnation temperature

$$c_o = \sqrt{\gamma R T_o} \tag{6-6}$$

Finally, a third reference velocity is the critical velocity, i.e., the velocity of the fluid at which the sound speed and the fluid speed are equal. Using an asterisk * to denote the conditions for which $q = c = q^* = c^*$, the temperature at which critical speed is attained is given by Equation (6-4)

$$q^* = \sqrt{\frac{2\gamma}{\gamma-1} R (T_o - T^*)} = \sqrt{\gamma R T^*} \tag{6-7}$$

from which

$$\frac{T^*}{T_o} = \frac{2}{\gamma+1} \tag{6-8}$$

and

$$q^* = \sqrt{\frac{2\gamma}{\gamma+1} R T_o} \tag{6-9}$$

From the foregoing equations, the following relations for the three reference speeds, together with the numerical values for $\gamma = 1.4$ are obtained:

$$\frac{c^*}{c_o} = \sqrt{\frac{2}{\gamma+1}} = .913 \tag{6-10}$$

$$\frac{q_{max}}{c_o} = \sqrt{\frac{2}{\gamma-1}} = 2.24 \tag{6-11}$$

$$\frac{q_{max}}{c^*} = \sqrt{\frac{\gamma+1}{\gamma-1}} = 2.45 \tag{6-12}$$

The local speed of sound decreases from ($c_o^2 = \gamma R T_o$) at $v = 0$ to zero at the maximum speed attainable by the fluid ($= \sqrt{\frac{2\gamma}{\gamma-1} R T_o}$).

The variation of c with q is shown in Figure (6-2).

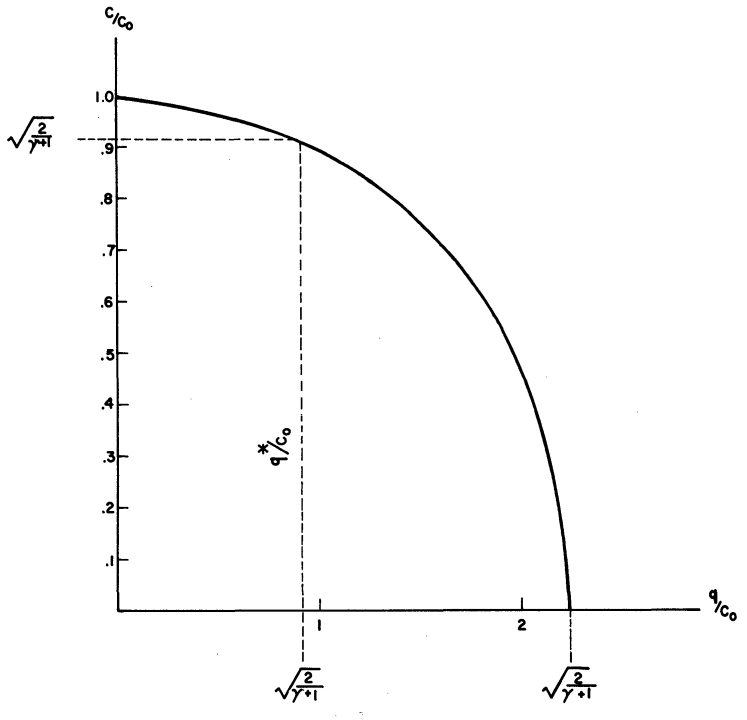

Figure 6-2. Variation of Sound-Speed with Velocity

The energy equation for adiabatic flow

$$\frac{q^2}{2} + c_p T = \text{constant}$$

becomes, with $c_p T = \frac{c_p}{\gamma R}\gamma RT = \frac{c^2}{\gamma - 1}$

$$\frac{q^2}{2} + \frac{c^2}{\gamma - 1} = \text{constant} \qquad (6\text{-}13)$$

The constant in Equation (6-13) may be evaluated at the three reference conditions of: zero speed, zero temperature, and sonic or critical speed. Thus

$$\frac{q^2}{2} + \frac{c^2}{\gamma - 1} = \frac{c_o^2}{\gamma - 1} \qquad (6\text{-}13a)$$

$$= \frac{q_{max}^2}{2} \qquad (6\text{-}13b)$$

$$= \frac{1}{2}\frac{\gamma + 1}{\gamma - 1} c^{*2} \qquad (6\text{-}13c)$$

6.3 Mach Number

Dimensional analysis leads to the dimensionless number

$$M = \frac{q}{c} \tag{6-14}$$

the usefulness of which is seen by introducing the speed of sound

$$c_o^2 = \frac{\gamma p_o}{\rho_o}$$

into Bernoulli's equation, Equation (6-3b), and solving for $\frac{p}{p_o}$

$$\left(\frac{p}{p_o}\right)^{\gamma-1/\gamma} = 1 - \frac{\gamma-1}{2}\frac{\rho_o}{\gamma p_o} q^2 = 1 - \frac{\gamma-1}{2}\frac{q^2}{c_o^2} \tag{6-15}$$

Multiplying and dividing the last term by c^2, and noting that

$$\frac{c^2}{c_o^2} = \frac{T}{T_o} = \left(\frac{p}{p_o}\right)\left(\frac{\rho}{\rho_o}\right) = \left(\frac{p}{p_o}\right)^{\gamma-1/\gamma}$$

Equation (6-15) becomes

$$\frac{p}{p_o} = \left[1 + \frac{\gamma-1}{2} M^2\right]^{-(\gamma/\gamma-1)} \tag{6-16}$$

Similar operations yield

$$\frac{\rho}{\rho_o} = \left[1 + \frac{\gamma-1}{2} M^2\right]^{-(\gamma/\gamma-1)} \tag{6-17}$$

$$\frac{T}{T_o} = \left[1 + \frac{\gamma-1}{2} M^2\right]^{-1} \tag{6-18}$$

$$\frac{c}{c_o} = \left[1 + \frac{\gamma-1}{2} M^2\right]^{1/2} \tag{6-19}$$

The Mach number thus uniquely determines the static to stagnation ratios of all the flow parameters. Curves of the static to stagnation ratios versus Mach numbers are drawn in Figure (6-3).

They will serve as work curves throughout the present analysis.

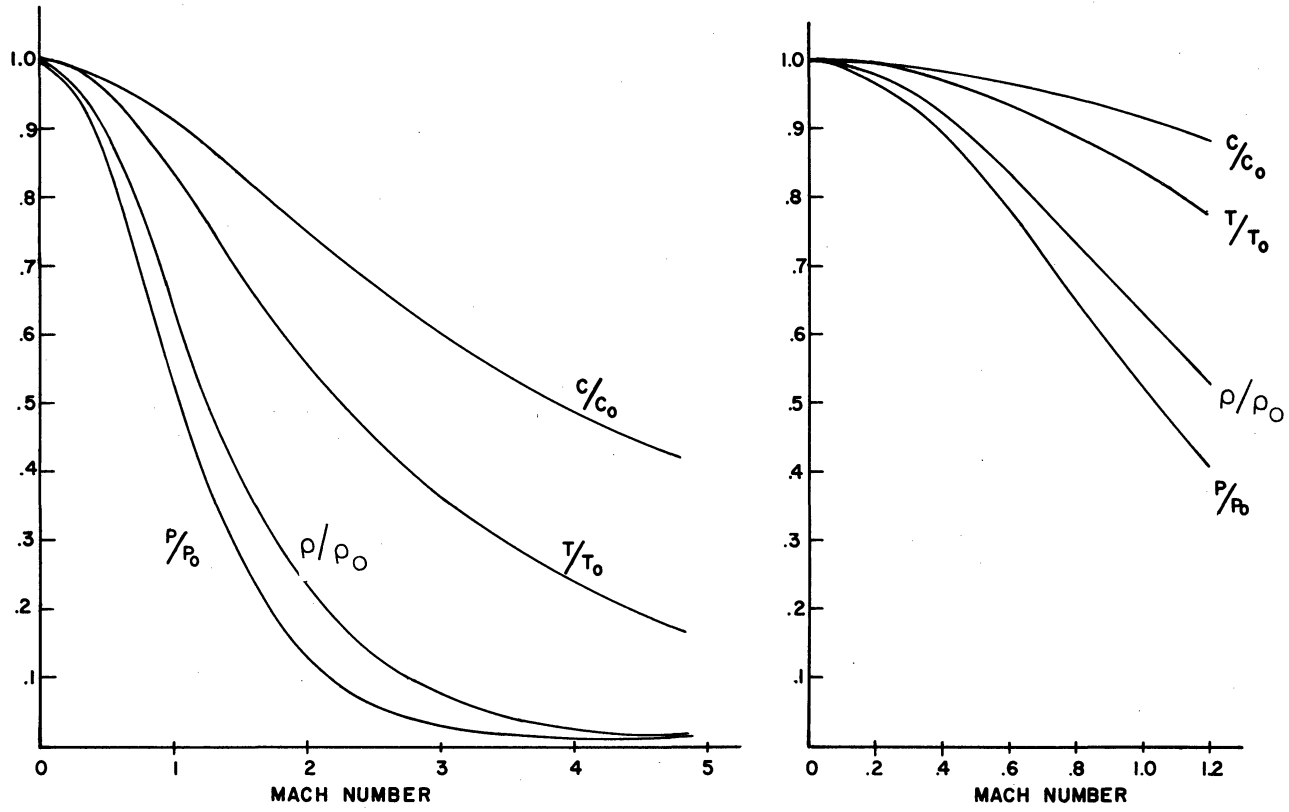

Figure 6-3. Parameter-Curves for Isentropic Flow

CHAPTER 7

POTENTIAL EQUATION AND STREAMLINE EQUATION

7.1 Preliminary Statement

The kinematical problem of finding the flow pattern for the vortex tube is eased by developing a single differential equation of flow in terms of the velocity potential and the stream function respectively. Since the tangential components of velocity in the vortex tube are appreciably greater than the axial and radial components, the flow outside the wall boundary layer is considered as two dimensional in the present chapter. The solution for the general spatial flow pattern is deferred to Chapter 9.

7.2 Existence of Potential Function

With the assumption of irrotational motion, the circulation, as calculated in Chapter 4 turns out to be zero. From this, it follows that the line integral of the velocity between any two points of the flow field depends only on the location of the points, and not on the path of integration. Referring to Figure (7-1), and to the fact that the circulation around a closed curve is zero, the existence of a velocity potential is established in the following manner.

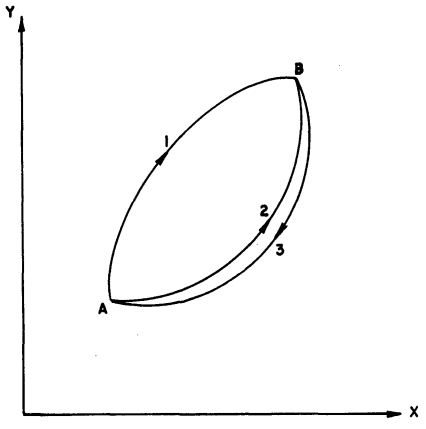

Figure 7-1. Existence of Point-Function for Irrotational Flow

Consider the closed curves (A-1-B-2-A) and (A-2-B-3-A) respectively. The circulation for a closed curve being zero:

$$\int_{A}^{B}{}_{1} \vec{q} \cdot \vec{dl} + \int_{B}^{A}{}_{3} \vec{q} \cdot \vec{dl} = 0$$

$$\int_{A}^{B}{}_{2} \vec{q} \cdot \vec{dl} + \int_{B}^{A}{}_{3} \vec{q} \cdot \vec{dl} = 0$$

from which results

$$\int_{A}^{B}{}_{1} \vec{q} \cdot \vec{dl} = \int_{A}^{B}{}_{2} \vec{q} \cdot \vec{dl} \qquad (7\text{-}1)$$

Since paths (1) and (2) may be arbitrarily chosen, it follows that $\vec{q} \cdot \vec{dl}$ is an exact differential, and may therefore be considered as the differential of a point function whose value depends only on x and y. This point function is called the velocity potential, φ, and is defined by the relation

$$\vec{q} \cdot \vec{dl} = d\varphi \qquad (7\text{-}2)$$

Equation (7-2) indicates that the derivative of the velocity potential in a given direction represents the component of velocity in that direction. In Cartesian coordinates, it means that

$$u = \frac{\partial \varphi}{\partial x} = \varphi_x \qquad (7\text{-}3a)$$

$$v = \frac{\partial \varphi}{\partial y} = \varphi_y \qquad (7\text{-}3b)$$

where u and v are the x and y components of the velocity $\vec{q}$.

Equations (7-3) show that the condition of irrotationality is automatically satisfied by the existence of a velocity potential φ. For, the order of differentiation being immaterial,

$$\frac{\partial^2\varphi}{\partial x\partial y} - \frac{\partial^2\varphi}{\partial y\partial x} = \frac{\partial v}{\partial x} - \frac{\partial u}{\partial y} = 0 \qquad (7\text{-}4)$$

which is precisely the condition for irrotationality developed in Chapter 4. Nor is the existence of a potential function confined to two-dimensional flow, for, if $\vec{q} = \nabla\varphi$, then

$$2\omega = \nabla \times \vec{q} = \nabla \times \nabla\varphi = 0 \qquad (7\text{-}5)$$

since the last term becomes zero because the cross product of two parallel vectors is zero.

Equations (7-3) indicate that φ is a number having magnitude, but not direction, which is assigned to each point in the flow field so that, at every point, the change of this number in unit distance in a given direction is equal to the component of velocity in that direction. This is the concept of velocity potential, and the purpose is to find such number-distributions. The concept of velocity potential derives historically from the concept in mechanics of the potential of a force. It is recalled that for conservative systems, the work, or line integral of the force, is zero around a closed curve, and hence a force potential exists whose derivative in any direction is the force in that direction. Because a velocity potential always exists for irrotational flow, the terms "potential flow" and "irrotational flow" are used interchangeably.

7.3 Potential Equation

To derive a single differential equation of flow in terms of the velocity potential, the equation of continuity and Euler's equation

are combined as follows. Starting with the equation of continuity, Equation (5-5), it is written in two-dimensional form in terms of the velocity potential as

$$\frac{\partial}{\partial x}(\rho u) + \frac{\partial}{\partial y}(\rho v) = \frac{\partial}{\partial x}(\rho \varphi_x) + \frac{\partial}{\partial y}(\rho \varphi_y) = 0$$

or, expanding

$$\rho(\varphi_{xx} + \varphi_{yy}) + \varphi_x \rho_x + \varphi_y \rho_y = 0 \qquad (7\text{-}6)$$

where the subscripts denote partial derivatives.

Euler's equation, Equation (5-23), becomes, in terms of the velocity potential:

$$dp = -\rho\, d\left(\frac{q^2}{2}\right) = -\rho\, d\left(\frac{u^2 + v^2}{2}\right) = -\rho\, d\left(\frac{\varphi_x^2 + \varphi_y^2}{2}\right) \qquad (7\text{-}7)$$

The velocity of sound, being given by $c^2 = \frac{dp}{d\rho}$, its use in Equation (7-7) results in

$$d\rho = -\frac{\rho}{c^2}\, d\left(\frac{\varphi_x^2 + \varphi_y^2}{2}\right)$$

from which

$$\rho_x = -\frac{\rho}{c^2}(\varphi_x \varphi_{xx} + \varphi_y \varphi_{xy})$$

$$\rho_y = -\frac{\rho}{c^2}(\varphi_x \varphi_{xy} + \varphi_y \varphi_{yy})$$

Substitution of these into Equation (7-6) then yields

$$\rho(\varphi_{xx} + \varphi_{yy}) - \frac{\rho}{c^2}\varphi_x(\varphi_x \varphi_{xx} + \varphi_y \varphi_{xy}) - \frac{\rho}{c^2}\varphi_y(\varphi_x \varphi_{xy} + \varphi_y \varphi_{yy}) = 0$$

and, upon simplification

$$\left(1 - \frac{\varphi_x^2}{c^2}\right)\varphi_{xx} + \left(1 - \frac{\varphi_y^2}{c^2}\right)\varphi_{yy} - \frac{2}{c^2}\varphi_x \varphi_y \varphi_{xy} = 0 \qquad (7\text{-}8)$$

where

$$c^2 = f(u^2 + v^2) = f(\varphi_x^2 + \varphi_y^2) = c_o^2 - \frac{\gamma-1}{2}(\varphi_x^2 + \varphi_y^2) \qquad (7\text{-}9)$$

Equation (7-8) is a single differential equation which is equivalent to the two equations

$$(c^2 - u^2)u_x - uv(u_y + v_x) + (c^2 - v^2)v_y = 0 \qquad (7\text{-}10)$$

$$v_x - u_y = 0 \qquad (7\text{-}11)$$

in the two unknowns u and v of the independent variables x and y. Equation (7-8) is an equation which simultaneously satisfies the continuity principle, Newton's second law of motion, and the laws of thermodynamics.

7.4 Existence of Stream Function

Just as the condition of irrotationality can be satisfied by the introduction of the potential function φ, so can the equation of continuity for steady, two-dimensional flow be satisfied by the introduction of a function ψ, the stream function.

For steady, two-dimensional flow, the equation of continuity is

$$\frac{\partial}{\partial x}(\rho u) + \frac{\partial}{\partial y}(\rho v) = 0 \qquad (7\text{-}12)$$

and it is obviously satisfied if

$$\rho u = \frac{\partial \psi}{\partial y} \qquad (7\text{-}13a)$$

$$\rho v = -\frac{\partial \psi}{\partial x} \qquad (7\text{-}13b)$$

For, if $\psi(x,y)$ is a point function, then the order of differentiation is immaterial, and

$$\frac{\partial}{\partial x}(\rho u) + \frac{\partial}{\partial y}(\rho v) = \frac{\partial^2 \psi}{\partial x \partial y} - \frac{\partial^2 \psi}{\partial y \partial x} = 0$$

Equations (7-13) define the stream function, though it is usually more convenient to alter them into

$$u = \frac{\rho_o}{\rho} \frac{\partial \psi}{\partial y} \tag{7-14a}$$

$$v = -\frac{\rho_o}{\rho} \frac{\partial \psi}{\partial x} \tag{7-14b}$$

where ρ_o is the density at the stagnation point.

The magnitude of the velocity vector at any point is given in terms of the stream function by

$$v^2 = u^2 + v^2 = \left(\frac{\rho_o}{\rho}\right)^2 (\psi_x^2 + \psi_y^2) \tag{7-15}$$

The physical interpretation of the stream function is the following. Since ψ is a point function, it may be written as

$$d\psi = \frac{\partial \psi}{\partial x} dx + \frac{\partial \psi}{\partial y} dy = \frac{1}{\rho_o} (\rho u \, dy - \rho v \, dx)$$

In Figure (7-2), let dm denote the mass rate of flow across any surface AB connecting two neighboring lines ψ and ψ and $d\psi$.

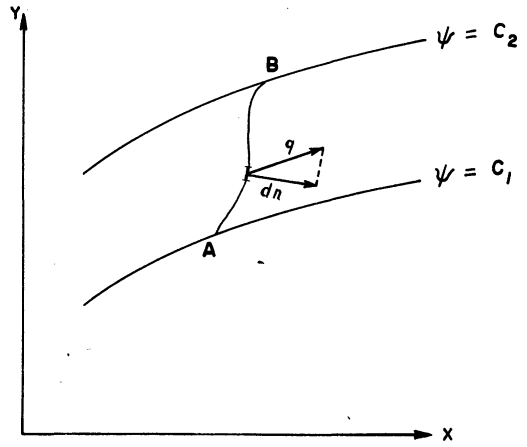

Figure 7-2. Stream Function in Two-Dimensional Flow

Let $\vec{q}$ be the velocity and $\vec{dn}$ the normal. Then

$$dm = \rho\, \vec{q} \cdot \vec{dn} = \rho(u\, dy - v\, dx) = \rho\left(\frac{\rho_o}{\rho} \frac{\partial \psi}{\partial y}\, dy + \frac{\rho_o}{\rho} \frac{\partial \psi}{\partial x}\, dx\right)$$

and

$$m = \rho_o \int_A^B \left(\frac{\partial \psi}{\partial y}\, dy + \frac{\partial \psi}{\partial x}\, dx\right) = \rho_o \int_A^B d\psi = \rho_o\, (\psi_B - \psi_A) = \rho_o\, (C_2 - C_1) \qquad (7\text{-}16)$$

Equation (7-16) shows that the mass flow rate between two neighboring ψ's is constant. Since the mass flow rate is also constant between streamlines, it follows that lines of constant ψ are streamlines, and ψ is thus termed the stream function.

7.5 Stream Function Equation

Just as a single differential equation of flow was developed in terms of the velocity potential, so will a single differential equation be developed in terms of the stream function.

First, the equation of continuity is automatically satisfied with the introduction of the point function ψ:

$$\frac{\rho_o}{\rho} \psi_y = u$$

$$-\frac{\rho_o}{\rho} \psi_x = v$$

whence

$$\frac{\partial}{\partial x}(\rho u) + \frac{\partial}{\partial y}(\rho v) = \rho_o \left(\frac{\partial^2 \psi}{\partial x \partial y} - \frac{\partial^2 \psi}{\partial y \partial x}\right) = 0 \qquad (7\text{-}17)$$

Second, the condition of irrotationality takes the form

$$\frac{\partial u}{\partial y} - \frac{\partial v}{\partial x} = 0 = \frac{\partial}{\partial y}\left(\frac{\rho_o}{\rho} \frac{\partial \psi}{\partial y}\right) - \frac{\partial}{\partial x}\left(-\frac{\rho_o}{\rho} \frac{\partial \psi}{\partial x}\right)$$

which, after differentiation and rearrangement, becomes

$$\rho\ (\psi_{xx} + \psi_{yy}) - (\psi_x \frac{\partial \rho}{\partial x} + \psi_y \frac{\partial \rho}{\partial y}) = 0 \qquad (7\text{-}18)$$

Third, Euler's equation, and the expression for the velocity of sound

$$\frac{dp}{\rho} + d(\frac{u^2 + v^2}{2}) = 0$$

$$c^2 = \frac{dp}{d\rho}$$

yield, upon elimination of dp:

$$d\rho = \frac{dp}{c^2} = - \frac{\rho}{2c^2}\ d\ (u^2 + v^2)$$

$$= - \frac{\rho}{2c^2}\ d \left[(\frac{\rho_o}{\rho})^2\ \psi_y{}^2 + (\frac{\rho_o}{\rho})^2\ \psi_x{}^2 \right]$$

or

$$d\rho = - \frac{\rho}{c^2} \left[(\frac{\rho_o}{\rho})^2\ (\psi_x d\psi_x + \psi_y d\psi_y) - (\psi_x{}^2 + \psi_y{}^2)\ (\frac{\rho_o}{\rho})^2\ \frac{d\rho}{\rho} \right] \qquad (7\text{-}19)$$

Equation (7-19) now enables the formation of the partial derivatives ρ_x and ρ_y. Upon substitution of these derivatives in Equation (7-18) and simplifying, there results

$$\left[1 - \frac{1}{c^2} (\frac{\rho_o}{\rho})^2\ \psi_y{}^2 \right] \psi_{xx} + \left[1 - \frac{1}{c^2} (\frac{\rho_o}{\rho})^2\ \psi_x{}^2 \right] \psi_{yy} + \frac{2}{c^2} (\frac{\rho_o}{\rho})^2\ \psi_x \psi_y \psi_{xy} = 0 \qquad (7\text{-}20)$$

where

$$c^2 = f(u^2 + v^2) = c_o{}^2 - \frac{\gamma - 1}{2}\ (u^2 + v^2)$$

$$= c_o{}^2 - \frac{\gamma - 1}{2} (\frac{\rho_o}{\rho})^2\ (\psi_x{}^2 + \psi_y{}^2) \qquad (7\text{-}21)$$

and

$$\frac{\rho_o}{\rho} = \left(1 + \frac{\gamma-1}{2} M^2\right)^{1/\gamma-1} = \left[1 + \frac{\gamma-1}{2} \left(\frac{\rho_o}{\rho}\right)^2 \frac{\psi_x^2 + \psi_y^2}{c^2}\right]^{1/\gamma-1} \qquad (7\text{-}22)$$

Substitution of Equations (7-21) and (7-22) into (7-20) yields a single differential equation of the second order for ψ in terms of x and y which is completely equivalent to the differential equation of flow in terms of the velocity potential. However, the differential equation in terms of φ are simpler in form than that in terms of ψ, and hence Equation (7-8) will be the one to work with.

7.6 Relation Between Streamlines and Equipotentials

The velocity potential and stream function are related through Equations (7-3) and (7-14):

$$u = \frac{\partial \varphi}{\partial x} = \frac{\rho_o}{\rho} \frac{\partial \psi}{\partial y}$$

$$v = \frac{\partial \varphi}{\partial y} = -\frac{\rho_o}{\rho} \frac{\partial \psi}{\partial x}$$

Since ψ is a point-function, it can be written as

$$d\psi = \frac{\partial \psi}{\partial x} dx + \frac{\partial \psi}{\partial y} dy \qquad (7\text{-}23)$$

For a constant ψ, Equation (7-23) is set to zero, and the slope of a line of constant ψ is thus found to be

$$\left(\frac{dy}{dx}\right)_{\text{constant } \psi} = -\frac{\psi x}{\psi y} = -\frac{-\frac{\rho}{\rho_o} v}{\frac{\rho}{\rho_o} u} = \frac{v}{u} \qquad (7\text{-}24a)$$

But, by definition, the slope of a streamline is

$$\left(\frac{dy}{dx}\right)_{\text{streamline}} = \frac{v}{u} \qquad (7\text{-}24b)$$

Equations (7-24a) and (7-24b) show that the lines of constant ψ and streamlines are identical.

As for the equipotential lines, the total differential

$$d\varphi = \frac{\partial \varphi}{\partial x} dx + \frac{\partial \varphi}{\partial y} dy$$

when set to zero for φ = constant, yields with the aid of Equation (7-3)

$$\left(\frac{dy}{dx}\right)_{\text{constant } \varphi} = - \frac{\varphi_x}{\varphi_y} = - \frac{u}{v} \qquad (7\text{-}25)$$

Comparison of Equations (7-24) and (7-25) reveals that

$$\left(\frac{dy}{dx}\right)_{\varphi} = - \frac{1}{\left(\frac{dy}{dx}\right)_{\psi}} \qquad (7\text{-}26)$$

Thus, the lines of constant φ and the lines of constant ψ are normal to each other, i.e., equipotential lines and streamlines form an <u>orthogonal network</u>.

7.7 Spacing of Net Lines

To investigate the relative spacing of the network, it is noted that the gradient of the potential in any direction is the velocity component in that direction.

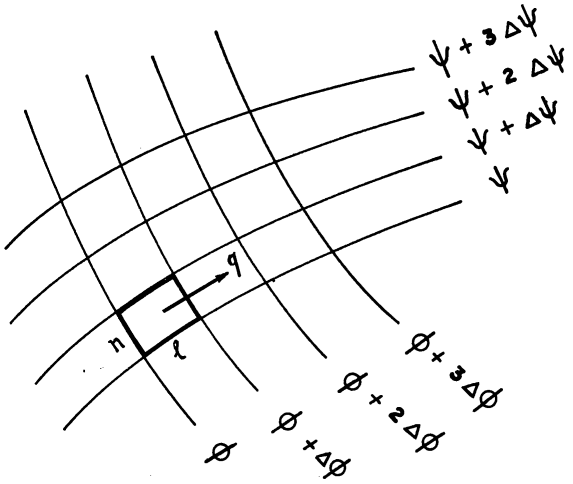

Figure 7-3. Network Spacing

Referring to Figure (7-3), the gradient of φ along the streamline gives the magnitude of the velocity vector,

$$\vec{q} = \frac{\Delta\varphi}{\ell} \tag{7-27}$$

On the other hand, the gradient of ψ in a given direction is related to the velocity component normal to that direction:

$$\vec{q} = \frac{\rho_o}{\rho} \frac{\Delta\psi}{n} \tag{7-28}$$

If, for convenience, equal numerical magnitudes for $\Delta\varphi$ and $\Delta\psi$ are selected between neighboring lines in the grid, then Equations (7-27) and (7-28) yield

$$\frac{\ell}{n} = \frac{\rho}{\rho_o} \tag{7-29}$$

Equation (7-29) shows that for incompressible flow, each element of the net is, in the limit, a square. However, for compressible flow, the ratio ℓ/n becomes proportional to the density ratio between $\Delta\varphi$ and $\Delta\psi$. Since ρ/ρ_o cannot be greater than unity, it follows that the potential lines are more closely spaced than the streamlines. Also, ρ/ρ_o being close to unity at low Mach numbers, and a great deal less than unity at high Mach numbers, the difference between the spacings will be most marked in those regions of high Mach numbers.

For incompressible flow, the conditions of irrotationality and steady-flow are purely kinematic, and only these conditions enter into the derivation of Laplace's equation for the velocity potential or stream function. The dynamic conditions represented by Bernoulli's equation are not involved in the determination of the streamline pattern.

Two-dimensional, incompressible, irrotational flow may thus be considered as a problem in pure geometry with φ and ψ lines interchangeable, so that any single flow pattern embodies two possible solutions.

For compressible flow, the situation is different, and it is not possible, in general, to use superposition. For, although the condition of irrotationality remains kinematic, the equation of continuity contains the density, which in turn is related to the pressure and, therefore, to dynamic requirements. Thus, the φ and ψ lines, when interchanged, do not represent a solution.

Having obtained Equations (7-8) and (7-20), what technique may be employed for their solution? Mathematically speaking, Equations (7-8) and (7-20) are nonlinear differential equations. A differential equation is linear when the dependent variable and its derivatives appear only in linear form. Such, unfortunately, is not the case with the aforementioned equations. This complicates tremendously the treatment of the problem. However, the situation here is not as hopeless as it seems. For, although the differential equations for φ and ψ are still nonlinear, they are now in terms of only two space coordinates. For this condition, they are amenable to exact solution by means of the hodograph transformation which follows in the next chapter.

CHAPTER 8

EXACT SOLUTION OF INVISCID FLOW IN THE PLANE

8.1 Nature of Solution

The exact solution applies to that region of flow outside the boundary layer. By excluding the latter from the field of flow, the behavior of the fluid becomes irrotational, and it becomes possible to use superposition to obtain the general solution.

Although the solution applies essentially to a perfect gas, it nevertheless describes very aptly the flow of a gas of low viscosity (such as air) as it enters a vortex tube. For, starting with this "idealized" solution, the viscous forces transform it in Chapter 10 into the "real" solution which is to provide comparison with the experimental results. Lastly, the solution has the merit of being exact in that it is free of any assumption of small perturbations or other successive approximations required for linearization. This exactness is achieved by a transformation from "physical" coordinates to "velocity" coordinates, the mathematical theory of which is briefly sketched in the following section.

8.2 Hodograph Transformation

In the general theory, denote by u and v the dependent variables, and by x and y the independent variables. Then the general form of the system of differential equations, Equations (7-8) and (7-20), is

$$A_1 u_x + B_1 u_y + C_1 v_x + D_1 v_y + E_1 = 0 \qquad (8\text{-}1)$$

$$A_2 u_x + B_2 u_y + C_2 v_x + D_2 v_y + E_2 = 0 \qquad (8\text{-}2)$$

where A_1, A_2, . . ., E_2 are known functions of x, y, u, and v. Let it be assumed that all functions occurring are continuous, and possess as many continuous derivatives as may be required.

If $E_1 = E_2 = 0$ (homogeneous system), and the coefficients A_1, A_2, . . ., D_2 are functions of u, v alone, the equations are called reducible. In this case, for any region where the Jacobian

$$j = u_x v_y - u_y v_x \tag{8-3}$$

is not zero, the system of Equations (8-1) and (8-2) can be transformed into an equivalent linear system by interchanging the roles of dependent and independent variables.

In such a case, x and y may be considered as functions of u and v, and from

$$j\, x_u = v_y, \; -j\, x_v = u_y \tag{8-4}$$

$$-j\, y_u = v_x, \; j\, y_v = u_x \tag{8-5}$$

it is seen that x(u,v) and y(u,v) satisfy the linear differential equations

$$A_1 y_v - B_1 x_v - C_1 y_u + D_1 x_u = 0 \tag{8-6}$$

$$A_2 y_v - B_2 x_v - C_2 y_u + D_1 x_u = 0 \tag{8-7}$$

Vice versa, every solution x, y of Equations (8-6) and (8-7) leads to a solution of Equations (8-1) and (8-2) if the Jacobian

$$J = x_u y_v - x_v y_u \tag{8-8}$$

does not vanish.

The described transformation of the (x,y)-plane into the (u,v)-plane is the <u>hodograph transformation</u>. The term stems from the

choice of the velocity coordinates u and v as the independent variables in place of the physical coordinates u and y. The advantage gained is that the differential equations for φ and ψ as functions of u and v are linear, thus allowing solutions to be formed by superposition. If, in addition, a fictitious gas is introduced by replacing the isentropic pressure-density relation by a tangent-gas relation, the hodograph equations are reducible to the Laplace equations, and solution may then be obtained by making use of analytic functions of a complex variable.

Equations (8-4) and (8-5) give the derivatives of x and y in terms of u and v. With them, Equations (7-10) and (7-11) are transformed into two linear differential equations

$$x_v - y_u = 0 \tag{8-9}$$

$$(c^2 - u^2)y_v + uv(x_v + y_u) + (c^2 - v^2)x_u = 0 \tag{8-10}$$

The first equation implies that a function $\varphi = \varphi(u,v)$ exists such that

$$x = \varphi_v \tag{8-11}$$

$$y = \varphi_u \tag{8-12}$$

and the second equation then takes the form

$$(c^2 - u^2)\varphi_{vv} + 2\,u\,v\,\varphi_{uv} + (c^2 - v^2)\varphi_{uu} = 0 \tag{8-13}$$

Equation (8-13) is now linear for $\varphi(u,v)$ as against Equation (7-8) being nonlinear for $\varphi(x,y)$. Provided the Jacobian

$$J = \varphi_{uu}\,\varphi_{vv} - \varphi_{uv}^2 = x_u y_v - x_v y_u \tag{8-14}$$

does not vanish, every solution φ (u,v) defined in the (u,v)-plane leads to a flow pattern given by u and v as functions of x and y.

Actually, a slightly different procedure is found to be more convenient. In it, φ is retained as dependent variable, together with the stream-function ψ, and the magnitude q and direction θ of the velocity are used as independent variables instead of $u = q \cos \theta$ and $v = q \sin \theta$.

8.3 Relation Between Physical Plane and Hodograph Plane

Since at every point on the physical plane there exists a definite velocity vector, q, the coordinates x and y can be considered as functions of q and θ. This is a point to point correspondence (but not a unique one), and it transforms the physical plane (x,y) into the hodograph plane (q,θ). A streamline in the physical plant thus describes a continuous sequence of end points and velocity vectors (q,θ) and will appear as a curve on the hodograph plane. This curve is called the hodograph of the streamline.

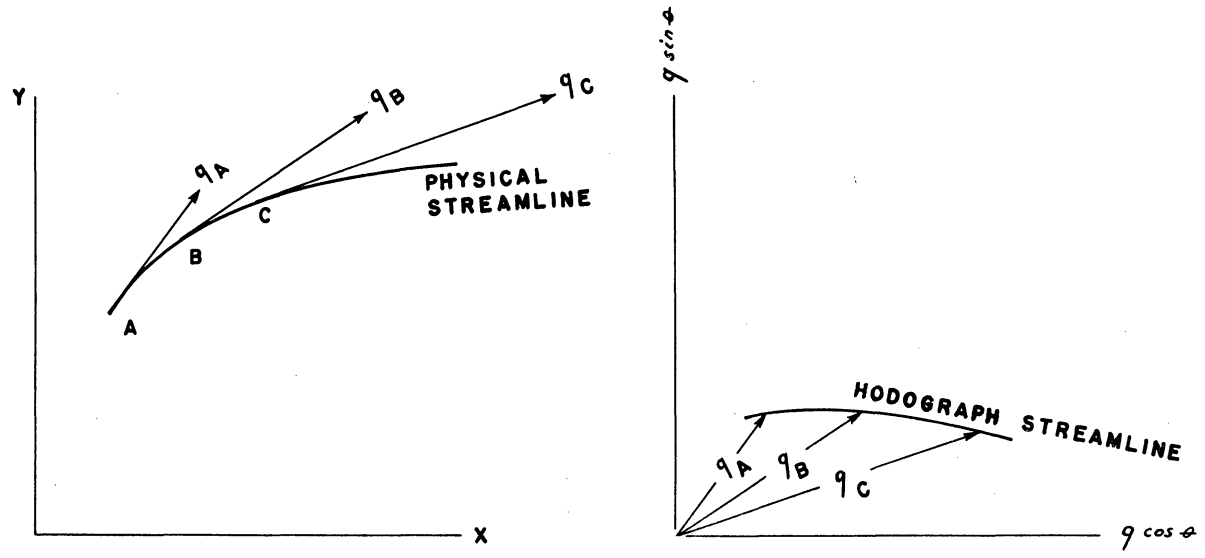

Figure 8-1. Correspondence Between Physical Plane and Hodograph Plane

It should be noted that, while the physical streamlines, by their definition, generally do not intersect, their hodographs can do so, since it is entirely possible that the same velocity vector (q,θ) may occur at more locations than one, either on the same streamline or on others, i.e., different points on the physical plane may have same velocities. Hence, there is the possibility that the hodograph plane may consist of several layers or leaves.

The nature of the transformation between the physical and hodograph planes is illustrated in Figure (8-2) by considering the flow past the symmetrical profile.

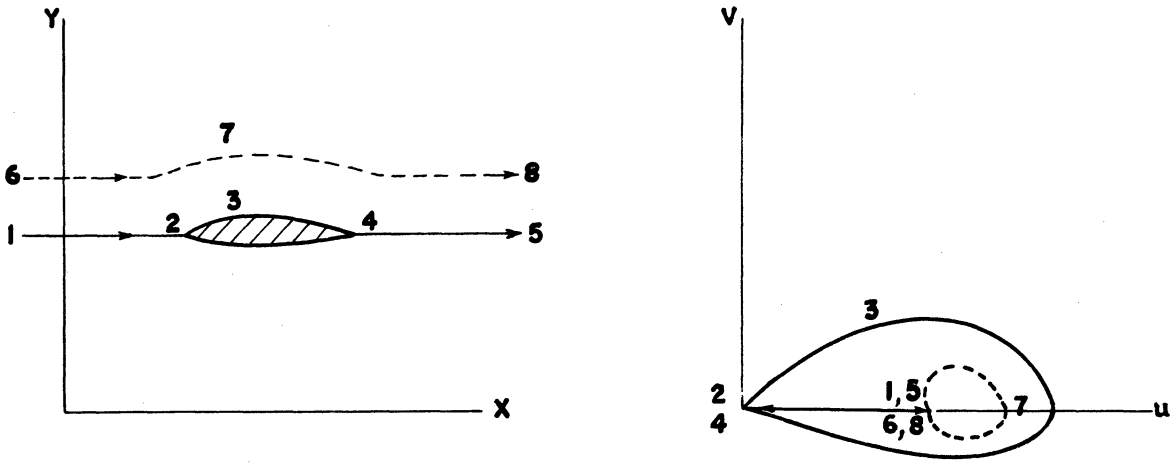

Figure 8-2. Streamlines in Physical and Hodograph Planes

Two streamlines have been sketched: the boundary streamline 1-2-3-4-5, and an external streamline 6-7-8-9.

8.4 Hodograph Equation

Let x and y be the coordinates of the physical or actual flow plane, and q and θ be the polar coordinates of the hodograph or velocity plane. The differential equations of flow will now be derived in terms of q and θ as independent variables.

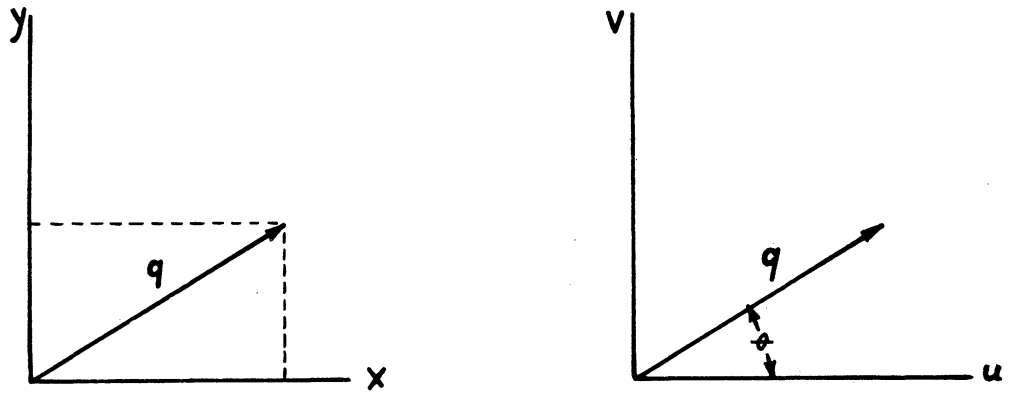

Figure 8-3. Velocity Coordinates

From Figure (8-3) it is seen that

$$u = q \cos \theta \tag{8-14a}$$

$$v = q \sin \theta \tag{8-14b}$$

The condition of irrotationality is satisfied through the introduction of a velocity potential:

$$u = \frac{\partial \varphi}{\partial x} \tag{8-15a}$$

$$v = \frac{\partial \varphi}{\partial y} \tag{8-15b}$$

The equation of continuity is satisfied through the introduction of a stream function:

$$u = \frac{\rho_o}{\rho} \frac{\partial \psi}{\partial y} \tag{8-16a}$$

$$v = \frac{\rho_o}{\rho} \frac{\partial \psi}{\partial x} \tag{8-16b}$$

Since

$$d\varphi = \frac{\partial \varphi}{\partial x} dx + \frac{\partial \varphi}{\partial y} dy$$

$$d\psi = \frac{\partial \psi}{\partial x} dx + \frac{\partial \psi}{\partial y} dy$$

these may be written with the aid of Equation (8-15) and (8-16):

$$d\varphi = u\, dx + v\, dy = q\,(\cos\theta\, dx + \sin\theta\, dy) \tag{8-17}$$

$$d\psi = -\frac{\rho}{\rho_o} V\, dx + \frac{\rho}{\rho_o} u\, dy = \frac{\rho}{\rho_o} q(-\sin\theta\, dx + \cos\theta\, dy) \tag{8-18}$$

Equations (8-17) and (8-18) can be considered as two simultaneous equations for dx and dy, thus obtaining

$$dx = \frac{\cos\theta}{q} d\varphi - \frac{\rho_o}{\rho} \frac{\sin\theta}{q} d\psi \tag{8-19a}$$

$$dy = \frac{\sin\theta}{q} d\varphi + \frac{\rho_o}{\rho} \frac{\cos\theta}{q} d\psi \tag{8-19b}$$

Now, considering φ and ψ as functions of q and θ, their total differentials may be written as

$$d\varphi = \frac{\partial \varphi}{\partial q} dq + \frac{\partial \varphi}{\partial \theta} d\theta$$

$$d\psi = \frac{\partial \psi}{\partial q} dq + \frac{\partial \psi}{\partial \theta} d\theta$$

Substituting these into equations (8-19) results in

$$dx = \frac{\cos\theta}{q}\left(\frac{\partial \varphi}{\partial q} dq + \frac{\partial \varphi}{\partial \theta} d\theta\right) - \frac{\rho_o}{\rho} \frac{\sin\theta}{q}\left(\frac{\partial \psi}{\partial q} dq + \frac{\partial \psi}{\partial \theta} d\theta\right)$$

$$= \left(\frac{\cos\theta}{q} \frac{\partial \varphi}{\partial q} - \frac{\rho_o}{\rho} \frac{\sin\theta}{q} \frac{\partial \psi}{\partial q}\right) dq + \left(\frac{\cos\theta}{q} \frac{\partial \varphi}{\partial q} - \frac{\rho_o}{\rho} \frac{\sin\theta}{q} \frac{\partial \psi}{\partial \theta}\right) d\theta$$

$$= \left(\frac{\cos\theta}{q}\varphi_q - \frac{\rho_o}{\rho}\frac{\sin\theta}{q}\psi_q\right) dq + \left(\frac{\cos\theta}{q}\varphi_q - \frac{\rho_o}{\rho}\frac{\sin\theta}{q}\psi_\theta\right) d\theta \quad (8\text{-}20a)$$

$$dy = \frac{\sin\theta}{q}\left(\frac{\partial\varphi}{\partial q}dq + \frac{\partial\varphi}{\partial\theta}d\theta\right) + \frac{\rho_o}{\rho}\frac{\cos\theta}{q}\left(\frac{\partial\psi}{\partial q}dq + \frac{\partial\psi}{\partial\theta}d\theta\right)$$

$$= \left(\frac{\sin\theta}{q}\frac{\partial\varphi}{\partial q} + \frac{\rho_o}{\rho}\frac{\cos\theta}{q}\frac{\partial\psi}{\partial q}\right) dq + \left(\frac{\sin\theta}{q}\frac{\partial\varphi}{\partial\theta} + \frac{\rho_o}{\rho}\frac{\cos\theta}{q}\frac{\partial\psi}{\partial\theta}\right) d\theta$$

$$= \left(\frac{\sin\theta}{q}\varphi_q + \frac{\rho_o}{\rho}\frac{\cos\theta}{q}\psi_q\right) dq + \left(\frac{\sin\theta}{q}\varphi_\theta + \frac{\rho_o}{\rho}\frac{\cos\theta}{q}\psi_\theta\right) d\theta \quad (8\text{-}20b)$$

from which

$$\frac{\partial x}{\partial q} = x_q = \frac{\cos\theta}{q}\varphi_q - \frac{\rho_o}{\rho}\frac{\sin\theta}{q}\psi_q \quad (8\text{-}21a)$$

$$\frac{\partial x}{\partial\theta} = x_\theta = \frac{\cos\theta}{q}\varphi_\theta - \frac{\rho_o}{\rho}\frac{\sin\theta}{q}\psi_\theta \quad (8\text{-}21b)$$

and

$$\frac{\partial y}{\partial q} = y_q = \frac{\sin\theta}{q}\varphi_q + \frac{\rho_o}{\rho}\frac{\cos\theta}{q}\psi_q \quad (8\text{-}22a)$$

$$\frac{\partial y}{\partial\theta} = y_\theta = \frac{\sin\theta}{q}\varphi_\theta + \frac{\rho_o}{\rho}\frac{\cos\theta}{q}\psi_\theta \quad (8\text{-}22b)$$

The objective is to obtain φ and ψ in terms of q and θ. To this end, x and y are eliminated from Equations (8-21) and (8-22) by making use of the independence of order in partial differentiation:

$$\frac{\partial^2 x}{\partial\theta\partial q} \quad \frac{\partial^2 x}{\partial q\partial\theta} \text{ and } \frac{\partial^2 y}{\partial\theta\partial q} \quad \frac{\partial^2 y}{\partial q\partial\theta}$$

resulting, after simplification (and noting that ρ depends only on q):

$$-\frac{\sin\theta}{q}\varphi_q - \frac{\rho_o}{\rho}\frac{\cos\theta}{q}\psi_q = \frac{\cos\theta}{q^2}\varphi_\theta + \frac{\rho_o}{\rho}\frac{\sin\theta}{q^2}\psi_\theta - \frac{\sin\theta}{q}\left[\frac{d}{dq}\left(\frac{\rho_o}{\rho}\right)\right]\psi_\theta$$

(8-23a)

$$\frac{\cos\theta}{q}\varphi_q - \frac{\rho_o}{\rho}\frac{\sin\theta}{q}\psi_q = -\frac{\sin\theta}{q}\varphi_\theta - \frac{\rho_o}{\rho}\frac{\cos\theta}{q^2}\psi_\theta + \frac{\cos\theta}{q}\left[\frac{d}{dq}\left(\frac{\rho_o}{\rho}\right)\right]\psi_\theta \tag{8-23b}$$

Multiplying Equation (8-23a) by sin θ, Equation (8-23b) by cos θ, subtracting, and similarly, multiplying Equation (8-23a) by cos θ, Equation (8-23b) by sin θ, and adding, there results the equation for φ in terms of q and θ:

$$\varphi_q = q\left[\frac{d}{dq}\left(\frac{1}{q}\frac{\rho_o}{\rho}\right)\right]\psi_\theta \tag{8-24a}$$

$$\varphi_\theta = \frac{\rho_o}{\rho}\, q\, \psi_q \tag{8-24b}$$

Equations (8-24) are the equivalent of the Cauchy-Rieman equations for incompressible flow.

Using Euler's equation $\frac{dp}{\rho} + q\,dq = 0$ and the expression for the speed of sound $c^2 = \frac{dp}{dq}$ to form the relation

$$\frac{d}{dq}\left(\frac{\rho_o}{\rho}\right) = -\frac{\rho_o}{\rho^2}\frac{d\rho}{dq} = -\frac{\rho_o}{\rho}\frac{d\rho}{dp}\frac{dp}{dq}$$

$$= -\frac{\rho_o}{\rho}\left(\frac{1}{c^2}\right)(-\rho\, q) = \frac{\rho_o}{\rho}\frac{q}{c^2} \tag{8-25}$$

Equation (8-25) is substituted into Equation (8-24a) to result, after rearrangement

$$\varphi_q = -\frac{\rho_o}{\rho}\frac{1}{q}\left(1 - \frac{q^2}{c^2}\right)\psi_\theta = -\frac{\rho_o}{\rho}\frac{1}{q}\left(1 - M^2\right)\psi_\theta \tag{8-26}$$

Finally, φ is eliminated from Equations (8-26) and (8-24b) by setting $\varphi_{\theta q} = \varphi_{q\theta}$. Thus, noting that ρ and M depend only on q, and making use of Equation (8-25) there is obtained:

$$\varphi_{\theta q} = \frac{\partial}{\partial \theta}\left[-\frac{\rho_o}{\rho}\frac{1}{q}(1 - M^2)\,\psi_\theta\right] = -\frac{\rho_o}{\rho}\frac{1}{q}(1 - M^2)\,\psi_{\theta\theta}$$

$$\varphi_{q\theta} = \frac{\partial}{\partial q}\left(\frac{\rho_o}{\rho}\,q\,\psi_q\right) = \frac{\rho_o}{\rho}(q\,\psi_{qq} + \psi_q) + q\,\psi\left(\frac{\rho_o}{\rho}\frac{q}{c^2}\right)$$

and, equating $\varphi_{\theta q}$ to $\varphi_{q\theta}$ and simplifying:

$$q^2\psi_{qq} + q(1 + M^2)\psi_q + (1 - M^2)\psi_{\theta\theta} = 0 \qquad (8\text{-}27)$$

Equation (8-27) is the hodograph equation giving ψ as function of the new variables q and θ. It is linear in the dependent variable $\psi(q,\theta)$ since $M = \frac{q}{c}$ is a function of q only.

An alternate form may be given Equation (8-27) by replacing M^2 by $\frac{q^2}{c^2}$ and eliminating c^2 through the Bernoulli relation

$$c^2 + \frac{\gamma - 1}{2}\,q^2 = c_o^2$$

This results in

$$q^2\left(1 - \frac{\gamma-1}{2}\frac{q^2}{c_o^2}\right)\psi_{qq} + q\left(1 - \frac{\gamma-3}{2}\frac{q^2}{c_o^2}\right)\psi_q + \left(1 - \frac{\gamma+1}{2}\frac{q^2}{c_o^2}\right)\psi_{\theta\theta} = 0 \qquad (8\text{-}28)$$

Equations (8-28) and (8-27) are also known as Chaplygin's equation. They represent the differential equation of flow in the (q,θ)-plane as against the physical (x,y)-plane.

8.5 Obtainment of Streamline

The general procedure for the solution of Equation (8-27) is as follows: i) assuming that a number of simple functions $\psi_1, \psi_2, \ldots$ have been found to satisfy Equation (8-27), more complex solutions are found by linear superposition:

$$\psi(q,\theta) = C_1 \psi_1(q,\theta) + C_2 \psi_2(q,\theta) + \ldots \qquad (8\text{-}29)$$

ii) the derivatives ψ_q and ψ_θ as functions of q and θ are found by partial differentiation of the solution $\psi = \psi(q,\theta)$, iii) using the Cauchy-Rieman equations for compressible flow, Equations (8-24):

$$\varphi_q = -\frac{\rho_o}{\rho}\frac{1}{q}(1 - M^2)\psi_\theta \qquad (8\text{-}24a)$$

$$\varphi_\theta = \frac{\rho_o}{\rho} q \psi_q \qquad (8\text{-}24b)$$

φ_q and φ_θ are found as functions of q and θ, iv) knowing φ_q and φ_θ, the partial derivatives x_q, x_θ, y_q, and y_θ of the physical variables are found by use of Equations (8-21) and (8-22)

$$x_q = \frac{\cos\theta}{q}\varphi_q - \frac{\rho_o}{\rho}\frac{\sin\theta}{q}\psi_q \qquad (8\text{-}21a)$$

$$x_\theta = \frac{\cos\theta}{q}\varphi_\theta - \frac{\rho_o}{\rho}\frac{\sin\theta}{q}\psi_\theta \qquad (8\text{-}21b)$$

and

$$y_q = \frac{\sin\theta}{q}\varphi_q + \frac{\rho_o}{\rho}\frac{\cos\theta}{q}\psi_q \qquad (8\text{-}22a)$$

$$y_\theta = \frac{\sin\theta}{q}\varphi_\theta + \frac{\rho_o}{\rho}\frac{\cos\theta}{q}\psi_\theta \qquad (8\text{-}22b)$$

v) the derivatives x_q, x_θ, y_q and y_θ are then integrated to yield x and y as functions of q and θ. This maps the streamlines $\psi(q,\theta)$ from the hodograph plane (q,θ) back to the original physical plane (x,y), thus obtaining a streamline $\psi(x,y)$.

8.6 Solution for Vortex Tube

The solution for the streamline pattern in the vortex tube is obtained by combining a "free" vortex flow with a "sink" flow. The

respective solutions of these individual flows, however, is first presented.

8.7 Vortex Flow

For this case, a particular solution of Equation (8-27) is sought, in which ψ depends only on q. Then $\psi_\theta = \psi_{\theta\theta} = 0$, and the differential equation becomes

$$q^2 \psi_{qq} + q\left(1 + \frac{q^2}{c^2}\right) \psi_q = 0 \qquad (8\text{-}30)$$

or

$$q^2 \left(1 - \frac{\gamma-1}{2} \frac{q^2}{c_o^2}\right)\psi_{qq} + q\left(1 - \frac{\gamma-3}{2} \frac{q^2}{c_o^2}\right)\psi_q = 0 \qquad (8\text{-}31)$$

Equation (8-31) cannot be integrated in closed form except for certain values of γ. For the particular value of $\gamma = 1.4$, a closed solution, however, is possible. It is

$$\psi = C_1 \int e^{-\int \frac{1 - \frac{\gamma-3}{2} \frac{q^2}{c_o^2}}{1 - \frac{\gamma-1}{2} \frac{q^2}{c_o^2}} \frac{dq}{q}} dq + C_2$$

which integrates to

$$\psi = C_1 \left[1/2 \ln \frac{1 - \left(1 - \frac{\gamma-1}{2} \frac{q^2}{c_o^2}\right)^{1/2}}{1 - \left(1 + \frac{\gamma-1}{2} \frac{q^2}{c_o^2}\right)^{1/2}} + \left(1 - \frac{\gamma-1}{2} \frac{q^2}{c_o^2}\right)^{1/2} + 1/3 \left(1 - \frac{\gamma-1}{2} \frac{q^2}{c_o^2}\right)^{3/2} + 1/5 \left(1 - \frac{\gamma-1}{2} \frac{q^2}{c_o^2}\right)^{5/2} \right] + C_2 \qquad (8\text{-}32)$$

Equation (8-32) is more conveniently written in the form of

$$\psi = C_1 J + C_2 \tag{8-33}$$

where

$$J = 1/2 \ln \frac{1-j}{1+j} + j + 1/3\, j^3 + 1/5\, j^5 \tag{8-34}$$

and

$$j = \left(1 - \frac{\gamma-1}{2} \frac{q^2}{c_o^2}\right)^{1/2} = \left(\frac{\rho}{\rho_o}\right)^{1/5} \tag{8-35}$$

From this, and Equations (8-24), it is seen that

$$\psi_q = \frac{C_1}{q} j^5, \quad \psi_\theta = 0 \tag{8-36a}$$

$$\varphi_\theta = C_1 \frac{\rho_o}{\rho} j^5, \quad \varphi_q = 0 \tag{8-36b}$$

Substitution of Equations (8-36) into Equations (8-21) and (8-22) yields

$$x_q = - C_1 \frac{\sin \theta}{q^2} \tag{8-37a}$$

$$x_\theta = C_1 \frac{\cos \theta}{q} \tag{8-37b}$$

$$y_q = C_1 \frac{\cos \theta}{q^2} \tag{8-38a}$$

$$y_\theta = C_1 \frac{\sin \theta}{q} \tag{8-38b}$$

Integrating Equations (8-37) and (8-38), and omitting unessential additive constants, the equations for the streamlines in the physical (x,y)-plane are finally obtained.

$$x = C_1 \frac{\sin \theta}{q} \tag{8-39a}$$

$$y = C_1 \frac{\cos \theta}{q} \tag{8-39b}$$

Choosing the constant to be $C_1 = rq = r^*c^*$ where r^* is the radius corresponding to a Mach number of unity, Equations (8-39) may be rewritten in the form

$$\frac{x}{r^*} = \frac{\sin \theta}{\frac{q}{c^*}} \tag{8-40a}$$

$$\frac{y}{r^*} = \frac{\cos \theta}{\frac{q}{c^*}} \tag{8-40b}$$

The streamlines ψ = constant of this flow are lines of constant velocity; they are also concentric circles in the physical plane. The velocity variation is that of a potential or free vortex, i.e., qr is constant. The flow pattern shows the velocity to increase with decreasing radius to a maximum of $M^* = \sqrt{\frac{\gamma+1}{\gamma-1}}$.

Figure (8-4) shows the velocity distribution for the vortex flow. It is of interest to note that the flow is not limited by a "sonic" radius r^*, but by a smaller radius r_{min} corresponding to a maximum attainable velocity of $\frac{q_{max}}{c^*} = \sqrt{6}$, a zero density, and a zero temperature. In terms of the strength of the vortex, this minimum or "limit" circle is

$$r_{min} = \frac{\Gamma}{2\pi c^*} \sqrt{\frac{\gamma-1}{\gamma+1}} = \frac{\Gamma}{2\pi q_{max}} \tag{8-41}$$

At any radius r, the radius ratio is given by

$$\left(\frac{r}{r_{min}}\right)^2 = \frac{1}{1 - \left(\frac{\rho}{\rho_o}\right)^{\gamma-1}} \tag{8-42}$$

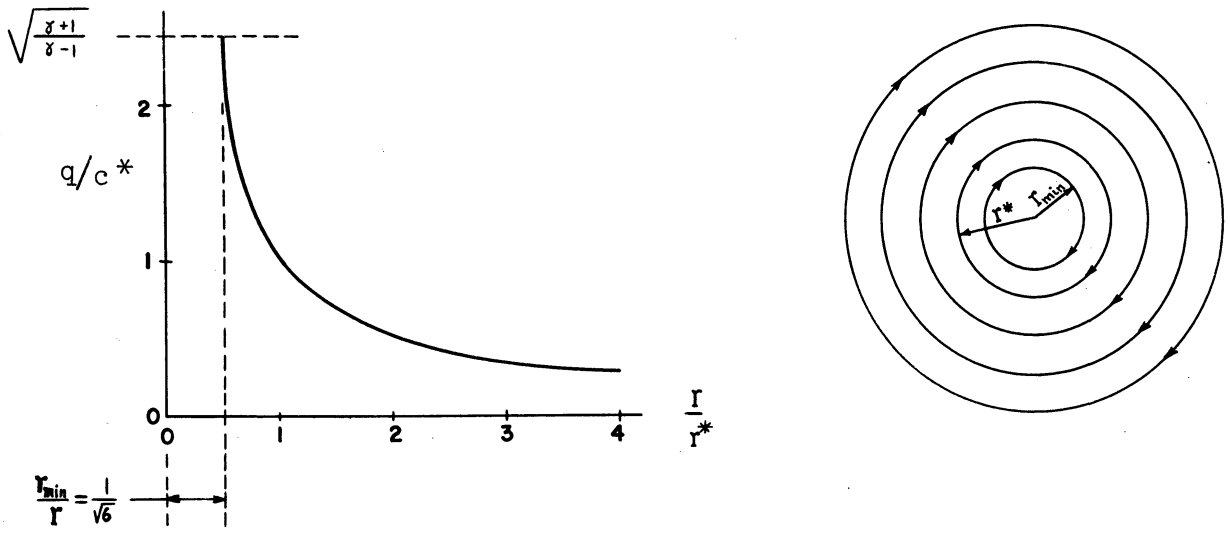

Figure 8-4. Velocity Distribution for Vortex Flow

The density (and similarly the pressure) decreases from the stagnation value at infinity, to zero at radius r_{min}. The variation of density, pressure, and speed with radius is shown in Figure (8-5).

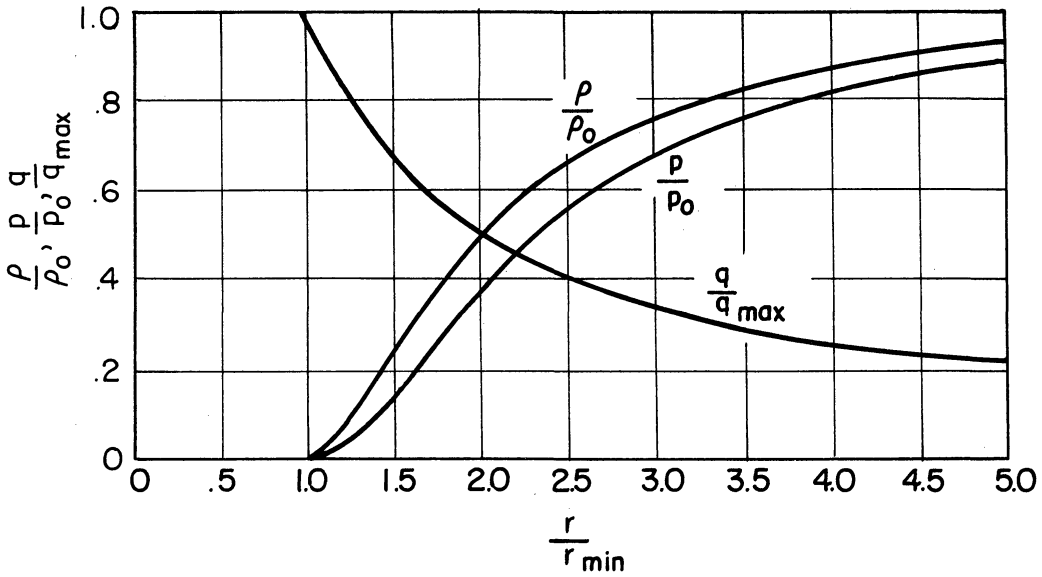

Figure 8-5. Solution-Curves for Vortex Flow

8.8 Sink (Source) Flow

Let a stream function ψ which depends only on θ be sought for Equation (8-27). Then $\psi_q = \psi_{qq} = 0$, and Equation (8-27) becomes simply

$$\psi_{\theta\theta} = 0 \tag{8-43}$$

the solution of which is

$$\psi = C_1 \theta + C_2 \tag{8-44}$$

where C_1 and C_2 are constants of integration. The streamlines ψ = constant are lines of constant flow direction, and therefore are straight lines passing through the origin.

The derivatives of ψ as obtained from Equation (8-44) are now $\psi_q = 0$, $\psi_\theta = C_1$, and substituting these values in the Cauchy-Rieman equations, Equations (8-24), results in

$$\varphi_q = -\frac{\rho_o}{\rho}\frac{1}{q}(1 - M^2)\psi_\theta = -C_1\frac{\rho_o}{\rho}\frac{1}{q}(1 - M^2) = C_1\frac{\rho_o}{\rho}\frac{1}{q}\left(1 - \frac{q^2}{c^2}\right)$$

$$\varphi_\theta = \frac{\rho_o}{\rho} q \psi_q = 0$$

The partial derivatives x_q, x_θ, y_q, and y_θ are then found by means of Equations (8-21) and (8-22).

$$x_q = \frac{\cos\theta}{q}\varphi_q - \frac{\rho_o}{\rho}\frac{\sin\theta}{q}\psi_q = -C_1\frac{\rho_o}{\rho}\frac{\cos\theta}{q^2}\left(1 - \frac{q^2}{c^2}\right) \tag{8-45a}$$

$$x_\theta = \frac{\cos\theta}{q}\varphi_\theta - \frac{\rho_o}{\rho}\frac{\sin\theta}{q}\psi_\theta = -C_1\frac{\rho_o}{\rho}\frac{\sin\theta}{q} \tag{8-45b}$$

and

$$y_q = \frac{\sin\theta}{q}\varphi_q + \frac{\rho_o}{\rho}\frac{\cos\theta}{q}\psi_q = -C_1\frac{\rho_o}{\rho}\frac{\sin\theta}{q^2}(1 - M^2) \qquad (8\text{-}46a)$$

$$y_\theta = \frac{\sin\theta}{q}\varphi_\theta + \frac{\rho_o}{\rho}\frac{\cos\theta}{q}\psi_\theta = C_1\frac{\rho_o}{\rho}\frac{\cos\theta}{q} \qquad (8\text{-}46b)$$

Equations (8-45) and (8-46) must now be integrated to obtain x and y as functions of q and θ. To obtain $x(q,\theta)$, it is easier to work with Equation (8-45b):

$$x_\theta = -C_1\frac{\rho_o}{\rho}\frac{\sin\theta}{q}$$

which gives

$$x = C_1\frac{\rho_o}{\rho}\frac{\cos\theta}{q} + f(q) \qquad (8\text{-}47)$$

To determine f(q), Equation (8-47) is differentiated with respect to q and the result compared with Equation (8-45a). Thus,

$$x_q = \frac{d}{dq}\left[C_1\frac{\rho_o}{\rho}\frac{\cos\theta}{q}\right] + f'(q)$$

$$= C_1\frac{\cos\theta}{q}\frac{d}{dq}\left(\frac{\rho_o}{\rho}\right) - C_1\frac{\rho_o}{\rho}\frac{\cos\theta}{q^2} + f'(q)$$

recalling that $\frac{d}{dq}\left(\frac{\rho_o}{\rho}\right) = \frac{\rho_o}{\rho}\frac{q}{c^2}$, this becomes

$$x_q = C_1\frac{\rho_o}{\rho}\frac{\cos\theta}{c^2} - C_1\frac{\rho_o}{\rho}\frac{\cos\theta}{q^2} + f'(q) \qquad (8\text{-}48)$$

Comparison of Equation (8-48) with Equation (8-45a) shows that $f'(q) = 0$. It follows that $f(q) = C_3$, and the complete expression for x as obtained from Equation (8-47) is thus

$$x = C_1\frac{\rho_o}{\rho}\frac{\cos\theta}{q} + C_3 \qquad (8\text{-}49)$$

In the same manner, integration of Equation (8-46b) and comparison with Equation (8-46a) results in

$$y = C_1 \frac{\rho_o}{\rho} \frac{\sin \theta}{q} + C_4 \tag{8-50}$$

The constants C_2, C_3, and C_4 merely involve displacements of the entire streamline pattern, and without loss of generality can be set to equal zero. The parametric equation for the streamlines is thus

$$x = C_1 \frac{\rho_o}{\rho} \frac{\cos \theta}{q} \tag{8-51a}$$

$$y = C_1 \frac{\rho_o}{\rho} \frac{\sin \theta}{q} \tag{8-51b}$$

Equations (8-15) show, by division of y by x, that the lines of constant flow direction θ are also lines of constant $\frac{y}{x}$. The latter are radial lines through the origin on the (x,y)-plane, and the former were previously shown to be lines of constant ψ. Therefore, the physical streamlines are those of a two-dimensional source or sink. The constant C_1 is determined in the following manner. From Equations (8-51):

$$r = (x^2 + y^2)^{1/2} = C_1 \frac{\rho_o}{\rho} \frac{1}{q} \tag{8-52}$$

If C_1 is set to satisfy the equation of continuity

$$\rho \; r \; q = \rho^* \; r^* \; c^* \tag{8-53}$$

it is seen that its value must be

$$C_1 = \frac{\rho^*}{\rho_o} c^* \; r^* \tag{8-54}$$

where the * superscript denotes the condition where the Mach number is unity.

The graph of $\frac{q}{c^*}$ versus $\frac{r}{r^*}$ as plotted in Figure (8-6) shows that there are two branches for the curve.

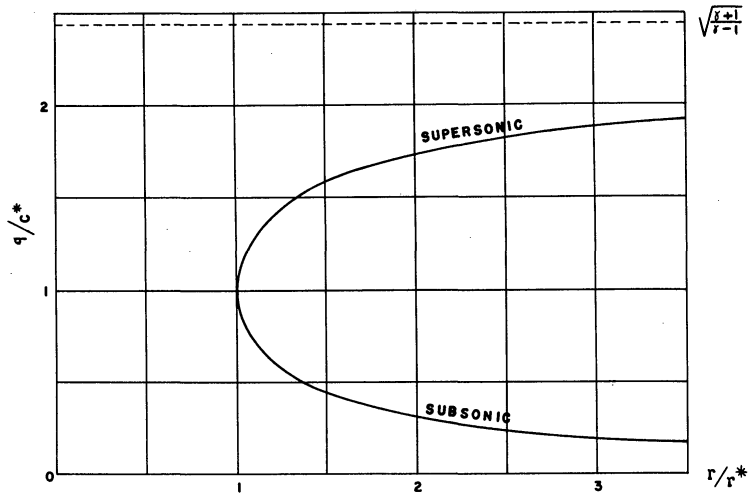

Figure 8-6. Velocity Distribution for Compressible Sink (Source)

One branch tends to zero, and the other tends to $(\frac{\gamma+1}{\gamma-1})^{1/2} = \sqrt{6}$ as $\frac{r}{r^*}$ tends to infinity. There is no value of $\frac{q}{c^*}$ for $r < r^*$. Thus, source, or sink flow cannot exist inside the "sonic" radius r^*, which is the limit line. This is in contrast to incompressible flow whose streamlines come to a point at the origin.

For any $r > r^*$, there are two possible values of q, one representing supersonic or "diverging" flow, and the other representing subsonic or "converging" flow. Physically, of course, only one curve may exist at a time, which means that the velocity may either be subsonic or supersonic, but not both. The minimum radius is given by

$$r_{min} = \frac{\sigma}{2\pi q^* \left(\frac{\rho_o}{\rho}\right)} \qquad (8\text{-}55)$$

where $\sigma = \frac{2\pi r q}{\rho_o}$ is a measure of the sink (source) strength. The dependence of speed, density, and pressure upon radius is shown by the curves in Figure (8-7).

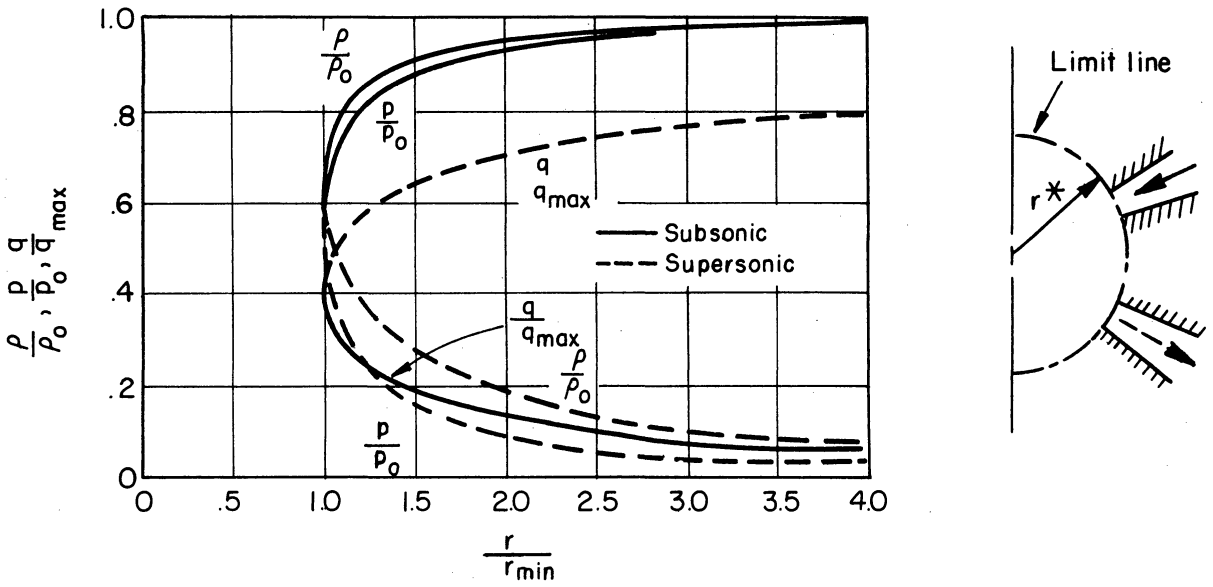

Figure 8-7. Solution-Curves for Sink (Source)

The portions corresponding to subsonic conditions are drawn in full lines, and those, corresponding to supersonic conditions in dotted lines. They represent the two cases of inward and outward flow. Regardless of the type of flow, however, if $\rho > \rho^*$, the speed is everywhere subsonic, and if $\rho < \rho^*$, the speed is everywhere supersonic.

The occurrence of a minimum radius is a characteristic property of compressible flow, namely the existence of limit lines or surfaces across which the fluid does not penetrate. This is most acutely evident in the case of an inward flow starting from the stagnation pressure at infinity, and continually accelerated until it arrives at the limit circle. The acceleration at the limit circle is found from

$$a = \frac{dq}{dt} = q \frac{dq}{dr} \tag{8-56}$$

Using Equations (8-51) and the relation $(dr)^2 = (dx)^2 + (dy)^2$, and recalling that

$$\frac{d\left(\frac{\rho_o}{\rho}\right)}{dq} = \frac{\rho_o}{\rho}\frac{q}{c^2} \tag{8-57}$$

Equation (8-56) becomes

$$a = \pm \frac{\rho}{\rho^*}\frac{q^3}{rc^*}\frac{1}{\left(\frac{q^2}{c^2} - 1\right)} \tag{8-58}$$

and it is seen that the fluid acceleration at the sonic line $\left(\frac{q^2}{c^2} = 1\right)$ becomes infinite.

8.9 Spiral Flow

The compressible vortex flow and the compressible sink flow of the previous sections are now combined for the final solution of the spiral flow in the vortex tube.

Let the mass rate of sink flow be denoted by $\rho_o\varphi = 2\pi\rho^* r^* c^*$ where Q is the corresponding volume rate of flow at the density ρ_o. The several results for sink flow as derived from the previous section then become

$$\psi = \frac{\varphi}{2\pi}\theta \tag{8-59}$$

$$x = \frac{\varphi}{2\pi c_o}\frac{\cos\theta}{\frac{\rho}{\rho_o}\frac{q}{c_o}} \tag{8-60a}$$

$$y = \frac{\varphi}{2\pi c_o}\frac{\sin\theta}{\frac{\rho}{\rho_o}\frac{q}{c_o}} \tag{8-60b}$$

$$r = \frac{\varphi}{2\pi c_o}\frac{1}{\frac{\rho}{\rho_o}\frac{q}{c_o}} \tag{8-61}$$

For the vortex flow, let $2\pi c^* r^* = \Gamma$ where Γ is the circulation for any closed curve enclosing the origin. Then the results for vortex flow may be written as

$$\psi = \frac{\Gamma}{2\pi} J \tag{8-62}$$

$$x = \frac{\Gamma}{2\pi c_o} \frac{\sin \theta}{\frac{q}{c_o}} \tag{8-63a}$$

$$y = - \frac{\Gamma}{2\pi c_o} \frac{\cos \theta}{\frac{q}{c_o}} \tag{8-63b}$$

$$r = \frac{\Gamma}{2\pi c_o} \frac{1}{\frac{q}{c_o}} \tag{8-64}$$

Superposing the vortex flow with the sink flow results in

$$\psi = \frac{Q}{2\pi} \theta + \frac{\Gamma}{2\pi} J \tag{8-65}$$

$$x = \frac{Q}{2\pi c_o} \frac{\cos \theta}{\frac{\rho}{\rho_o} \frac{q}{c_o}} + \frac{\Gamma}{2\pi c_o} \frac{\sin \theta}{\frac{q}{c_o}} \tag{8-66a}$$

$$y = \frac{Q}{2\pi c_o} \frac{\sin \theta}{\frac{\rho}{\rho_o} \frac{q}{c_o}} - \frac{\Gamma}{2\pi c_o} \frac{\cos \theta}{\frac{q}{c_o}} \tag{8-66b}$$

$$R = \frac{2\pi c_o}{\sqrt{Q^2 + \Gamma^2}} r \tag{8-67}$$

where the constants Q and Γ may be regarded as the strengths of the sink and vortex, $\sqrt{Q^2 + \Gamma^2}$ as the strength of the combined flow, and R the radius of curvature of streamline. Equations (8-65), (8-66), and (8-67) may be rearranged into

$$\frac{2\pi\psi}{\sqrt{Q^2 + \Gamma^2}} = \frac{\theta}{\sqrt{1 + \left(\frac{\Gamma}{Q}\right)^2}} + \frac{J}{\sqrt{1 + \left(\frac{Q}{\Gamma}\right)^2}} \tag{8-68}$$

$$\frac{2\pi c_o}{\sqrt{Q^2 + \Gamma^2}}\, x = \frac{\cos\theta}{\left(\frac{\rho}{\rho_o}\right)\left(\frac{q}{c_o}\right)\sqrt{1 + \left(\frac{\Gamma}{Q}\right)^2}} + \frac{\sin\theta}{\left(\frac{q}{c_o}\right)\sqrt{1 + \left(\frac{Q}{\Gamma}\right)^2}} \tag{8-69a}$$

$$\frac{2\pi c_o\, y}{\sqrt{Q^2 + \Gamma^2}} = \frac{\sin\theta}{\left(\frac{\rho}{\rho_o}\right)\left(\frac{q}{c_o}\right)\sqrt{1 + \left(\frac{\Gamma}{Q}\right)^2}} - \frac{\cos\theta}{\left(\frac{q}{c_o}\right)\sqrt{1 + \left(\frac{Q}{\Gamma}\right)^2}} \tag{8-69b}$$

$$R = \frac{1}{q/c_o}\sqrt{\frac{1}{\left(\frac{\rho}{\rho_o}\right)^2\left[1 + \left(\frac{\Gamma}{Q}\right)^2\right]} + \frac{1}{1 + \left(\frac{Q}{\Gamma}\right)^2}} \tag{8-70}$$

To plot a physical streamline for selected values of Q and Γ, a value of ψ is chosen and corresponding pairs of values for q/c_o and θ are solved for from Equation (8-68). These are then substituted into Equations (8-69) to determine the corresponding values of x and y on the streamline. The general streamline pattern is shown in Figure (8-8).

Or, a corresponding pair of values of q/c_o and θ may be determined from experiment and substituted into Equations (8-68) and (8-69) to give a streamline ψ corresponding to a certain strength of vortex and sink. The streamlines ψ = constant are spirals which meet the limiting circle r_{min} at the angle $\sin^{-1}\frac{c}{q}$. The physical plane is mathematically covered twice by the streamline pattern. Physically, however, only one set of streamlines at a time is possible. At the limit line, the two streamlines meet in a cusp. One set of streamlines is purely supersonic, whereas the other set is partly subsonic and partly supersonic. The fluid acceleration is infinite, and the component of velocity in the radial direction is equal to the local speed of sound.

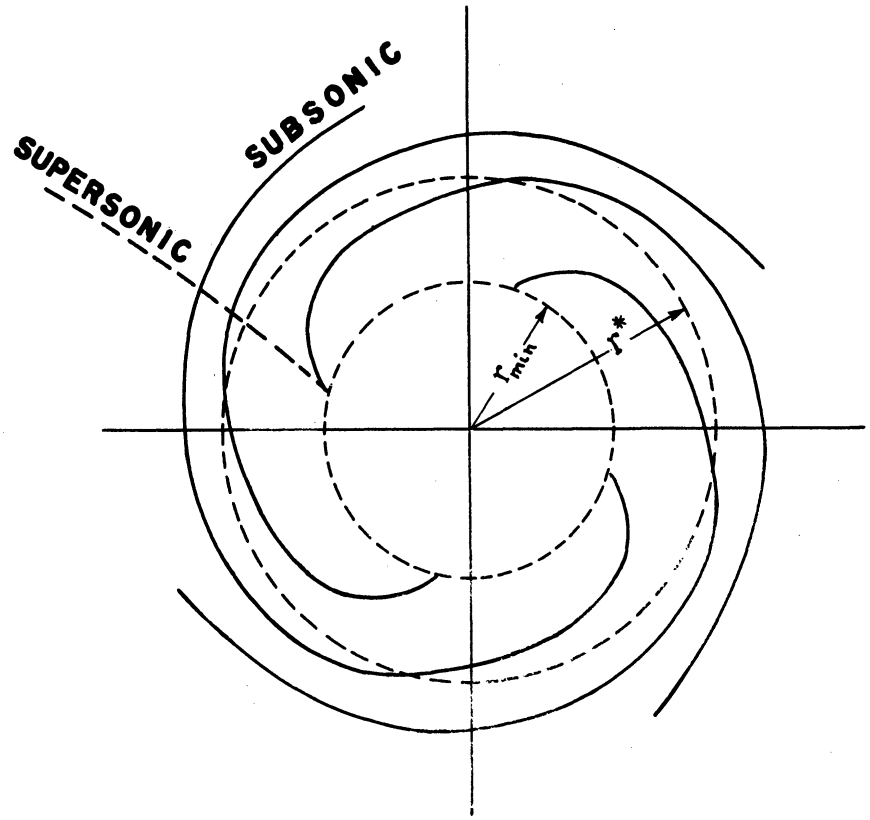

Figure 8-8a. Spiral Flow Pattern

It is interesting to note that the limit circle, being smaller than the sonic circle, deceleration from supersonic speeds to subsonic speeds is possible without shocks. The relation between q/c^* and r/r^* for various strength ratios Q/Γ is shown in Figure (8-9).

For each direction of flow, inward or outward, there are two possible régimes. In one, the density tends to zero at infinity, and the speed is everywhere supersonic. In this case, the resultant velocity becomes more and more nearly radial as r increases. In the other, the density is ρ_o at infinity, and the radial component of the velocity is everywhere subsonic. In this case, the flow is spiral, and the streamlines approach equiangular spirals ($r \alpha \exp \frac{\sigma\theta}{\Gamma}$) as r increases.

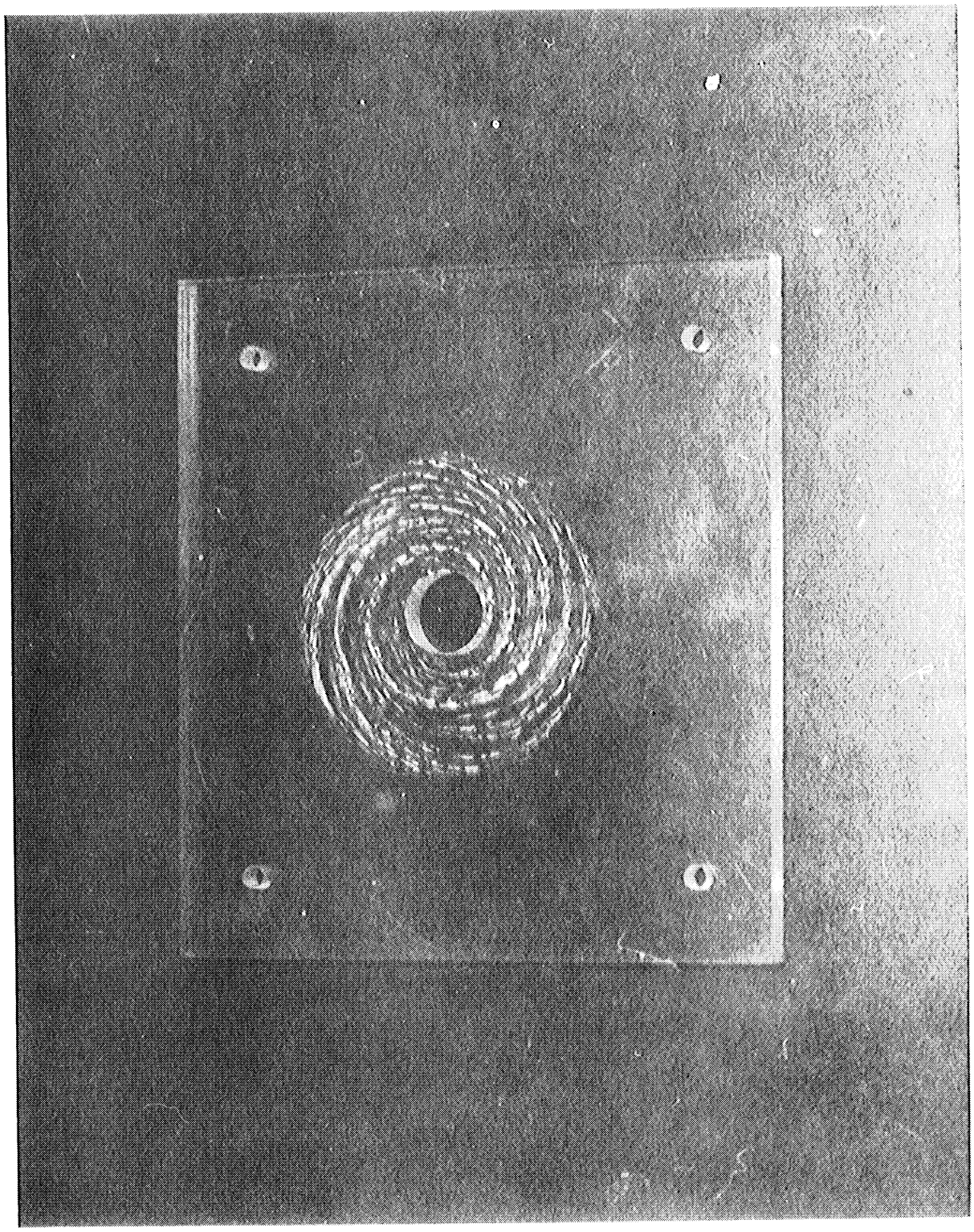

Figure 8-8b. Flow Pattern from Experimental Study (Light Injection)

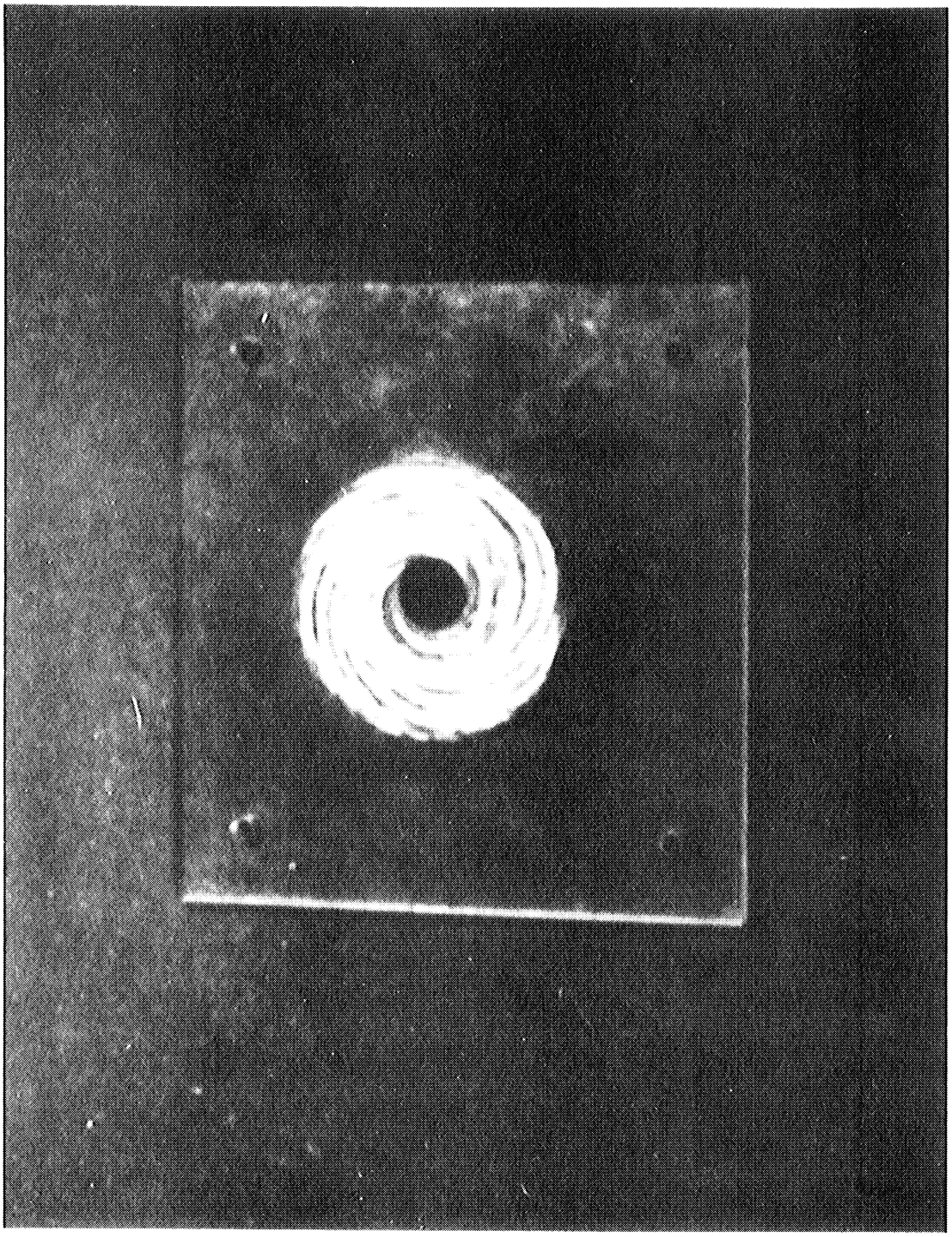

Figure 8-8c. Flow Pattern from Experimental Study (Heavy Injection)

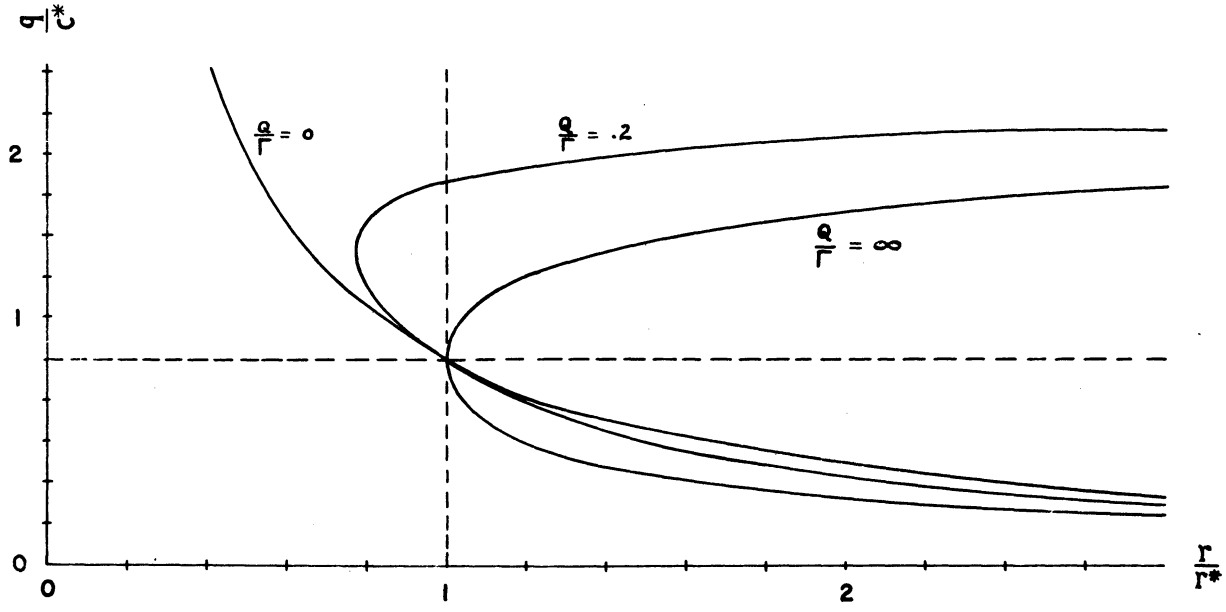

Figure 8-9. Dimensionless Speed for Spiral Flow

A plot of the streamlines is more conveniently determined by introducing the variable

$$A = \frac{c}{c_o} \tag{8-71}$$

and expressing the stream function ψ in finite terms. The result is

$$\psi = \frac{\sigma}{2\pi}\left[\theta + \tan^{-1}\frac{A^5\Gamma}{\sigma}\right] - \frac{\Gamma}{2\pi}\left[1/2\ \ln\frac{1+A}{1-A} - A - \frac{A^3}{3} - \frac{A^5}{5}\right] \tag{8-72}$$

$$r^2 = \frac{1}{4\pi^2 q^2_{max}}\,\frac{A^{10}\Gamma^2 + \sigma^2}{(1-A^2)\,A^{10}} \tag{8-73}$$

$$\frac{\partial\psi}{\partial r} = -\frac{\rho}{\rho_o}V = -\frac{\Gamma}{2\pi r}\frac{\rho}{\rho_o} \tag{8-74a}$$

$$\frac{\partial\psi}{\partial\theta} = r\frac{\rho}{\rho_o}u = \frac{\sigma}{2\pi} \tag{8-74b}$$

$$q^2 = u^2 + v^2 \tag{8-75}$$

Elimination of A between Equations (8-72) and (8-73) enables the streamlines to be drawn. As $\rho/\rho_o \to 0$, $\psi \to \frac{\sigma\theta}{2}$ and $x \to \infty$, so that the streamlines become asymptotically radial. This is the first flow regime. As $\rho/\rho_o \to 1$, $r \to \infty$, and $(\sigma\theta - \Gamma \ln r)$ constant, so that the streamlines become asymptotically the equiangular spirals $r \alpha \exp \sigma\theta/\Gamma$. This is the second regime, and the one that exists in the vortex tube. Figure (8-10) shows the detailed construction of a streamline for both flow regimes. The full line corresponds to the type of flow that exists in the vortex tube.

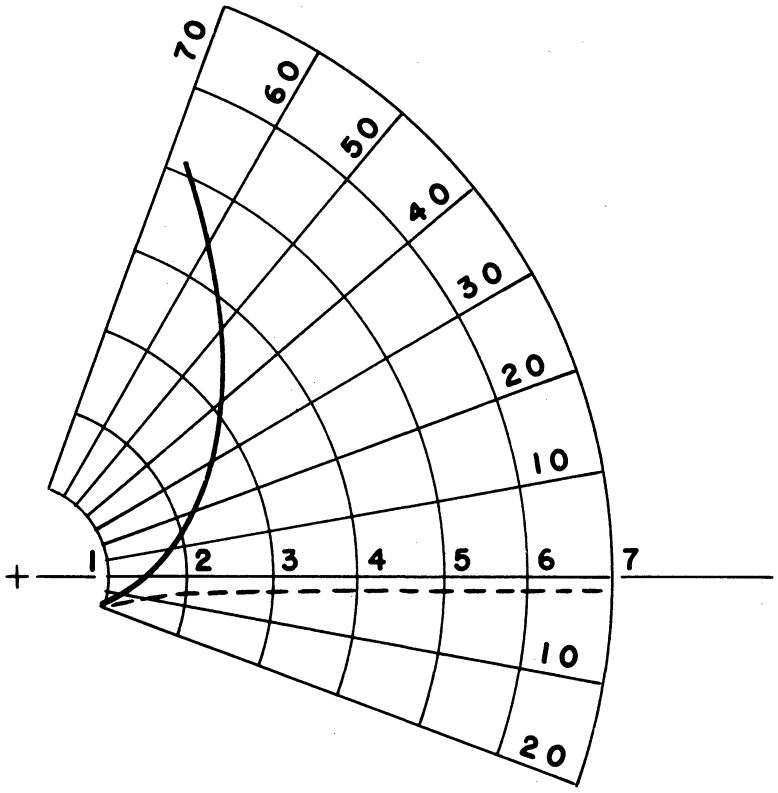

Figure 8-10. Construction of Streamline

CHAPTER 9

THREE-DIMENSIONAL SOLUTION BY ADDITION OF AXIAL VELOCITY

9.1 Preliminary Statement

The solution presented in the preceding chapter is an exact solution in that it became mathematically solvable after transformation of coordinates. But it was achieved at the expense of adopting one restriction, namely, that the third velocity component be relatively small, and is thus neglected. When a more general solution in terms of three space coordinates is sought, however, the mathematical difficulties become so great that formal solution is not possible. It is the purpose of the present chapter to circumvent this difficulty.

9.2 Potential Equation in Space

In the preceding chapter on two-dimensional flow, the equation of continuity, the equation of motion, and the relations for the existence of a velocity potential were combined to yield the differential equation of flow

$$\left(1 - \frac{\varphi_x}{c^2}\right) \varphi_{xx} + \left(1 - \frac{\varphi_y^2}{c^2}\right) \varphi_{yy} - \frac{2}{c^2} \varphi_x \varphi_y \varphi_{xy} = 0 \qquad (9\text{-}1)$$

$$c^2 = f(u^2 + v^2)$$

which, being in terms of two space coordinates, was solved by means of a hodograph transformation.

For three-dimensional flow, similar proceedings yield the differential equation in Cartesian coordinates:

$$\left(1 - \frac{\varphi_x^2}{c^2}\right) \varphi_{xx} + \left(1 - \frac{\varphi_y^2}{c^2}\right) \varphi_{yy} + \left(1 - \frac{\varphi_z^2}{c^2}\right) \varphi_{zz} - \text{(cont'd)}$$

$$- 2 \frac{\varphi_x \varphi_y}{c^2} \varphi_{xy} - 2 \frac{\varphi_y \varphi_z}{c^2} \varphi_{yz} - 2 \frac{\varphi_z \varphi_x}{c^2} \varphi_{zx} = 0 \qquad (9\text{-}2)$$

$$c^2 = f(u^2 + V^2 + w^2)$$

In cylindrical coordinates, the three coordinates, u, v, and w are the velocity components in the r, θ, and z directions as shown in Figure (9-1).

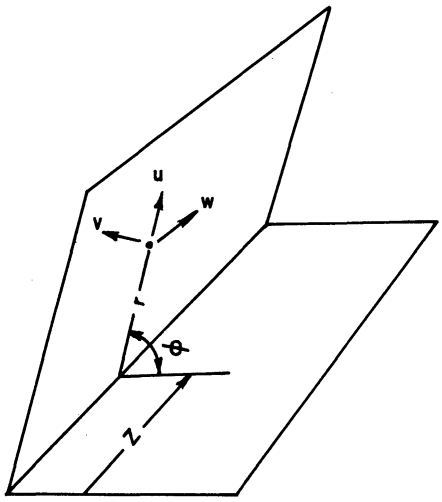

Figure 9-1. Cylindrical Coordinate System

With $x = r \cos \theta$, $y = r \sin \theta$, $z = z$, the flow relations become the following:

$$\frac{\partial u}{\partial \theta} - \frac{\partial (Vr)}{\partial r} = 0, \quad \frac{\partial (Vr)}{\partial z} - \frac{\partial w}{\partial \theta} = 0, \quad \frac{\partial w}{\partial r} - \frac{\partial u}{\partial z} \qquad (9\text{-}3)$$

(Condition of irrotationality)

$$u = \frac{\partial \varphi}{\partial r} \; ; \; v = \frac{1}{r} \frac{\partial \varphi}{\partial \theta} \; ; \; w = \frac{\partial \varphi}{\partial z} \qquad (9\text{-}4)$$

(Definition of velocity potential)

$$\frac{\partial}{\partial r} (\rho u r) + \frac{\partial}{\partial \theta} (\rho v) + r \frac{\partial}{\partial z} (\rho w) = 0 \qquad (9\text{-}5)$$

(Equation of continuity)

$$dp = -\frac{\rho}{2} d(\varphi_r^2 + \frac{1}{r^2}\varphi_\theta^2 + \varphi_z^2) \qquad (9\text{-}6)$$

(Equation of motion)

$$c^2 = \frac{dp}{d\rho} \qquad (9\text{-}7)$$

(Velocity of sound)

Combination of these equations yields the differential equation for three-dimensional flow in cylindrical coordinates.

$$(1 - \frac{\varphi_r^2}{c^2})\varphi_{rr} + (1 - \frac{\varphi_\theta^2}{r^2 c^2})\frac{\varphi_{\theta\theta}}{r^2} + (1 - \frac{\varphi_z^2}{c^2})\varphi_{zz}$$

$$- \frac{2}{r^2 c^2}(\varphi_r\varphi_\theta\varphi_{r\theta} - \varphi_\theta\varphi_z\varphi_{\theta z}) - \frac{2}{c^2}\varphi_z\varphi_r\varphi_{zr} + \frac{\varphi_r}{r}(1 + \frac{\varphi_\theta^2}{r^2 c^2}) = 0 \qquad (9\text{-}8)$$

$$c^2 = c_o^2 - \frac{\gamma - 1}{2}(\varphi_r^2 + \frac{1}{r^2}\varphi_\theta^2 + \varphi_z^2)$$

Neither Equation (9-2) nor Equation (9-8) is linear, and there is no possibility of rendering them so. What recourse then? The answer lies in bypassing Equations (9-2) and (9-8), and adding to the exact solution of two-dimensional flow, a velocity component such that it does not disturb the initial equation. It is in the nature of a trick, but it is imminently successful.

9.3 Addition of Axial Velocity

The technique for the successful solution of flow in three-dimensional space consists in starting with the two-dimensional flow previously solved, and superposing upon it, a velocity of constant magnitude and direction along the axis of the vortex tube, while at the same time leaving the pressure, density and temperature of the fluid unchanged (85).

The three-dimensional flow thus obtained is labeled the modified flow, and that it obeys the same set of equations as the flow previously solved in Chapter 8 may be shown in the following manner. Let w = constant (in time and space) be the velocity component which is added to the two-dimensional flow. The question is: Does the resulting velocity field represent a physically possible flow? The answer lies with the equations developed in Chapter 5 governing steady-state compressible flow, namely

i) the continuity equation

$$\frac{\partial(\rho u)}{\partial x} + \frac{\partial(\rho v)}{\partial y} + \frac{\partial(\rho w)}{\partial z} = 0 \qquad (9\text{-}9)$$

ii) the dynamical equations

$$u \frac{\partial u}{\partial x} + v \frac{\partial u}{\partial y} + w \frac{\partial u}{\partial z} + \frac{1}{\rho} \frac{\partial p}{\partial x} = 0 \qquad (9\text{-}10a)$$

$$u \frac{\partial v}{\partial x} + v \frac{\partial v}{\partial y} + w \frac{\partial v}{\partial z} + \frac{1}{\rho} \frac{\partial p}{\partial y} = 0 \qquad (9\text{-}10b)$$

$$u \frac{\partial w}{\partial x} + v \frac{\partial w}{\partial y} + w \frac{\partial w}{\partial z} + \frac{1}{\rho} \frac{\partial p}{\partial z} = 0 \qquad (9\text{-}10c)$$

and iii) the isentropy relation

$$p = \frac{p_o}{\rho_o^{\gamma}} \rho^{\gamma} \qquad (9\text{-}11)$$

For the case of two-dimensional flow, the last term in Equation (9-9) does not exist; for the modified flow, it becomes

$$\frac{\partial(\rho w)}{\partial z} = \rho \frac{\partial w}{\partial z} = 0 \qquad (9\text{-}12)$$

since the w = constant, and since the addition of the component w was done without changing ρ, thereby leaving ρ independent of z. The

continuity equation is thus the same for both the two-dimensional flow and the modified flow.

For the case of two-dimensional flow, the third relation in Equation (9-10) does not exist, and the terms $w \frac{\partial u}{\partial z}$, $w \frac{\partial v}{\partial z}$ in the first two relations are zero. For the modified flow, the third relation in Equation (9-10) vanishes due to the independence of w(= constant) with respect to x, y, z, and the independence of p with respect to z. The terms $w \frac{\partial u}{\partial z}$, $w \frac{\partial v}{\partial z}$ in the first two relations likewise vanish because neither u nor v are dependent of z. Thus, the two-dimensional flow and the modified flow obey a common dynamical equation.

Lastly, the isentropy equation, Equation (9-11) remains unchanged since p, ρ, and T are not affected by the addition of a constant axial velocity, and since an observer traveling uniformly with the gas would not be aware of the axial velocity.

Thus, the same set of differential equations describe both flows, which is equivalent to saying that these equations represent a family of flows, of which the foregoing two are examples of particular interest here. Since these equations were linearized and solved in Chapter 8, what remains then is simply to superpose the stream function of the two-dimensional flow with the stream function of the axial flow to obtain the general solution in space.

Nor does the addition of a constant velocity in the axial direction alter the conditions of irrotationality. For, if the original two-dimensional flow possesses a velocity potential φ such that

$$u = \frac{\partial \varphi}{\partial x} \qquad (9\text{-}13a)$$

$$v = \frac{\partial \varphi}{\partial y} \qquad (9\text{-}13b)$$

then the addition of a constant velocity w still leads to an irrotational flow field with

$$\varphi + w\, z \tag{9-14}$$

as its velocity potential.

On the other hand, if the flow possesses vorticity so that no scalar velocity potential exists, then the addition of a constant velocity w does not affect the vorticity either in magnitude or direction.

The only change involves the stagnation pressure: while the same (p, ρ)-curve represents both the two-dimensional and the modified flow, the stagnation or total pressure p_o is different for the two cases, since the velocity-square term in the Bernoulli relation

$$\frac{q^2}{2} + c_p T \tag{9-15}$$

differs by the constant $\frac{w^2}{2}$. Thus, for a given (p, $\frac{1}{\rho}$) on the pressure-specific volume diagram of Figure (9-2), the stagnation pressure p_o of the modified flow is greater than the stagnation pressure of the two-dimensional flow. The areas to the left of the (p, $\frac{1}{\rho}$)-curve represent the values of $\frac{q^2}{2}$ for the two-dimensional flow and the modified flow. The shaded area, being the difference between the two cases, is equivalent to $\frac{w^2}{2}$.

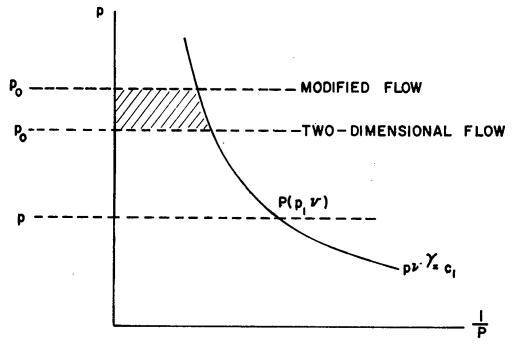

Figure 9-2. Stagnation Pressures for Two-Dimensional and Modified Flow

The plot of the resultant flow pattern shows spiraling streamlines whose projections on a transverse plane are logarithmic spirals, and whose pitch along the axial direction is constant. The helix angle, however, increases with decreasing radius, so that the flow pattern is very much of a spiral near the wall of the tube, but becomes more and more axial as the center of the tube is approached. Figure (9-3) shows the theoretical streamlines; Figure (9-4) shows a streamline as actually obtained from an experimental run by injection of colored liquid. The correspondence between theory and experiment is rewarding.

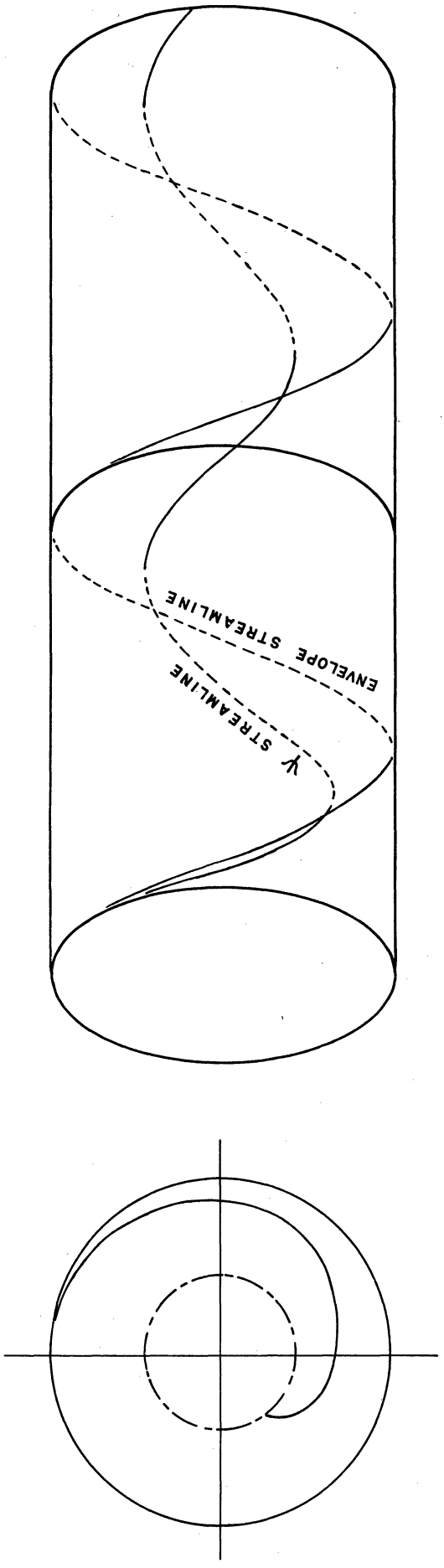

Figure 9-3. Theoretical Streamlines for Vortex Tube

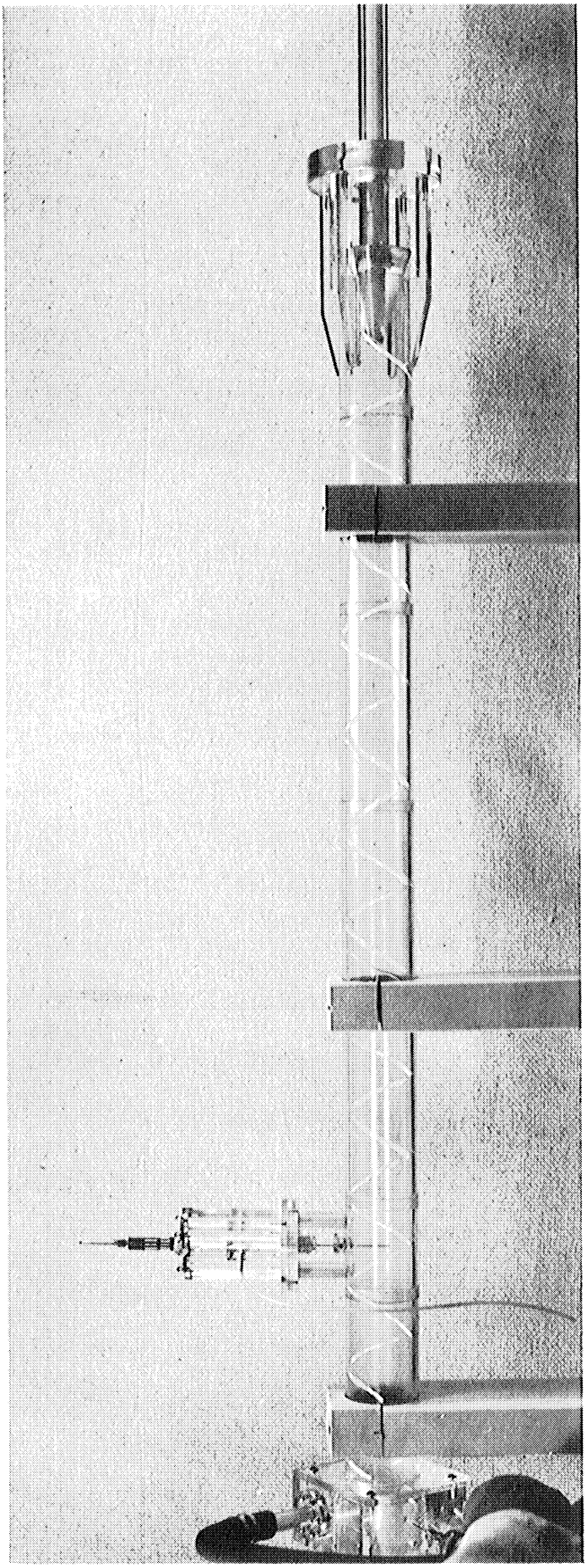

Figure 9-4. Experimental Streamline for Vortex Tube

CHAPTER 10

VISCOUS EFFECTS IN VORTEX TUBE

10.1 General Stress System

In the general case of fluid motion in space, let the velocity field be specified by

$$\vec{q} = u\vec{i} + v\vec{j} + w\vec{k} \qquad (10\text{-}1)$$

Then the equations of motion can be written in vector form as

$$\rho \frac{D\vec{q}}{Dt} = \vec{F} + \vec{p} \qquad (10\text{-}2)$$

where

$$\vec{F} = X\vec{i} + Y\vec{j} + Z\vec{k} \qquad = \text{body force}$$

$$\vec{p} = p_x\vec{i} + p_y\vec{j} + p_z\vec{k} \qquad = \text{surface force}$$

$$\frac{D}{Dt} = u\frac{\partial}{\partial x} + v\frac{\partial}{\partial y} + z\frac{\partial}{\partial z} + \frac{\partial}{\partial t}$$

The body forces are to be regarded as given external forces, but the surface forces depend on the state of strain (velocity field) of the fluid. The system of surface forces determines a state of stress, and a relationship between stress and strain must thus exist. In the case of elastic solid bodies, this relation is given by Hooke's law, and for liquids and gases, it is given by Stokes' law of friction.

Let a cube (dx, dy, dz) be isolated from the fluid continuum. There are nine stress components which are in evidence, and they act as shown in Figure (10-1). Normal stresses are indicated by σ, and shear stresses by τ. The first subscript indicates the direction of the normal to the plane over which the stress acts, and the second subscript

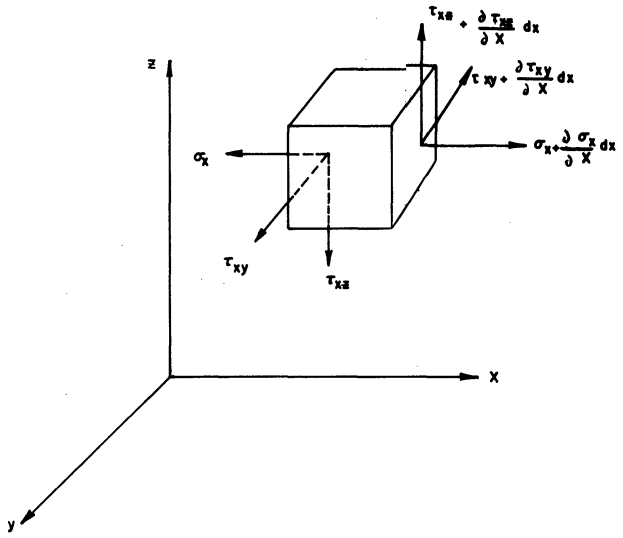

Figure 10-1. Stress System for Fluid Continuum

indicates the direction of the stress. The stress system requires nine scalar quantities for its description, and these nine quantities form a stress tensor of rank two:

$$II = \begin{pmatrix} \sigma_x & \tau_{xy} & \tau_{xz} \\ \tau_{yx} & \sigma_y & \tau_{yz} \\ \tau_{zx} & \tau_{zy} & \sigma_z \end{pmatrix} \qquad (10\text{-}3)$$

Equilibrium conditions, however, require that $\tau_{xy} = \tau_{yx}$, $\tau_{xz} = \tau_{zx}$, $\tau_{yz} = \tau_{zy}$, and the stress tensor is thus symmetric with respect to the principal diagonal:

$$II = \begin{pmatrix} \sigma_x & \tau_{xy} & \tau_{xz} \\ \tau_{xy} & \sigma_y & \tau_{yz} \\ \tau_{xz} & \tau_{yz} & \sigma_z \end{pmatrix} \qquad (10\text{-}4)$$

By considering each column as representing the stress in the directions x, y, and z, Equation (10-4) enables the surface force per unit volume to be calculated:

$$\vec{p} = \left[\frac{\partial\sigma_x}{\partial x} + \frac{\partial\tau_{xy}}{\partial y} + \frac{\partial\tau_{xz}}{\partial z}\right]\vec{i}$$

$$= \left[\frac{\partial\tau_{xy}}{\partial x} + \frac{\partial\sigma_y}{\partial y} + \frac{\partial\tau_{yz}}{\partial z}\right]\vec{j} \qquad (10\text{-}5)$$

$$= \left[\frac{\partial\tau_{xz}}{\partial x} + \frac{\partial\tau_{yz}}{\partial y} + \frac{\partial\sigma_z}{\partial z}\right]\vec{k}$$

From this, it is seen that the presence of shear stresses causes the pressure to be different in different directions. Introducing Equation (10-5) into Equation (10-2), and resolving into components, the three equations of motion become

$$\rho\frac{Du}{Dt} = X + \frac{\partial\sigma_x}{\partial x} + \frac{\partial\tau_{xy}}{\partial y} + \frac{\partial\tau_{xz}}{\partial z} \qquad (10\text{-}6a)$$

$$\rho\frac{Dv}{Dt} = Y + \frac{\partial\tau_{xy}}{\partial x} + \frac{\partial\sigma_y}{\partial y} + \frac{\partial\tau_{yz}}{\partial z} \qquad (10\text{-}6b)$$

$$\rho\frac{Dw}{Dt} = Z + \frac{\partial\tau_{xz}}{\partial x} + \frac{\partial\tau_{yz}}{\partial y} + \frac{\partial\sigma_z}{\partial z} \qquad (10\text{-}6c)$$

For a frictionless fluid, all shearing stresses vanish, and only the normal stresses remain. These are, moreover, equal, and their negative is defined as the pressure at the point (x,y,z).

$$\tau_{xy} = \tau_{yz} = \tau_{zx} = 0 \qquad (10\text{-}7a)$$

$$\sigma_x = \sigma_y = \sigma_z = -p = 1/3(\sigma_x + \sigma_y + \sigma_z)$$

$$= \bar{\sigma} \qquad (10\text{-}7b)$$

The system of Equations (10-6) contains the six stresses σ_x, σ_y, σ_z, τ_{xy}, τ_{yz}, and τ_{zx}. The next task is to determine the relation between them and the strains so as to enable the introduction of the velocity components u, v, and w into Equations (10-6).

10.2 Relation Between Stress Tensor and Rate of Strain Tensor

The strain system of any continuum, whether elastic solid, liquid, or gas, can be described in two alternate ways. The first method is to describe the deformation of a given volume by three elongations ξ_x, ξ_y, ξ_z and by three angular displacements γ_{xy}, γ_{yz}, γ_{zx}, i.e., by six strains. The quantities ξ_x, ξ_y, ξ_z denote changes in length along the coordinate axes, and the quantities γ_{xy}, γ_{yz}, γ_{zx} denote changes in angle between the (x-y), (y-z), and (z-x) axes. The second method of describing the state of strain consists in the use of the displacement vector

$$\vec{S} = \xi\vec{i} + \eta\vec{j} + \zeta\vec{k} \qquad (10\text{-}8)$$

of a point. If the coordinates of a point before deformation are (x,y,z), after deformation they become $(x + \xi, y + \eta, z + \zeta)$. The state of strain is fully determined if for every point the displacement vector is given, i.e., if

$$\xi = \xi\,(x,y,z);\ \eta = \eta\,(x,y,z);\ \zeta = \zeta\,(x,y,z).$$

The six strain parameters ξ_x, ξ_y, ξ_z, γ_{xy}, γ_{yz}, and γ_{zx} are related to the three displacement parameters ξ, η, and ζ by

$$\xi_x = \frac{\partial\xi}{\partial x}\ ;\ \xi_y = \frac{\partial\eta}{\partial y}\ ;\ \xi_z = \frac{\partial\zeta}{\partial z} \qquad (10\text{-}9)$$

$$\gamma_{xy} = \frac{\partial\xi}{\partial y} + \frac{\partial\eta}{\partial x}\ ;\ \gamma_{yz} = \frac{\partial\eta}{\partial z} + \frac{\partial\zeta}{\partial y}\ ;\ \gamma_{zx} = \frac{\partial\zeta}{\partial x} + \frac{\partial\xi}{\partial z} \qquad (10\text{-}10)$$

$$\xi_x + \xi_y + \xi_z = e = \text{volume dilatation} = \operatorname{div}\vec{S} \qquad (10\text{-}11)$$

The six stress parameters σ_x, σ_y, σ_z, τ_{xy}, τ_{yz}, and τ_{zx} are related to the three displacement parameters ξ, η, and ζ by

$$\sigma_x = \bar{\sigma} + 2G \frac{\partial \xi}{\partial x} - 2/3\ G\ \text{div}\ \vec{S} \qquad (10\text{-}10a)$$

$$\sigma_y = \bar{\sigma} + 2G \frac{\partial \eta}{\partial y} - 2/3\ G\ \text{div}\ \vec{S} \qquad (10\text{-}10b)$$

$$\sigma_z = \bar{\sigma} + 2G \frac{\partial \zeta}{\partial z} - 2/3\ G\ \text{div}\ \vec{S} \qquad (10\text{-}10c)$$

$$\tau_{xy} = G\left(\frac{\partial \xi}{\partial y} + \frac{\partial \eta}{\partial x}\right);\ \tau_{yz} = G\left(\frac{\partial \eta}{\partial z} + \frac{\partial \zeta}{\partial y}\right);\ \tau_{zx} = G\left(\frac{\partial \zeta}{\partial x} + \frac{\partial \xi}{\partial z}\right) \qquad (10\text{-}11)$$

where G is the modulus of elasticity in torsion.

Equations (10-10) and (10-11) can be written in better form by use of matrix notation from Equation (10-4) The result is

$$\begin{vmatrix} \sigma_x & \tau_{xy} & \tau_{xz} \\ \tau_{xy} & \sigma_y & \tau_{yz} \\ \tau_{xz} & \tau_{yz} & \sigma_z \end{vmatrix} = \begin{vmatrix} \bar{\sigma} & 0 & 0 \\ 0 & \bar{\sigma} & 0 \\ 0 & 0 & \bar{\sigma} \end{vmatrix}$$

$$+ G \begin{vmatrix} \frac{\partial \xi}{\partial x} & \frac{\partial \xi}{\partial y} & \frac{\partial \xi}{\partial z} \\ \frac{\partial \eta}{\partial x} & \frac{\partial \eta}{\partial y} & \frac{\partial \eta}{\partial z} \\ \frac{\partial \zeta}{\partial y} & \frac{\partial \zeta}{\partial x} & \frac{\partial \zeta}{\partial z} \end{vmatrix} + G \begin{vmatrix} \frac{\partial \xi}{\partial x} & \frac{\partial \eta}{\partial x} & \frac{\partial \zeta}{\partial x} \\ \frac{\partial \xi}{\partial y} & \frac{\partial \eta}{\partial y} & \frac{\partial \zeta}{\partial y} \\ \frac{\partial \xi}{\partial z} & \frac{\partial \eta}{\partial z} & \frac{\partial \zeta}{\partial z} \end{vmatrix}$$

$$- 2/3\ G \begin{vmatrix} \text{div}\ \vec{S} & 0 & 0 \\ 0 & \text{div}\ \vec{S} & 0 \\ 0 & 0 & \text{div}\ \vec{S} \end{vmatrix} \qquad (10\text{-}12)$$

Equation (10-12) is the general form of Hooke s law for an elastic solid body. It is based on the stresses being proportional to the strain. In the case of the flow of liquids and gases, Stokes' law of friction can by derived readily from Equation (10-12) by making the stresses proportional

to the rate of strain. Therefore, in Equation (10-12), G is replaced by μ, σ is by -p, (ξ,η,ζ) by (u,v,w), and $\vec{S}$ by $\vec{q}$:

$$\begin{vmatrix} \sigma_x & xy & \tau_{yz} \\ \tau_{xy} & \sigma_y & \tau_{yz} \\ \tau_{xz} & \tau_{yz} & \sigma_z \end{vmatrix} = \begin{vmatrix} -p & 0 & 0 \\ 0 & -p & 0 \\ 0 & 0 & -p \end{vmatrix}$$

$$+ \mu \begin{vmatrix} \frac{\partial u}{\partial x} & \frac{\partial u}{\partial y} & \frac{\partial u}{\partial z} \\ \frac{\partial v}{\partial x} & \frac{\partial v}{\partial y} & \frac{\partial v}{\partial z} \\ \frac{\partial w}{\partial x} & \frac{\partial w}{\partial y} & \frac{\partial w}{\partial z} \end{vmatrix} + \mu \begin{vmatrix} \frac{\partial u}{\partial x} & \frac{\partial v}{\partial x} & \frac{\partial w}{\partial x} \\ \frac{\partial u}{\partial y} & \frac{\partial v}{\partial y} & \frac{\partial w}{\partial y} \\ \frac{\partial u}{\partial z} & \frac{\partial v}{\partial y} & \frac{\partial w}{\partial z} \end{vmatrix}$$

$$- 2\mu/3 \begin{vmatrix} \text{div } \vec{q} & 0 & 0 \\ 0 & \text{div } \vec{q} & 0 \\ 0 & 0 & \text{div } \vec{q} \end{vmatrix} \qquad (10\text{-}13)$$

Equation (10-13) is the general relation between the stress tensor and the rate of strain tensor. Using the summation convention that repetition of a suffix in a single term or in a product is to imply summation over all values of the suffix, it is sometimes rewritten as

$$p_{\alpha\beta} = - (p + 2/3\ \mu\Delta)\ \delta_{\alpha\beta} + \frac{\partial q_\alpha}{\partial x_\beta} + \frac{\partial q_\beta}{\partial x_\alpha} \qquad (10\text{-}14)$$

where

Δ = div $\vec{q}$ = volume dilation

$\alpha,\beta = 1,2,3$

$\delta_{\alpha\beta}$ = Kroneker delta = 1 when $\alpha = \beta$, 0 when $\alpha \neq \beta$.

10.3 Navier Stokes Equations

It is convenient to subtract the pressure from the normal stresses by putting

$$\sigma_x = \sigma_x' - p; \quad \sigma_y = \sigma_y' - p; \quad \sigma_z = \sigma_z' - p \qquad (10\text{-}15)$$

so that the frictional terms of the stress components can be written as

$$\sigma_x' = \mu \left(2 \frac{\partial u}{\partial x} - 2/3 \text{ div } \vec{q}\right) \qquad (10\text{-}16a)$$

$$\sigma_y' = \mu \left(2 \frac{\partial v}{\partial y} - 2/3 \text{ div } \vec{q}\right) \qquad (10\text{-}16b)$$

$$\sigma_z' = \mu \left(2 \frac{\partial w}{\partial z} - 2/3 \text{ div } \vec{q}\right) \qquad (10\text{-}16c)$$

$$\tau_{xy} = \mu \left(\frac{\partial u}{\partial y} + \frac{\partial v}{\partial x}\right) \qquad (10\text{-}17a)$$

$$\tau_{yz} = \mu \left(\frac{\partial v}{\partial z} + \frac{\partial w}{\partial y}\right) \qquad (10\text{-}17b)$$

$$\tau_{zx} = \mu \left(\frac{\partial w}{\partial x} + \frac{\partial u}{\partial z}\right) \qquad (10\text{-}17c)$$

Equation (10-15) enables the non-viscous pressure terms to be separated in the equations of motion, so that Equations (10-6) become:

$$\rho \frac{Du}{Dt} = X - \frac{\partial p}{\partial x} + \left(\frac{\partial \sigma_x'}{x} + \frac{\partial \tau_{xy}}{\partial y} + \frac{\partial \tau_{xz}}{\partial z} \right) \qquad (10\text{-}18a)$$

$$\rho \frac{Dv}{Dt} = Y - \frac{\partial p}{\partial y} + \left(\frac{\partial \tau_{yx}}{\partial x} + \frac{\partial \sigma_y'}{\partial y} + \frac{\partial \tau_{yz}}{\partial z} \right) \qquad (10\text{-}18b)$$

$$\rho \frac{Dw}{Dt} = Z - \frac{\partial p}{\partial z} + \left(\frac{\partial \tau_{zx}}{\partial x} + \frac{\partial \tau_{zy}}{\partial y} + \frac{\partial \sigma_z'}{\partial z} \right) \qquad (10\text{-}18c)$$

Equations (10-16) and (10-17) enable the surface forces in Equation (10-5) to be calculated:

$$p_x = \frac{\partial \sigma_x}{\partial x} + \frac{\partial \tau_{xy}}{\partial y} + \frac{\partial \tau_{xz}}{\partial z}$$

$$= - \frac{\partial p}{\partial x} + \frac{\partial \sigma'_x}{\partial x} + \frac{\partial \tau_{xy}}{\partial y} + \frac{\partial \tau_{xz}}{\partial z}$$

$$= - \frac{\partial p}{\partial x} + \frac{\partial}{\partial x} \left[\mu \left(2 \frac{\partial u}{\partial x} - 2/3 \text{ div } \vec{q} \right) \right]$$

$$+ \frac{\partial}{\partial y} \left[\mu \left(\frac{\partial u}{\partial y} + \frac{\partial v}{\partial x} \right) \right] + \frac{\partial}{\partial z} \left[\mu \left(\frac{\partial w}{\partial x} + \frac{\partial u}{\partial z} \right) \right] \qquad (10\text{-}19a)$$

$$p_y = \frac{\partial \tau_{xy}}{\partial x} + \frac{\partial \sigma_y}{\partial y} + \frac{\partial \tau_{yz}}{\partial z}$$

$$- \frac{\partial p}{\partial y} + \frac{\partial}{\partial y} \left[\mu \left(2 \frac{\partial v}{\partial y} - 2/3 \text{ div } \vec{q} \right) \right]$$

$$+ \frac{\partial}{\partial z} \left[\mu \left(\frac{\partial v}{\partial z} + \frac{\partial w}{\partial y} \right) \right] + \frac{\partial}{\partial x} \left[\mu \left(\frac{\partial u}{\partial y} + \frac{\partial v}{\partial x} \right) \right] \qquad (10\text{-}19b)$$

$$p_z = \frac{\partial \tau_{xz}}{\partial x} + \frac{\partial \tau_{yz}}{\partial y} + \frac{\partial \sigma_z}{\partial z}$$

$$= - \frac{\partial p}{\partial z} + \frac{\partial}{\partial z} \left[\mu \left(2 \frac{\partial w}{\partial z} - 2/3 \text{ div } \vec{q} \right) \right]$$

$$+ \frac{\partial}{\partial x} \left[\mu \left(\frac{\partial w}{\partial x} + \frac{\partial u}{\partial z} \right) \right] + \frac{\partial}{\partial y} \left[\mu \left(\frac{\partial v}{\partial z} + \frac{\partial w}{\partial y} \right) \right] \qquad (10\text{-}19c)$$

Finally, when Equations (10-19) are introduced into the equations of motion (10-6), there is obtained

$$\rho \frac{Du}{Dt} = X - \frac{\partial p}{\partial x} + \frac{\partial}{\partial x} \left[\mu \left(2 \frac{\partial u}{\partial x} - 2/3 \text{ div } \vec{q} \right) \right]$$

$$+ \frac{\partial}{\partial y} \left[\mu \left(\frac{\partial u}{\partial y} + \frac{\partial v}{\partial x} \right) \right] + \frac{\partial}{\partial z} \left[\mu \left(\frac{\partial w}{\partial x} + \frac{\partial u}{\partial z} \right) \right] \qquad (10\text{-}20a)$$

$$\rho \frac{Dv}{Dt} = Y - \frac{\partial p}{\partial y} + \frac{\partial}{\partial y}\left[\mu \left(2 \frac{\partial v}{\partial y} - 2/3 \operatorname{div} \vec{q}\right)\right]$$

$$+ \frac{\partial}{\partial z}\left[\mu \left(\frac{\partial v}{\partial z} + \frac{\partial w}{\partial y}\right)\right] + \frac{\partial}{\partial x}\left[\mu \left(\frac{\partial u}{\partial y} + \frac{\partial v}{\partial x}\right)\right] \qquad (10\text{-}20b)$$

$$\rho \frac{Dw}{Dt} = Z - \frac{\partial p}{\partial z} + \frac{\partial}{\partial z}\left[\mu \left(2 \frac{\partial w}{\partial z} - 2/3 \operatorname{div} \vec{q}\right)\right]$$

$$+ \frac{\partial}{\partial x}\left[\mu \left(\frac{\partial w}{\partial x} + \frac{\partial u}{\partial z}\right)\right] + \frac{\partial}{\partial y}\left[\mu \left(\frac{\partial v}{\partial z} + \frac{\partial w}{\partial y}\right)\right] \qquad (10\text{-}20c)$$

Equations (10-20) are the Navier-Stokes equations of fluid motion. They, along with the equation of continuity, the equation of state, the energy equation, and the viscosity-temperature relation constitute seven equations for the seven unknowns, u, v, w, p, ρ, T, and μ.

10.4 Change of Circulation

As stated in Chapter 4, the circulation, in a frictionless fluid, is constant along a vortex filament, and remains constant with respect to time.

In the case of a viscous fluid, however, the circulation

$$\Gamma = \oint \vec{q} \cdot \vec{dl} = \oint q_\alpha \, dx_\alpha \; ; \; \alpha = 1, 2, 3$$

changes with time, so that

$$\frac{D\Gamma}{Dt} = \oint \frac{Dq_\alpha}{Dt} dx_\alpha + \oint q_\alpha \frac{D}{Dt} dx_\alpha$$

$$= \oint \left(X_\alpha + \frac{1}{\rho} \frac{p_{\alpha\beta}}{x_{\alpha\beta}}\right) dx_\alpha$$

$$= \oint \frac{1}{\rho} \frac{p_{\alpha\beta}}{x_{\alpha\beta}} dx_\alpha \qquad (10\text{-}21)$$

After some rearrangement, this can be written as

$$\frac{D\Gamma}{Dt} = -\oint \frac{1}{\rho} [dp + \mu(\text{curl } \vec{\omega}) \cdot \vec{dr} + 2/3\ \Delta\ d\mu$$

$$- 4/3\ \mu\ d\ \Delta - 2(\text{grad } \mu) \cdot \vec{dq} + (\text{grad } \mu \times \vec{\omega}) \cdot \vec{dr}] \quad (10\text{-}22)$$

Equation (10-22) is the general expression for the circulation around a closed curve in a viscous compressible flow field. It reduces to Kelvin's Theorem of Chapter 4 when viscosity is neglected and flow is isentropic. Unfortunately, neither Equation (10-20) nor Equation (10-22) is linear. Both defy present day methods of mathematical analysis, and instead of working with them, the method of Kassner and Knoernachild (58) will be adopted.

10.5 Shear Stress in Circular Flow

While the laws of Newton and Prandtl have yielded well established methods for determining shear stresses in straight laminar and turbulent flow, there is, in the case of circular flow, no general agreement as to theory. One theory is that, in accordance with the concept of laminar fluid friction, shear stresses are proportional to shear velocity. The other theory, based on the concept of momentum-transfer, holds that shear stresses are proportional to the rotation of the fluid.

According to the first theory, which is applicable to straight laminar or circular laminar flow, the stresses caused in the fluid by friction correspond to the stresses caused by elastic deformation in a solid, differing only in that, instead of the deformation themselves, the rates of change of deformations are considered. This means that the shear stress, which in solid bodies is proportional to the shear angle, in viscous flow, is proportional to the so-called shear velocity, i.e., the

rate of change of the angle between two surfaces of an originally rectangular element of fluid.

According to the second theory, the shear stress in circular motion is proportional to the rotation, i.e., to the mean angular velocity of the rotating fluid element. This is the so-called momentum-transfer theory.

Neither theory contradicts the other, so long as they are applied to straight flow. However, if applied to circular flow, the first theory means that there would be no shear stresses in a fluid rotating according to the law $q = \omega r$ (forced vortex), because there is no relative gliding or shearing, whereas the second theory means that shear stresses would occur in rotational flow ($q = \omega r$), but not in irrotational flow ($q r$ = constant).

The notion that frictional stress in turbulent circular flow is proportional to rotation is ascribed to Prandtl. Taylor, however, has pointed out that the results of Prandtl's Theory do not confirm with experience, and has advanced a vorticity transport theory, according to which turbulent friction is determined by shear velocity. Recently, Kassner (58) modified Prandtl's theory to yield results which, in the laminar case, are consistent with the general theory of laminar friction, and which, in the turbulent circular case, are in agreement with Taylor's results.

Adapting Kassner's concept, the shear stress for the type of flow occurring in the vortex tube is now determined. It was established in Chapter 4 that, in terms of the natural coordinates, the fluid rotation is given by

$$2\omega = \frac{dq}{dr} + \frac{q}{r} \qquad (10\text{-}23)$$

In the case of irrotational flow, the concept of shear stress being proportional to rotation would lead to no shear, since $\frac{dq}{dr} = -\frac{q}{r}$ for irrotational flow. On the other hand, in the case of rotational flow, the same concept would lead to considerable shear stress. These conclusions are incompatible with experience, which shows that an irrotational flow is unstable, and that it converts to a rotational flow. In consequence of all this, Kassner considers the shear stress to be a function of $(\frac{dq}{dr} - \frac{q}{r})$. Thus

$$\tau_{lam.} = \mu \left(\frac{dq}{dr} - \frac{q}{r}\right) \qquad (10\text{-}24)$$

for laminar flow. And for turbulent flow:

$$\tau_{turb.} = \epsilon \left(\frac{dq}{dr} - \frac{q}{r}\right) \qquad (10\text{-}25)$$

where ξ is the "turbulent exchange rate", or virtual viscosity, and the ratio of the turbulent shear stress to the laminar shear stress is in the order of the Reynold's number.

Applying Equations (10-24) and (10-25) to the case of irrotational flow ($q\,r$ = constant), the result is

$$r\,dq + q\,dr = 0$$

$$\frac{dq}{dr} = -\frac{q}{r}$$

and Equations (10-24) and (10-25) become

$$\tau_{lam.} = \mu \left(-\frac{q}{r} - \frac{q}{r}\right) = -2\mu\frac{q}{r} \qquad (10\text{-}26)$$

$$\tau_{turb.} = \epsilon \left(-\frac{q}{r} - \frac{q}{r}\right) = -2\epsilon\frac{q}{r} \qquad (10\text{-}27)$$

The distribution of shear stress is shown in Figure (10-2).

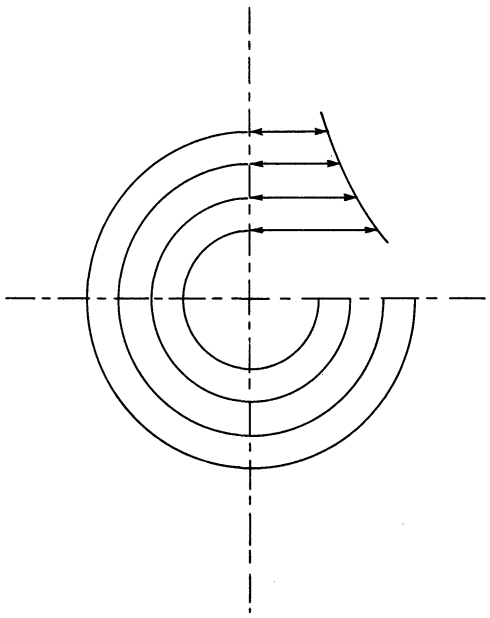

Figure 10-2. Shear Stress Distribution in Irrotational Flow

It is seen in the following that irrotational flow represents flow with constant moment of shear stresses, as against rotational flow which represents flow with no shear stresses.

10.6 Conversion of Irrotational to Rotational Flow

The experimental results of Part III indicate that there is a sort of energy transfer from one part of the flow to the other, thus decreasing the total temperature of the one part, and increasing the total temperature of the other. The shear stresses occurring in circular flow furnish an explanation for this.

When the compressed air enters the vortex tube, a velocity profile is built up inside the tube, which complies with the law of constant angular momentum (irrotational flow). Coupled with this velocity profile, is a pressure and temperature profile as shown. The question is whether or not these profiles can be maintained. To answer this, consider the shearing force which acts on an annular element of fluid at a distance r from the center, and which tends to reduce the velocity difference

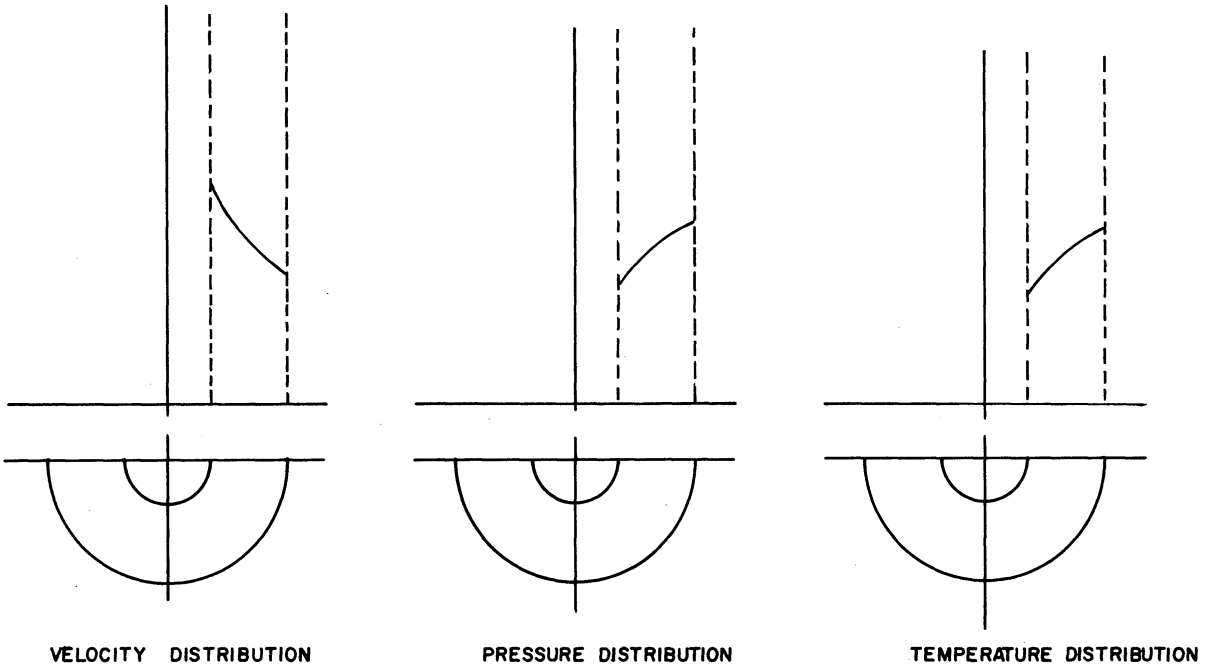

Figure 10-3. Initial Flow in Vortex Tube

between two neighboring elements. From Equation (10-24) the shearing force for laminar flow is

$$F_i = \mu \left(\frac{dq}{dr} - \frac{q}{r}\right) 2\pi r$$

and the moment of the shearing force about the center is

$$M_i = F_i \, r = \mu \left(\frac{dq}{dr} - \frac{q}{r}\right) 2 \pi r^2 \qquad (10\text{-}28)$$

Similarly, for turbulent flow

$$M_i = F_i \, r = \epsilon \left(\frac{dq}{dr} - \frac{q}{r}\right) 2 \pi r^2 \qquad (10\text{-}29)$$

Now, in the case of irrotational flow: $q\,r = K$, hence $r\,dq + q\,dr = 0$, and

$$\frac{dq}{dr} = -\frac{q}{r} = -\frac{K}{r^2} \qquad (10\text{-}30)$$

Substitution of Equation (10-30) into Equations (10-28) and (10-29) then results in

$$M_i = \mu \left(-\frac{2K}{r^2}\right) (2\pi r^2) = -4\pi\mu K \qquad (10\text{-}31)$$

for laminar flow, and

$$M_i = \epsilon \left(-\frac{2K}{r^2}\right) (2\pi r^2) = -4\pi\epsilon K \qquad (10\text{-}32)$$

for turbulent flow.

Equations (10-31) and (10-32), in addition to being independent of r, show that for both laminar and turbulent flow, the moment of the friction forces is of a finite and constant amount for each annulus.

In the case of rotational flow: $q = \omega r$, $dq = \omega\, dr$, hence

$$\frac{dq}{dr} = \omega = \frac{q}{r} \qquad (10\text{-}33)$$

and substitution of Equation (10-32) into Equations (10-31) and (10-32) results in the moment of the friction force being zero.

Thus, while irrotational flow is stable for a frictionless fluid, for a viscous fluid, it is unstable, for, in the latter case, the summation of internal moments of friction forces must be zero, since there is no external moment that is acting. The relationship between the internal moments of friction forces and the external moment being

$$\int_{r_1}^{r_2} M_i \, dr = M_{external} = 0$$

This can be satisfied only if M_i is zero everywhere, since by Equations (10-31) and (10-32), no summation of quantities of like sign can be zero unless all the quantities are zero individually. But the latter case

represents precisely the condition for rotational flow, which means that after a time, the flow, initially irrotational, becomes rotational.

The conversion from irrotational to rotational flow starts from both sides of the vortex tube, i.e., from the inner radius of the tube outward, from the outer radius of the tube inward, so that the variation of velocity profile with time is as shown in Figure (10-4). Here, three transient velocity profiles are sketched out.

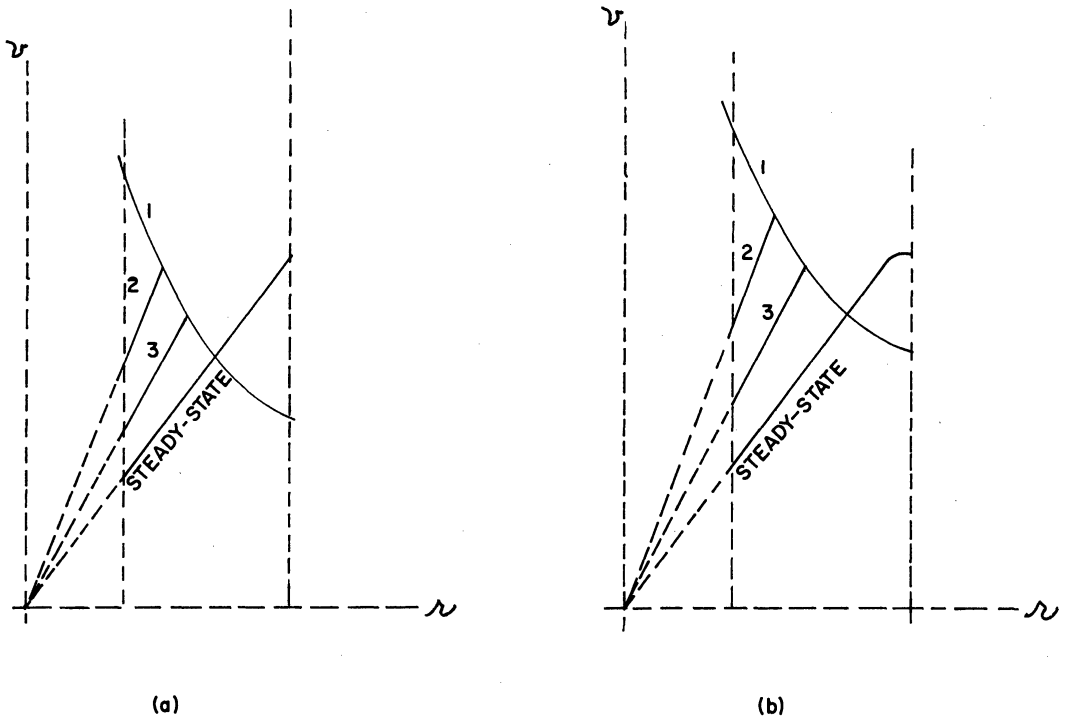

Figure 10-4. Velocity-Profile Conversion

Figure (10-4a) shows the velocity change neglecting wall effect, whereas Figure (10-4b) shows the velocity change with the wall effect taken into account. Here, there is a force by wall friction, which tends to decelerate the fluid in its vicinity, and the velocity profile is "rounded out" instead of being sharp.

With the flow establishing itself as rotational in the steady-state, the temperature and velocity profiles become those of rotational flow, and they are shown in Figure (10-5).

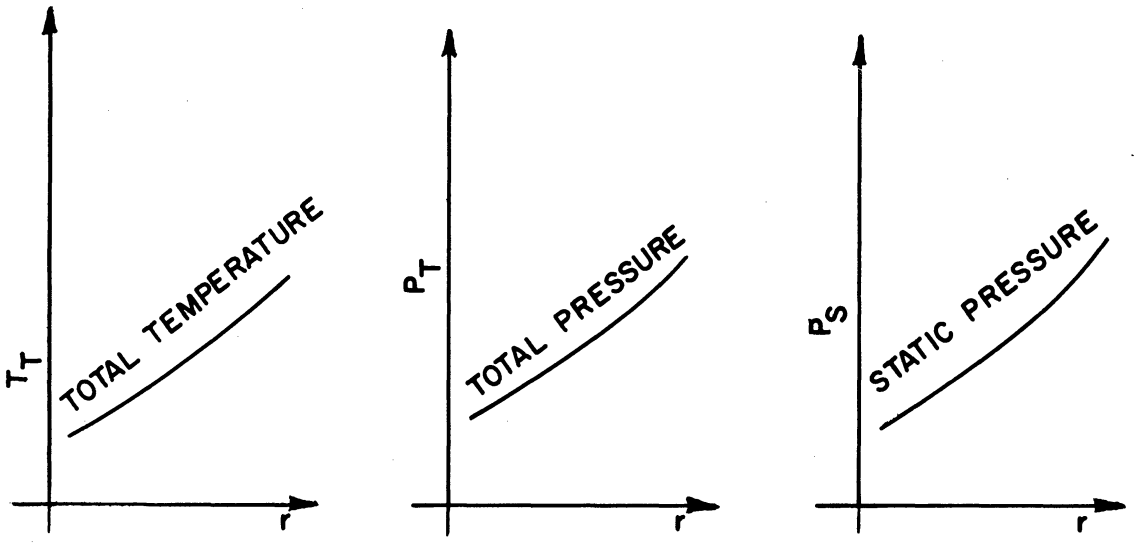

Figure 10-5. Temperature, Pressure-Profile for Rotational Flow

A noteworthy feature of these curves is that they are in marked agreement with the experimental curves of Chapter 3, thus attesting to the soundness of the theory.

10.7 Velocity Relation

A comparison of the magnitudes of velocity before and after conversion is afforded by determining the moment of momentum for both irrotational and rotational flow, and equating them to each other. First the moment of momentum for irrotational flow is

$$M_{irrot.} = \int \omega \, dI \qquad (10\text{-}35)$$

where

$$\omega = \text{angular velocity} = \frac{q}{r} = \frac{K}{r^2}$$

$$dI = \text{moment of inertia of annular element} = r^2 \, dm = r^2(2\pi r \rho \, dr)$$

Thus:

$$M_{irrot.} = \int_{r_1}^{r_2} \frac{K}{r^2} (r^2)(2\pi r\rho\ dr)$$

$$= \pi\ \rho\ K\ (r_2^2 - r_1^2) \qquad (10\text{-}36)$$

For the case of rotational flow, the moment of momentum is

$$M_{rot.} = \int \omega\ dI$$

$$= \int_{r_1}^{r_2} \omega\ (r^2)\ (2\pi r\rho\ dr)$$

$$= \frac{r\ \rho\ \omega}{2}\ (r_2^4 - r_1^4) \qquad (10\text{-}37)$$

Setting Equations (10-36) and (10-37) equal to each other results in

$$\pi\rho K\ (r_2^2 - r_1^2) = \frac{\pi\rho\omega}{2}\ (r_2^4 - r_1^4)$$

and, with $K = rq_{irrot.}$

$$\omega = \frac{q_{rot.}}{r}$$

this becomes

$$q_{rot.} = \frac{2\ r^2}{r_2^2 + r_1^2}\ q_{irrot.} \qquad (10\text{-}38)$$

From Equation (10-38), it is seen that as $r \to 0$, $q_{rot.} \to 0$, and as $r \to r_2$, $q_{rot.} \to 2\ q_{irrot.}$ This not only checks with the steady-state velocity profile of Figure (10-4) but gives the velocity of the

converted flow at the wall to be approximately twice the velocity of the original flow at the same location.

10.8 Energy Relation

The energy possessed by the flow can be obtained by taking summation of kinetic energies of the annuli. Thus, for the initial irrotational flow,

$$E_{irrot.} = \int_{r_1}^{r_2} \frac{1}{2} q^2 \, dm$$

$$= \int_{r_1}^{r_2} \frac{1}{2} \frac{K^2}{r^2} 2 \pi \rho \, r \, dr$$

$$= \pi \rho K^2 \ln \frac{r_2}{r_1} \qquad (10\text{-}39)$$

Similarly, for the steady-state rotational flow,

$$E_{rot.} = \int_{r_1}^{r_2} \frac{1}{2} q^2 \, dm$$

$$= \int_{r_1}^{r_2} \frac{1}{2} \omega^2 r^2 \, 2 \pi \rho \, r \, dr$$

$$= \frac{\pi \rho \omega^2}{4} (r_2^4 - r_1^4) \qquad (10\text{-}40)$$

Equations (10-38), (10-39), and (10-40) afford a comparison of energies possessed in rotational and irrotational flow. Letting $r = r_2$ in Equations (10-38), this yields

$$q_{rot.} = \omega r_2 = \frac{2\, r_2^2}{r_2^2 + r_1^2} \qquad q_{irrot.} = \frac{2\, r_2^2}{r_2^2 + r_1^2}\ \frac{K}{r_2}$$

or, combining the second and last terms:

$$\omega = \frac{2\, k}{r_2^2 + r_1^2} \tag{10-41}$$

Replacing ω by this value in Equation (10-40), the latter becomes:

$$E_{rot.} = \frac{\pi\rho}{4} \left(\frac{2\, K}{r_2^2 + r_1^2}\right)^2 (r_2^4 - r_1^4)$$

$$= \frac{\pi\, \rho\, K^2\, (r_2^2 - r_1^2)}{r_2^2 + r_1^2} \tag{10-42}$$

Comparison of Equations (10-42) and (10-39) shows that the energy possessed by rotational flow is less than that possessed by irrotational flow. In fact, of all possible velocity profiles, that of rotational flow has the minimum kinetic energy. The difference between the energies of irrotational and rotational flow represents the energy lost from one configuration to another. Thus, from Equations (10-39) and (10-42):

$$E_{loss} = \pi\, \rho\, K^2 \ln \frac{r_2}{r_1} - \pi\, \rho\, K^2\, \frac{r_2^2 - r_1^2}{r_2^2 + r_1^2}$$

$$= \pi\, \rho\, K^2 \left[\ln \frac{r_2}{r_1} - \frac{1 - \left(\frac{r_1}{r_2}\right)^2}{1 + \left(\frac{r_1}{r_2}\right)^2}\right] \tag{10-43}$$

The kinetic energy given up by the fluid in transforming itself rom irrotational flow to rotational flow goes to heating up the fluid as a whole, and the increase in temperature is superimposed upon the temperature distribution of the resultant rotational flow.

The efficiency of the vortex tube may be expressed as

$$\eta(r) = 1 - \frac{E_{rot.}}{E_{irrot.}} = 1 - \frac{\pi\rho K^2 \dfrac{r_2^2 - r_1^2}{r_2^2 + r_1^2}}{\pi\rho K^2 \ln \dfrac{r_2}{r_1}}$$

$$= 1 - \left[\frac{\left(\dfrac{r_2}{r_1}\right)^2 - 1}{\left(\dfrac{r_2}{r_1}\right)^2 + 1} \cdot \frac{1}{\ln \dfrac{r_2}{r_1}} \right] \qquad (10\text{-}44)$$

the plot of which is shown in Figure (10-6).

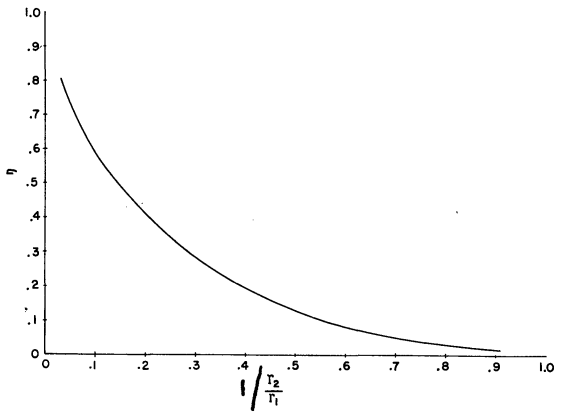

Figure 10-6. Efficiency Curve for Vortex Tube

It is seen that the coldest portions of the flow lie near the center of the tube, and that the optimum diameter of the diaphragm for tapping cold air is around a radius ratio of .2. This not only checks well with the experimental results in Chapter 3, but also gives the performance of the vortex tube to be calculated.

CHAPTER 11

THREE-DIMENSIONAL VISCOUS-COMPRESSIBLE SOLUTION

11.1 Preliminary Statement

The latter part of Chapter 10 gave the solution of the viscous vortex flow in the plane. A consideration of the shear stresses showed that the initial free vortex of inviscid compressible flow was transformed into a forced vortex of viscous compressible flow. What remains then in way of general solution is to superimpose the forced vortex flow of the preceding chapter to that of a viscous compressible sink. The forced vortex was developed in Chapter 10; the viscous sink will now be developed prior to adding it to the vortex for the general solution.

11.2 Viscous Compressible Sink

The solution for the inviscid compressible sink was presented in Chapter 8. It contained a limit circle (the sonic circle) to the exterior of which the solution had two branches, one having its stagnation point at infinity (the subsonic branch), and the other having its maximum velocity at infinity (the supersonic branch). Both branches terminate at the limit line with theoretically infinite velocity gradient.

The problem of viscous compressible sink (source) flow, because of its cylindrical symmetry, is one of the few nonlinear flows in more than one dimension which can be described by only one independent variable, the radial distance. Consequently, it is solvable, though not without pains, and has attracted the attention of a number of writers (136).

The momentum equation for viscous compressible sink, as evolved from the Navier-Stokes equation of Chapter 10 is

$$\rho q \frac{du}{dr} = - \frac{dp}{dr} + \frac{d}{dr} \left[2 \mu \frac{dq}{dr} + \frac{2}{3} (\xi - \mu) \frac{1}{r} d(rq) \right] + 2\mu \frac{d}{dr} \left(\frac{q}{r}\right) \qquad (11\text{-}1)$$

where ρ, q, r, p, μ, and ξ denote respectively density, radial velocity, radial distance, pressure, coefficient of shear viscosity, and coefficient of bulk viscosity.

The energy equation for viscous compressible sink, as evolved from the general expression of the energy equation is

$$\rho q r \frac{d}{dr} \left[\frac{q^2}{2} + c_p T \right] = \frac{d}{dr} \left[rk \frac{dT}{dr} + \mu r \frac{dq^2}{dr} + \frac{2r(\xi - \mu)}{3} \left(\frac{1}{2} \frac{dq^2}{dr} + \frac{q^2}{r} \right) \right] \qquad (11\text{-}2)$$

where c_p, T, and k denote respectively specific heat at constant pressure, absolute temperature, and thermal conductivity.

The equation of continuity for viscous compressible sink flow is

$$2 \pi \rho r q = -m \qquad (11\text{-}3)$$

where m denotes the sink strength.

Lastly, the equation of state is

$$p = \rho R T \qquad (11\text{-}4)$$

where R is the gas constant.

Equations (11-1) to (11-4) form a system of nonlinear differential equations in the four variables q, p, ρ, and T. They are solved after Wu (136) by reducing to non-dimensional form by the introduction of

$$r_1 = \frac{r}{r^*} \; ; \; \eta = \log r \; ; \; w = - \frac{q}{c^*} \; ; \; \Theta = \frac{T}{T^*}$$

$$p_1 = \frac{p}{p^*} \; ; \; \rho_1 = \frac{\rho}{\rho^*} ; \; \mu_1 = \frac{\mu}{\mu^*} \; ; \text{ and } \epsilon_1 = \frac{\epsilon}{\epsilon^*} \tag{11-5}$$

where the * quantities are those occurring at the local Mach number of unity for inviscid gas.

Eliminating p and ρ in Equation (11-1) by use of Equations (11-3) and (11-4), and introducing the non-dimensional quantities with η as the independent variable results in

$$\frac{dw}{d\eta} + \frac{1}{\gamma} \left[\frac{d}{d\eta} \left(\frac{\Theta}{w}\right) - \frac{\Theta}{w} \right] = - 2 \alpha \left[\mu_1 (1 + \lambda) \left(\frac{d^2 w}{d\eta^2} - w\right) \right.$$

$$\left. + (1 + \lambda) \frac{dw}{d\eta} \frac{d\mu_1}{d\eta} + \lambda w \frac{d\mu_1}{d\eta} \right] \tag{11-6}$$

where

$$\alpha = (Re)^{-1} = \frac{2\pi\mu^*}{m} \; ; \; \epsilon = (1 + 3\lambda)\mu$$

Thus, α denotes the inverse of the Reynolds number, and is smaller than unity throughout, whereas λ expresses the relation between the two viscosity coefficients.

Using Equation (11-3), the energy Equation (11-2) is integrated to yield

$$\frac{w^2}{2} + \frac{\Theta}{\gamma - 1} + \alpha\mu_1 \left[\frac{Pr^{-1}}{\gamma - 1} \frac{d\Theta}{d\eta} + (1 + \lambda) \frac{dw^2}{d\eta} + 2 \lambda w^2 \right] = \frac{\gamma + 1}{2(\gamma - 1)} \tag{11-7}$$

where $Pr = \frac{\mu c_p}{k}$ = Prandtl's number.

Equations (11-6) and (11-7) are two equations for the two unknowns w and Θ. The boundary conditions for them are determined by requiring that they tend to their respective inviscid solutions as

$\eta \to \infty$. As a check, setting $\alpha = 0$ in these equations gives the solution for the inviscid compressible sink flow. The result is

$$\frac{1}{w}\left(\frac{\gamma+1}{2} - \frac{\gamma-1}{2} w^2\right)^{-(\gamma/\gamma-1)} = \frac{r}{r^*} \qquad (11\text{-}8)$$

This solution is plotted in Figure (11-1) and it is seen that it checks with that of Chapter 8.

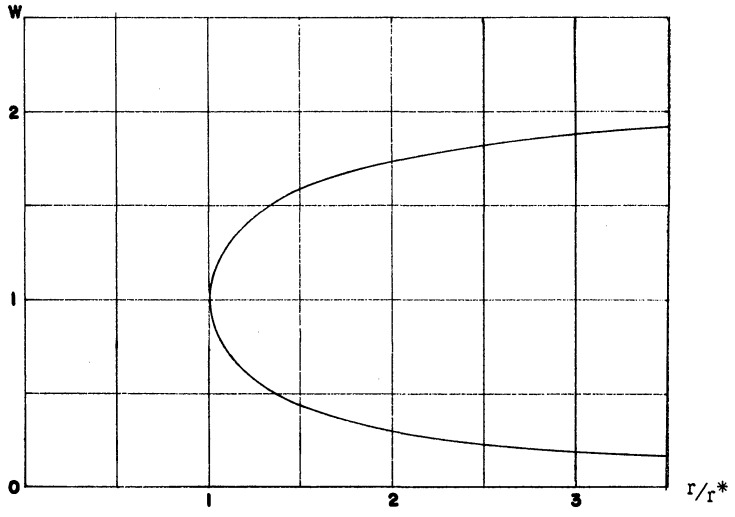

Figure 11-1. Inviscid Solution for $\alpha = 0$

The inviscid solution is now used as a guide to solve the sink flow of a real fluid described by Equations (11-6) and (11-7) by ascribing the limit of the viscous solution for vanishing viscosity to approach the inviscid solution as r tends to infinity. By continuing the viscous solution backwards in r, the viscous effects become more and more prominent, and it is found that the case of a real fluid flow does cross the sonic circle. By means of this technique, Wu (136) obtained several solutions corresponding to both the subsonic and supersonic regimes discussed in Chapter 8. However, only the subsonic solution need be of interest here. Its plot and comparison with the inviscid solution is shown in Figure (11-2).

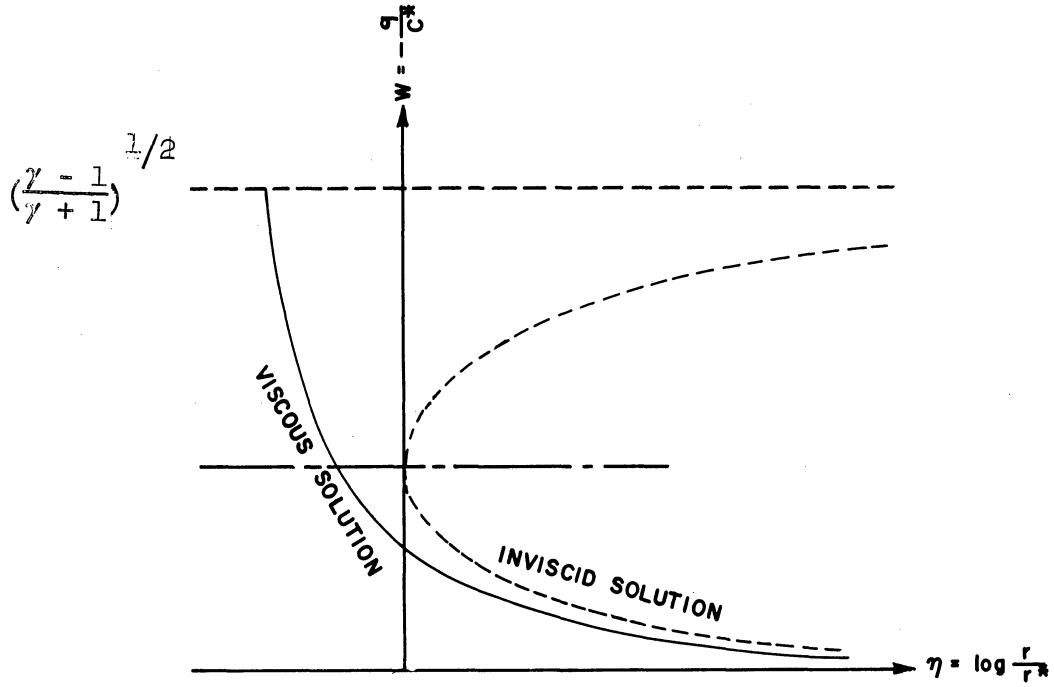

Figure 11-2. Viscous Sink Flow Solution

It is seen that at every $\eta = \ln \frac{r}{r^*}$, the velocity is slowed down from its inviscid solution due to viscous effect. The viscous solution for subsonic flow is, nevertheless, very close to the inviscid solution. There is no single expression available for the solution throughout the entire flow region, but the calculation is performed in three different ranges of r. The present work proceeds from Wu's solution curve, but substitutes an exponential for it, thus obtaining a single expression throughout the flow region from $\frac{r}{r^*} \gg 1$ to $\frac{r}{r^*} = 1$. The least squares calculation for doing this is shown in Appendix C with the solution as an exponential function.

11.3 Superposition of Rotational Flow and Sink Flow

The superposition of the rotational flow of Chapter 10 with the sink flow calculated in the preceding section results in the general solution for the flow in the vortex tube. The technique being the same

as that presented in Chapter 8, its details are not repeated here. The flow pattern in the plane is shown in Figure (11-3).

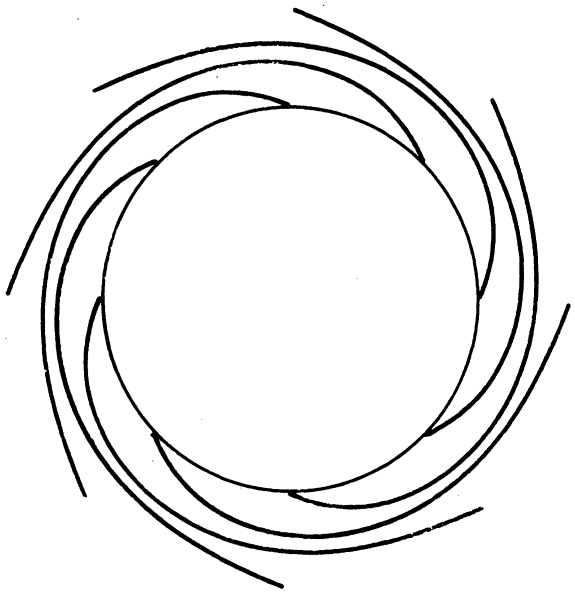

Figure 11-3. Viscous Flow Pattern

It is seen that the general appearance is similar to that of the inviscid flow pattern of Chapter 8, except that the free vortex of inviscid flow has been replaced by the forced vortex of viscous flow. In fact, the rotational characteristics of the latter flow make it somewhat easier to plot the streamlines.

To obtain the flow pattern in space, the technique of Chapter 9 is again employed, i.e., an axial velocity is added to the two-dimensional flow pattern of Figure (11-3). The magnitude of this axial velocity is gotten from the experimental data of Chapter 3. The streamlines are similar in character to the solution obtained in Chapter 9 except that the particles of fluid now possess rotational properties. Because of the latter reason, neither potential function φ nor stream function ψ technically exists here, and the streamlines in in Figure (9-3) are therefore labeled lines of "pseudo ψ" in compliance with mathematical language.

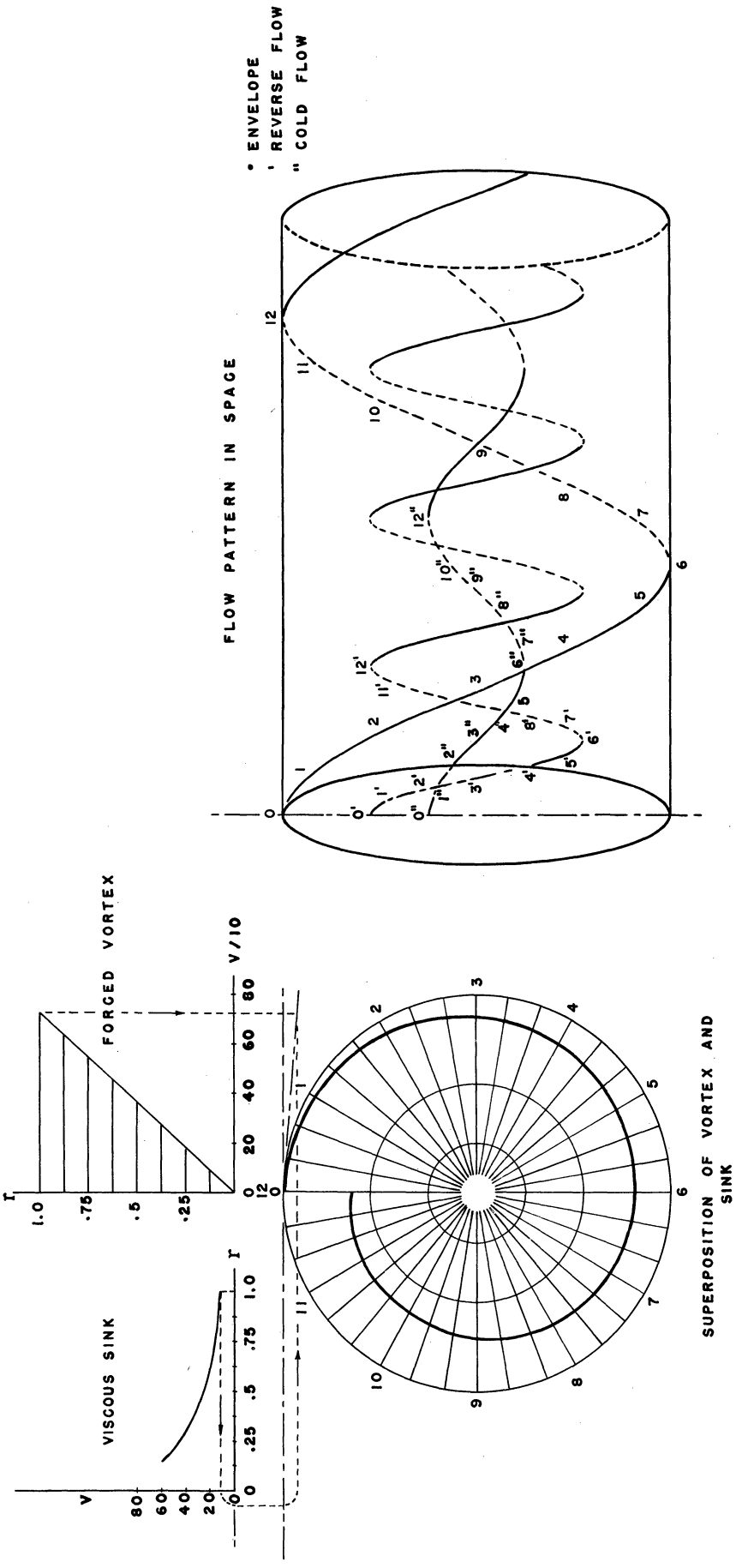

Figure 11-4. General Solution of Vortex Tube (P_{inlet} = 20 psig; Configuration A)

PART IV

DISCUSSION AND CONCLUSION

Chapter 12

BOUNDARY LAYER AND ENERGY SEPARATION

12.1 Nature of Solution

The current work represents an analytical and experimental study of compressible flow in a uniflow vortex field. It consists of a mathematical treatment based on experimental facts, and requires no special assumptions or elaborate models for comparison. The explanation of the phenomenon is in the solutions of the flow and energy equations, and it is the simplest and best explanation. The alternative to the mathematical approach would have involved various conjectures as to the mechanism of energy transfer, and as to the apparent alteration of the Maxwell-Boltzmann velocity distribution. With such assumptions, the study would have taken on an artificial character.

The mathematical results arrived at are dependable, because the initial assumptions are few in number, and the physical laws upon which the equations are written are those of classical physics. The assumptions made were that the fluid be a continuum, and that the flow field be divided into two regions, the one outside the boundary layer, and the other the boundary layer itself. The physical laws upon which the equations were based are non other than the principle of continuity, Newton's law of motion, the isentropic change of state relation, and the equation of state for the medium.

The assumption of a continuum is equivalent to working with the macroscopic properties of the fluid rather than with its molecular properties. This is valid, since the mean free path of the molecular (3.5×10^{-6} in. for air) is nowhere comparable in size with the

smallest significant dimension of the problem. The division of the flow field into two regions enables the problem to be solved. For, in the region outside the boundary layer, the viscous forces being very small compared to the inertia forces, the flow can be treated as potential, and the equations can be greatly simplified. The method of isolating the boundary layer is due to Prandtl, and it is appropriate to the present work, for in subsonic flow, the presence of a boundary layer influences the potential flow only in a secondary manner (110). True, viscous stresses within the boundary layer do shearing work on the fluid particles, and this shearing work tends to alter the temperature distribution, thus leading to heat conduction and changes in viscosity and density. However, for the flow of most liquids and gases at low Mach numbers past an insulated surface, such heat transfers are relatively unimportant, inasmuch as the internal heat transfers within the boundary layer are then of the same order of magnitude as the viscous shearing work, and the latter is not very large, except at high Mach numbers.

12.2 Boundary Layer

To illustrate the events taking place withing the boundary layer, consider the high-speed boundary layer next to an insulated wall. Because of the condition of no-slip, the outer layers of fluid do viscous shearing work on the inner layers, and consequently, the internal energy and temperature of the fluid in the inner layers tend to rise. When there is no heat conduction from the wall (case of insulated wall), the inner layers and the wall become progressively hotter. However, the temperature gradients now created by the viscous shearing work lead to a conduction of heat through the gas, and away

from the wall which ultimately counterbalances the effects of the viscous shearing work. The resulting steady-state temperature distrubution is as shown in Figure (12-1). Here, the temperature distributions for the three cases of insulated, hot, and cold wall are shown.

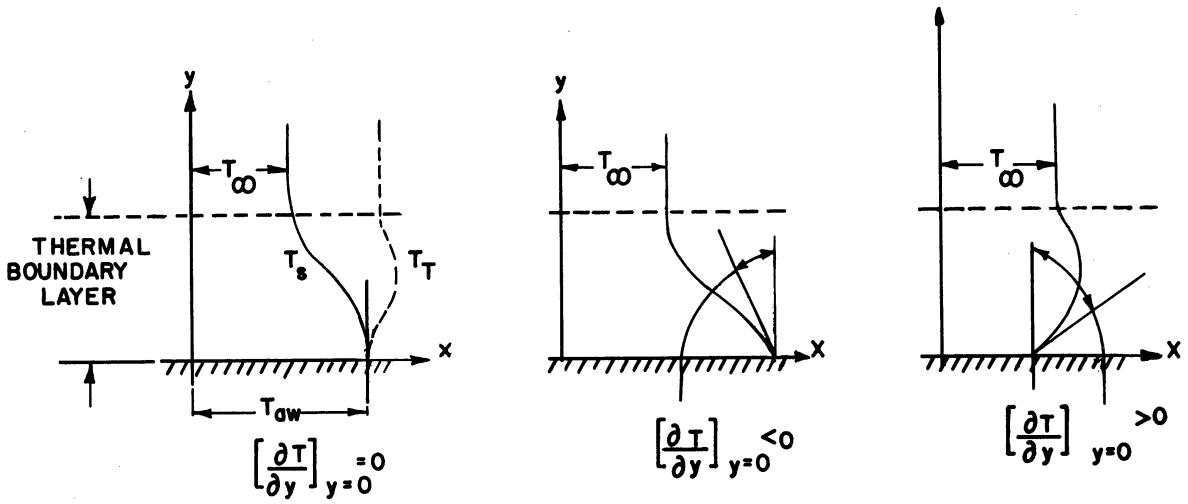

Figure 12-1. Temperature Distribution within Boundary Layer

The adiabatic wall temperature (T_{aw}) is greater than the free-stream temperature T_∞ . However, the temperature gradient at the wall is zero, in accordance with the Fourrier heat conduction equation ($Q = - k \frac{\partial T}{\partial y}$) and the assumption of zero heat flux for an insulated wall. In gases, the adiabatic wall temperature is always less than the free stream stagnation temperature T_T. For practical purposes, it is convenient to express the temperature at the wall in terms of a "recovery factor", defined by the relation

$$T_{aw} = T_\infty + \eta \frac{u_\infty^2}{2gJc_p} \qquad (12\text{-}1)$$

where η is the recovery factor. Incidently, T_{aw} is the temperature attained by the thermocouple and hot-wire probe if the latter were

also used to check temperatures. The value of η may be determined experimentally, but the commonly accepted value for the type of experiments involved in the present work is around .65.

Another feature is that since the wall temperature is less than the free-stream stagnation temperature, it follows that the distribution of stagnation temperature within the boundary layer is of the form shown in Figure (12-1a), with some portion of the boundary layer having a stagnation temperature greater than the free-stream stagnation temperature. When the wall is uninsulated, the temperature distributions within the boundary layer are as shown in Figures (12-1b, 1c). The slope of the curve is given by the value of $\frac{\partial T}{\partial y}$ at the wall (y=0).

12.3 Energy Separation and Prandtl's Number

In connection with the discussion of the boundary layer, it is of interest to note that whereas in steady, inviscid, isentropic flow, the total temperature remains constant, the situation is rather different in cases of fluids with viscosity and conductivity, even when there is no energy flow through the wall. Eckert and Hartnett (30) have studied several such cases of possible energy separation in terms of the Prandtl number. Some of the cases are summarized and discussed here for purposes of comparison with the vortex tube phenomenon.

i) Couette Flow

In the simple Couette flow between two parallel plates, one of which is at rest, the velocity distribution is

$$u = u_1 \frac{y}{\ell} \qquad (12\text{-}2)$$

and the energy equation is

$$k \frac{d^2 T}{dy^2} = - \mu \left(\frac{du}{dy}\right)^2 \qquad (12\text{-}3)$$

Referring to Figure (12-2), if the plate at y = 0 is assumed adiabatic, and that at y = ρ is cooled to a temperature T_1, then the following boundary conditons exist

$$\frac{dT}{dy} = 0 \quad \text{at} \quad y = 0 \tag{12-4a}$$

$$T = T_1 \quad \text{at} \quad y = \ell \tag{12-4b}$$

The static temperature field, obtained by integration, is

$$T = T_1 + \left(\frac{\mu c_p}{k}\right) \frac{u_1^2}{2c_p} \left[1 - \left(\frac{y}{\ell}\right)^2\right] \tag{12-5}$$

Noting that the stagnation or total temperature is related to the static temperature by

$$T_T = T + \frac{u^2}{2c_p} \tag{12-6}$$

the expression for the difference between the total temperature at y and the total temperature at y = 0 is finally obtained:

$$(T_T)_{y=\ell} - (T_T)_{y=0} = \left(\frac{u_1^2}{2c_p}\right)(1-p_r)\left(\frac{y}{\ell}\right)^2 \tag{12-7}$$

The velocity and temperature distribution is shown in Figure (12-2). The temperature distribution is that due to heat generated by friction when the lower wall is non-conducting (thermometer-plate problem).

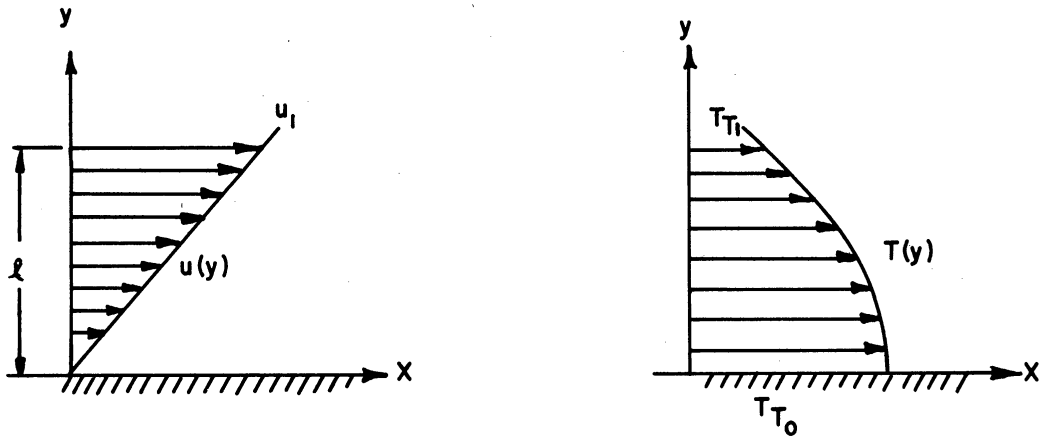

Figure 12-2. Velocity and Temperature Distribution for Couette Flow

Equation (12-7) indicates that for a Prandtl number of unity, the total temperature is constant across the flow, but that for all other Prandtl numbers there will be a "separation", i.e., a region of high total temperature and a region of low total temperature.

ii) Laminar Channel Flow

Consider the Poiseuille flow through a channel formed by two parallel flat walls a distance q apart. The velocity distribution is

$$u = \frac{3}{2} u_m \left[1 - \left(\frac{y}{\frac{\ell}{2}}\right)^2 \right] \tag{12-8}$$

where u_m denotes the mean velocity. The energy equation is

$$\rho c_p u \frac{\partial T}{\partial n} = k \frac{\partial^2 T}{\partial y^2} + \mu \left(\frac{du}{dy}\right)^2 \tag{12-9}$$

If the boundary conditions

$$\frac{\partial T}{\partial y} = 0 \quad \text{at} \quad y = 0$$

$$\frac{\partial T}{\partial y} = 0 \quad \text{at} \quad y = \frac{\ell}{2}$$

are imposed, Equation (12-9) is solved by setting $T = Ax + g(y)$ and integrating to yield

$$T = 12 \frac{\mu u_m}{\rho c_p \ell^2} x - \frac{9}{8} p_r \left(\frac{u_m^2}{c_p}\right) \left[1-4\left(\frac{y}{\ell}\right)^2\right]^2 \tag{12-10}$$

and the difference of total temperatures becomes

$$(T_T)_{y=\frac{\ell}{2}} - (T_T)_{y=0} = \left(\frac{u_c^2}{2c_p}\right)(1-p_r) \left[1-4 \left(\frac{y}{\ell}\right)^2\right]^2 \tag{12-11}$$

where u_c is the center-line velocity. The velocity and temperature distribution is shown in Figure (12-3).

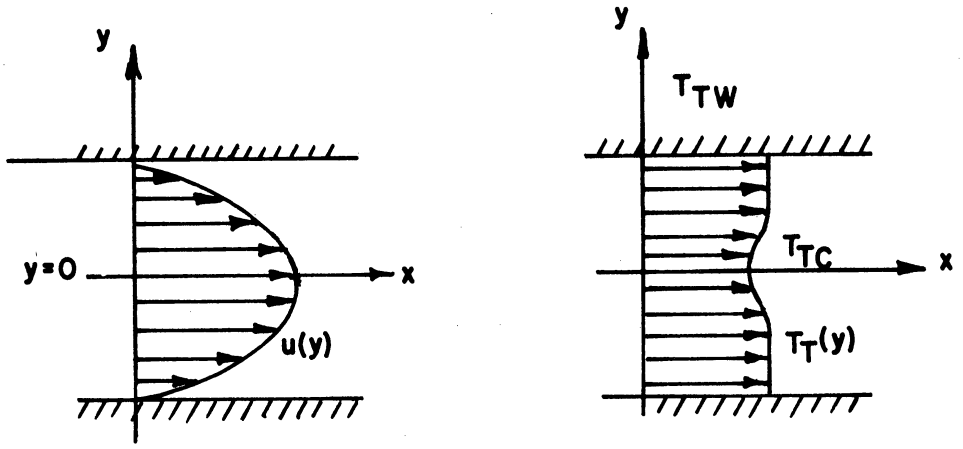

Figure 12-3. Velocity and Temperature Distribution for Channel Flow

Equation (12-11) indicates that a variation in total temperature occurs only for Prandtl numbers differing from unity.

iii) Poiseuille Flow in Circular Tube

The velocity distribution for laminar flow in a circular tube is

$$u = 2u_m \left[1-\left(\frac{r}{R}\right)^2 \right] \tag{12-12}$$

where R is the radius of the tube, and u_m is the mean velocity. The energy equation is

$$\rho c_p u \frac{\partial T}{\partial x} = \frac{k}{r} \frac{\partial}{\partial r} \left[\left(r \frac{\partial T}{\partial r} \right) \right] + \mu \left(\frac{du}{dr} \right)^2 \tag{12-13}$$

If the boundary conditions imposed are

$$\frac{\partial T}{\partial r} = 0 \qquad \text{at} \qquad r = 0$$

$$\frac{\partial T}{\partial r} = 0 \qquad \text{at} \qquad r = R$$

the static temperature integrates into

$$T = \frac{8\mu u_m}{\rho c_p R^2} x - 4 \left(\frac{u_m^2}{2c_p} \right) \left(\frac{\mu c_p}{k} \right) \left[1-\left(\frac{r}{R} \right)^2 \right]^2 \tag{12-14}$$

and the total temperature into

$$(T_t)_{r=r} - (T_t)_{r=R} = \left(\frac{u_c^2}{2c_p}\right)(1-P_r)\left[1-\left(\frac{r}{R}\right)^2\right]^2 \qquad (12\text{-}15)$$

where u_c is the center-line velocity. Equation (12-15) is essentially the same as that of channel flow. Again variation in total temperature occurs only for Prandtl numbers different from unity.

iv) Solid Body Rotation

Consider a laminar solid-body rotational flow with the velocity distribution

$$V = \frac{r}{R} V_1 \qquad (12\text{-}16)$$

Since there are no shearing stresses present, the energy equation becomes

$$\frac{\partial}{\partial r}\left[\left(r \frac{\partial T}{\partial r}\right)\right] = 0 \qquad (12\text{-}17)$$

Imposing the boundary conditions of

$$T = T_w \quad \text{at} \quad r = R$$

$$\frac{\partial T}{\partial r} = 0 \text{ at } r = 0$$

results in no heat flowing across the wall, and in a total temperature difference of

$$(T_T)_{r=R} - (T_T)_{r=0} = \left(\frac{V_1^2}{2c_p}\right)\left[1-\left(\frac{r}{R}\right)^2\right] \qquad (12\text{-}18)$$

where V_1 is the peripheral speed. Equation (12-18) shows a marked difference from the cases of rectilinear flow, namely that the "separation" effect is independent of the Prandtl number, i.e., there is energy spearation even for a Prandtl number of unity. Thus, for gases which have a Prandtl number close to unity (.7 for air), the separation effect, while small for rectilinear flow, becomes considerable for rotational flow. This is precisely what happens in the vortex tube, where it was shown in chapter 10 that the flow is indeed rotational. Equation (12-18) furnishes a check on the theory of the

vortex tube developed earlier. It shows that the central total temperature is the lowest, a situation which is analogous to that found in the vortex tube.

v) Solid Body Rotation - Turbulent Flow

The same situation prevails in the case of turbulent solid-body rotational flow. Consider the turbulent flow with velocity and pressure distributions given by

$$V = \frac{r}{R} V_1 \tag{12-19}$$

$$\frac{\partial p}{\partial r} = \rho \frac{v^2}{r} \tag{12-20}$$

Substituting the value for V from Equation (12-19) into Equation (12-20) and separating variables yields

$$\int_o^R \frac{dp}{\rho} = \int_o^R V_1^2 \frac{r}{R^2} dr \tag{12-21}$$

It is commonly accepted hypothesis that the equilibrium temperature distribution in a highly turbulent gas flow in which pressure gradients exist normal to the flow direction should correspond to the isentropic variation with pressure. That is, if a small mass of fluid at temperature T_1 and pressure p_1 moves to a new position where the pressure is p_2, the small mass will take up a temperature T_2 which is given by the isentropic relation $T_2 = T_1 \left(\frac{p_2}{p_1}\right)^{\frac{\gamma-1}{\gamma}}$. If the temperature of the fluid at the new position already corresponds to this temperature T_2, no heat transfer will occur, but if it is different, then a heat transfer will result and tend to establish the temperature T_2. Thus, introducing the isentropic relation

$$\frac{p}{\rho^\gamma} = \frac{p_o}{\rho_o^\gamma} = \frac{p_1}{\rho_1^\gamma} \tag{12-22}$$

and the perfect gas relation

$$p = \rho RT \tag{12-23}$$

into Equation (12-21), the latter integrates into

$$\frac{\gamma}{\gamma-1}\left[R(T_1 - T_o) \right] = \frac{V_1^2}{2} \tag{12-24}$$

and, in terms of total temperatures, this may be expressed as

$$(T_T)_{r = R} - (T_T)_{r = 0} = \frac{V_1^2}{c_p} \tag{12-25}$$

Equation (12-25) indicates not only an energy separation independent of the Prandtl number, but an amount of separation even greater than that obtained in the case of laminar rotation. The results of the solid-body rotation case are summarized in Figure (12-4) for the entire region of r = R to r = 0.

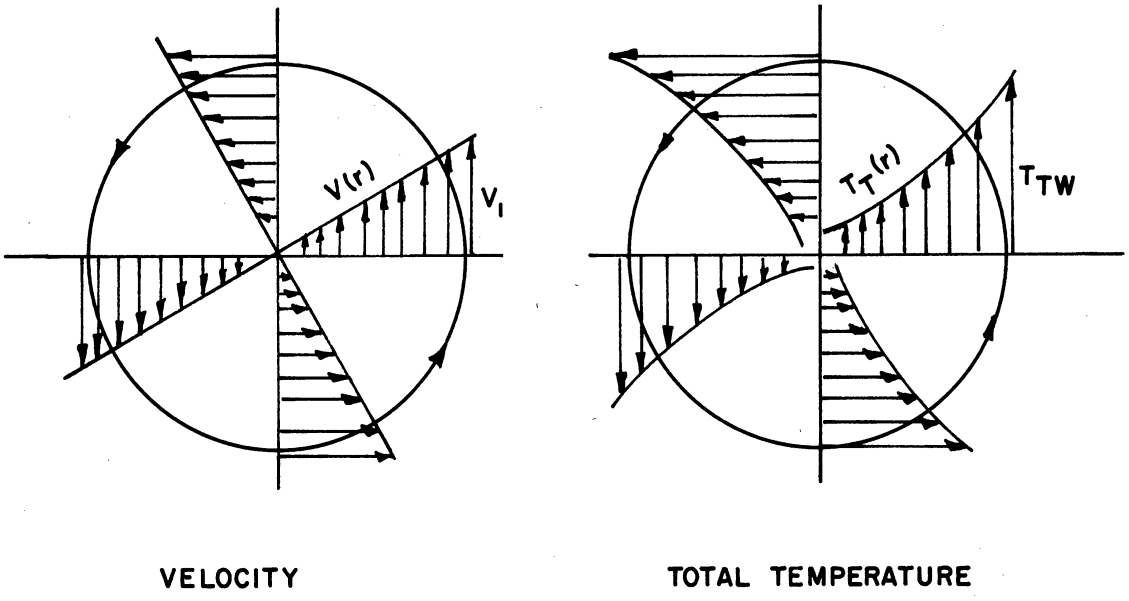

Figure 12-4. Velocity and Energy Distribution for Solid-Body Rotational Flow

It can be seen that except for "end effects" at r = 0 and r = R, the computed profiles have the same shape as the experimental profiles previously obtained. The "separation factor" in Equations (12-18) and (12-25) is theoretically .5 for laminar flow, and 1.0 for turbulent

flow. The experimental separation factor turns out to be between .7 and .9, a value greater than that for laminar flow, but somewhat lower than that for turbulent flow. Since the flow in the vortex tube is mostly turbulent, the result is consistent. The presence of an axial component of velocity prevents the separation factor from reaching its maximum obtainable value under pure rotation.

12.4 Conclusion

The conclusion of the study on the vortex tube is summarized by the following statements.

i) Upon entrance into the tube, the motion of the gas is that of a "free" vortex, having the characteristics of irrotational flow.

ii) By isolating the thin boundary layer from the flow field proper, the problem of the vortex tube becomes amenable to exact solution through the superposition of a vortex and a sink. The compressible nature of the flow gives rise to the existence of limit or sonic circles, inside which there is no flow "in the plane".

iii) Under the influence of viscous shearing forces, the free vortex "locks" itself, and changes to a "forced" vortex. The character of the flow changes from irrotational to rotational. This in agreement with the experimental traverses obtained at various stations along the tube.

iv) A more realistic solution is obtained by superposing a viscous rotational flow to a viscous compressible sink flow to replace the superposition under ii). The performance of the vortex tube is obtained in terms of a parameter representing the ratio of the strength of vortex to sink.

v) The three-dimensional solution for the flow pattern is obtained by the additon of an axial velocity to the combination of vortex and sink flows in the planes.

vi) The results are in agreement with the circular shear theory of Kassner and Knoernschild (58), and the energy separation case studies of Eckert and Harnett (30).

12.5 Applications of Vortex Tube

The vortex tube is a relatively new device, having been invented in 1932, and re-discovered in 1945. For this reason, its knowledge and application are not widespread. Although its efficiency is low compared to a standard refrigerating machine, it has several possible advantages. First, the construction is very simple, involving no moving or wearing parts. Second, it starts functioning immediately with no warm-up period required. A vortex tube has been built into a small air liquefier of 3.5 liters per hour capacity (78). The tube is of small dimensions, and is fed by laboratory air supply at about 10 atm. pressure. The cold stream emerges at -40°C and joins the upward-streaming air from the expansion valve and liquid air chamber. It thus serves as a precooler and as part of the steady cooling of the high pressure stream at 200 atm. going down through the heat exchanger to the expansion valve. The entire liquefier is very quick to get into operation. Starting at room temperature, liquid air is produced three minutes after the air supply is turned on and continues thereafter at the rate of 3.5 liters per hour. The cold air from the vortex tube is used to make up the volume of air liquefied. This has the advantage that water vapor is held to a minimum, since the air entering the vortex tube has already been through the laboratory compressor where the water

vapor is mostly removed.

Another application of the vortex tube is the temperature conditioning of parts or sections of high-speed aircraft. Its extreme simplicity makes it very attractive for this purpose. This is particularly true when the airplane speed is high (in the sonic range), but the altitude is not too excessive (under 20,000 feet). In such cases, the aerodynamic heating which is caused by the skin friction reaches temperatures in excess of 1000°F. Cooling for the sake of human comfort and in the interest of strength considerations of structural parts or equipment thus becomes necessary. The use of the vortex tube is indicated, since it can take advantage of the ram air (61).

Still another application of the vortex tube is the measurement of true air temperature in high-speed flight. If a conventional type thermometer is used on the aircraft, the aerodynamic heating would cause a much higher reading on the thermometer than that corresponding to the true air temperature. It is therefore desired to have a cooling effect around the thermometer pick-up that will compensate for the heating effect. The vortex tube accomplishes this purpose. Suppose the inlet nozzle of the vortex tube is in the direction of motion of the airplane such that the air is rammed through the nozzle. If the airplane is flying at a Mach number M relative to the air, then the stagnation temperature T_T is related to M and the free air temperature T_f by the relation

$$T_T = (1 + 0.2\ M^2)\ T_f \qquad (12\text{-}26)$$

In the case of an airplane flying at sonic speed (M = 1), a thermocouple placed at the entrance of the nozzle would read a temperature of 1.2 T_f. Now, if the stagnation probe is located in the cold

portion of the vortex tube, the cooling effect of the tube would compensate for the aerodynamic heating, and the temperature of the thermocouple can be made to read T_f. The extent of the compensation and the design of the vortex-thermometer installation are under current study (127, 59, 81).

APPENDICES

APPENDIX A

HOT WIRE ANEMOMETRY

1. Hot Wire Realtions

The relation between the rate of heat loss from a heated wire immersed in a fluid and the speed of the fluid has been developed by Boussinesq, King, et al., to

$$H = L(T - T_o)(A + B\,V^{1/2}) \qquad (1)$$

where H = heat loss per unit time

L = length of wire

T = temperature of wire

T_o = temperature of airstream

V = velocity of airstream normal to wire

A,B = constants

In the velocity dependence relation $(A + B\,V^{1/2})$, the constant A represents the loss of heat due to free convection and radiation, and $B\,V^{1/2}$ represents the forced convection heat loss.

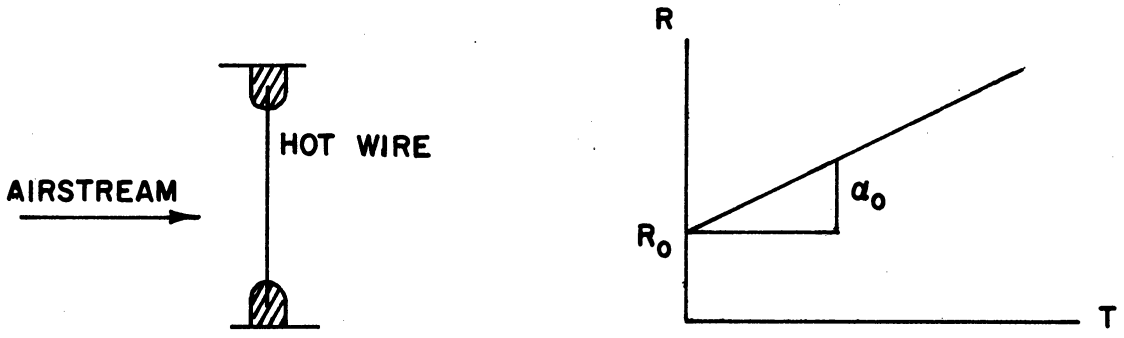

Figure A-1. Hot-Wire Anemometer and Linearity of Resistance Versus Temperature

If a current of I amperes is made to flow in the wire of resistance R, a second expression for the heat loss may be written:

$$H = I^2R \tag{2}$$

since the rate of heat loss from the wire is equal to the rate at which electrical energy is being converted into heat in the wire. Equation (1) and (2) yield

$$I^2R = L(T - T_o)(A + B\ V^{1/2}) \tag{3}$$

If α_o denotes the temperature-coefficient of resistivity at T_o, then

$$R = R_o\ [1 + \alpha_o(T - T_o)] \tag{4}$$

where R_o is the wire resistance at T_o, and R is the wire resistance at T (Figure A-1). Equation (4) shows that the product $\alpha_o R_o$ is the slope of the resistance-temperature curve at T_o. This slope is very nearly constant over a wide range of T_o for most wire materials, and $(T-T_o)$ may be replaced by its value of $(\frac{R-R_o}{\alpha_o R_o})$ from Equation (4) to put into Equation (3), thus resulting in

$$I^2R = L(\frac{R-R_o}{\alpha_o R_o})(A + B\ V^{1/2})$$

or

$$(\frac{I\ \alpha_o R_o}{L})[\frac{(R/R_o)}{(R/R_o)\ -1}] = A + B\ V^{1/2} \tag{5}$$

Equation (5) is the fundamental hot wire anemometer relation between wire current, wire resistance, and stream speed.

Suppose that the resistance ratio R/R_o is held fixed; then as the velocity of the stream changes, the current through the wire must be changed in order to preserve equality in Equation (5). This means that at any fixed resistance ratio, there is a definite relationship between I and V which may be determined by calibration, and subsequently used to measure unknown velocities. Note that it is not necessary to measure stream temperature, since it does not appear in Equation (5).

There are two ways in which the hot wire may be operated: i) keeping R(or T) constant, and measuring I, so that V is proportional

to I^4, or ii) keeping I constant, and measuring R, so that V is proportional to $(\frac{R}{R-R_o})^2$. The present work uses the first method.

2. Wire Calibration

Equation (5) suggests a linear calibration curve in which $I^2 (\frac{\alpha_o R_o}{L})[\frac{R/R_o}{(R/R_o)-1}]$ is plotted versus $V^{1/2}$. Such a plot will be a straight line having a slope B/ $(\frac{\alpha_o R_o}{L})$ $[\frac{R/R_o}{(R/R_o)-1}]$and a y-intercept A/ $(\frac{\alpha_o R_o}{L})$ $[\frac{R/R_o}{(R/R_o)-1}]$. Incorporating these as new constants C and D, the calibration curve simply becomes the straight line I^2 versus $V^{1/2}$ of Figure (A-2).

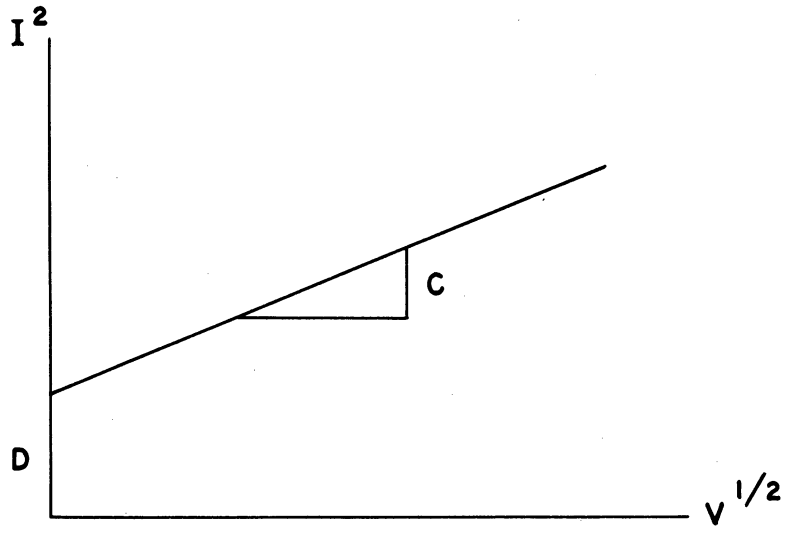

Figure A-2. Hot Wire Constants

Before calibration, it is convenient to decide at what constant temperature level (or R) the wire is to be operated. This is usually expressed as the overheating ratio, a, defined as

$$\frac{R}{R_o} = 1 + a \qquad (6)$$

The higher the overheating ratio, the greater the sensitivity of the wire, but also the greater the danger of burning the wire. Common overheating ratio for platinum wire is between 0.5 and 1.0 while those for

tungsten wires are approximately 1.0 and 2.0. After a has been decided upon, and R_o determined, Equation (6) serves to determine the value of R. At this constant R setting, the hot wire is placed in the airstream, and for various values of the velocity V, the current I, necessary to keep the wire at the constant temperature (corresponding to the constant R) is measured. The velocity is measured with a pitot tube in conjunction with a precision manometer. From these results, a calibration curve similar to the curve of Figure (A-2) is plotted for each particular wire that is used. Figure (A-4) shows the calibration curves of some of the wires that were used in the present work.

3. Measurement Circuit

The basic circuit for measuring the current through the hot wire is shown in the simplified diagram of Figure (A-3). The actual circuit is boxed in, and operates from a panel Figure (A-5).

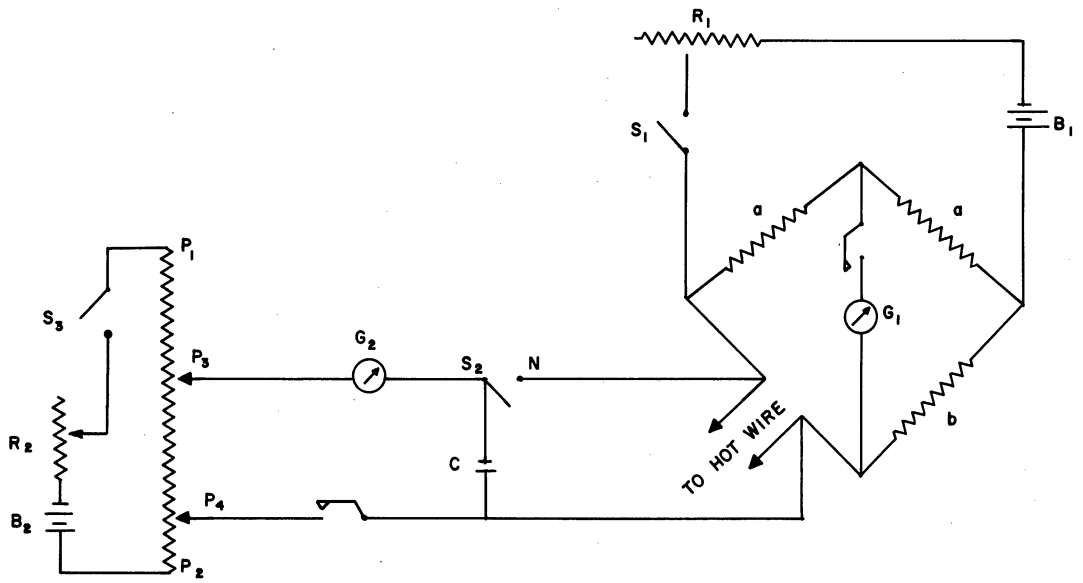

Figure A-3. Measurement Circuit

The bridge is used to measure the resistance and the current of the hot wire. The potentiometer measures the voltage drop between the ends of the hot wire, and since this voltage drop is the product of the constant resistance and the current, the reading is proportional to the current.

The sequence of operations is the following. 1) The hot wire is placed in the airstream. 2) Switch s_1 is closed, and the rheostat R_1 adjusted until the Wheatstone bridge shows balance. This makes the resistance of the hot wire equal to b. 3) The potentiometer contacts p_3 and p_4 are brought to the ends p_1 and p_2; switch s_2 is brought to the standard cell c, switch s_3 is closed, and the rheostat R_2 is adjusted till the voltage drop from p_1 to p_2 balance the voltage of the standard cell c_4. 4) Switch s_2 is brought to N, and the contacts p_3 and p_4 moved to give balance. This gives the voltage drop across the hot wire and completes the reading. 5) Switch s_1 is opened before retracting the hot wire from the airstream so as to avoid burning the wire.

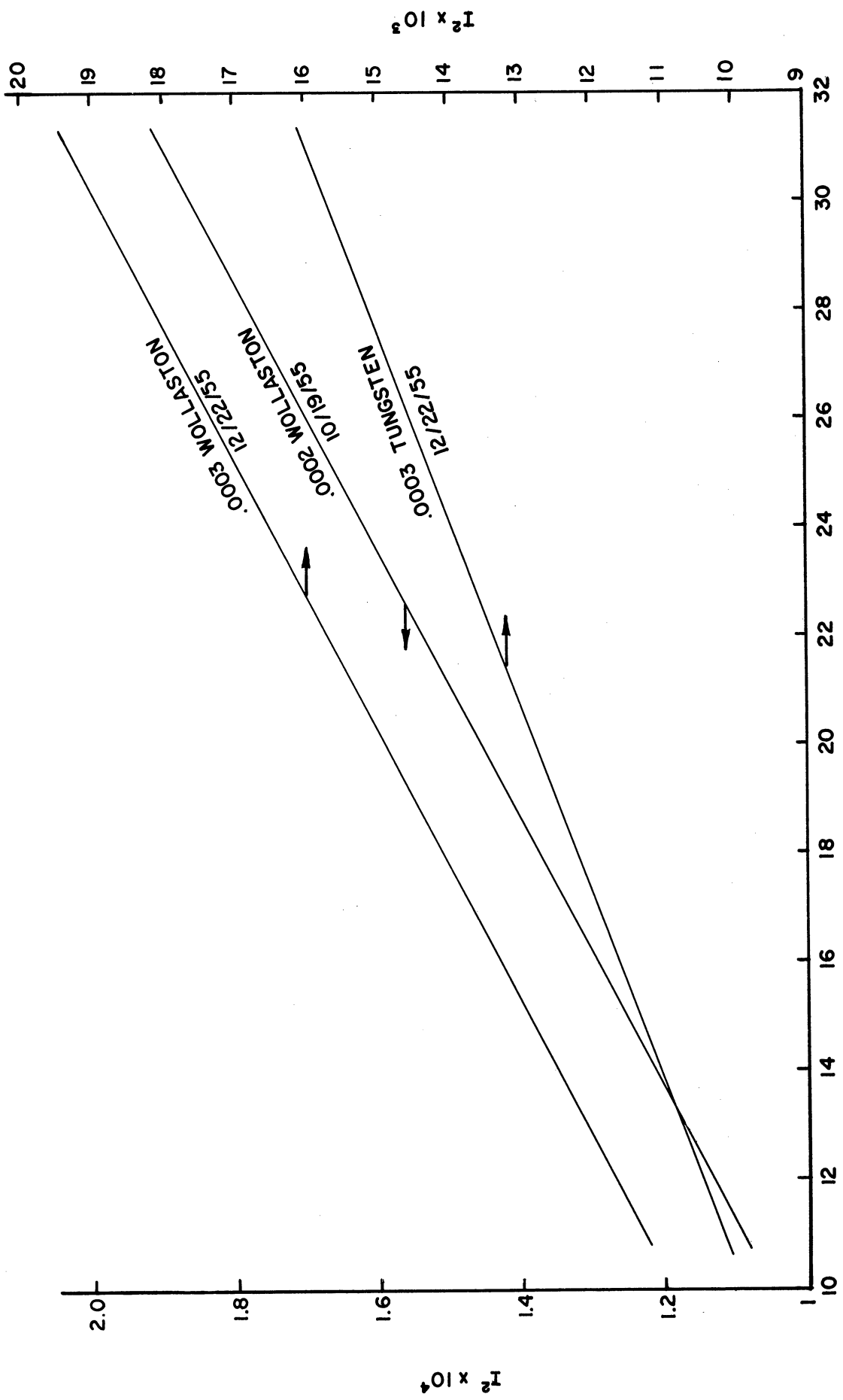

Figure A-4. Hot Wire Calibration Curves

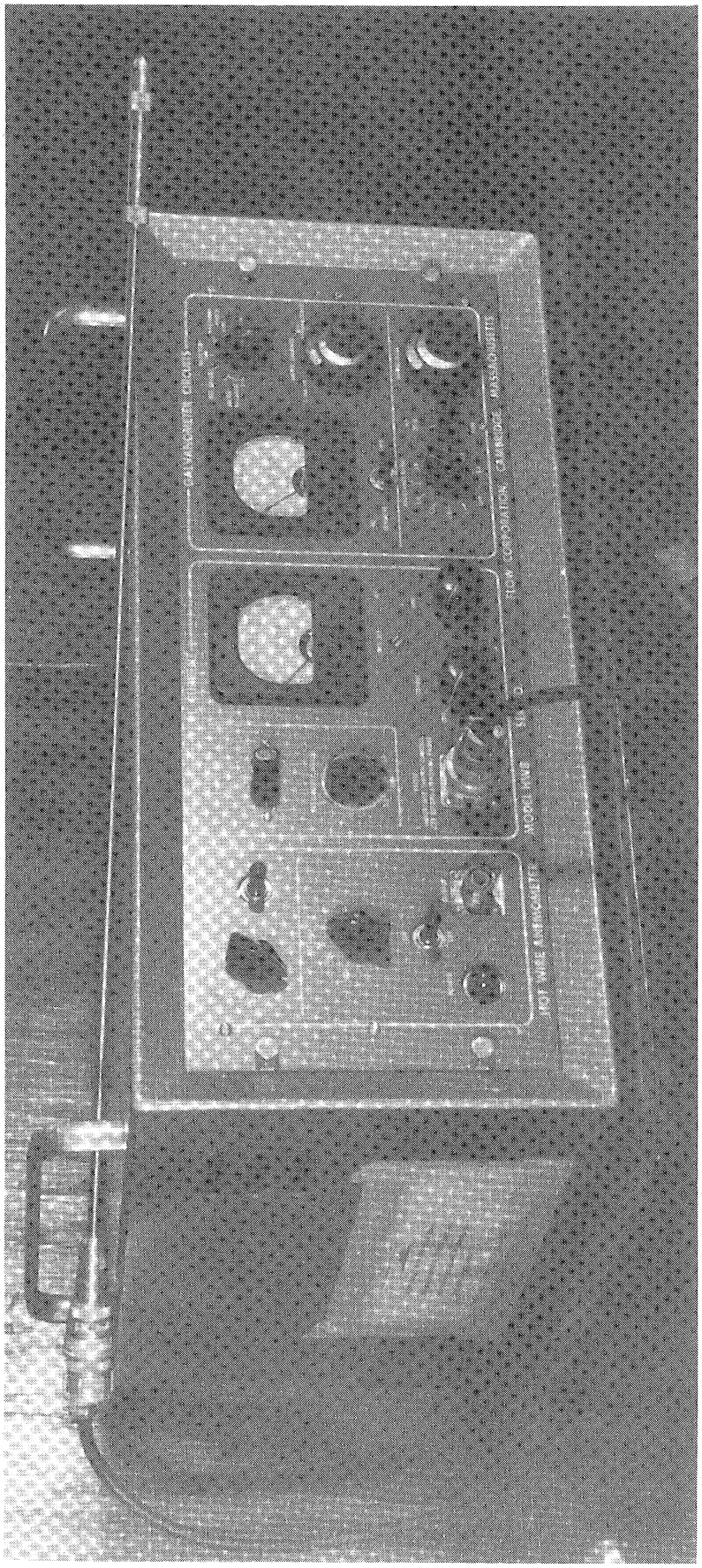

Figure A-5. Flow Corporation Hot Wire Anemometer

APPENDIX B

TEMPERATURE CORRECTION

After calibration of the thermocouple by comparison with a Bureau of Standards certified thermometer, the readings of the thermocouple must be corrected to indicate true temperatures of the airstream. The present purpose is to develop the necessary corrections.

1. Sources of Errors

If, when a thermocouple is placed in a gas at a given temperature, the heat transfer between it and the gas ceases, the couple will be at the same temperature as the gas, and the corresponding voltage of the couple will represent the temperature of the gas. Thus, the true temperature of the gas would be measured only under the following idealized conditions: 1) The walls of the enclosure have the same temperature as the gas. 2) The gas temperature is uniform in all directions. 3) The gas is stagnant or moving very slowly. 4) No temperature gradient exists along the thermocouple wires. Under these conditions, thermal equilibrium then exists between the wall, the gas, and the thermocouple measuring junction.

In practice, however, these conditions are never met, and the junction does not measure the true gas temperature. The principal sources of errors are shown in Figure (B-1).

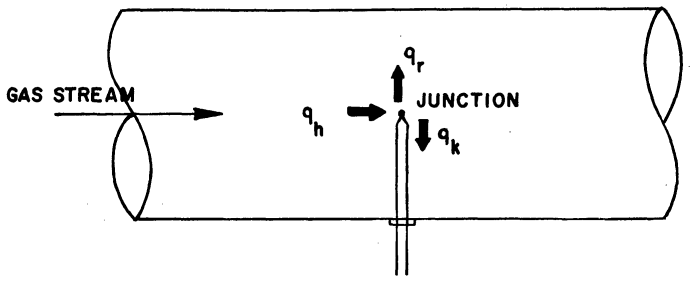

Figure B-1. Heat Transfers in Gas Temperature Measurement

2. Evaluation of Errors

The walls of the enclosure are at a different temperature from the thermocouple junction. The junction then "sees" the walls, and heat is exchanged by radiation, with the result that the junction assumes a temperature between that of the gas itself and the walls that it "sees". This heat exchange is shown schematically as q_r in Figure (B-1), and it is evaluated by

$$q_r = \epsilon \sigma A_1 (T_T^4 - T_w^4) \qquad (1)$$

where q_r = net rate of heat transfer by radiation

ϵ = emissivity of junction

σ = Stefan-Boltzmann constant

A_1 = exposed area of junction

T_T = thermocouple temperature

T_w = wall temperature

A temperature gradient may exist along the thermocouple wires, the temperature being higher at the junction than where the wires enter the enclosure. Consequently, heat is lost by conduction (q_k in Figure B-1), and the junction will assume a lower temperature than that of the gas, other things being equal. The heat conduction is evaluated by

$$q_k = \frac{kA_2(T_T - T_w)}{L} \qquad (2)$$

where q_k = rate of heat transfer by conduction

k = thermal conductivity

L = length of wire from junction to inlet

A_2 = cross sectional area of thermocouple wires

Convective heat transfer (q_h) occurs from the gas to the junction, and its general expression is

$$q_h = h\, A_1 (T_G - T_T) \tag{3}$$

where q_h = rate of heat transfer by convection.

h = Convection coefficient, computed from the cross-convection equation $(Nu) = 0.3\ (Re)^{0.57}$

T_G = gas temperature

In the case of static-temperature measurements, a fourth and final error is present: that due to the velocity of the gas stream However, this is usually taken care of by means of the adiabatic-temperature-rise (chapter 12), and will not be considered further here. Thus, when the junction reaches a constant temperature, which lies between that of the gas and of the walls, a heat balance may be written to the effect that the heat lost from the junction by radiation and conduction is balanced by convective heat transfer from the gas to the junction:

$$q_r + q_k = q_h \tag{4}$$

Making use of Equations (1), (2) and (3), this can be written as

$$\epsilon \sigma A_1 (T_T^4 - T_w^4) + \frac{2\ (T_T - T_w)}{L} = hA_1 (T_G - T_T)$$

and, solving for $(T_G - T_T)$ results in

$$T_G - T_T = \frac{\epsilon \sigma (T_T^4 - T_w^4)}{h} + \frac{kA_2 (T_T - T_w)}{hA_1 L} \tag{5}$$

Equation (5) is the basic equation for the difference between the true gas temperature and the thermocouple reading, and thus represents the "error" in gas temperature measurement. The working curve of error versus junction temperature is plotted in Figure (B-2).

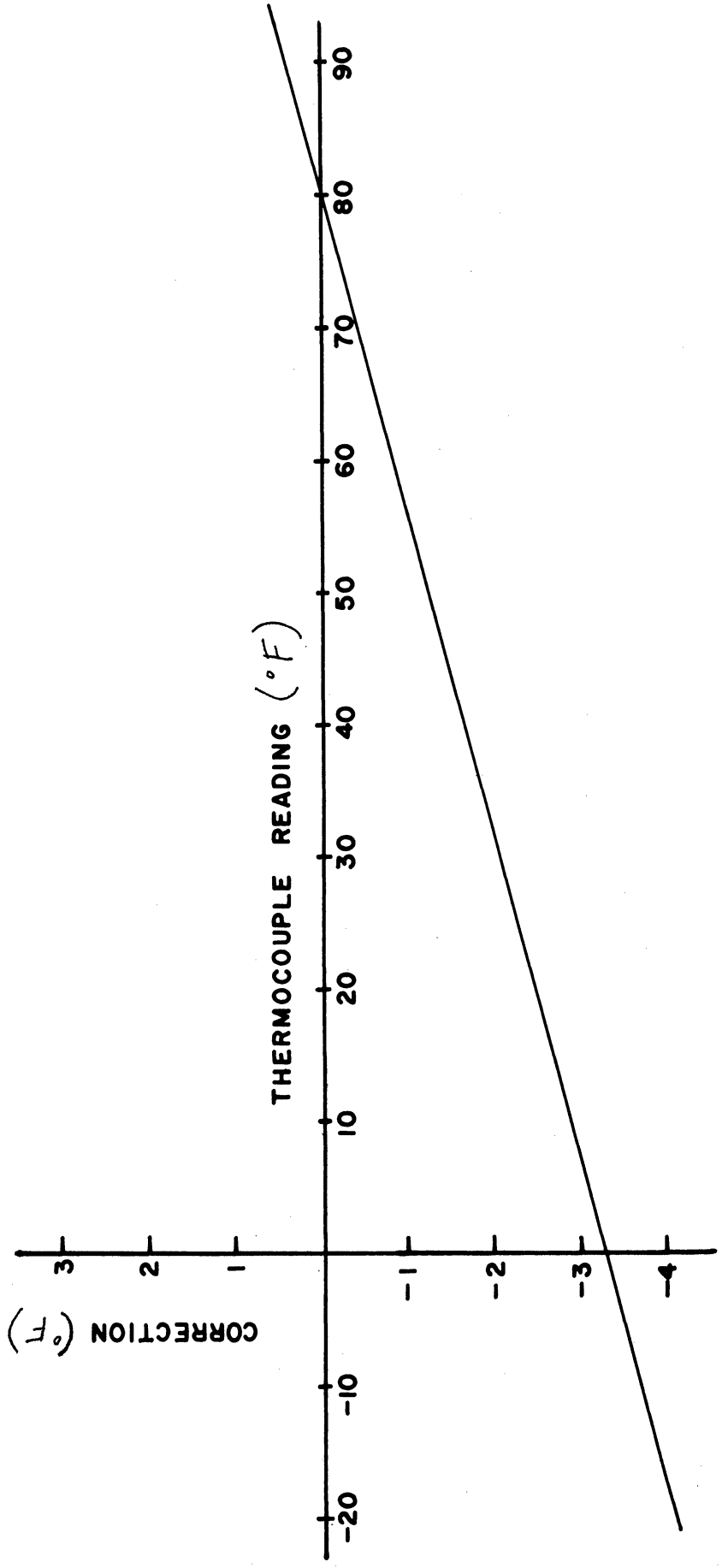

Figure B-2. Working Curve for Junction Temperature Correction

APPENDIX C

COMPUTATION FOR VISCOUS SINK SOLUTION BY METHOD OF LEAST SQUARES

It was stated in Chapter 11 that Wu (136) obtained mathematically the viscous compressible sink solution in three parts, since it was found that there was no single expression available for the solution that was uniformly valid in the entire flow region.

The present work proceeds from Wu's solution, and obtains a single expression for the viscous solution, uniformly valid in the range of values of r for the vortex tube. It is the purpose here to give the details of calculation by least squares that were not included in Chapter 11.

1. Method of Least Squares

Viewed in general terms, the method of least squares is simply a process for finding the best possible values of a set of m unknowns $x_1, x_2, \ldots . x_m$, connected by n(>m) linear equations

$$a_{11} x_1 + a_{12} x_2 + - - - - - + a_{1m} x_m = b_1$$

$$a_{21} x_1 + a_{22} x_2 + - - - - - + a_{2m} x_m = b_2$$

$$a_{n1} x_1 + a_{n2} x_2 + - - - - - + a_{nm} x_m = b_n$$

Since the number of equations exceeds the number of unknowns, the foregoing system does not admit an exact solution, i.e., there is no set values $x_1, x_2, \ldots . x_m$, for which each equation is exactly satisfied. Therefore, consider the discrepancies

$$\Delta_1^2 = (a_{11}\, x_1 + a_{12}\, x_2 + - - - - - a_{1m}\, x_m - b_1)^2$$

$$\Delta_2^2 = (a_{21}\, x_1 + a_{22}\, x_2 + - - - - - a_{2m}\, x_m - b_2)^2$$

- -

$$\Delta_i^2 = (a_{i1}\, x_1 + a_{i2}\, x_2 + - - - - - a_{im}\, x_m - b_i)^2$$

and let it be attempted to find the values of $x_1, x_2, \ldots . x_m$, for which the sum of the squares of the errors

$$E^2 = \sum_{i=1}^{n} \Delta_i^2 = \sum_{i=1}^{n} (a_{i1}\, x_1 + a_{i2}\, x_2 + - - - a_{im}\, x_m - b_i)^2$$

is as small as possible.

To minimize E^2, the conditions for minimizing a function of several variables, namely that the first partial derivatives of each variable be zero is applied. Thus,

$$\frac{\partial E^2}{\partial x_1} = \sum_{i=1}^{n} 2(a_{i1}\, x_1 + a_{i2}\, x_2 + - - - a_{im}\, x_m - b_i)(a_{i1}) = 0$$

$$\frac{\partial E^2}{\partial x_2} = \sum_{i=1}^{n} 2(a_{i1}\, x_1 + a_{i2}\, x_2 + - - - a_{im}\, x_m - b_i)(a_{i2}) = 0$$

which can be rewritten as

$$x_1 \sum_{i=1}^{n} a_{i1}\, x_{i1} + x_2 \sum_{i=1}^{n} a_{i1}\, a_{i2} + - - - + x_m \sum_{i=1}^{n} a_{i1}\, a_{im} = \sum_{i=1}^{n} a_{i1}\, b_i$$

$$x_1 \sum_{i=1}^{n} a_{i2}\, x_{i1} + x_2 \sum_{i=1}^{n} a_{i2}\, a_{i2} + - - - + x_m \sum_{i=1}^{n} a_{i2}\, a_{im} = \sum_{i=1}^{n} a_{i2}\, b_i$$

- -

- -

$$x_1 \sum_{i=1}^{n} a_{im} x_{i1} + x_2 \sum_{i=1}^{n} a_{im} a_{i2} + - - - + x_m \sum_{i=1}^{n} a_{im} x_{im} = \sum_{i=1}^{n} a_{im} b_i$$

The above represents a system of m linear equations in the m unknowns $x_1, x_2, \ldots . x_m$, whose solution is now a routine matter. These equations are labeled normal equations, and they can be written down instantly from the following rule: Let each of the original equations be multiplied by the coefficient of x_i in that equation, and let all the resulting equations be added. The sum represents the ith normal equation.

2. Equation for Viscous Sink Flow

From Figure (11-2), it is seen that the best expression to select for the viscons sink flow is that of decaying exponential:

$$w = c_1 e^{- a \ln \frac{r}{r^*}}$$

where c_1 and a are unknown constants to be determined. However, it is more realistic and convenient to simply work with the radius ratio r/r^*. Thus, without loss of generality, and with the understanding that a new set of constants is involved:

$$w = c_1 e^{- a \frac{r}{r^*}} \qquad (1)$$

From chapter 11, the data is

r/r^*	.5	1.0	1.5	2.0	2.5	3
w	.80	.55	.25	.16	.10	.06

From Equation (1):

$$\ln w = \ln c_1 - a \left(\frac{r}{r^*}\right) \qquad (2)$$

and the conditions to be satisfied by the unknowns c_1 and a become

$$\ln .80 = \ln c_1 - .5a$$

$$\ln .55 = \ln c_1 - a$$

$$\ln .25 = \ln c_1 - 1.5a$$

$$\ln .16 = \ln c_1 - 2a$$

$$\ln .10 = \ln c_1 - 2.5a$$

$$\ln .06 = \ln c_1 - 3a$$

or

$$-0.223 = \ln c_1 - .5a \tag{3}$$

$$-0.598 = \ln c_1 - a \tag{4}$$

$$-1.386 = \ln c_1 - 1.5a \tag{5}$$

$$-1.833 = \ln c_1 - 2a \tag{6}$$

$$-2.303 = \ln c_1 - 2.5a \tag{7}$$

$$-2.813 = \ln c_1 - 3a \tag{8}$$

Equations (3) to (8) represent six equations of condition for the two unknowns c_1 and a. The normal equations, as obtained by the rule set forth in the preceeding section are:

$$- 0.223 - .598 - 1.386 - 1.833 - 2.303 - 2.813 =$$
$$6 \ln c_1 - (0.5 + 1 + 1.5 + 2 + 2.5 + 3) a$$

or

$$-9.156 = 6 \ln c_1 - 10.5a \tag{9}$$

$$1.115 + 0.598 - 2.08 + 3.666 + 5.76 + 8.439 =$$
$$- (0.5 + 1 + 1.5 + 2 + 2.5 + 3) \ln c_1 +$$
$$(0.25 + 1 + 2.25 + 4 + 6.25 + 9) a$$

or

$$21.658 = - 10.5 \ln c_1 + 22.75a \tag{10}$$

The solution of the two normal equations (9) and (10) is

$$\ln c_1 = .753 \tag{11}$$

$$a = 1.301 \tag{12}$$

Replacement of Equations (11) and (12) into Equation (2) results in

$$\ln w = .753 - 1.301 \left(\frac{r}{r^*}\right)$$

or

$$w = 2.14\, e^{-1.301(r/r^*)} \tag{13}$$

which is the expression for the viscous compressible sink flow in the vortex tube. Its plot is shown in Figure (C-1). It corresponds to the convergent branch of the inviscid solution.

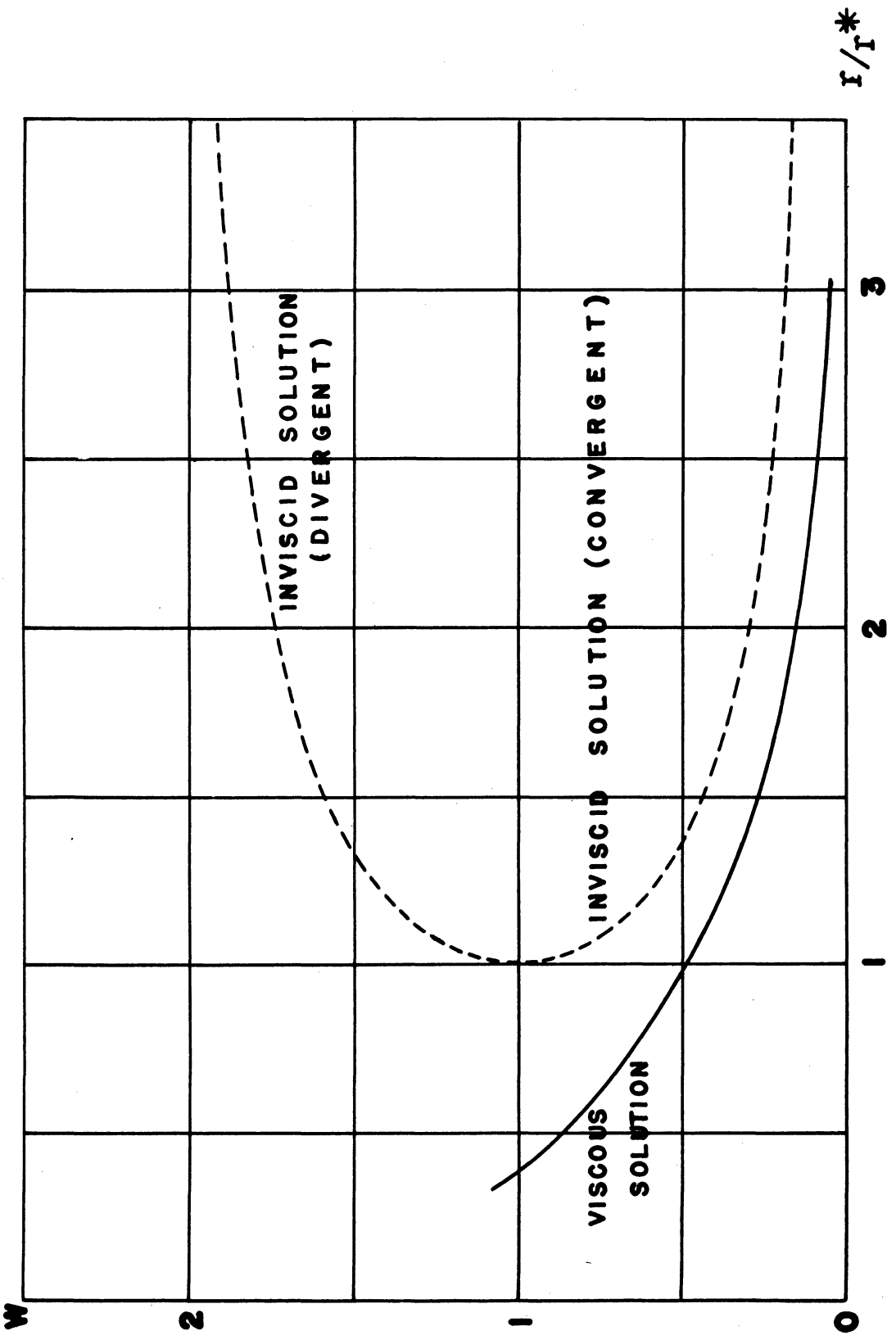

Figure C-1. Exponential Solution for Viscous Compressible Sink (Source)

APPENDIX D

PERFORMANCE CALCULATION

The performance of the vortex tube can be evaluated by superposing a rotational flow with an axial flow, i.e., by combining cases iii) and iv) of Chapter 12.

1. Solution for Superposed Flow

For mathematical simplicity, consider a rotational flow being superposed with a Poiseuille flow in a circular tube. For such a case, the Navier-Stokes equations reduce to

$$\frac{\partial p}{\partial r} = \rho \frac{V_T^2}{r}$$

$$(1) \qquad \frac{d^2 v_T}{dr^2} + \frac{1}{r}\frac{dV_T}{dr} - \frac{V_T}{r} = 0$$

$$\frac{d^2 V_A}{dr^2} + \frac{1}{r}\frac{dV_A}{dr} = \frac{1}{\mu}\frac{\partial p}{\partial z}$$

where V_T, V_A are the tangential and axial velocities respectively. The boundary conditions imposed on V_T and V_A are

$$(2) \qquad \begin{cases} V_T = 0 & \text{at} \quad r = 0 \\ V_T = V_{T1} & \text{at} \quad r = R \\ \dfrac{dV_A}{dr} = 0 & \text{at} \quad r = 0 \\ V_A = 0 & \text{at} \quad r = R \end{cases}$$

The velocity components as obtained by solution of the equations are

$$V_A = 2\bar{V}_A\left[1-\left(\frac{r}{R}\right)^2\right] \tag{3}$$

$$V_T = V_{T1}\left(\frac{r}{R}\right) \tag{4}$$

The energy equation is

$$\rho c_p V_A \frac{\partial T}{\partial z} = \frac{k}{r}\frac{\partial}{\partial r}\left(r\frac{\partial T}{\partial r}\right) + \mu\left(\frac{dV_A}{dr}\right)^2 \tag{5}$$

with the imposed boundary conditions of

$$\begin{aligned} \frac{\partial T}{\partial r} &= 0 \quad \text{at} \quad r = 0 \\ \frac{\partial T}{\partial r} &= 0 \quad \text{at} \quad r = R \end{aligned} \tag{6}$$

The solution is

$$T = 8\frac{\mu\bar{V}_A}{\rho c_p R^2} z - 4\left(\frac{\bar{V}_A^2}{2c_p}\right)\left(\frac{\mu c_p}{k}\right)\left[1-\left(\frac{r}{R}\right)^2\right]^2 \tag{7}$$

which can be rewritten in terms of the total temperature as

$$\frac{T_T - T_{TW}}{\frac{\bar{V}_A^2}{2c_p}} = 4[1-P_r]\left[1-\left(\frac{r}{R}\right)^2\right]^2 - \left(\frac{V_{T1}}{\bar{V}_A}\right)^2\left[1-\left(\frac{r}{R}\right)^2\right] \tag{8}$$

where T_{TW} is the total temperature at the wall.

2. Performance Curve

Equation (8) is the performance equation of the laminar case of superposition. It was chosen because it is amenable to solution, whereas the turbulent case is not. The solution for the turbulent case, however, may yet be evaluated from the discussion in Chapter 12 by multiplying the laminar solution by a factor of 1.8.

Experimental results indicate that the factor is closer to 1.6, and this is the value that is adopted for the plot of the performance curve in Figure (D-1). It is seen that the performance or energy separation of the vortex tube is the higher when the ratio of whirl velocity to axial velocity is the higher, and when the ratio of the cold tube diameter to hot tube diameter is the lower. In actual practice the ratio of whirl to axial velocities is controlled by the exit cone valve, whereas the ratio of the cold to hot tube diameters is controlled by the size of the cold outlet.

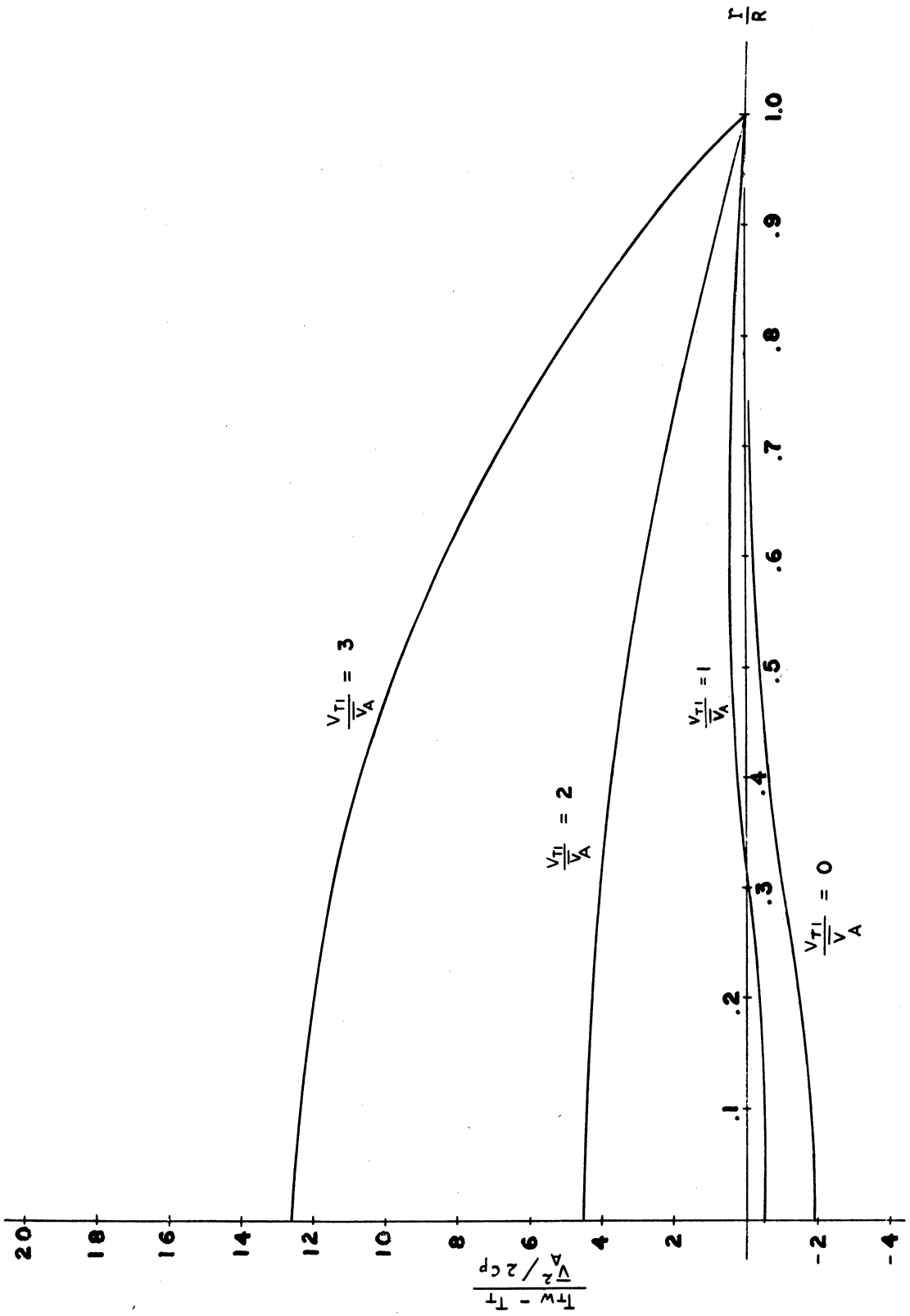

Figure D-1. Performance Curve for Vortex Tube ($P_r = 0.7$)

BIBLIOGRAPHY

1. Ackeret, J., "On Aerodynamic Cooling Effects", Ricerca Sc., Vol. 20, 1950, No. 12, pp. 1926-27.

2. Ambrose, W., "The Hilsch Tube", Carnegie Technical, December, 1949, pp. 8-10.

3. Applegate, M., Air Research Manufacturing Co., Los Angeles, "Vortex Tube Applications", Proceedings of the conference on cooling of Airborne Electronic Equipment, March, 1952, Ohio State University, Engineering Bulletin No. 148, pp. 207-209, July, 1952.

4. Arthur, P. D., "Operation and Theory of the Hilsch Tube," M. S. Thesis, University of Maryland, 1948.

5. Bailey, N. P., "Discussion," on Webster's paper. Refrigerating Engineering, 58, 169 Reb., 1950.

6. Barnes, W. P., Jr., "Energy Transfer in a Vortex," M. S. Thesis, Massachusetts Institute of Technology, 1948.

7. Baumeister, P. A., "Hot-Cold Tube Phenomenon Explained," Compressed Air Magazine, 52, 200, August, 1947.

8. Bertin, J. "Modified Hilsch Apparatus for Producing Hot and Cold Air Streams," (French Patent No. 521,736, Sept. 1946) Journal of Scientific Instruments, Vol. 28, Aug., 1951, No. 8, pp. 251.

9. Bickley, W. G., "Some Exact Solutions of the Equations of Steady Homentropic Flow of an Inviscid Gas," Modern Developments in Fluid Dynamics, Vol. I., Edited by L. Howarth, Oxford at the Clarendon Press, (1953).

10. Binnie, A. M., and Hooker, S. G., "The Radial and Spiral Flow of a Compressible Fluid," Philosophical Magazine, Vol. 23, January - June, 1937, pp. 597-606.

11. Blaber, M. P., "A Simply Constructed Vortex Tube for Producing Hot and Cold Air Streams", Journal of Scientific Instruments 27, 168-9, June, 1950.

12. Boer, J. De, "Theorie Van de Ranque - Hilsch Koelmethod," Nederlandsch Tijdschrift Voor Natuurkunde, Vol. 14, Angustus, 1948, pp. 240-241.

13. Bolsted, M. M., University of Missouri, "Discussion" on Webster's Paper, Refrigerating Engineering, 58, 169, Feb., 1950.

14. Brun, E., "Comments on Paper by G. J. Ranque," Journal de Physique et le Radium, Tome IV, Série VII, Juin 1933, No. 6., No. 343 Bulletin Bi-Mensuel, Juin, 1933, p. 122, s-123, s.

15. Burkhardt, G., "Theoretical Contribution to the Work of R. Hilsch on the Vortex Tube," (Translation by R. C. Murray, from Zeitschrift fur Naturforschung, Vol. 3a, No. 1., January 1948, pp. 46-51, R.A.E. Library) Translation No. 345, June, 1951.

16. Burkhardt, G., "The Hilsch Centrifugal Jet," Zeitschr. Naturforschung, e, 46, 1948, Condensed and reported by Plank, R., Journal of ASRE, Refrigerating Engineering, ST, 448-9, May, 1949.

17. Chapman, S., "The Ranque-Hilsch Tube and Its Application to Air Temperature Measurements," Cornell Aeronautical Laboratory Report, HF-686-F-1, (1950).

18. Cob, B. N., "Recent Developments in Gas Dynamics," Engineering, London, Vol. 170, (4418), 29th September, 1950, pp. 277.

19. Comassar, S., "The Vortex Tube," Journal of American Society of Naval Engineers, 63, 99-108, February 1951.

20. Compressed Air Magazine, 52, 131, May 1947, "T-Tube Both Heats and Cools Air," Comp. Air Mag., August 1947, pp. 206, "Hot-Cold Tube Phenomenon Explained."

21. Corliss, R. J. and Solnick, R. L., "Experimental Investigation of Vortex Refrigeration." B. S. Thesis, Massachusetts Institute of Technology, September 1947.

22. Corr, J. E., "The Vortex Tube," Unpublished report, Research Laboratory, Mechanical Investigation Division, General Electric Co., Data Folder No. 45289, July, 1948.

23. Courant, R., and Friedrichs, K. O., "Supersonic Flow and Shock Waves," Interscience Publishers, Inc., N. Y., (1948).

24. Curley, W. R., "Report on the Hilsch Vortex Tube," Journal of Boston College Physics Society, May 1950, pp. 3-9.

25. Curley, W., and MacGee, R., Jr., "Bibliography of the Vortex Tube," Refrigerating Engineering, 59, 2, pp. 166, 191-93, February 1951.

26. Dalitz, R. H., "Some Mathematical Aspects of Compressible Flow," Australian Council for Aeronautics Report, ACA-20, (1946).

27. De Havilland Aircraft Co. Ltd., "Vortex Tube Cooler," Test Report No. T. R. 100147, Structural Test House, "E" block, De Havilland Aircraft Co., Ltd., Hatfield, Herts, (1950).

28. Dornbrand, H., "Theoretical and Experimental Study of Vortex Tubes," A. F. Tech. Report 6123, Contract No. AF 33(038)5770, E.O. No. 664-776, Republic Aviation Corporation, (June 1950).

29. Eckert, E., "Temperature Recording in High-Speed Gases," NACA, TM 985, (1941).

30. Eckert, E. R. G., and Hartnett, J. P., "Experimental Study of the Velocity and Temperature Distribution in a High Velocity Vortex Type Flow," Stanford University Heat Transfer Institute Conference, (June 1956).

31. Elsler, K. and Hoch, M., "Das Verhalten Verschiedener Gase Und Die Trennung Von Gasgemischen in Einem Wirbelrohr" Zeitschrift fur Naturforschung, 6a, pp. 25-31, (January 1951), "The Behaviour of Various Gases and the Separation of Mixtures of Gases in a Vortex Tube," Translation by G. Coldewood, R.A.E. Library Translation, No. 400, February 1952.

32. Fattah, M. N. and Sweeny, A. N., "An Experimental Study of Centrifugal Refrigeration,: B. S. Thesis, Massachusetts Institute of Technology, (September 1947).

33. Finnemore, O. B., "A Method for the Experimental Investigation of the Hilsch Tube," Report No. HF-566-A-1, ATI-35748, Air Doc. Div. ATTn. MCIDKD, Cornell Aeronautical Laboratory, (1948).

34. First, M. W., "Cyclone Dust Collector Design," Paper No. 49-A-127, American Society of Mech. Eng'rs (November 1949).

35. Fortune Magazine, "Blows Hot and Cold," December 1948, pp. 180-3.

36. Franklin Institute of Laboratories for Research and Developement, Electronics and Instruments Division, Interim Report No. F-2015-4, (December 1948), "Investigation to Determine Most Practical Method of Obtaining Free Air Temperature at Transonic and Supersonic Speeds."

37. Fulton, C. D., "Energy Migration in the Vortex Refrigerator," Report on Term Project, No. 31, (Course 2,492), Department of Mechanical Engineering, Massachusetts Institute of Technology, (May 21, 1948).

38. Fulton, C. D., " Thermodynamics of the Vortex Refrigerator," Report on Term Project No. 1,(Course 2,452), Department of Mechanical Engineering, Massachusetts Institute of Technology, (May 27, 1948).

39. Fulton, C. D., "Ranque's Tube," Journal of the ASRE, Refrigerating Engineering, 58, 473-9, (May, 1950).

40. Fulton, C. D., "Comments on the Vortex Tube," Refrigerating Engineering, 59, 984 (October, 1951).

41. Garrick, I. E., and Kaplan, C., "On the Flow of a Compressible Fluid by the Hodograph Method: II - Fundamental Set of Particular Flow Solutions of the Chaplygin Differential Equation," NACA Tech. Ref., No. 790, (1944).

42. General Electric Company Educational Service News, Vol. II, No. 6, p. 4 (March 1950), "Measuring Cloud Temperatures."

43. Goetz, A., Discussion on Webster's Paper, Refrigerating Engineering, 58, 2, pp. 169-71, (February 1950).

44. Greene, R. L., "A Study of Centrifugal Refrigeration," M. S. Thesis, Massachusetts Institute of Technology, (January 1947).

45. Haar, D. Ter, and Wergeland, H., "On the Working Principle of the Hilsch Gadget," Det Kongelige Norske Videnskabers Selskab, Forhandlinger, B. D. SS, Nr. 15, pp. 55-8, (January 1948).

46. Haddox, R., Jr., Hunter, J. W., and Plunkett, W. H., "Experimental Investigation of Centrifugal Refrigeration," B. S. Thesis, Massachusetts Institute of Technology, (June 1947).

47. Hansell, C. W., "Low Temperature Physics," Miscellaneous Developments in German Science and Industry, C-6, Report No. 68, June, 1945, pp. 29-31, The Joint Intelligence Objective Agency, Washington, D. C.

48. Hansell, C. W., "Miscellaneous Development in German Science and Industry," Report PB-1638, Publications Board, Department of Commerce, Washington, D. C., pp. 36-7.

49. Heffner, F. E., "The Vortex Tube," M. S. Thesis, Wayne University, (1951).

50. Hilsch, R., "Die Expansion von Gasen im Zentrifrigalfeld als Kalteprozess," Zeitschrift fur Naturforschung, Bend I, Heft 4, April 1946, pp. 208-14. Hilsch, R, "The Use of the Expansion of Gases in a Centrifugal Field in Cooling Process," Review of Scientific Instruments, 18, 2, 108-113 (1947), (unabridged translation).

51. Hooper, F. C., and Juhasz, I. C., "Electric Dew Point Meter Cooled by Vortex Tube," Refrigerating Engineering, 60, 1196-7, (Nov., 1952).

52. Hottel, H. C., and Kalitinsky, A., "Temperature Measurements in High Velocity Airstreams," Trans, ASME, 67, A-0 (1945).

53. Industrial and Engineering Chemical Reports on the Chemical World Today, Technology, p. 5, May, 1946, "The Maxwellian Demon."

54. Industrial and Engineering Chemistry, December 1946, pp. 5-14, "Low Temperature Research."

55. Iron Age, "Tube Both Heats and Cools Air," 8th, May, 1947, pp. 145-146.

56. Johnson, A. V., "Quantitive Study of the Hilsch Heat Separator," Canadian Journal of Research, 25, 299, (September 1947).

57. Joint Int. Objective Agency, Washington D. C. Report No. 68, p. 29, "Miscellaneous Developments in German Science and Industry."

58. Kassner, R., and Knoernschild, E., "Friction Laws and Energy Transfer in Circular Flow," Technical Report No. F-TR-2198-ND, GS-USAF Wright - Patterson Air Force Base No. 78, (March 1948).

59. Kafader, A. D., and Teichmann, O. E., "Mysterious Hilsch Tube," Bulletin of the Armour Research Foundation (1952).

60. Knudsen, J. A., and Katz, D. L., "Fluid Dynamics and Heat Transfer," Engineering Research Institute Bulletin No. 37, University of Michigan Press, (1953).

61. Knoernschild, E., and Morgenson, "Application of Hilsch Tube to Aircraft and Missiles," A I T 33095, Army Air Force, Air Material Command, Engineering Division, Equipment Laboratory, Serial No. MCREXE-664-510A, 45-USAF-Wright Patterson 128, June 10, 1948.

62. Kraft, H., and Dibble, C., "Some Two-Dimensional Adiabatic Compressible Flow Patterns," Journal of the Aeronautical Sciences, 2, 4, October 1944, pp. 283-298.

63. Kramer, A. W., "Common Phenomena are not Scientific," Power Engineering, June 1950, pp. 79-80.

64. Kuethe, A. M., and Schetzer, J. D., "Foundations of Aerodynamics," John Wiley & Sons, Inc., N. Y., (1950).

65. Levitt, B. B., "A Study of the Characteristics of Converging Vortex Flow," A T I - 66647, from C. A. D. C., Rensselaer Polytechnic Institute, (1944).

66. Lewis, W., and Perkins, P. J., "Recorded Pressure Distribution in the Outer Portion of a Tornado Vortex," Monthly Weather Review, Vol. 31, Number 12, December 1953.

67. Lighthill, M. J., "The Hodograph Transformation in Trans-sonic Flow," Proc. Roy. Soc. (A), Vol. 191, (1947), p. 323; Vol. 191, (1947), p. 341; Vol. 191, (1947), p. 352; Vol. 192, (1947), p. 135.

68. Lunbeck, R. J., "De Ranque-Hilsch Koelmethode," Nederlandsch Tijdschrift Voor Naturkunde, Vol. 14, Feb./maart 1948/pp 83.

69. Lustick, L., "A Theoretical Investigation of the Hilsch Tube," M. S. Thesis, Syracuse University, (1950).

70. Mace, A. G., Mrs., "A Summary of Literature on the Ranque-Hilsch-Vortex Tube," British Scientific Instrument Research Association, B. S. I.R.A. Research Report No. M 16 Nov. 1953.

71. MacGee R., Jr., "The Vortex Tube," M. A. Thesis, Boston University (1950).

72. MacGee, R., Jr., "Fluid Action in the Vortex Tube," Refrigerating Engineering, 58, 974-5, (October, 1950).

73. MacGee, R. L., "The Vortex Tube Today," Power Engineering, Chicago, Vol. 55, No. 3, March, 1951, pp. 82-3.

74. Mayer, B. H., and Hunter, J. W., "Centrifugal Refrigeration," B. S. Thesis, Massachusetts Institute of Technology, (January 1947).

75. Miler, R. C., "Supersonic Aerodynamics - A Theoretical Introduction," McGraw - Hill, New York, (1950).

76. Milton, R. M., "Maxwellian Demon at Work, "Industrial and Engineering Chemistry, (Ind. Ed.), Vol. 38, No. 5, pp. 5.

77. Modern Developments in Fluid Dynamics - High Speed Flow, Vol. I, Edited by L. Howarth, The Oxford Engineering Science Series, Oxford at the Clarendon Press, (1953).

78. Naval Research, "Low Temperature Research at the University of Erlangen," Technical Report O A N A R -15-50, office of Naval Research, London Branch.

79. Nickerson, Jr. R., "Vortex Flow of a Compressible Fluid," B. S. Thesis, Massachusetts Institute of Technology, (1949).

80. Packer, L. S., "Phase A, Report Vortex Free Air Thermometer," Report No. IH-775-P-1, Contract No. a(S)51-832-C, Physics Department, Cornell Aeronautical Laboratory, (February 1952).

81. Packer, L. S., and Box, N. C., "Vortex-Tube Free Air Thermometry," Cornell Aeronautical Laboratory Inc., Buffalo, New York, ASME Diamond Jubilee Annual Meeting, Chicago, Illinois, Paper #55-A-22, (November 1955).

82. Planck, R. P., "The Ranque-Hilsch Centrifugal Jet," Refrigerating Engineering, 56, 58-9, (July, 1948).

83. Plank, R., "The Centrifugal Jet," (Abstract from "Theoreticher Beitrag Zur Arbeit von R. Hilsch uber das Wirbelrohr," by Burkhardt, Zeitschrift fur Naturforschung), 3a, January, 1948, pp. 46-51, Refrigerating Engineering, Vol. 57, May 1949, pp. 448-49.

84. Plank, R. P., "Cold Air Refrigerating Cycle," Refrigerating Engineering, Vol. 58, No. 1 (July 1948).

85. Poritsky, H., "Compressible Flows Obtainable From Two-Dimensional Flows Through the Addition of a Constant Normal Velocity," Journal of Applied Mechanics, 13, 1, (March 1946).

86. Power Plant Engineering, August 1947, pp. 87, "Tube Both Heats and Cool Air."

87. Prim, 3rd, R. C., "Steady Rotational Flow of Ideal Gases," Ph.D. Thesis in Mathematics, Princeton University, 1949, reprinted in Journal of Rational Mechanics and Analysis," I, 425-497, (1952).

88. Prins, J. A., "Brief aan de Redactie," Nederlandsch Tijdschrift Voor Naturkunde, Vol. 14, Augustus 1948, pp. 241.

89. Rannie, W. D. "Three-Dimensional Flow in Axial Turbomachines with Large Free Stream Vorticity," Advisory group for Aeronautical Research and Development, North Atlantic Treaty Organization, Paris de Chaillot, France, (June 1954).

90. Ranque, G. J., "Experiences sur la Détente Giratoire avec Productions Simultanées d'un Echappement d'Air chaud et d'Air Froid." Journal de Physique et le Radium, suppl. p. 112,(1933). (Translation: G. E. Schnectady Works Library, T. F. 3294).

91. Ranque, G. J., "Method and Apparatus for Obtaining from Fluid Under Pressure Two Currents of Fluids at Different Temperatures," United States Patent 1, 952,281 (March, 1934).

92. Reed, G. A., "Vortex Tube Refrigeration." M. S. Thesis, Massachusetts Institute of Technology, (May 1947).

93. Refrigerating Engineering 60, 379, April 1952, "Vortex Tube Principle Used by Navy in Thermometer for High Speed Planes.

94. Ringleb, F., "Exakte Losungen der Differentialgleichungen einer Adiabatischen Gasstromung," Zeitschrift fur Angewandte Mathematik und Mechanik 20, 185-198, (1940). Abstract in the "Journal of the Royal Aeronautical Socity," 46, 403-404, (1942), Translation, "Ministry of Aircraft Production," Great Britain, R.T.P. Translation 1609 (1942).

95. Roebuck, J. R., "A Novel Form of Refrigerator," Journal of Applied Physics, 15, 5, pp. 285, 245, (May 1945).

96. Ruskin, R. E., Schuter, R. M., Merrill, J. E., and Dinger, J. E., "Vortex Thermometer for Measurement of True Air Temperature in Flight," Naval Research Laboratory Annual Meeting, American Meteoroligical Society, New York City, (January, 1952).

97. Ruskin, R. E., Schuter, R. M., Dinger, J. E., and Merrill, J. E., "Development of the NRL Axial Flow Vortex Thermometer," Naval Research Laboratory Report No. 4008, (Sept., 1952).

98. Ryan, L. F., "Experiments on Aerodynamic Cooling," (Remarks on the Hilsch Vortex Tube). Mitteilung (No. 18) des Institute fur Aerodynamick an der E. T. H. (1950), pp. 49-50.

99. Sauer, R., "Introduction to Theoretical Gas Dynamics," Translation by Hill, F. K., and Alpher, R. A., J. W. Edwards Bros. Inc., Ann Arbor, Michigan, (1947).

100. Scheper, G. W., Jr., "The Vortex Tube-Internal Flow Data and a Heat Transfer Theory," Refrigerating Engineering, 59, 985-9, (October 1951).

101. Scheper, G. W., Jr., "Flow Patterns and a Heat Transfer Theory for the Vortex Heating and Refrigerating Tube," M. S. Thesis, Union College, (1949).

102. Scheper, G. W. Jr., "Internal Flow Data and Heat Transfer Theory for the Vortex Refrigerating Tube," Bulletin of Heat Transfer and Fluid Mechanics Institute (Stanford University). June, 1951, pp. 159-176.

103. Schlichting, H., "Boundary Layer Theory," Translated by J. Kestin, McGraw - Hill Book Co., Inc. New York, (1955).

104. Schmidt, K., "Experimentelle Unterschungen am Ranque-Wirbelrohr," F. Naturf. Vol. 7a, July, 1952, No. 1, pp. 480-86.

105. Schneider, F. B., "The Reduction of Pressure Drop Across Vortex Dust Collectors," Paper No. 49-A-126. American Society of Mechanical Engineers, (November 1949).

106. Schultz-Grunow, F., "Turbulenter Warmedurchgang im Zentrifugalfeld," Forschung Ing. Wes. 17, 1951, No. 3, pp. 65-76, Reviewed in Z. Angew. Math. Mech. Vol. 31, Aug./Sept., 1951, No. 8/9, pp. 293-94.

107. Schultz-Grunow, F., "How the Ranque-Hilsch Vortex Tube Operates," Refrigerating Engineering, 59, 52-3, (January 1951).

108. Science News Letter, "Whirling in Simple Tube Separates Hot and Cold Air," April 26th Issue, 1947, pp. 263.

109. Scientific American, 177 p. 29-30, (July 1947), "Blows Hot and Cold."

110. Shapiro, A. H., "The Dynamics and Thermodynamics of Compressible Fluid Flow," Vols. I and II. The Ronald Press Co., New York, 1953.

111. Shepherd, C. B., and Lapple, C. E., "Flow Pattern and Pressure Drop in Cyclone Dust Collectors," Industrial and Engineering Chemistry, 32, 9, pp. 1246-48, (1940).

112. Shepherd, C. B., and Lapple, C. E., "Flow Pattern and Pressure Drop in Cyclone Dust Collectors," Industrial and Engineering Chemistry, 32, 9, pp. 1246-48, (1940).

113. Sochor, J. J., "A Report on the Hilsch Tube," Chemical Engineering Report, Syracuse University, (May 1949).

114. Sprenger, H., Beobachtungen an Wirbelrohren," "Observation on the Vortex Tube," (Translation by a. O'Donnel from Zeitschrift fur Angewandte Mathematick und Physik, II, 1951, 5, pp. 293-300), R.A.E. Library Translation, No. 394, (December, 1951).

115. Sprenger, H., "Uber Thermische Effekte Bei Rezonanzrohren," Referat Gehalten anlasslich der Jahrewersammlung der Schweizerishen Physikalishen Gesellschaft in Bern am 24 August, 1952.

116. Stern, J., "A Study of the Hilsch Tube," Thesis, M. E. Dept. Purdue University.

117. Stern, M., "The Rolling up of a Vortex Sheet", Ph.D. Thesis in Mathematics at the New York University (1953-54).

118. Still, E. W., "Temperature Control of Jet-Engined Aircraft," Journal R.AE.S., February, 1953, pp. 93.

119. Sweeney, R. J., "Measurement Technique in Mechanical Engineering," John Wiley & Sons, Inc., (1953).

120. Taylor, G. I., "Distribution of Velocity and Temperature Between Concentric Rotating Cylinders," Proceedings of the Royal Society, London, 151, 494-512 (1935).

121. Truesdell, C. A., "The Kinematics of Vorticity," University of Indiana Press (1955).

122. Tsien, H. S., "The Limiting Line in Mixed Subsonic and Supersonic Flow of Compressible Fluids," N A C A Tech. Note, No. 961, (1944).

123. Tsien, H. S., and Kuo, Y. H., "Two-Dimensional Irrotational Mixed Subsonic and Supersonic Flow of a Compressible Fluid and the Upper Critical Mach Number," N A C A Tech. Note, No. 995, (1946).

124. Van Deemter, J. J., "On the Theory of the Ranque-Hilsch Cooling Effect," Applied Scientific Research, Section A, Vol. 3, No. 3, pp. 174-196 (1952).

125. Van Der Maas, H. J., and Wyrria, S., "Corrections on Thermometer Readings in an Air Stream," N A C A, T M 956, (1940).

126. Vonnegut, B., "Vortex Thermometer for Measuring True Air Temperature and True Air Speeds in Flight," Occasional Report No. 14, Project Cirrus, Contract W-36-039-SC-38141, Report No. PB99102 (September 1949).

127. Vonnegut, B., "Vortex Thermometer for Measuring True Air Temperature and True Air Speed in Flight," The Review of Scientific Instruments, 21, 136-141 (February 1950).

128. Vonnegut, B., "Operation Cirrus uses Principle of Hilsch Tube to Measure Temperature," Refrigerating Engineering. 58, p. 267 (March 1950).

129. Weber, H. E., "The Boundary Layer Inside a Conical Surface Due to Swirl," 1956 ASME National Applied Mechanics Conference. Reprint of Paper No. 56-APM-31.

130. Webster, D. S., "An Analysis of the Hilsch Vortex Tube," Journal of the ASRE, Refrigerating Engineering, 58, 163-9; Discussion, 107-71, (February 1950).

131. Wenig, H. G., "The Ranque-Hilsch Effect in a Vortex Tube, Ph. D. Thesis, New York University, (1952).

132. Weske, J. R., "Discrete Vortices in the Transition Range of Flow in a Pipe," Advisory group for Aeronautical Research and Development, North Atlantic Treaty Organization, Palais de Chaillot, Paris, (June 1954).

133. Westley, R., "A Bibliography and Survey of the Vortex Tube," The College of Aeronautics Cranfield (1954).

134. Westley, R., "A Note on the Application of the Vortex Tube to Ventilated Suits," Tech. Note Aero., College of Aeronautics, Cranfiedl, (April 1953).

135. Williamson, U.A.F. and Tompkins, J. A. (Miss), "Practical Notes on the Design of a Vortex Tube," R.A.E. Technical Note, No. Mech. Eng. 67, (March 1951).

136. Wu, T. Yao-Tsu, "Two-Dimensional Sink Flow of a Viscons, Heat-Conducting, Compressible Fluid," Quaterly of Applied Mathematics, Vol. XIII, No. 4, (January 1956).